CANADIAN THESES ON MICROFICHE

I.S.B.N.

THESES CANADIENNES SUR MICROFICHE

National Library of Canada
Collections Development Branch

Canadian Theses on
Microfiche Service

Ottawa, Canada
K1A 0N4

Bibliothèque nationale du Canada
Direction du développement des collections

Service des thèses canadiennes
sur microfiche

NOTICE

The quality of this microfiche is heavily dependent upon the quality of the original thesis submitted for microfilming. Every effort has been made to ensure the highest quality of reproduction possible.

If pages are missing, contact the university which granted the degree.

Some pages may have indistinct print especially if the original pages were typed with a poor typewriter ribbon or if the university sent us a poor photocopy.

Previously copyrighted materials (journal articles, published tests, etc.) are not filmed.

Reproduction in full or in part of this film is governed by the Canadian Copyright Act, R.S.C. 1970, c. C-30. Please read the authorization forms which accompany this thesis.

THIS DISSERTATION
HAS BEEN MICROFILMED
EXACTLY AS RECEIVED

AVIS

La qualité de cette microfiche dépend grandement de la qualité de la thèse soumise au microfilmage. Nous avons tout fait pour assurer une qualité supérieure de reproduction.

S'il manque des pages, veuillez communiquer avec l'université qui a conféré le grade.

La qualité d'impression de certaines pages peut laisser à désirer, surtout si les pages originales ont été dactylographiées à l'aide d'un ruban usé ou si l'université nous a fait parvenir une photocopie de mauvaise qualité.

Les documents qui font déjà l'objet d'un droit d'auteur (articles de revue, examens publiés, etc.) ne sont pas microfilmés.

La reproduction, même partielle, de ce microfilm est soumise à la Loi canadienne sur le droit d'auteur, SRC 1970, c. C-30. Veuillez prendre connaissance des formules d'autorisation qui accompagnent cette thèse.

LA THÈSE A ÉTÉ
MICROFILMÉE TELLE QUE
NOUS L'AVONS REÇUE

NL-339 (r. 82/08)

Canada

MEASUREMENT AND PREDICTION OF TRANSITION BOILING HEAT TRANSFER OF SUBCOOLED WATER AT LOW FLOW AND ATMOSPHERIC PRESSURE

BY

HELMY S. RAGHEB

THESIS SUBMITTED TO THE SCHOOL OF GRADUATE STUDIES OF THE UNIVERSITY OF OTTAWA AS A PARTIAL FULFILLMENT OF THE REQUIREMENTS FOR THE DEGREE OF DOCTORAT EN PHILOSOPHIE IN MECHANICAL ENGINEERING

DEPARTMENT OF MECHANICAL ENGINEERING

UNIVERSITY OF OTTAWA

JANUARY 1984

© Helmy S. Ragheb, Ottawa, Canada, 1984

UNIVERSITÉ D'OTTAWA
UNIVERSITY OF OTTAWA

ACHNOWLEDGEMENTS

I am indebted to many for assistance in preparing this thesis. Foremost is my wife, Mona, who endured me during the preparation.

I also appreciate the support, guidance and encouragement of Professor S.C. Cheng who initiated the present investigation.

I would like to pay particular thanks to Dr. D.C. Groeneveld of AECL who offered constructive comments throughout this work.

Thanks also are due to the technical staff of the Mechanical Engineering Workshop for their cooperation.

Finally, I wish to acknowledge the financial support of U.S. NRC and Argonne National Laboratory, Illinois, U.S.A.

ABSTRACT

A relatively simple technique has been developed to obtain transition boiling data using a high thermal inertia test section. Complete boiling curves have been obtained for subcooled water at low flow and atmospheric pressure.

The following effects on the transition boiling section of the boiling curve were studied in detail (a) flow conditions (mass flux, subcooling), (b) method of analysis (1-D, 2-D conduction), (c) method of operation (transient, steady-state), and (d) experimental equipment (test section arrangement, test section construction, heated surface properties).

Two computational models to predict the transition boiling heat transfer for subcooled water at low flow and atmospheric pressure are presented. The models incorporate the effects of mass flux, local enthalpy (or inlet subcooling) and thermal properties of the heated surface. Comparisons of the predicted results with the experimental data show fair agreement in the nucleate and transition boiling regions.

TABLE OF CONTENTS

LIST OF TABLES

LIST OF FIGURES

FIGURES (Cont'd)

FIGURES (Cont'd)

NOMENCLATURE

A	area (Chapter 4) or vapour flow area (Chapter 7)
b	$= -in$ = growth coefficient
c	velocity of harmonic wave
C	constant
C_p, c	specific heat at constant pressure
d	vapour film thickness
D_w	diameter of the heated surface
F	force acting on liquid-vapour interface
f	fraction of wetted area or frequency of contacts
g	acceleration of gravity or gap thickness (Fig. 4.3)
G	mass flux
h	enthalpy or heat transfer coefficient
i	$= \sqrt{-1}$
k	thermal conductivity
KE	kinetic energy
L	length of test section
m	wave number $= \frac{2\pi}{\lambda}$ or wave mass in equation (7.29)

NOMENCLATURE (Cont'd)

M°	vapour mass flow
n	wave frequency
p	pressure
q	heat flux
Q	heat content of test section
r	radial distance in cylindrical coordinates
Δr	regular radial increment
Δr_o	radial distance between inner wall and location of T.C. (Fig. 4.1)
R	radias of the vapour jet (Zuber's model) or radius of tube
R_e	Reynolds number
R_{eo}	transition Reynolds number
S	wall thickness
t	time
T	temperature
V	velocity of vapour or approach velocity of the wave
x	quality
y	thermal boundary layer in liquid phase
z	vertical distance in cylindrical coordinates

GREEK LETTERS

α thermal diffusivity = $\frac{k}{\rho C_p}$

β ratio of liquid core radius/tube radius (see Fig. 7.2)

δ distance perpendicular to liquid-vapour interface (see Fig. II.2)

δ amplitude of harmonic wave

Δ change

λ wave length

ρ density

σ surface tension

θ angle in cylindrical coordinates

μ viscosity

SUBSCRIPTS

CHF critical heat flux

c critical, convection , thermodynamic critical state or copper

d conduction

SUBSCRIPTS (Cont'd)

f	saturated liquid (Chapter 6)
fg	change from liquid to vapour saturation condition
FB	film boiling
G	mass flux
i	ith nodal point
I	isothermal
in	inner wall or inlet in Chapter 6
l	liquid
m	modified
min	minimum
o	location of thermocouple
out	outer wall
s	saturation
sat	saturated (Chapter 6)
sub	subcooled
TB	transition boiling

SUBSCRIPTS (Cont'd)

v	vapour
w	wall
x	quality
wm	Wood's metal
-1	nodal point at inner wall
Z	Zircaloy

CHAPTER 1

INTRODUCTION

Safety analysis of water-cooled nuclear reactors aims at the accurate predictions of fuel sheath temperature during postulated accidents that could lead to a situation where the fuel elements are not adequately cooled. Inadequate cooling occurs due to either an accidental increase in power or a decrease in flow. As a result, the heat transfer mode changes from forced convection into nucleate boiling where the fuel sheath transmits high heat fluxes. A further increase in the heat flux is limited by the Critical Heat Flux (CHF). At this point any attempt to increase the heat flux will result in an inordinate increase in surface temperature. This phenomenon is usually referred to as the boiling crisis.

Immediately following the CHF, the heated surface can no longer support the continuous liquid-solid contact, and heat transfer deteriorates due to the spread of area covered by dry patches. The heat transfer mode, therefore, changes into less efficient transition boiling. At higher surface superheat the transition boiling mode will gradually change to the inefficient film boiling mode.

The transition boiling mode could also occur in a reversed manner, in the reactor core, during the Emergency Core Cooling (ECC) phase following a Loss of Coolant Accident (LOCA). In this case, the injected

flow in the core attempts to establish a continuous liquid-solid contact with fuel sheath. Here, the heat transfer mode changes from film boiling to transition boiling before nucleate boiling can be re-established.

The transition boiling heat transfer mode is unique among heat transfer modes in that surface heat flux decreases with an increase in surface temperature. As shown in Fig. 1.1, the transition boiling is an intermediate heat transfer mode where the heated surface temperature is too high to maintain nucleate boiling but too low to maintain stable film boiling. At the low temperature boundary, where the transition boiling is most efficient, the heat flux can be predicted by a variety of correlations for the critical heat flux (CHF). At the high temperature boundary lies the minimum stable film boiling point (MSFB). Little is known about this point except that it is affected by flow, subcooling, pressure and surface conditions. Between the two boundaries there is a scarcity of experimental data and their conditions are limited. This is due to the unique nature of transition boiling in which heat flux decreases with an increase of surface temperature; such a heat transfer mode is unstable in a heat flux controlled system and usually requires a temperature controlled system.

A review by Groeneveld[1] showed that existing correlations for transition boiling do not agree with each other and their data base is questionable. The apparent discrepancies between the available correlations and the suspected experimental data have provided the motivation for this study.

This thesis presents an experimental and analytical investigation of the transition boiling regime using a simple technique. The technique involves the employment of high thermal inertia test sections to stablize the transition boiling. Data were obtained for subcooled water at atmospheric pressure under forced convective conditions. The study identifies the following effects on the transition and film boiling section of the boiling curve:

(a) flow conditions (mass flow and degree of subcooling)

(b) experimental procedure (transient and steady state modes of operation)

(c) methods of analysis (one dimensional model and two dimensional model)

(d) experimental equipments (types of test section, heated surface thermal material, etc.)

This study also presents two computational models to predict transition boiling heat transfer for water at low flow and atmospheric pressure. The first model is semi-empirical and the second is analytical. The models incorporate effects of mass flux, local enthalpy and thermal properties of heated surface. Comparisons of the predicted results with experimental data show fair agreement in the transition boiling region.

REFERENCES

1. Groeneveld, D.C. and Fung, K.K. "Forced Convective Transition Boiling Review of Literature and Comparison of Prediction Methods", AECL-5543. (1976).

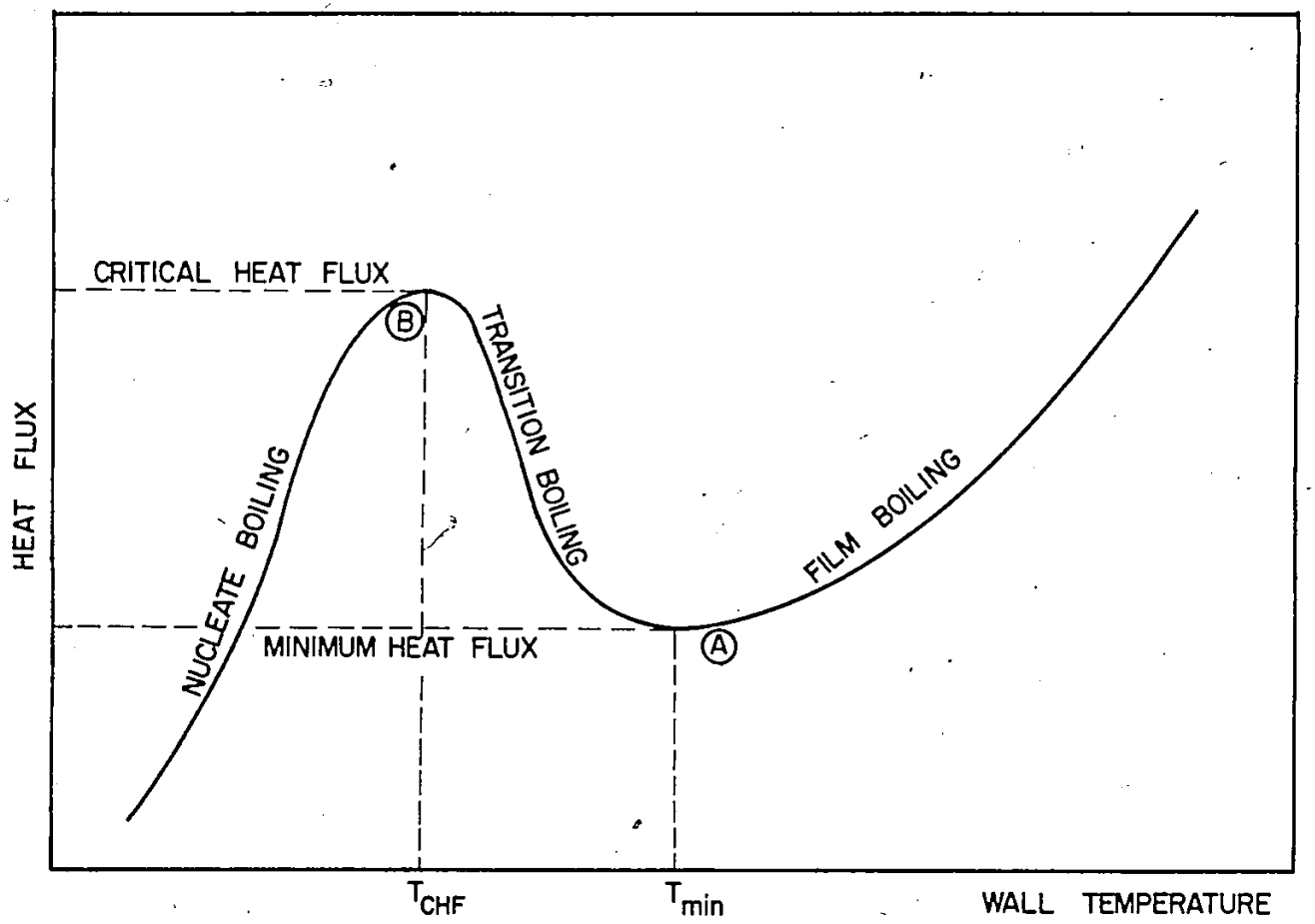

FIG. I.I BOILING CURVE

CHAPTER 2

THE TRANSITION BOILING - SURVEY OF LITERATURE

2.1 History

It was commonly known that the heat flux, q, transmitted from a metallic surface to boiling water, increases with their temperature difference ΔT. However, it was not known whether the heat flux, q, had a maximum and minimum value until 1935, when Nukiyama[1] observed the existence of several modes of boiling over an electrically heated wire submerged in a pool of water. In his experiment it was found that the heat flux, q, reached its maximum value at point (b) as shown in Fig. 2.1, when the wire was heated in pool boiling. Beyond point (b), the fluid could not accept heat as fast as being supplied by constant electric heating. Thus the heat added was stored partially in the wire, causing the surface temperature to rise drastically from (b) to (a), and the wire melted. On the other hand, it was shown by experiment - using a platinum wire to prevent melting - that at very high temperatures, q could be large due to radiation along path (a-d). Therefore, Nukiyama expected that q has a minimum value between (a) and (b).

Indeed, by decreasing the electric power, the change of q traced along a smooth curve (a - c), followed by a sudden jump (c - e). He wrote: *"It must, however, be expected that though q decreases due to the increasing volume of steam in the vicinity of the surface, it must have its minimum value where it begins to increase again".*

The work of Nukiyama led Drew and Mueller[2] to hypothesize the existence of the transition boiling region. Looking back at previous work as long ago as 1888, they found some reported tests on a sea-water evaporator which gave an indication of an upper limit for the overall heat transfer coefficient at temperature differences between 40° and 50°C, and at least suggest an actual decrease in the rate of boiling when the temperature difference was raised to higher values. Therefore, they referred to Nukiyama's study as the first to deliberately investigate the possibility of a maximum limit for the heat transfer to occur at moderate temperature differences.

In their study on the behaviour of boiling organic liquids, Drew and Mueller considered the film boiling region to comprise all boiling at a temperature difference in excess of T_{CHF} (see Fig. 2.2). However, they referred to the possibility of the existence of a "transition" range just beyond T_{CHF}. In this range a mechanism distinct from film and nucleate boiling could exist.

The existence of the transition boiling mode was also observed by metallurgists who have obtained cooling curves during quenching processes. A typical of this curve is shown in Fig. 2.3. By following the curve from right to left, it can be seen that the result of plotting the rate of heat transfer of q versus T_w is the boiling curve. Such terms as 'partial' or 'unstable' film boiling were first introduced and then dropped in favour of the term 'transition' that did not commit anyone to a hypothetical mechanism.

Witte and Lienhard[3] have recently introduced an advanced idea which suggests that the 'transition' region ought to be viewed as an extension of either film boiling or nucleate boiling. In effect, they suggest two 'transition' boiling curves.

The two curves (see Fig. 2.4) are labelled 'nucleate' and 'film' boiling. As ΔT is increased independently, in the nucleate boiling regime, there will be an increase in nucleation sites and an increased tendency to separate liquid from the heated surface just beyond the Critical Heat Flux. As the surface grows hotter, the duration of liquid contact will be reduced. The film boiling curve is also extended to the left beyond conventional minimum heat flux point. When ΔT is reduced independently, there will be some liquid-solid contact. Although the contact is slight it leads to substantial increase in the rate of generation of vapour, thus q begins to rise. Here, the basic film boiling process is preserved but it is increasingly augmented by instances of liquid-solid contact.

2.2 Mechanisms of Transition Boiling

The mechanisms of transition boiling were described in the literature according to the method by which the transition regime is approached. During a heating process, the transition occurs when the maximum heat flux is exceeded while in a quenching process, the transition occurs following surface rewetting. In the following sections, a description of the mechanisms associated with each process is presented.

2.2.1 Transition Boiling Mechanism Following Rewetting

During a quenching process, the transition occurs from film boiling to nucleate boiling, in the manner in which it would occur during Emergency Core Cooling (ECC) in a nuclear reactor. This type of transition is associated with the collapse of the vapour film next to the heated surface.

In pool boiling, Zuber[4] expected a definite geometrical configuration for the transition boiling based on the observations of Westwater and Santangelo[5]. A schematic representation of this geometry and the process of transition boiling is shown in Fig. 2.5. Fig. 2.5a shows a vapour patch in transition boiling where the liquid-vapour interface is hydrodynamically unstable. The interface consists of spikes of liquid and of rounded regions of vapour. This shape of interface is defined in Fig. 2.5b as disturbances with a range of wave lengths. As liquid evaporates from the spikes the vapour flows in the region between two spikes. This region resembles rising bubbles (see Fig. 2.5c). As a row of bubbles is released an unstable interface is formed again. Because of the downward flow of the liquid a spike will be formed underneath the released bubble and the process is renewed (see Fig. 2.5d). The successive rows of bubbles will appear displaced, therefore, by half a wave length (see Fig. 2.5e). For such a system, Zuber expected that changes in heat transfer rates are associated with changes in the frequency of bubble release, i.e., of the vapour bursts. The minimum heat flux, therefore, corresponds to the minimum frequency of the system.

It should be noted here that, at a given heat flux, the process of transition boiling can continue indefinitely; it is therefore thermally stable. However, it is hydrodynamically unstable since this instability is the cause of the phenomenon.

A quantitative analysis of the above mechanism which was done by Zuber is described in Appendix II.

In flow boiling, a number of models have been suggested in the available literature, yet no complete answer exists.

Iloeje et al[6] identified three controlling mechanisms for forced convective rewet*. These are impulse cooling collapse, axial conduction controlled rewet, and dispersed flow rewet.

Impulse Cooling Collapse

At a temperature higher than T_{rewet}** the fluid is separated from the wall by a vapour film. If the wall temperature is lowered, the film thickness decreases, so that the crests of the wavy fluid-vapour interface may contact the wall. These repeated contacts, during a quenching process, decrease the wall temperature and allow rewetting.

---

* Surface rewetting refers to the phenomenon of establishing liquid contact with a solid surface whose initial temperature is greater than the rewetting temperature.

** T_{rewet} is the temperature below which the surface may wet.

This model has been proposed by Kalinin[7], who performed a conduction analysis to obtain the temperature at the beginning and end of the transition process T_{min} and T_{CHF}. In order for his analysis to be useful, the frequency of contacts before collapse needs to be known. The difficulty in obtaining such information would appear to make his solution useless. However, his solution showed that T_{min} and T_{CHF} increase with increasing the group parameter $1/(\rho C_p k)_w$. Therefore, he conducted experiments to study the effect of thermophysical properties of wall material on T_{min} and T_{CHF}, using annular channels made of different materials, and cooled by different liquids, in both pool and forced convective boiling. His data were correlated in terms of the ratio $\sqrt{\frac{(\rho C_p k)_l}{(\rho C_p k)_w}}$.

The dependence of T_{CHF} and T_{min} on the group parameter $\rho C_p k$ is due to the assumption that the heat transfer over the contact region is controlled by pure conduction. A local decrease of the temperature over this region depends on the rate of heat supplied from the heater material to the contact region. Therefore, if the material is highly conductive, the heat supply will be at such a high rate as to delay rewetting to a lower temperature.

In general, there are two shortcomings in this model: a) the model does not reflect the effect of flow velocity on T_{min} and T_{CHF}, and b) there maybe some error in ignoring the axial conduction.

Axial Conduction Controlled Rewet

Based on their visual observation of the hydrodynamic conditions existing at the minimum heat flux point, Simon and Simoneau[8], suggested that the transition from film boiling to nucleate boiling is controlled by axial conduction. Wall conduction transfers heat from the film boiling side to the nucleate boiling side and causes the surface temperature to drop. Transition will occur at a position on the wall where the rewetting temperature is reached.

In their analysis, they assumed that the rewetting temperature was equivalent to T_{min}, and used the theoretical equation of Spiegler et al.[9]

$$\frac{T_{rewet}}{T_c} = 0.13 \frac{P}{P_c} + 0.84 \qquad (2.1)$$

The above equation implies that both minimum heat flux and rewetting temperatures are solely determined by the thermodynamic properties of the boiling fluid. Experimental results showed that T_{min} varies considerably for the same fluid and system pressure, and in some cases much higher than T_c. For these reasons, one would conclude that T_{min} is not a thermodynamic property of the fluid.

Dispersed Flow Rewet

The variation of T_{min} for the same fluid and system pressure has been discussed by Iloeje et al[6], who attributed this variation to surface effects, namely scale deposits, and surface roughness.

In an attempt to encounter all the observed effects on T_{min}, they proposed a dual mode heat transfer model. Heat transfer to the flow is a sum of two components:

1. Heat transfer to droplets of water hitting the wall.
2. Heat transfer to vapour assuming no effect of the existence of droplets.

The sum of these two components give the total q and indicates T_{min}.

Modelling the collapse in this manner reflects the effect of mass flux which was absent in the other two models. At high mass fluxes there is a greater mixing of the flow, and it therefore reduces superheating of the vapour, while it provides a greater momentum of droplets. All these factors will increase the heat transfer, and consequently lead to transition occuring at higher wall superheat.

The difficulty with this model lies in the prediction of the heat transfer component of the droplets.

2.2.2 Transition Boiling Mechanisms at the CHF Point

In the preceding section (2.2.1), it was suggested that in pool boiling, the release of bubbles was spaced half a wave apart. As will be discussed in Appendix II, this wave length is determined by Taylor instability. At the CHF, because of the increasing evaporation rates,

bubble population continues to increase. The frequency of bubble emission increases until bubbles follow each other and consequently form vapour columns or vapour jets. The vapour velocity in these jets increase to a critical value determined by the stability of the vertical liquid-vapour interface which separates the vapour columns from the bulk of liquid. The stability of such jets is determined by the Helmholtz instability criterion. Since the jet spacing is determined by the Taylor instability, the critical heat flux is characterized by the combined effects of Taylor and Helmholtz instabilities. The mathematical formulation of this problem has been performed by Zuber[4] and is described in Appendix II.

The mechanism of transition in flow boiling is different from that in pool boiling. In addition to the convective effect of the flow, Tong[10] referred to two phenomena that further complicate the mechanism at the CHF:

(a) The existence of a bubble layer moving closely parallel to the heated surface that shields the surface from incoming cold liquid. This phenomenon is referred to as "Bubble Clouding".

(b) A premature boiling crisis may take place during local flow instability. The changing bulk velocity periodically retards the boundary layer, thus leading to overheating of the surface. Furthermore, during flow oscillation, a temporary decrease in the local pressure will cause an increase in the local superheat near the surface. This increase leads to an increase in bubble population resulting in the destruction of the liquid film.

The mechanism of transition in flow boiling will also depend on the flow conditions which may be classified into two categories:

(a) subcooled or low quality, and

(b) high quality region.

In the following discussion, attention will be focused on the former region since it closely relates to the conditions of the present investigation.

At the low temperature boundary, the transition in the subcooled region usually requires a high heat flux. The bubbles generated at the heated surface may be so crowded that they form a layer which prevents a sufficient amount of liquid from reaching the surface to maintain the liquid-solid contact. Such a bubbly layer was observed by Jiji and Clark[11] and Tong[12]. The occurence of this phenomenon has several implications:

(1) If it occurs at a high flow, the fluid in the neighbourhood of the heated surface may not be in thermodynamic equilibrium with the liquid bulk and therefore the initiation of transition will be controlled by the "surface proximity parameters" (Tong[10]).

(2) The severe accumulation of bubbles limits the upstream effects.

(3) The local heat flux is an important perameter regardless of the heat flux distribution. Tong et al[12] showed that the ratio of

the local CHF with uniform distribution to that of non-uniform distribution is close to unity.

At surface temperatures in excess of the boiling crisis temperature, the heated surface will be partially covered with unstable vapour patches (varying with space and time). This has been reported by Ellion[13] who studied forced convective transition boiling in subcooled water and observed frequent replacement of vapour patches by liquid. It is the formation of these dry patches that causes the severe reduction in heat transfer coefficient. The subsequent reduction in vapour generation will allow the liquid to momentarily rewet the heated surface. Ragheb and Cheng[14] showed experimentally that the fraction of wetted area under forced convective conditions, decreases with increasing wall superheat (Fig. 2.6). Vapour slug formation was also observed by Ragheb[15], who used a transparent test section upstream of the test section. The slugs were seen to force the flow toward both up-and-down-stream directions, causing a violent motion.

2.3 Parametric Effects

Since the transition boiling mode is an intermediate heat transfer mode, the effects of different parameters (such as subcooling, mass flux and thermal properties of the surface) can be determined by investigating their effect on the boundaries, i.e., CHF and minimum heat flux points.

2.3.1 Effect of Mass Flux

A summary of the experiments which reported the effect of mass flux on the transition boiling regime is given in Table 2.1. In general, the heat flux increases with the increase of mass flux. At the CHF point, the higher flow allows more efficient removal of bubbles, thus delaying the occurrence of the Departure of Nucleate Boiling (DNB) phenomenon. At the minimum heat flux point, the increase in mass flux destabilizes the vapour film allowing intermittent liquid-wall contact thus increasing the heat flux.

2.3.2 Effect of Subcooling

The effect of subcooling on heat flux and surface temperature at the boundaries of transition boiling is summarized in Table 2.2. In general, the increase in subcooling causes an increase in q_{CHF}, q_{min}, q_{TB} and T_{min}.

2.3.3 Effect of Surface Thermal Properties

Few observations were found in the literature on the effect of surface thermal properties on transition boiling. The minimum film boiling temperature T_{min} has been found to be well correlated to the parameter ρCk. T_{min} increases with the decrease in the value of ρCk. A summary of this effect is given in Table 2.3.

2.3.4 Effect of Hysteresis

Several investigators attempted to identify the difference between the pool boiling curve obtained via a cooldown process (quenching) and that obtained through a heat-up process.

Since most of the transient heat-up experiments and the quenching experiments have been performed separately, comparison between the two types of boiling has not been established.

Sakurai and Shiotsu[30] performed a computer controlled experiment to study the transient heat-up followed by quasi-steady cooldown in a pool. They observed a thermal hysteresis only near the CHF. Because the transient was very slow (2 K/s) they did not observe any hysteresis in the region away from CHF.

More recently, Salehpour and Yao[31] reported the existence of the thermal hysteresis under forced convective condition. They performed termperature controlled experiments for boiling of Freon 113 in a vertical annular channel. Fig. 2.7 shows their transient heat-up and cooldown data where the difference appears to be noticeable. They also found that the CHF of the cooldown process to be very close to the predicted steady state of Coffield[32].

2.3.5 Effect of Quenching Mechanism

Thermal hysteresis of boiling in heated channels is also dependent upon the type of quenching mechansim. In relatively long channels, the quenching could occur at both upstream and downstream ends and propagates toward the middle of the channel. Salehpour and Yao[31] showed that there are two boiling curves which correspond to the two quenching mechanisms. In Fig. 2.8 the solid line is the one corresponding to the quenching front propagating downstream and the broken line is the one corresponding to the quenching front propagating upstream. Since the CHF for the latter case is less than the first one, it is concluded that the thermal hysteresis of boiling is dependent upon the type of quenching mechanism.

2.3.6 Effect of Applied Electric Field

In a two-phase system which is subject to electric field, bubbles tend to migrate towards the anode. This is attributed to the charge distribution at the liquid-vapour interface; the negative charges are oriented towards the liquid phase and the positive charges toward the vapour phase. If a downward heating surface acting as a cathode faces an anode, the repulsion of bubbles away from the surface will occur. The resulting increase in liquid agitation augments heat transfer from the surface.

In the transition boiling region, an increase in heat transfer was observed by Markles and Durfee[33] when the electric field strength was

increased (see Fig. 2.9). They related the enhancement in heat transfer to the destabilization of the vapour film.

Table 2.1

EFFECT OF MASS FLUX

Experimenter	Equipment, Conditions	Observed Effect; Results
Pramuk & Westwater[16]	Agitated pool of methanol	q_{TB} increases due to the agitation
Kalinin[7]	Forced convection of fluids in vertical tubes	T_{min} and T_{CHF} are not affected by flow velocity
Groeneveld[17]	High quality and high flow of Freon-12; Heat flux controlled system	q_{TB} increases with increase in surface temperature
Iloeje[6]	Forced vertical flow of water in a tube -- high pressure and high quality	T_{min} increases with mass flux
Dhir[18]	Quenching of steel, copper and silver spheres in water -- free and forced convection	T_{min} is independent of flow velocity
Yilmaz & Westwater[19]	Flow of Freon-113 outside horizontal copper tube near atmospheric pressure	q_{TB} very sensitive to flow velocity (900% higher for a velocity 2.4 m/s than for zero velocity). See Fig. 2.10
Auracher & Albrodt[20]	Flow of Freon-114 in nickel tube soldered to copper block -- steady-state temperature controlled experiment	q_{TB} & T_{min} increase with the increase of mass flux. See Fig. 2.11

Table 2.2

EFFECT OF SUBCOOLING

Experimenter	Equipment, Conditions	Observed Effect, Results
Nishikawa[21]	Pool boiling - horizontal platinum wire	q_{min} improves with increasing subcooling
Bradfield[22]	Quenching of a copper sphere in a pool of water at atmospheric pressure	q_{TB} shifts to a higher superheat with increasing subcooling. T_{min} increases linearly with subcooling
Kalinin[7]	Free and forced convection of fluids in vertical tubes	T_{min} and T_{CHF} increase with increasing subcooling
Tachibana[23]	Pool boiling of water and oils on a horizontal surface using quenching and steady-state methods	q_{CHF} and q_{min} increase with subcooling. The effect of subcooling is remarkable with water and slight with oils
Dhir[18]	Quenching of steel, copper and silver spheres in water -- free and forced convection	T_{min} increases with liquid subcooling
Johannsen & Kleen[24]	Steady-state flow boiling of water on a copper surface at low pressure	q_{TB} increases with increasing subcooling. See Fig. 2.12
Veda et al.[25]	Flow boiling of Freon-113 on a copper surface	q_{TB} increases with increasing subcooling. See Fig. 2.13

Table 2.3

EFFECT OF SURFACE PROPERTIES

Experimenter	Equipment, Conditions	Observed Effect, Results
De Bertolli, et al[26]	Forced convective flow of water in rectangular and round tubes (Zirc. S.S. & Inc.)	No observed effect on CHF
Berenson[27]	Pool boiling on horizontal surface. Pentane with copper, nickel and Inconel surface	Critical heat flux and T_{min} are independent of surface material
Kalinin[7]	Free and forced convection of fluids in vertical tubes	T_{min} and T_{CHF} increase with the increase of $\sqrt{1/\rho C_p k}$
Henry[28]	Analysis of experimental data obtained on spheres, plates, etc	$T_{min} \propto 1/(k\rho C_p)$
Labuntsov, et al[29]	Pool boiling on horizontal tubes (liquid heated). Ethanol on copper, nickel, and stainless steel	CHF on nickel and stainless steel is higher than on copper

REFERENCES

1. Nukiyama, S., "The Maximum and Minimum Values of the Heat Transmitted from Metal to Boiling Water Under Atmospheric Pressure", J. Soc. Mech. Engres, Japan, 37, 367, (1934).

2. Drew, T.B. and A.C. Mueller, "Boiling", Trans. Am. Inst. Chem. Engres., 33, 449, (1937).

3. Witte L.C. and Lienhard, J.H., "On the Existence of Two 'Transition' Boiling Curves", Int. J. Heat Transfer, Vol. 25, No. 6, pp. 771-779 (1982).

4. Zuber, N., "Hydrodynamic Aspects of Boiling Heat Transfer", Ph.D. Thesis, AECN-4439 (1959).

5. Westwater, J.W. and Santangelo, J.G., "Photographic Study of Boiling", Ind. Engr. Chem., 47, 1955, 1605.

6. Iloeje, O.C., et al, "An Investigation of the Collapse and Surface Rewet in Film Boiling in Forced Vertical Flow", J. of Heat Transfer, May (1975).

7. Kalinin, E.K., et al, "Investigation of the Crisis in Film Boiling in Channels", Proceedings of Two-Phase Flow and Heat Transfer in Rod Bundles, ASME Winter Annual Meeting, Los Angeles, California (1969).

8. Simon, F.F. and R.J. Simoneau, "Transition from Film to Nucleate Boiling in Vertical Flow", ASME paper 69-HT-26, August (1969).

9. Spiegler, P., et al, "On-Set of Stable Film Boiling and the Foam Limit", Int. J. Heat Mass Trans., Vol. 6, pp. 987-994 (1963).

10. Tong, L.S., "Boiling Heat Transfer and Two-Phase Flow", Wiely, New York, (1965).

11. Jiji, L.M. and Clark, J.A. "Bubble Boundary Layer and Temperature Profiles for Forced Convection Boiling in Channel Flow", ASME paper 62-WA-141 (1962).

12. Tong, L.S., Currin, H.B., Larson, P.S. and O.G. Smith, "Influence of Axially Non-Uniform Heat Flux on DNB", AICHE Preprint 17, Eighth National Heat Transfer Conference, Los Angeles (1965).

13. Ellion, M.E., "A Study of the Mechanism of Boiling Heat Transfer", California Inst. of Technology Report JPL-MEMO-20-88 (1954).

14. Ragheb, H.S. and Cheng, S.C., "Surface Wetted Area During Transition Boiling in Forced Convective Flow", J. Heat Transfer 101, pp. 381-383, (1979).

15. Ragheb, H.S., Cheng, S.C. and D.C. Groeneveld, "Measurement of Transition Boiling Boundaries in Forced Convective Flow", Int. J. of Heat and Mass Transfer, (1978).

16. Pramuk, F.S. and J.W. Westwater, "Effect of Agitation on the Critical Temperature Difference for a Boiling Liquid", Chem. Eng. Prog. Symp. Ser. 18, 52, 79 (1956).

17. Groeneveld, D.C., "Post-Dryout Heat Transfer at Reactor Operating Conditions", Invited paper, A.N.S. Topical Meeting on Water Reactor Safety, Salt Lake City (1973).

18. Dhir, V.K., "Study of Transient Transition Boiling Heat Fluxes from Spheres Subjected to Forced Vertical Flow". Paper presented at 6th International Heat Transfer Conference, Toronto, August (1978).

19. Yilmaz, S. and Westwater, J.W., "Effect of Velocity on Heat Transfer to Boiling Freon-113", J. of Heat Transfer, Vol. 102, February (1980).

20. Auracher, H. and Albrodt, H., "Temperature Controlled Measurement of Boiling Curves for Low Quality Upward Forced Flow in Tubes", 3rd Multi-Phase Flow and Heat Transfer Symposium-Workshop, Miami Beach, Florida, April (1983).

21. Nishikawa, K. and Shimomura, R. "Boiling Heat Transfer at the Coexistence of Nucleate and Film Regions", Trans. Japan Soc. Mech. Engrs., 29, No. 204 (1963). Translation NSJ-Tr-47.

22. Bradfield, W.S., "On the Effect of Subcooling on Wall Superheat in Pool Boiling", J. of Heat Transfer, 89, pp. 269-270, (1967).

23. Tachibana, F. and E. Shinataro, "Heat Transfer Problems in Quenching", Bulletin of JSME, 16, No. 91 (1973).

24. Johannsen, K. and Kleen, V., "Steady-State Measurement of Forced Convection Surface Boiling of Subcooled Water at and Beyond Maximum Heat Flux Via Indirect Joule Heating of a Test Section of High Thermal Conductance", 3rd Multiphase Flow and Heat Transfer Symposium-Workshop, Miami Beach, Florida, April (1983).

25. Veda, T., Tsunenari, S. and Koyanagi, M., "An Investigation of Critical Heat Flux and Surface Rewet in Flow Boiling Systems", Int. J. Heat Mass Transfer, Vol. 26, No. 8, pp. 1189 (1983).

26. De Bortoli, R.A., et al, "Forced-Convective Heat Transfer Burnout Studies of Water in Rectangular Channels and Round Tubes at Pressures above 500 psia", Westinghouse Electric Corp., Report WAPD-188, October (1958).

27. Berenson, R.J., "Experiments on Pool-Boiling Heat Transfer", Int. J. Heat Mass Transfer, Vol. 5, pp. 985-999 (1962).

28. Henry, R.E., "A Correlation for the Minimum Film Boiling Temperature", AICHE Symposium Series, No. 138, Vol. 70, pp. 81-90 (1974).

29. Abuntsov, D.A., et al, "Critical Heat Fluxes in Boiling at Low Pressure Region", 6th International Heat Transfer Conference, Toronto, August (1978).

30. Sakurai, A. and Shiotsu, M., "Temperature Controlled Pool-boiling Heat Transfer", Proc. Heat Transfer Conf., Vol. 4, pp. 81-85 (1974).

31. Salehpour, A. and Yao, S.C., "Thermal Hystersis of Forced Convective Boiling", Int. J. Multiphase Flow, Vol. 9, No. 1, pp. 97-100 (1983).

32. Coffield, R.D., "A Subcooled DNB Investigation of Freon-113 and its Similarity to Subcooled Water Data", Ph.D. Thesis, University of Pittsburgh (1969).

33. Markles, M. and Durfee, R.L., "The Effect of Applied Voltage on Boiling Heat Transfer", AI Che J, 10(1), 106-109 (1964).

POOR PRINT
Epreuve illisible

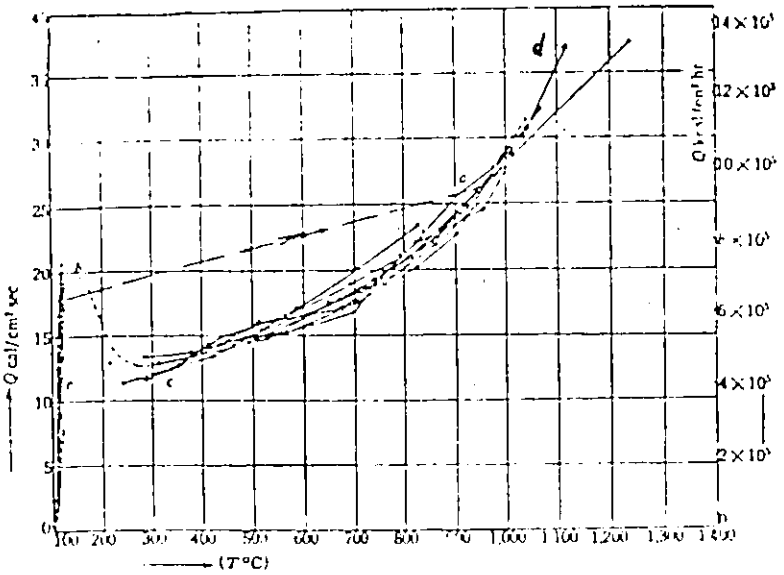

Fig.2.1 The Boiling Curve of Nukiyama [1]

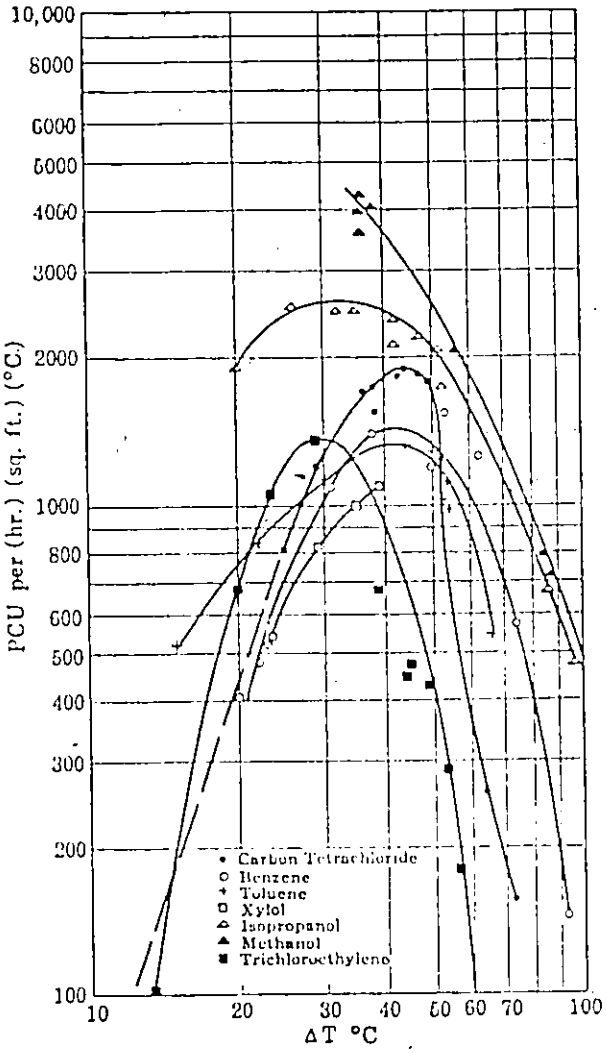

Experimental Data in the Transition region reported by Drew and Mueller [2].

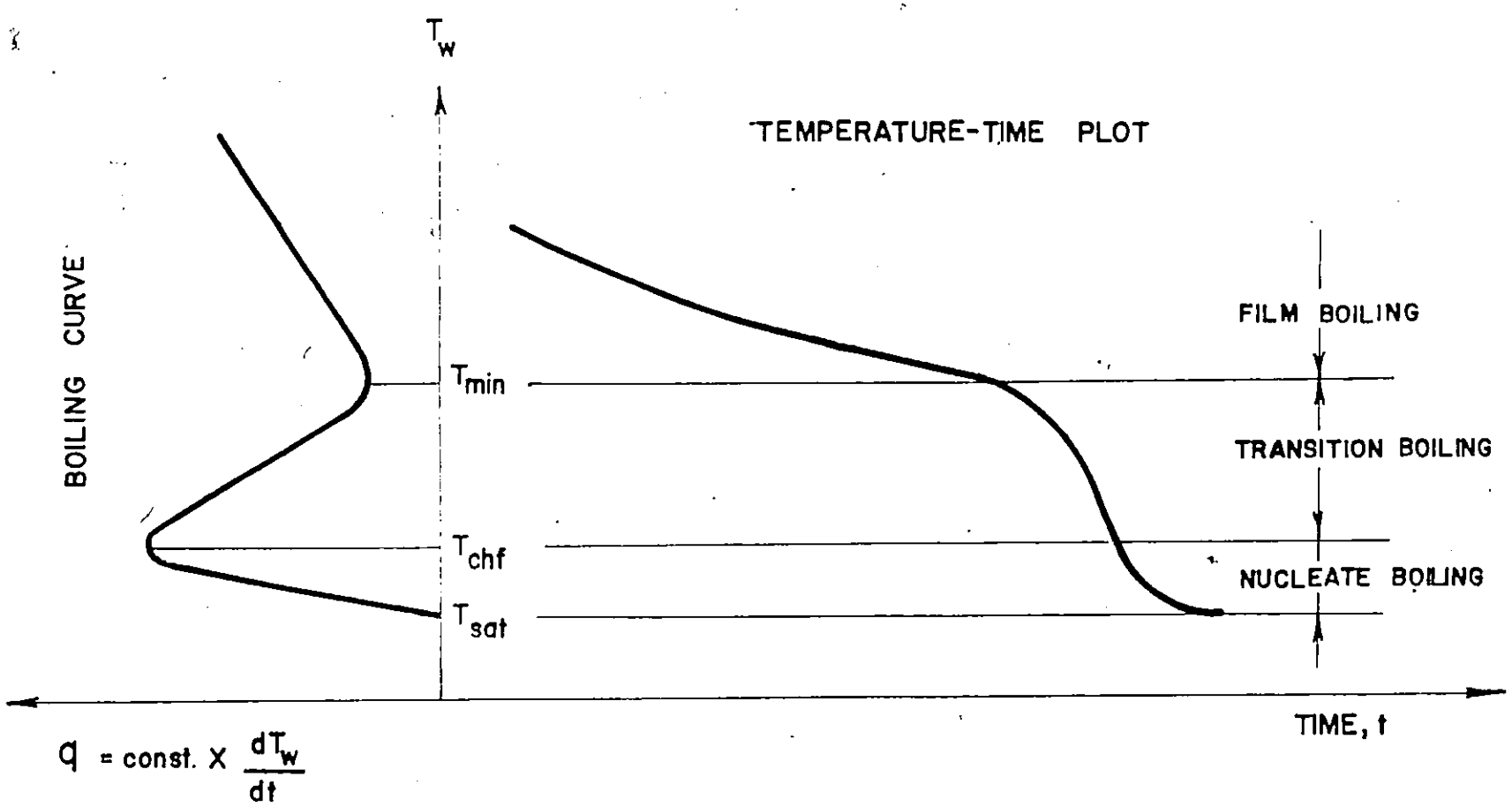

FIG. 2.3 DERIVATION OF BOILING CURVE FROM TEMPERATURE-TIME PLOT

POOR PRINT
Epreuve illisible

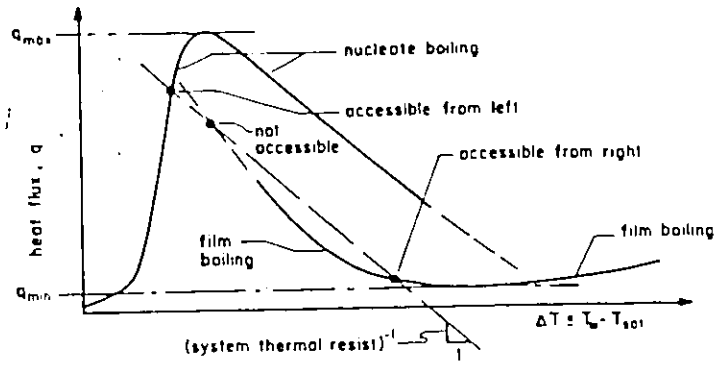

Fig. 2.4 The Two Boiling Curves
(Witte and Lienhard 1982)

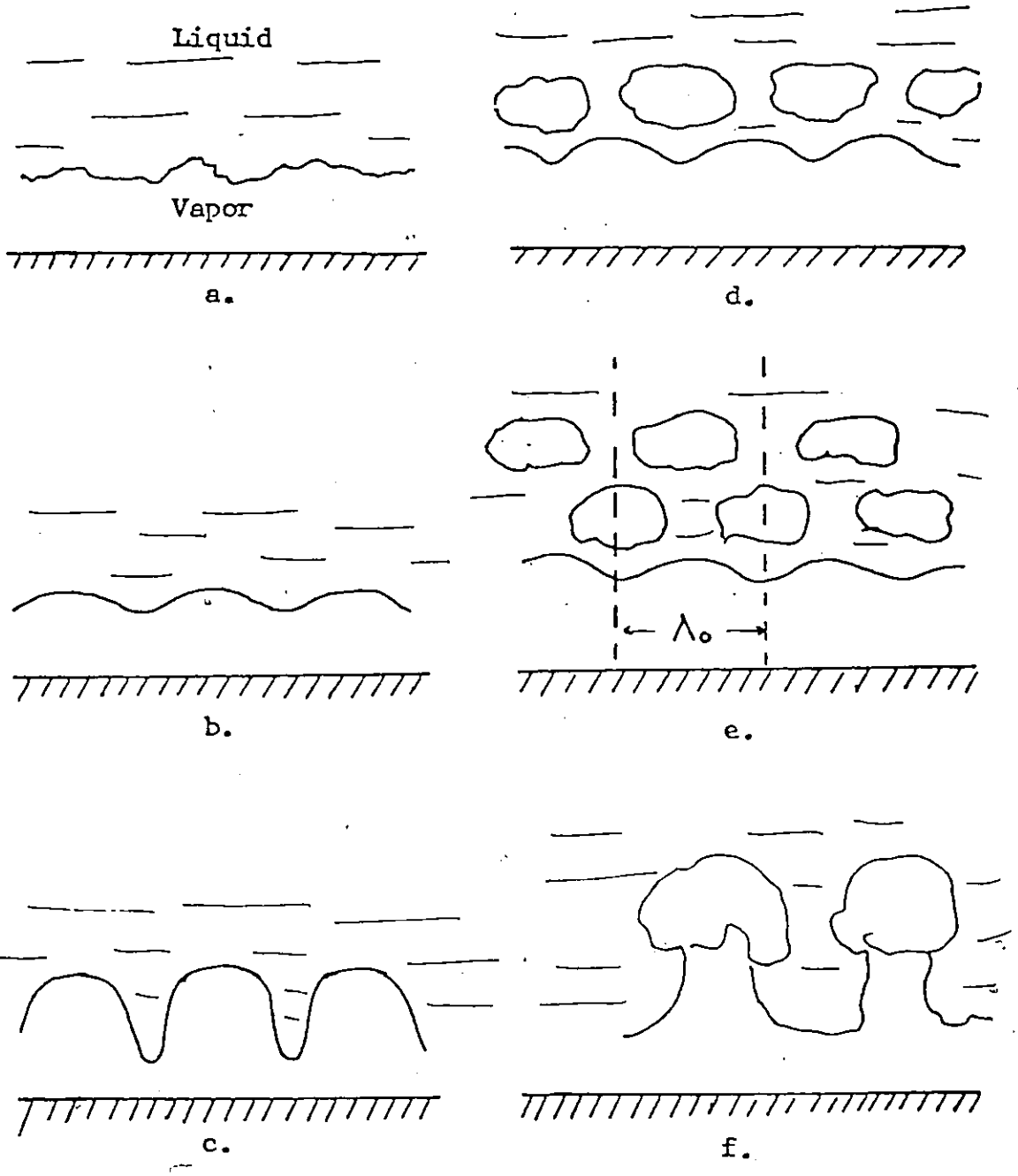

Fig. 2.5 Mechanisms of Transition in Pool boiling
(Zuber 1958)

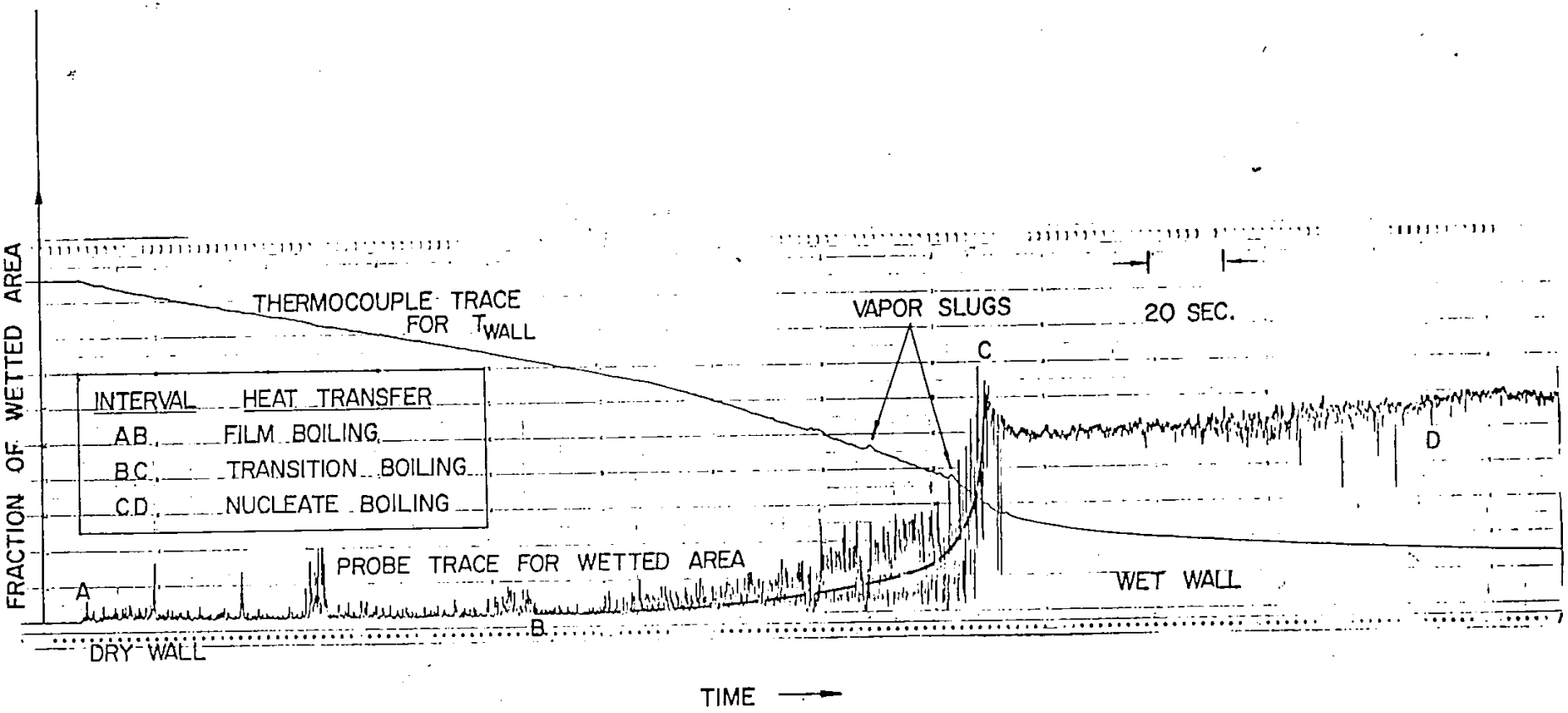

Fig. 2.6 Surface Wetted Area During Transition Boiling

POOR PRINT
Epreuve illisible

POOR PRINT
Epreuve illisible

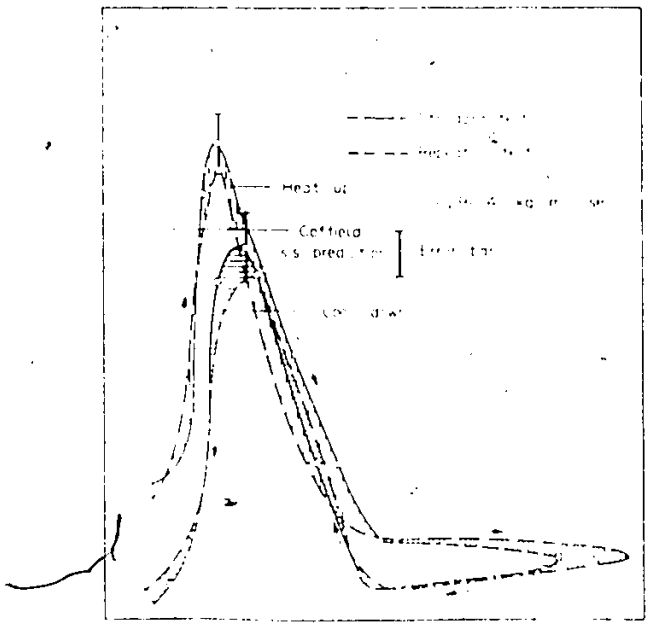

Fig. 2.7 Effect of Hysteresis on Boiling Curves
(Salehpour and Yao 1983)

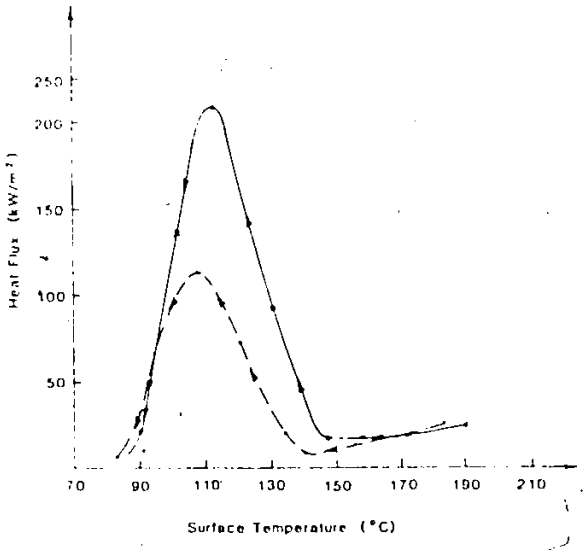

Fig. 2.8 Effect of Quenching Mechanism on the Boiling Curve
(Salehpour and Yao 1983)

POOR PRINT
Epreuve illisible

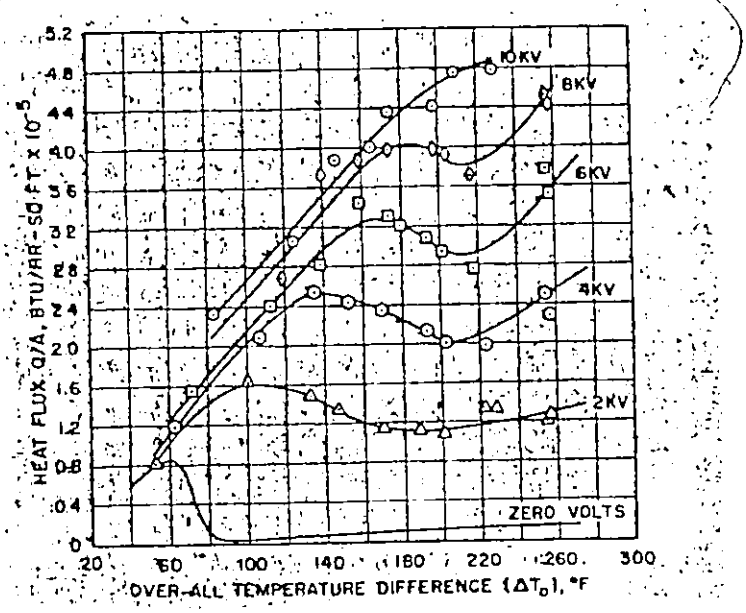

Fig. 2.9 Effect of Applied d.c. Voltage on Heat Transfer to Isopropanol

(Markles and Durfee 1964)

POOR PRINT
Epreuve illisible

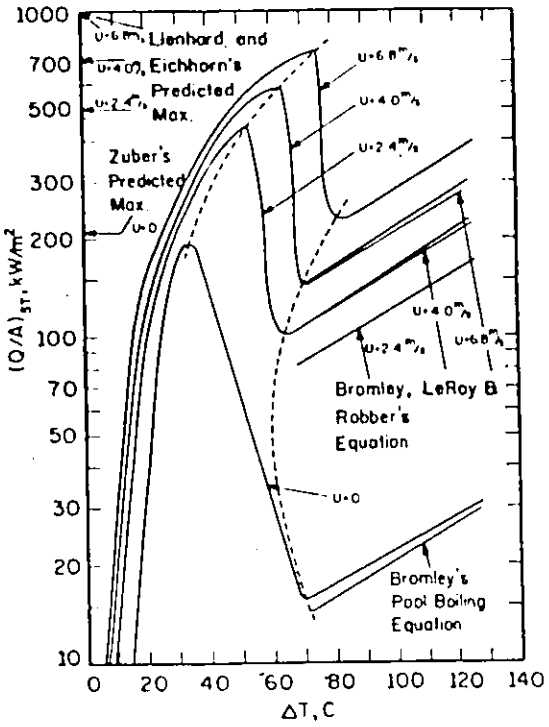

Fig. 2.10 Effect of Flow Velocity on Boiling Curves (Yilmaz and Westwater 1980)

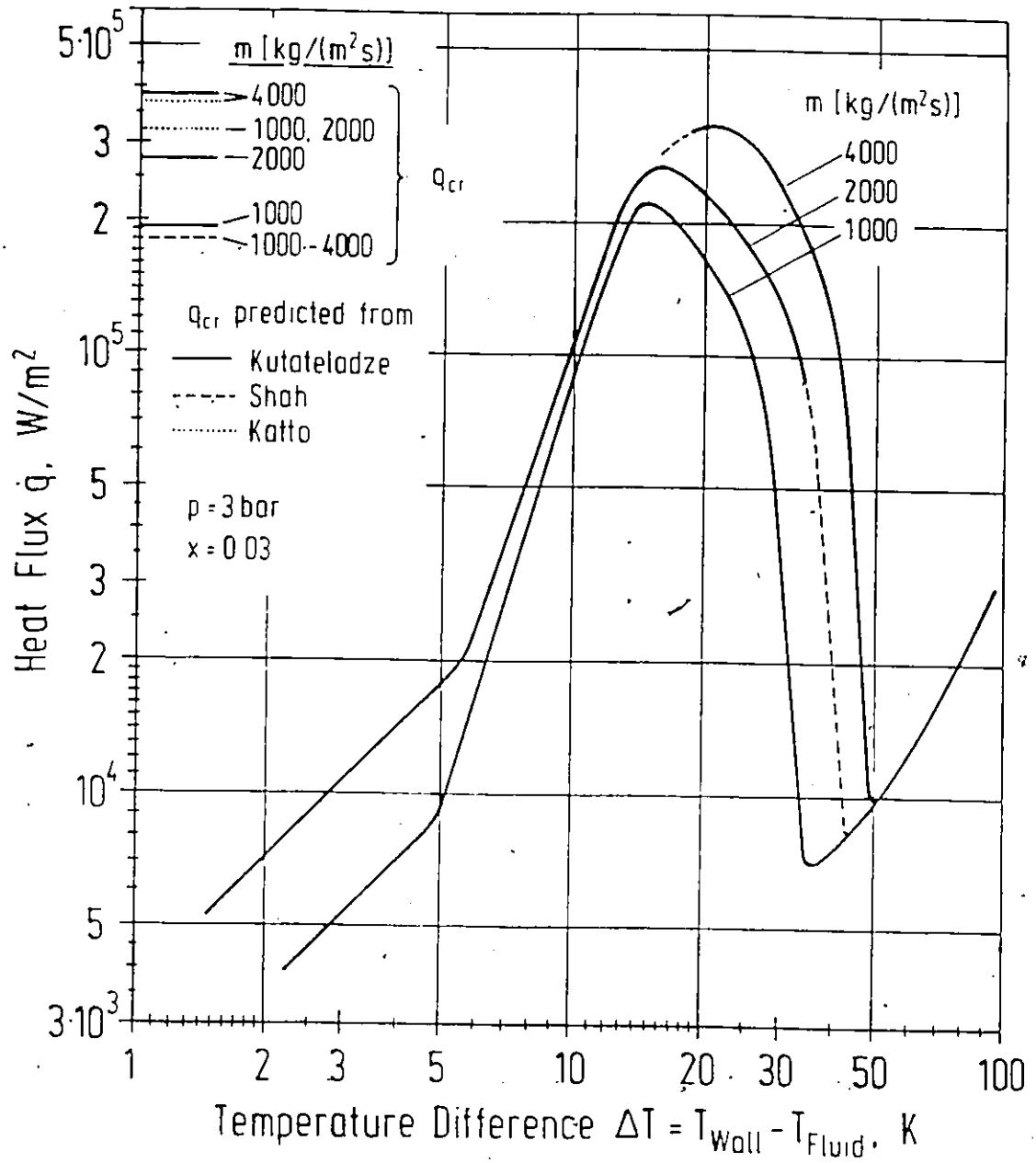

Fig. 2.11 Effect of Mass Flux on Boiling Curves of Freon-114
(Auracher and Albrodt 1983)

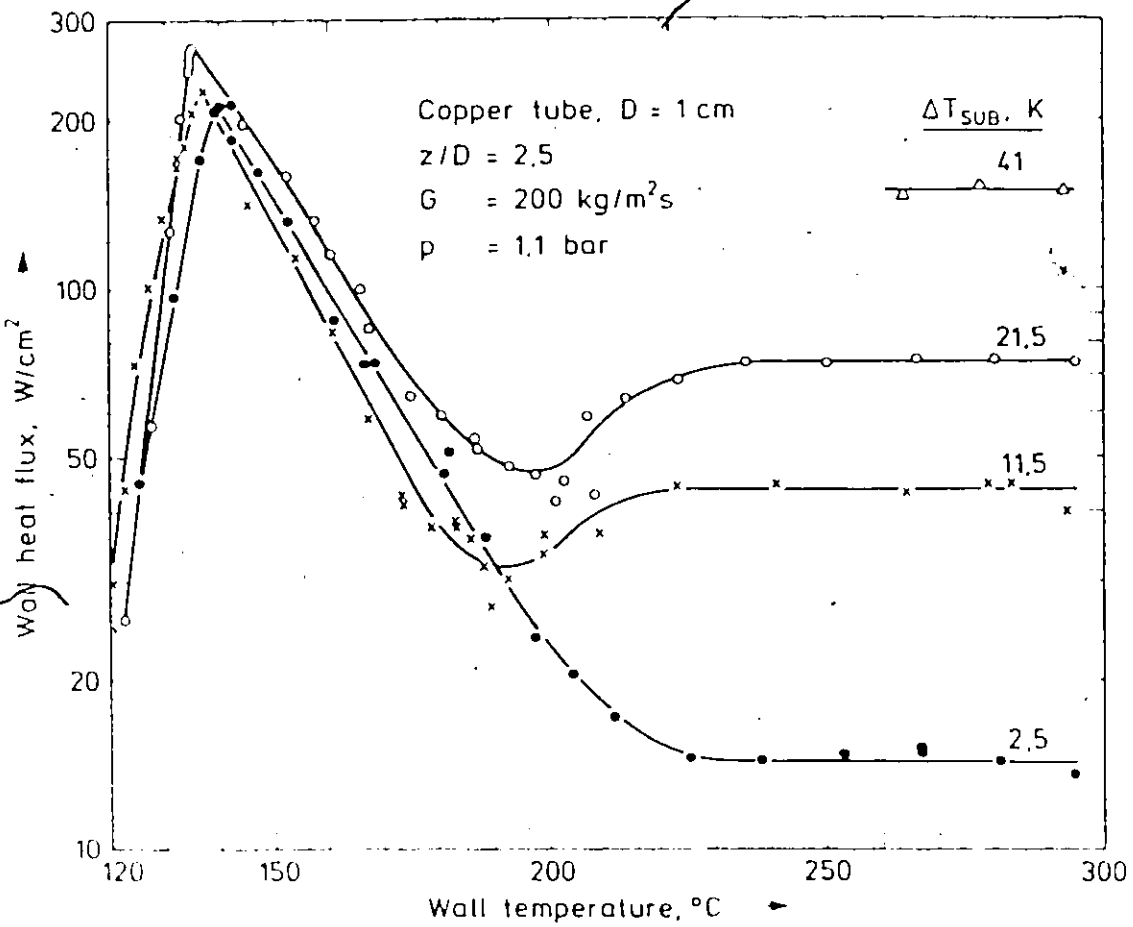

Fig. 2.12 Effect of Inlet Subcooling on Flow Boiling Curves of Water

(Johannsen and Kleen 1983)

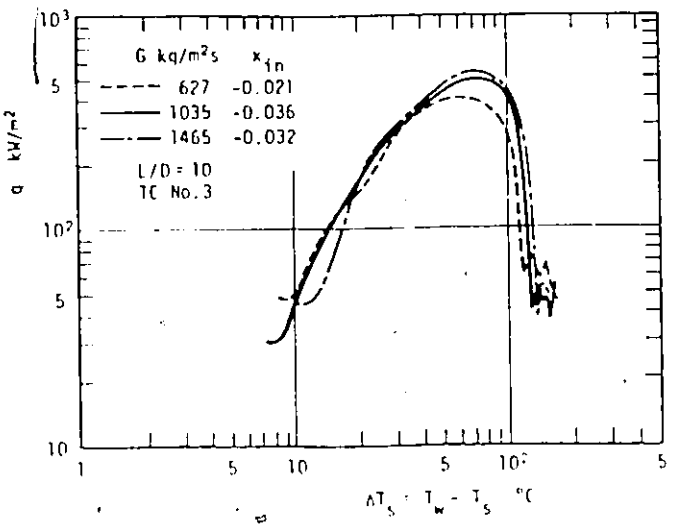

Fig. 2.13 Effect of Subcooling on Boiling Curves (Vera et al. 1983)

CHAPTER 3

EXPERIMENTS

3.1 Experimental Apparatus

The experimental apparatus consists primarily of a hot water storage tank, a flow meter, a pump and a test section assembly as shown in Fig. 3.1. Piping of the whole set-up is 1/2" copper pipe which is joined by soldering. Provisions of bypassing the pump and the test section assembly were incorporated to stabilize the flow. The flow rate was measured by a rotameter and the flow adjustment was done via the flow control valve 1. Valves 2 and 3 are ON-OFF valves which operate out-of-phase, i.e. valve 2 open and valve 3 closed or vice versa. Thermocouples I, II and III were installed to measure temperatures of the flow, the inlet, and the outlet of the entrance heater and the exit temperature of the test section, respectively.

A supply of Nitrogen is also included in the experimental apparatus. It serves the purpose of purging the centre passage to prevent oxidation at high temperatures.

The storage tank, which has a capacity of about 50 gallons of distilled water, is powered by three immersion heaters of 3 kW rating each. Temperature sensors are placed at strategic points so that the temperature of water can be measured with average value as the bulk

fluid temperature. A stirrer is also incorporated to ensure good mixing for the same reason. The heaters draw current via a thermostat which can be adjusted to the desired operating temperature.

3.2 Test Sections

Different types of test sections were employed and are shown in Fig. 3.2. The test sections basically consist of a high thermal inertia cylindrical block with or without a flow tube located along the centre line. The block is heated by cartridge heaters located in a concentric ring at some distances from the centre of the flow channel. Temperature measurements were taken at different axial planes within the test section using metal sheathed thermocouples located radially approximately 1.5 mm from the heated surface. A detailed description of the different types of test sections is given below.

3.2.1 Type I Test Section

The simplest version of test section used in the experiments is Type I test section consisting of a short cylindrical copper or brass block, heated by cartridge heaters. Physical dimensions of the test section and thermocouple locations are given in Fig. 3.3. It consists of a 5.72 cm long copper cylinder with a 9.53 cm outside diameter and a 1.27 cm diameter central flow channel. The location of the seven thermocouples and the twelve cartridge heaters are also shown. T.C's A3, B3 and C3 were used for data thermocouples.

3.2.2 Type II Test Section

Type II test section employed a combination of two copper blocks; a short block and a long block. In one series of experiments the short block was utilized as the test section while the long block remained unheated. In other series, the long block was used as the test section with the short block as an entrance heater.

The test assembly as shown in Fig. 3.4 consists of a long copper block test section and a short copper block which acts as an entrance heater to establish the required flow conditions and minimize heat losses. The short copper block is a type I test section. The long copper block test section is similar to the short copper block and is illustrated in Fig. 3.5, where T.C's A1, B1 and C1 were used for data thermocouples. Axial heat losses of the test section assembly were reduced by using asbestos gasket and asbestos spacer at the inlet and outlet of the two blocks as shown in Fig. 3.4. Heat losses from the outer surface of the test section assembly were minimized by lagging the two blocks with a 5 cm thick ceramic fiber insulation.

3.2.3 Type III Test Section

The Type III test section was designed to study the effect of heated surface thermal proporties on transition boiling, by brazing the material under investigation (e.g. Inconel) into the copper block using silver solder. The thermal properties of the different surfaces studied are given in Table 3.1.

A typical composite test section, as shown in Fig. 3.6, consists of a 5.08 cm long cylindrical copper block with 9.53 cm outside diameter and a center bore of 1.296 cm allowing for the insertion of an Inconel tube. The Inconel tube with O.D. = 1.27 cm and thickness = 0.038 cm is inserted into the copper block, with a gap of 0.013 cm between them provided for before silver soldering. The Inconel tube is sticking out from both ends of test section for piping connections. Cartridge heaters are spaced around the test section and a total of six thermocouples are embedded. Five of them -- located in the interface of the tube and silver solder -- are to be used for data thermocouples (T.C. 2.2, T.C. 2.3 ... T.C. 2.6).

3.2.4 Type IV Test Section

Because of problems in brazing a Zircaloy tube or an aluminum tube to copper a Type IV test section was designed in which Wood's metal (a liquid metal) was used instead to provide good thermal contact between the two materials. The schematic diagram for the test section is shown in Fig. 3.7. To ensure that no air is trapped when filling the gap, three evenly spaced vents were drilled at the bottom of the test section to allow the air to escape. These vents were plugged during the tests. At the top of the test section, a recess containing an excess quantity of Wood's metal was provided to compensate for any possible leak of Wood's metal. A cylindrical enclosure was placed on the top of test section with argon gas blown inside to minimize oxidation on the surface of Wood's metal in the recess during the experiments.

3.3. Instrumentation

The flow rate is measured by a rotameter (series 20-4000, S&K Instruments) and the flow adjustment is done via the regulatory needle valve 1.

Power supplied to the cartridge heaters is regulated by a Silicon Controlled Rectifier driver stage. Current indicator consists of a current transformer, an A.C. transmitter and a strip chart recorder. The D.C. level from the output stage is displayed on the strip chart recorder.

3.4 Procedure

Two modes of operation are used; the transient and the steady state methods.

3.4.1 Transient Method

(i) Water in the storage tank is first heated to the desired test temperature by immersion heaters which are thermostatically controlled. By means of a stirrer for mixing and a thermocouple to measure the tank temperature, the approximate initial desired value is obtained.

(ii) The pump is turned on for circulation and adjustment of flow via regulatory needle valve 1. The flow is passed through ON-OFF

valve 2 (valve 3 closed) and is drained back to the storage tank utilizing the second by-pass loop. This serves the purpose of stabilizing the flow and the system temperature.

(iii) Nitrogen is introduced into the test section assembly while both the test section and the entrance heater are heated up to set point values on temperature controllers.

(iv) At the start of the quenching test run, nitrogen supply is turned off then valve 2 is switched to OFF position and the flow is diverted to the test section assembly by opening valve 3.

(v) All the cartridge heaters in the test section are switched OFF prior to the start of passing the flow into the test section assembly. The temperature of the guarded heater is maintained at the constant set point value by the temperature controller throughout a given run. Instrumentations such as chart recorders are all ready and running at the beginning of every test run.

3.4.2 Steady-State Method

The experimental procedures for the steady-state method are very similar to those of the transient method except the following:

(i) Temperature of the test section is initially set well into the film boiling region and is maintained at that level by the temperature controller during an experimental run. Power measurement is required which in turn gives the heat flux.

(ii) Repeat the experiment run for lower temperature points until a complete boiling curve is obtained. It has been decided, prior to the run, that settings on the temperature controller start from higher values to lower ones in favour of better improvement of temperature stabilization.

3.5 Experimental Runs

A total of 24 series of experiments were run throughout this study, series 100 to 2400. In this thesis only the experimental runs representative of a test section type or a surface material will be presented. All experiments covered the range of mass flux from 68 to 203 $kg.m^{-2}.s^{-1}$ and subcooling 0°C to 27°C.

3.5.1 Series 500 (Type I test section)

This series was run using Type I test section; the boiling curves produced by these runs are those for a copper surface.

3.5.2 Series 400 (Type II test section)

Two copper blocks were used in this series. The long block was used as the test section while the short block was used as an entrance heater.

3.5.3 Series 1500 (Type III test section)

This is the first series run using an Inconel tube silver soldered to the copper block. Five thermocouples were located along the flow pass to facilitate the 2-D analysis. The boiling curves produced by this series are those for an Inconel surface.

3.5.4 Series 2100 to 2500 (Type IV test section)

Four different surface materials were used in these runs. Table 3.2 gives the tubing dimensions for each material used. Note that in series 2400 and 2500 Inconel and copper were used so that a comparison with other surfate materials tested in Type IV test section can be made.

3.5.5 Series 2700 (Type III test section)

Due to the solder contact resistance found in Type IV test section, a new material such as brass which can be soldered to copper (Type IV test section) was used to investigate the effect of thermal properties on boiling curve.

3.5.6 Series 2800 (Type I test section)

This series was run using Type I test section similar to the one used in series 500 but made of brass.

TABLE 3.1: Thermal Properties of Heated Surfaces and Solders at 20°C

Heated Surface	k (W/m°C)	ρ (kg/m^3)	c_p (J/kg°C)
Copper	379	8938	385
Inconel	17	8169	435
Zircaloy	15	6549	316
Aluminum	229	2707	896
Brass (70% cu, 30% Zn)	144	8522	385
Solder			
Silver solder	50	8938*	385*
Wood's metal	25**	9134	145**

*, Assuming the property of copper
** Approximate value

TABLE 3.2: Type IV Test Section Flow Tube Dimensions

Run Series	Tubing Material	Tubing Dimensions
2100	Zircaloy	OD = 1.31 cm, = 0.0559 cm
2300	Aluminum	OD = 1.40 cm, = 0.0635 cm
2400	Inconel	OD = 1.27 cm, = 0.038 cm
2500	Copper	OD = 1.27 cm, = 0.038 cm

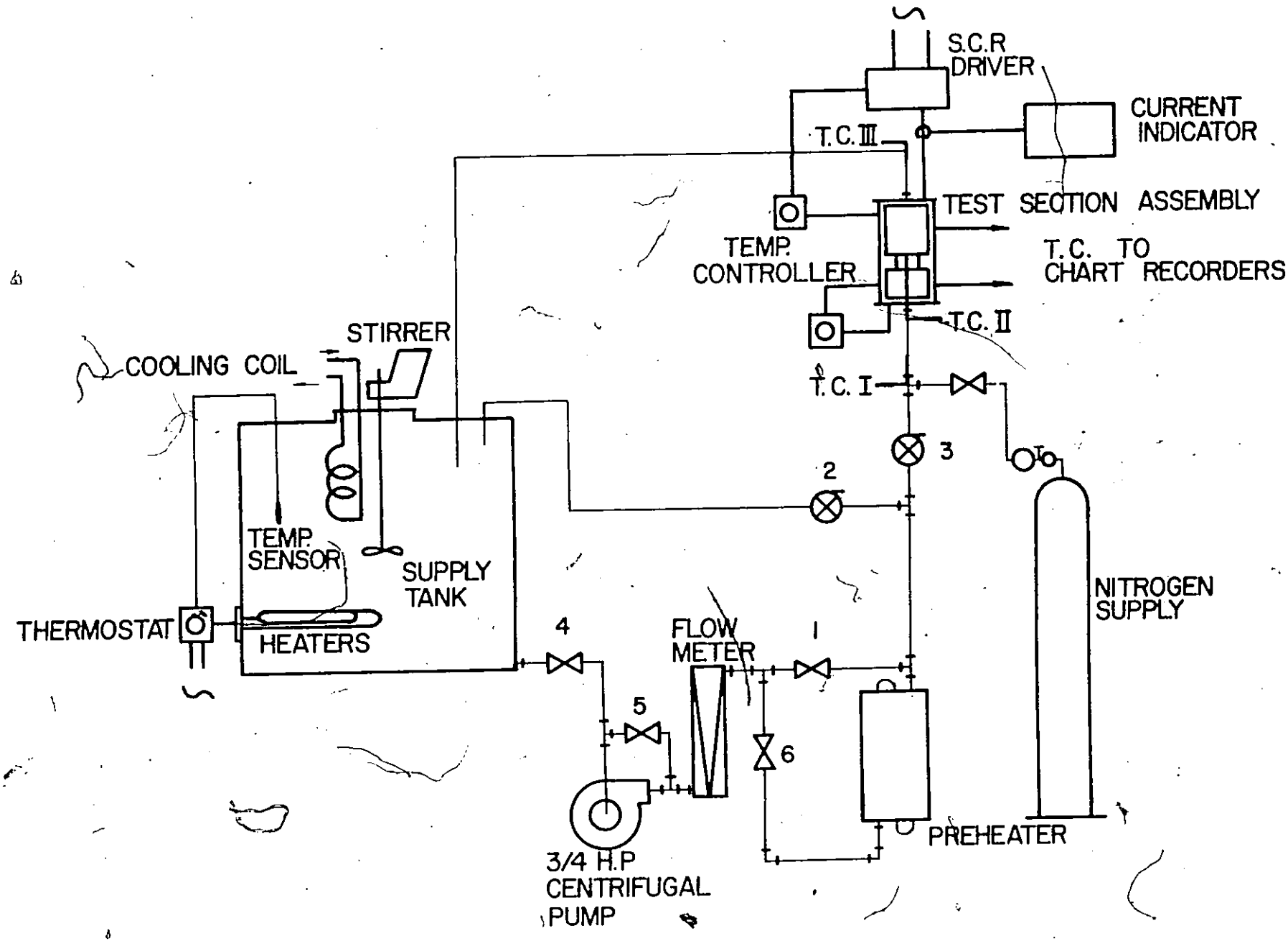

FIG. 3.1 SCHEMATIC DIAGRAM FOR THE EXPERIMENTAL LOOP

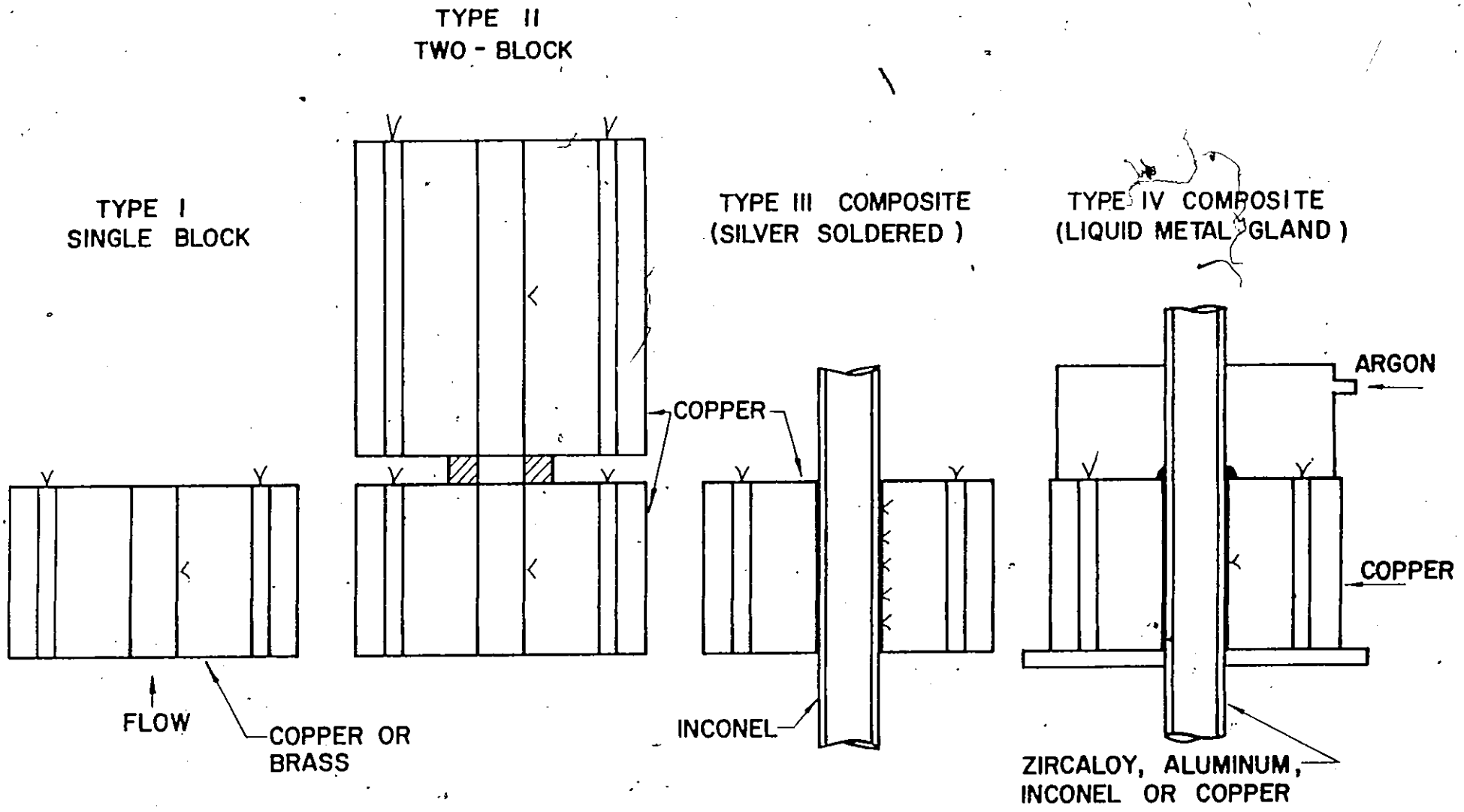

FIG. 3.2 TEST SECTION DESIGNS FOR TRANSITION BOILING STUDY

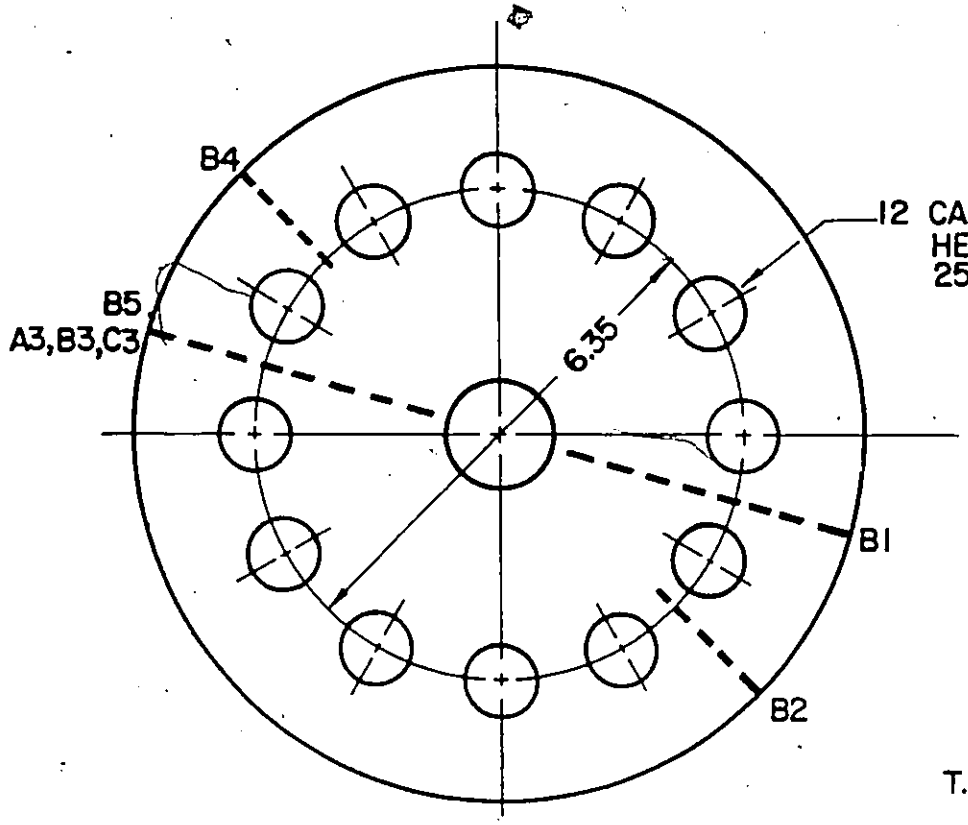

T.C. NO.	DIST. FROM INNER WALL
*A3	0.168
B1	0.462
B2	2.205
B3	0.175
B4	2.263
B5	ON THE OUTER WALL
C3	0.124

*A DESIGNATES PLANE A

ALL DIMENSIONS IN cm

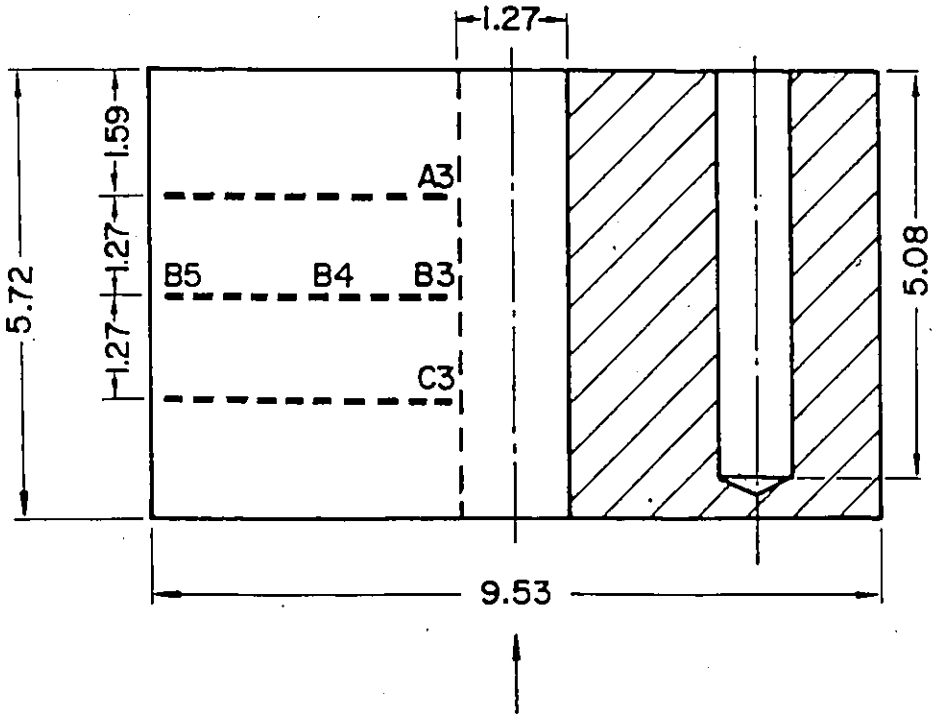

FIG. 3.3 TYPE I TEST SECTION

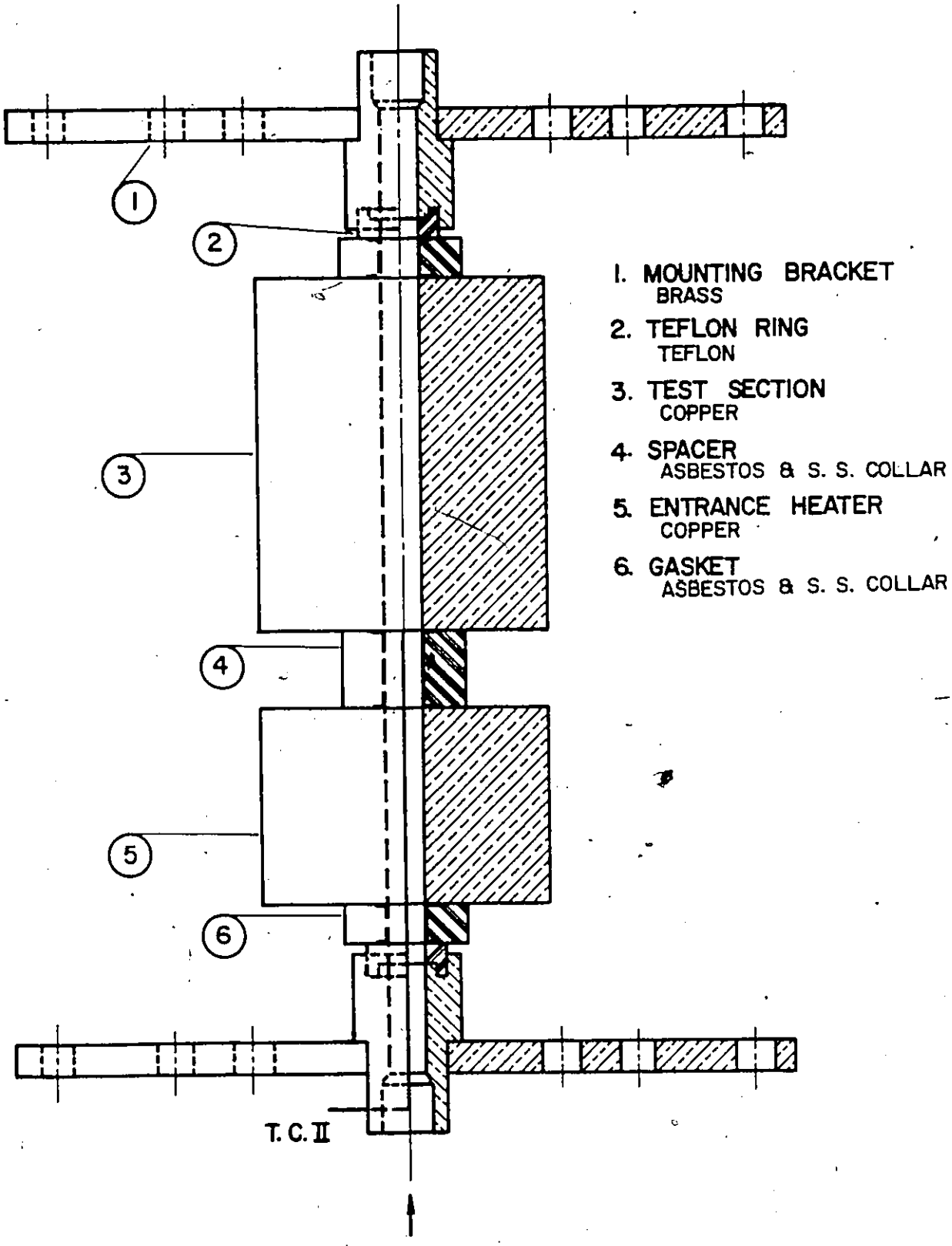

FIG. 3.4 TYPE II TEST SECTION

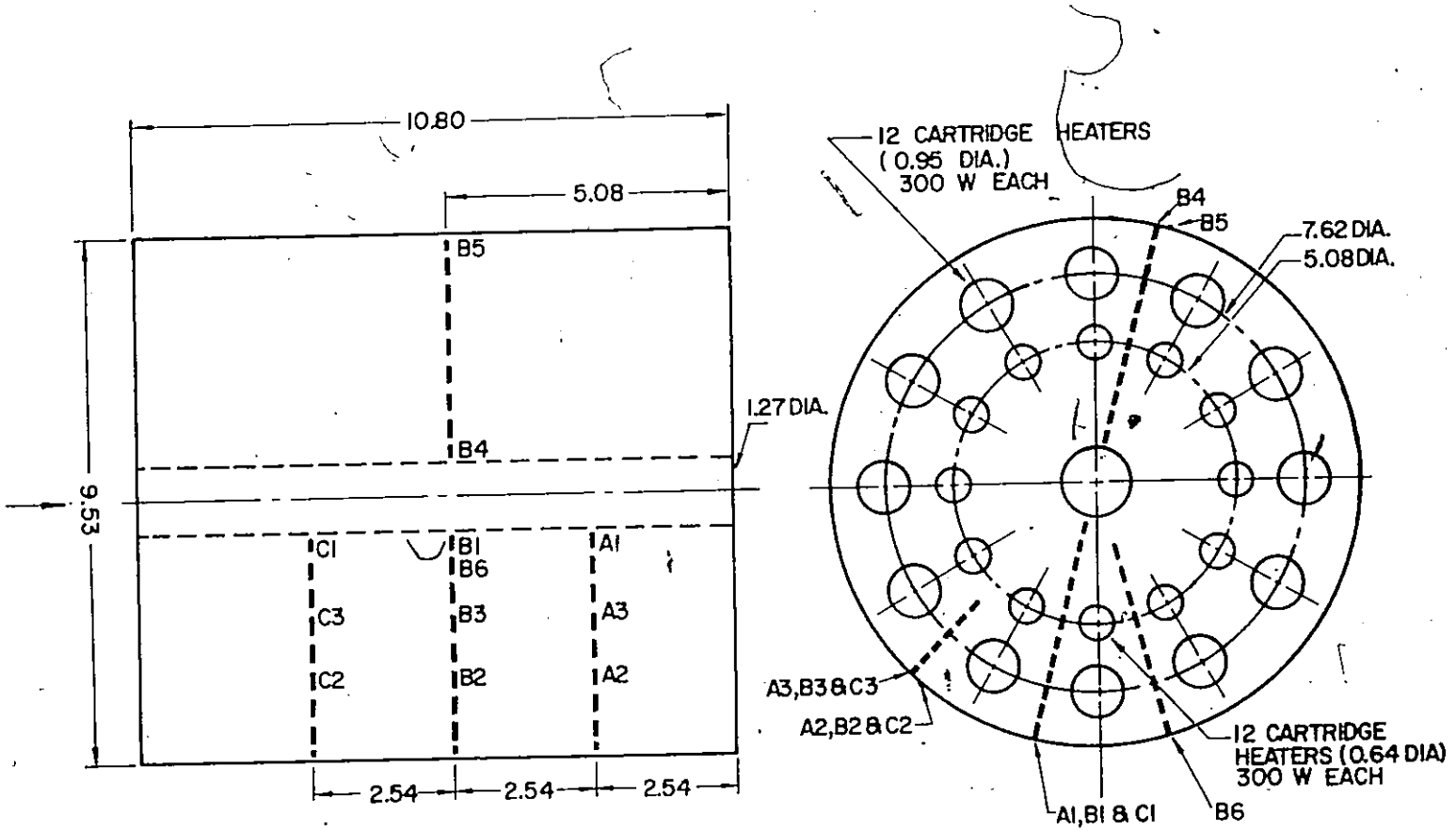

T.C. NO	DIST. FROM INNER WALL
A1	0.105
B1	0.090
B3	2.426
B5	ON THE OUTER WALL
C1	0.079

FIG. 3.5 LONG BLOCK OF TYPE II TEST SECTION

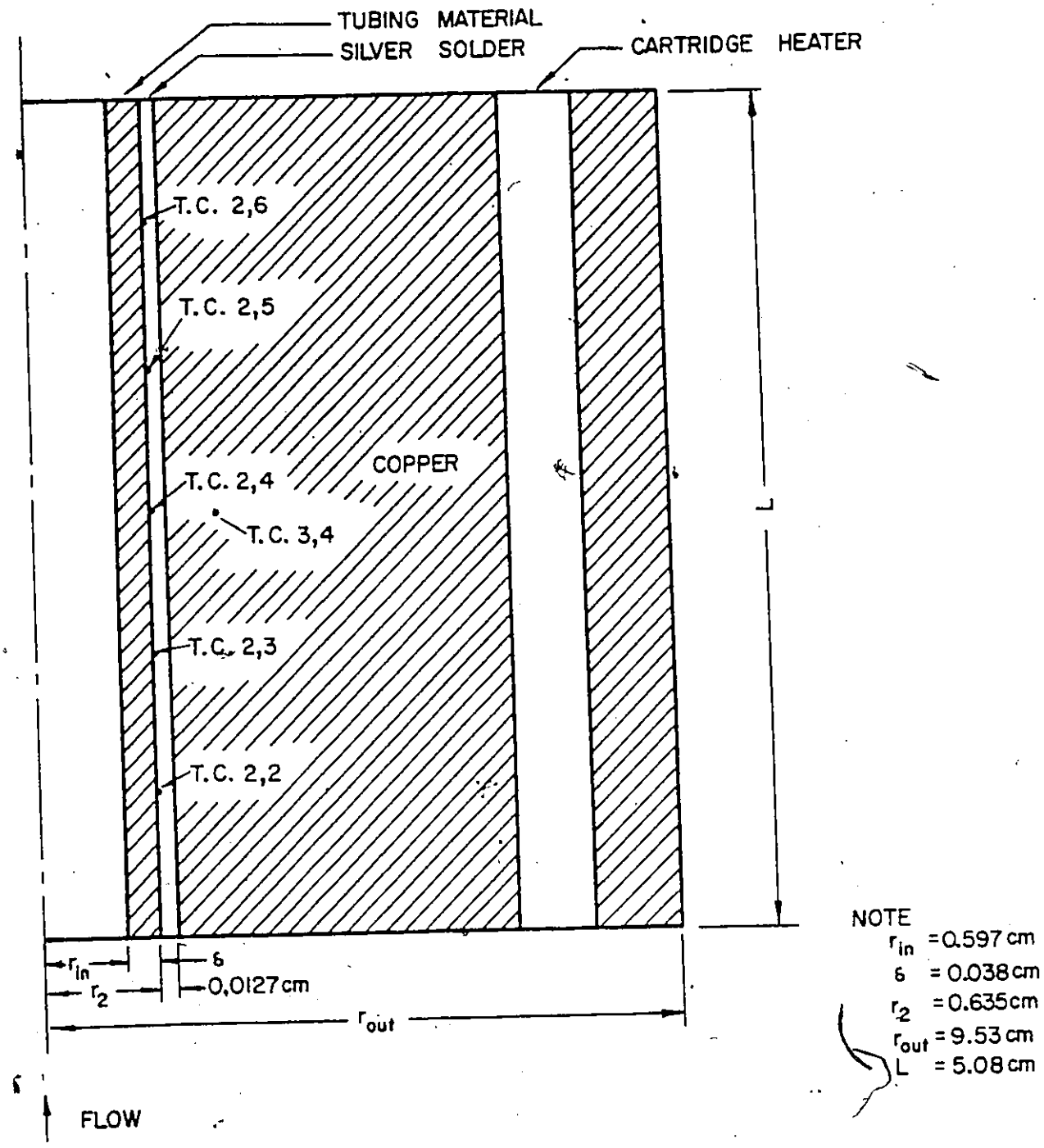

FIG. 3.6 TYPE III TEST SECTION

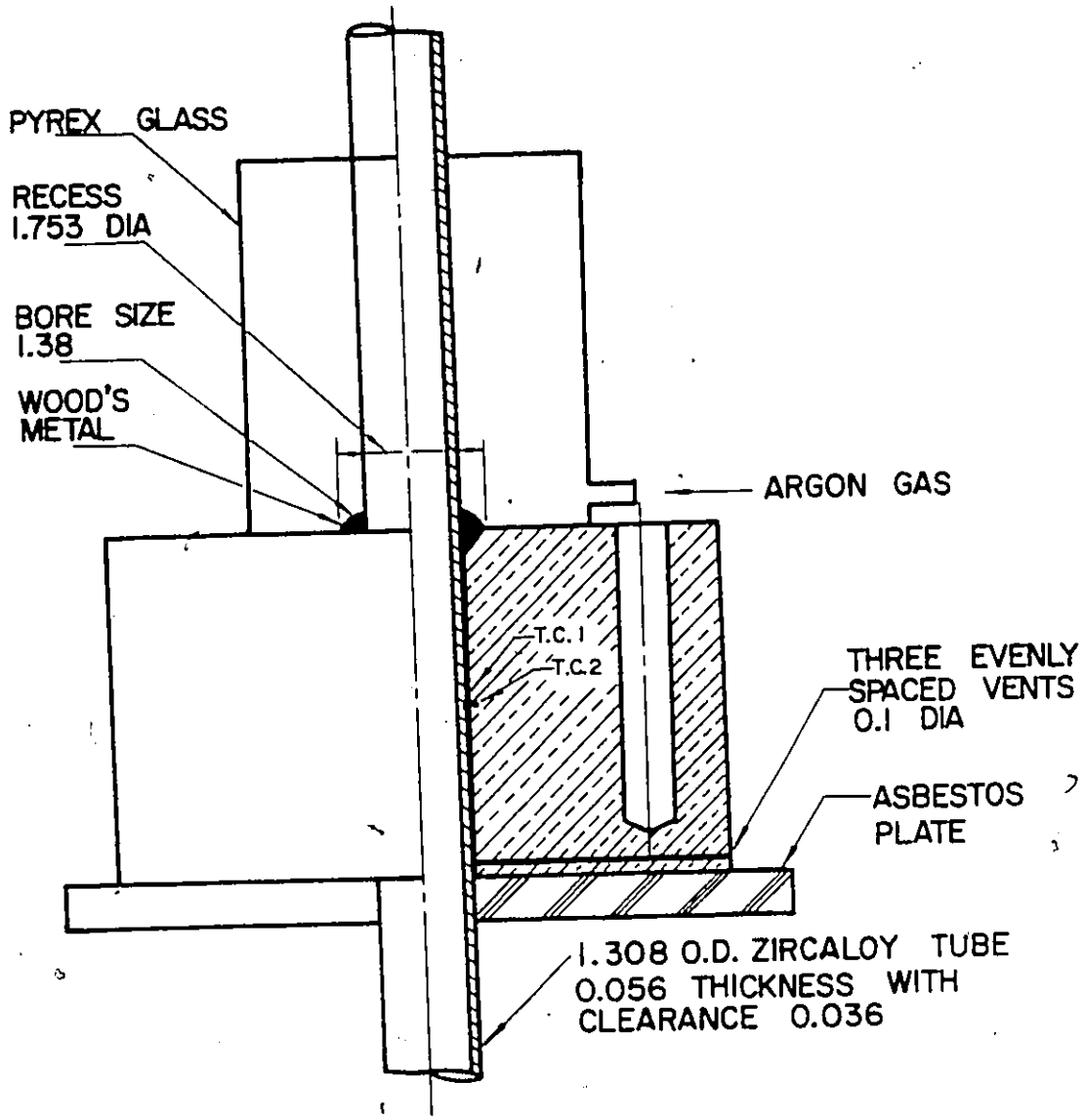

FIG.3.7 TYPE IV TEST SECTION (ZIRCALOY-COPPER)

CHAPTER 4

METHODS OF ANALYSIS

4.1 General

In order to obtain the boiling curves (heat flux-vs. wall temperature) from the temperature history as recorded from a thermocouple located near the wall, one has to solve the so-called inverse heat transfer problem. The inverse problem is one for which internal boundary conditions are described and the desired quantity is a surface condition (heat flux or wall temperature). This type of problem could be solved using the method of Burggraf[1], who obtained an exact solution in the form of rapidly convergent series. This solution involves the determination of third order derivative of T_o.

In this thesis, the mathematical models and computational techniques developed by Cheng, et al[2,3], are used to construct boiling curves. In general, these methods involve the calculation of heat flux by solving the Fourier transient equation and using the concept of rate of change of heat content within the test section.

4.2 One-Dimensional Conduction Models (1-D models)

The following methods were used when applying the 1-D models:

(a) Fourier equation method - The temperature profile across the test section is obtained through a solution of the Fourier conduction equation, assuming that the inner wall temperature equals the measured temperature at the location of data thermocouple (usually located within 1.5 mm of the inner surface).

(b) Refined Fourier equation method - This is similar to (a) except that the inner wall temperature is calculated by extrapolating the temperature distribution between the location of the data thermocouple and the outer wall, assuming perfect insulation at the outer surface of the test section.

(c) h-method - The heat loss through the outer wall is found from heat loss calibration runs and is included as a heat transfer coefficient h at the outer surface of the test section.

(d) Two-point method - The temperature recording at the outer surface is used as a boundary condition instead of h.

In the sections to follow, a detailed description is given for methods (c) and (d).

4.2.1 h method

Heat transfer from the test section to the fluid between time 0 to t is assumed equal to the change in heat content Q inside the cylinder minus heat loss through the outer wall during the same time interval. Q can be expressed as:

$$Q(t) = \rho c_p L \int_{r_{in}}^{r_{out}} 2\pi r T dr \qquad (4.1)$$

where L represents the length of the test section. The function T(r,t) is obtained as the solution to the one-dimensional Fourier equation in cylindrical coordinates:

$$\frac{\partial T}{\partial t} = \alpha \left(\frac{\partial^2 T}{\partial r^2} + \frac{1}{r} \frac{\partial T}{\partial r} \right) \qquad (4.2)$$

and is subject to the following initial and boundary conditions:

(1) $T = T(r,o)$ ... In general, at $t = 0$ the temperature across the test section is linear with about 4°C difference for our initial temperature condition. (4.3)

(2) $T(r_o,t) = T_o$ ... r_o and T_o are the location and recordings of the thermocouple, respectively (e.g., location B3 in Figure 3.3). (4.4)

(3) $$-k\left(\frac{\partial T}{\partial r}\right)_{r=r_{out}} = h(T_n - T_{amb})$$ ... h is the heat transfer coefficient at the outer wall and its determination will be explained later. (4.5)

The solution of Equation (4.2) can be obtained by reducing it to a system of linear first-order difference equations in t. This is achieved by discretizing along the r-direction (Fig. 4.1) using the approximation:

$$\frac{\partial T}{\partial r} = \frac{T_{i+1}(t) - T_{i-1}(t)}{2\Delta r} \tag{4.6}$$

and

$$\frac{\partial^2 T}{\partial r^2} = \frac{T_{i-1}(t) - 2T_i(t) + T_{i+1}(t)}{(\Delta r)^2} \tag{4.7}$$

where $T_i(t)$ represents the temperature at the ith nodal point. $(1 \leq i \leq n+1)$ and $\Delta r = \left[r_{out} - (r_{in} + r_o)\right]/n$

Using (4.6) and (4.7) along with initial and boundary conditions, the following system of equations can be inferred from (4.2).

$$\frac{dT_i}{dt} = \alpha \frac{T_{i-1} - 2T_i + T_{i+1}}{(\Delta r)^2} + \frac{\alpha}{r_i}\left(\frac{T_{i+1} - T_{i-1}}{2\Delta r}\right) \tag{4.8}$$

$$1 \leq i \leq n$$

where $r_i = r_{in} + \Delta r_o + i\Delta r$

and $$-\frac{k}{2}\left(\frac{T_i - T_{i-1}}{\Delta r} + \frac{T_{i+1} - T_i}{\Delta r}\right) = h(T_i - T_{amb}) \quad i = n \tag{4.9}$$

(4.7) is a direct consequence of (4.5). Furthermore, T_{n+1} in (4.8) can be eliminated by using (4.9).

(4.8) contains a system of n equations with n unknowns in T_i and are readily to be solved. Once T_1 up to T_n are solved and dT_o/dt determined experimentally, the inner wall temperature T_{-1} can then be calculated in the following Fourier equation based on the nodal point $i = 0$.

$$\frac{dT_o}{dt} = \alpha\left[\frac{\frac{T_1 - T_o}{\Delta r} - \frac{T_o - T_1}{\Delta r_o}}{\frac{1}{2}(\Delta r + \Delta r_o)}\right] + \frac{\alpha}{r_o}\left(\frac{T_1 - T_{-1}}{\Delta r + \Delta r_o}\right) \tag{4.10}$$

Equation (4.1) expressed in terms of summation, becomes

$$Q = 2\pi\rho\, c_p L\left[0.5T_{-1}\, r_{in}\, \Delta r_o + 0.5\, T_o(r_{in} + \Delta r_o)\, \Delta r_o + 0.5\, T_o(r_{in} + \Delta r_o)\, \Delta r + \left(\sum_{j=1}^{n-1} T_j r_j + 0.5\, T_n r_n\right)\Delta r\right] \tag{4.11}$$

The expression of net heat transfer to the fluid q in terms of Q and heat loss is:

$$q = \frac{-dQ}{dt}/A_{in} - hA_{out}\,(T_n - T_{amb})\,/A_{in}$$

$$= -\frac{1}{2\pi r_{in} L}\frac{dQ}{dt} - \frac{hr_{out}}{r_{in}}(T_n - T_{amb}) \tag{4.12}$$

where A_{in} and A_{out} represent the inner and the outer test section area, respectively.

The heat transfer coefficient h at the outer wall is determined experimentally under a no-flow condition. Its value stays nearly constant at 34 $W/m^2°C$ for most of the operating temperature range except at the lower temperature range where it drops to 22.7 $W/m^2°C$. For simplicity, a constant value of 34 $W/m^2°C$ has been assumed in the computation. However, a variable expression of h as a function of temperature can be simply incorporated within the capability of the CSMP computer package by using the function generator.

4.2.2 Two-Point Method

If the recordings of thermocouple No. 5 (Fig. 3.3) are known in the experiment, then T_n is known. Equation (4.8) can be solved directly for nodal points $1 \leq i \leq n - 1$ without involving (4.9). Thus, yields T_1 up to T_{n-1}; the determination of T_{-1} and q is the same as before.

4.3 Two-Dimensional Conduction Model (2-D Model)

In Type III test section larger axial temperature gradients were observed especially in the transition boiling regime. Thus, a 2-D model was necessary to properly account for the effect of axial temperature gradient.

A total of six thermocouples are embedded, five of them -- located in the interface of the tube and silver solder -- are to be used for data thermocouples as shown in Fig. 3.6.

The net heat transfer q_j from a given section j (inside the test section as shown in Fig. 4.2) to the fluid at time t can be expressed as the rate of change in heat content Q_j of that section, plus axial conduction from neighboring sections at the same time t. Q_j can be expressed as:

$$Q_j(z,t) = \rho\, c\, \Delta z \int_{r_{in}}^{r_{out}} 2\pi r T_{i,j}\, dr \qquad (4.13)$$

The function T(r,z,t) is obtained as the solution to the two dimensional Fourier equation in cylindrical coordinates:

$$\rho c \frac{\partial T}{\partial t} = \frac{\partial}{\partial r}\left(k \frac{\partial T}{\partial r}\right) + \frac{1}{r}\left(k \frac{\partial T}{\partial r}\right) + \frac{\partial}{\partial z}\left(k \frac{\partial T}{\partial z}\right) \qquad (4.14)$$

and is subject to the following initial and boundary conditions:

(1) $T = T(r,z,0)$ ... The initial test section temperatures are measured by the thermocouples; for simplicity, an average value T_i is used. (4.15)

(2) $T(r_2, z_2, t)$ = T.C. 2,2 ... r_2 and z_2 are the coordinates of T.C. 2,2. Similarly,

$$T(r_2, z_3, t) = \text{T.C. } 2,3$$
$$\vdots \qquad (4.16)$$
$$T(r_2, z_6, t) = \text{T.C. } 2,6$$

(3) $\left.\frac{\partial T}{\partial r}\right)_{r=r_{out}} = 0, \quad \left.\frac{\partial T}{\partial z}\right)_{z=0} = 0$ and $\left.\frac{\partial T}{\partial z}\right)_{z=z_7} = 0$ ... The test section is insulated. (4.17)

The solution of Equation (4.14) can be obtained by reducing it to a system of linear first-order difference equations in t. This is achieved by discretizing along both r-direction and z-direction as shown in Fig. 4.2 using the approximation

$$\frac{\partial T_{i,j}}{\partial r} = \frac{T_{i+1,j}(t) - T_{i-1,j}(t)}{2\Delta r} \qquad (4.18)$$

$$\frac{\partial^2 T_{i,j}}{\partial r^2} = \frac{T_{i-1,j}(t) - 2T_{i,j}(t) + T_{i+1,j}(t)}{(\Delta r)^2} \qquad (4.19)$$

and

$$\frac{\partial^2 T_{i,j}}{\partial z^2} = \frac{T_{i,j-1}(t) - 2T_{i,j}(t) + T_{i,j+1}(t)}{(\Delta z)^2} \qquad (4.20)$$

Using Equations (4.18) to (4.20) along with initial and boundary conditions, the following system of equations can be inferred from Equation (4.14).

$$\frac{d\,T_{i,j}}{dt} = \alpha_c \frac{T_{i-1,j} - 2T_{i,j} + T_{i+1,j}}{(\Delta r)^2} + \frac{\alpha_c}{r_i}\left(\frac{T_{i+1,j} - T_{i-1,j}}{2\Delta r}\right)$$

$$\alpha_c \frac{T_{i,j-1} - 2T_{i,j} + T_{i,j+1}}{(\Delta z)^2} \qquad (4.21)$$

$$(3 \leq i \leq n-1;\ 2 \leq j \leq 6)$$

where

$$r_i = r_{in} + \delta + (i - 2)\,\Delta r$$

and

$$\frac{dT_{n,j}}{dr} = \frac{2\alpha_c(T_{n-1,j} - T_{n,j})}{(\Delta r)^2} \qquad (4.22)$$

$$T_{i,2} = T_{i,1} \qquad (4.23)$$

$$T_{i,6} = T_{i,7}$$

Equations (4.22) and (4.23) are a direct consequence of Equation (4.17).

Equations (4.21) and (4.22) along with Equation (4.23) contain a system of 5x(n-2) equations with the same number of unknowns in $T_{i,j}(3 \leq i \leq n;\ 2 \leq j \leq 6)$. Once $T_{i,j}$ have been solved and $dT_{2,j}/dt$ determined from experimental data, the inner wall temperature $T_{1,j}$ can then be calculated in the following Fourier equation based on the nodal point (2,j).

$$\frac{\left[r_2^2 - (r_2 - \frac{\delta}{2})^2\right] \rho_t c_t + \left[(r_2 + \frac{\Delta r}{2})^2 - r_2^2\right] \rho_c c_c \frac{dT_{2,j}}{dt}}{(r_2 + \frac{\Delta r}{2})^2 - (r_2 - \frac{\delta}{2})^2}$$

$$= \frac{k_c \frac{T_{3,j} - T_{2,j}}{\Delta r} - k_t \frac{T_{2,j} - T_{1,j}}{\delta}}{\frac{1}{2}(\Delta r + \delta)} + \frac{1}{r_2} \frac{1}{2} \left(k_c \frac{T_{3,j} - T_{2,j}}{\Delta r} + k_t \frac{T_{2,j} - T_{1,j}}{\delta}\right)$$

$$+ k_m \left(\frac{T_{2,j-1} - 2T_{2,j} + T_{2,j+1}}{(\Delta z)^2}\right) \qquad (4.24)$$

where

$$k_m = k_t \frac{r_2^2 - (r_2 - \frac{\delta}{2})^2}{(r_2 + \frac{\Delta r}{2})^2 - (r_2 - \frac{\delta}{2})^2} + k_c \frac{(r_2 + \frac{\Delta r}{2})^2 - r_2^2}{(r_2 + \frac{\Delta r}{2})^2 - (r_2 - \frac{\delta}{2})^2} \qquad (4.25)$$

Equation (4.25) is the expression of mean thermal conductivity based on Ohm's law in parallel laminae. In solving Equation (4.24), Equation (4.23) has to be incorporated for i = 1 and 2.

Equation (4.13), expressed in terms of summation, becomes

$$Q_j = 2\pi\Delta z \left[0.5\, T_{1,j}\, r_{in}\, \delta\rho_t c_t + 0.5\, T_{2,j}(r_{in} + \delta)\, \delta\rho_t c_t\right.$$

$$+ 0.5\, T_{2,j}(r_{in} + \delta)\, \Delta r\, \rho_c c_c + \left(\sum_{i=3}^{n-1} T_{i,j}\, r_i\, \Delta r\, \rho_c c_c\right) \qquad (4.26)$$

$$\left. + 0.5\, T_{n,j}\, r_n\, \Delta r\, \rho_c c_c\right]$$

The expression of heat transfer q_j from section j through plane j to the fluid in terms of Q_j and axial conduction is:

$$q_j = -\frac{1}{A_{in}}\frac{dQ_j}{dt} + q_{j+1,j} - q_{j,j-1}$$

$$= -\frac{1}{2\pi r_{in}\Delta z}\frac{dQ_j}{dt} + q_{j+1,j} - q_{j,j-1} \qquad (4.27)$$

where $q_{j+1,j}$ the axial conduction from section j + 1 to section j, can be expressed as

$$q_{j+1,j} = \frac{2\pi}{\Delta z}\Big[0.5\, r_{in}\,\delta\, k_t(T_{1,j+1} - T_{1,j}) + 0.5(r_{in}+\delta)\,\delta k_t(T_{2,j+1} - T_{2,j})$$

$$+ 0.5(r_{in}+\delta)\,\Delta r\, k_c(T_{2,j+1} - T_{2,j}) + \sum_{i=3}^{n-1} r_i\,\Delta r\, k_c(T_{i,j+1} - T_{i,j})$$

$$+ 0.5\, r_n\,\Delta r\, k_c(T_{n,j+1} - T_{n,j})\Big] \qquad (4.28)$$

$q_{j,j-1}$ can be obtained in a similar manner.

The net heat transfer q_j can be approximated by

$$q_j = k_t\frac{T_{2,j} - T_{1,j}}{\delta} \qquad (4.29)$$

It has been found that q_j calculated from Equation (4.29) in general results in less than 10% error compared to that of Equation (4.27).

The above 2-D analysis can be reduced to a 1-D case by substituting all five data thermocouple inputs, i.e., T.C. 2,2 ...

T.C. 2.6, with a single data thermocouple input, resulting in five identical boiling curves.

4.4 One Dimensional Three-Layer Model

For certain types of composite test sections, e.g., Zircaloy-copper test sections, due to problems in brazing copper to Zircaloy, a liquid metal gland (Wood's metal) was used instead to provide good thermal contact between the two materials as shown in Fig. 3.7. Note that Wood's metal is in the liquid state (melting point 70°C) at test conditions. It is, therefore, suspected that the data thermocouple T.C. 1 (Fig. 4.3), may not be maintained at the interface position of the tube and Wood's metal. As a result, a new thermocouple T.C. 2 was used for the data thermocouple in this application. T.C. 2 is located on the copper side, but very close to the interface of Wood's metal and copper. It was found out later that the temperature measured at the T.C. 1 location is much higher than that predicted. This confirmed the earlier suspicion about the measurement of T.C. 1.

For simplicity, the 1-D model (two-layer), after some modification, was used in data reduction. Because of the location of the new data thermocouple T.C. 2, the low value of thermal conductivity of Wood's metal (Table 3.2) and its thickness (almost three times thicker than silver solder), the effect of the solder layer has to be included in the analysis. The derivation for 1-D three layer analysis in this case is essential, the same as that of 2-D cases, except two extrapolations (based on Fourier equation) are required to determine the inner wall temperature.

For the 1-D model, the Fourier equation on the copper side can be obtained from Equation (4.21) after neglecting axial conduction.

$$\frac{dT_i}{dt} = \alpha_c \frac{T_{i-1} - 2T_i + T_{i+1}}{(\Delta r)^2} + \frac{\alpha_c}{r_i} \frac{(T_{i+1} - T_{i-1})}{2\Delta r} \qquad (4.30)$$

$$(3 \leq i \leq n)$$

where

$$r_i = r_{in} + \delta + g + (i-2)\,\Delta r$$

and

$$-\frac{k_c}{2}\left(\frac{T_n - T_{n-1}}{\Delta r} + \frac{T_{n+1} - T_n}{\Delta r}\right) = h(T_n - T_{amb}) \qquad (4.31)$$

where Equation (4.31) is the boundary condition at the outer wall of the test section. All the symbols in this derivation are referred to Fig. 4.3.

Equation (4.30) contains a system of n-2 equations with n-2 unknowns in $T_i (3 \leq i \leq n)$, where T_{n+1} in the equation is to be eliminated from Equation (4.31). With T_i available and dT_2/dt determined from experimental data, T_1 can be calculated from the Fourier equation based on the nodal point 2.

$$\frac{\left[r_2^2 - (r_2 - \frac{g}{2})^2\right]\rho_{wm}c_{wm} + \left[(r_2 + \frac{\Delta r}{2})^2 - r_2^2\right]\rho_c c_c}{(r_2 + \frac{\Delta r}{2})^2 - (r_2 - \frac{g}{2})^2} \frac{dT_2}{dt} \qquad (4.32)$$

$$= \frac{k_c \frac{T_3 - T_2}{\Delta r} - k_{wm} \frac{T_2 - T_1}{g}}{\frac{1}{2}(\Delta r + g)} + \frac{1}{r_2}\frac{1}{2}\left(k_c \frac{T_3 - T_2}{\Delta r} + k_{wm} \frac{T_2 - T_1}{g}\right)$$

With T_1 known and from which dT_1/dt determined, the inner wall temperature T_o can then be computed from the Fourier equation based on the nodal point 1.

$$\frac{\left[r_1^2 - (r_1 - \frac{\delta}{2})^2\right]\rho_z c_z + \left[(r_1 + \frac{g}{2})^2 - r_1^2\right]\rho_{wm} c_{wm}}{(r_1 + \frac{g}{2})^2 - (r_1 - \frac{\delta}{2})^2} \frac{dT_1}{dt}$$

$$= \frac{k_{wm} \frac{T_2 - T_2}{g} - k_z \frac{T_1 - T_0}{\delta}}{\frac{1}{2}(g + \delta)} + \frac{1}{r_1}\frac{1}{2}\left(k_{wm} \frac{T_2 - T_1}{g} + k_z \frac{T_1 - T_0}{\delta}\right) \qquad (4.33)$$

where

$$r_1 = r_{in} + \delta$$

Finally, the heat content of the test section H and the average heat flux q to the fluid can be expressed as:

$$\begin{aligned} H = 2\pi L \Big[& 0.5\, T_0 r_{in} \delta \rho_z c_z + 0.5\, T_1 (r_{in} + \delta)\, \delta \rho_z c_z \\ & + 0.5\, T_1 (r_{in} + \delta)\, g \rho_{wm} c_{wm} + 0.5\, T_2 (r_{in} + \delta + g) g \rho_{wm} c_{wm} \\ & + 0.5\, T_2 (r_{in} + \delta + g) \Delta r \rho_c c_c \\ & + \Big(\sum_{i=3}^{n-1} T_i r_i \Delta r \rho_c c_c + 0.5\, T_n r_n \Delta r \rho_c c_c\Big] \end{aligned} \qquad (4.34)$$

and

$$q = -\frac{1}{2\pi r_{in} L} \frac{dH}{dt} \qquad (4.35)$$

4.5 Computer Simulation

All calculations were performed via the Continuous System Modelling Program[4] (CSMP). The Runge-Kutta fixed-step size method has been used in numerical intergration with selectionof n = 10 and t = 0.1 sec and its convergency checked. The NLFGEN function generation (nonlinear function generation) capability of CSMP was used to generate $T_{2,j}$ from measured data and DERIV (derivative) module used to compute $dT_{2,j}/dt$ from $T_{2,j}$ and dQ_j/dt from Q_j. A sample computer program for the 2-D model is shown in Appendix I.

REFERENCES

1. Burggraf, O.R., "An Exact Solution of the Inverse Problem in Heat Conduction Theory and Applications", Journal of Heat Transfer, pp. 373-382, August, 1964.

2. Cheng, S.C., Ragheb, H., Ng, W.W.L., Heng, K.T. and Roy, S. "Transition Boiling Heat Transfer in Forced Vertical Flow", NUREG/CR-0357, ANL-78-75.

3. Cheng, S.C., Ragheb, H., Ng, W.W.L., Heng, K.T., Roy, S. and Poon, K.T., "Transition Boiling Heat Transfer in Forced Vertical Flow", Final Report for the period June 1978 to June 1979, under contract with Argonne National Laboratory, Argonne, Illinois; Contract No. 31-109-38-3564.

4. IBM System/360 Continuous System Modelling Program, User's Manual, Program No. 360 A-CX-16X, 1972.

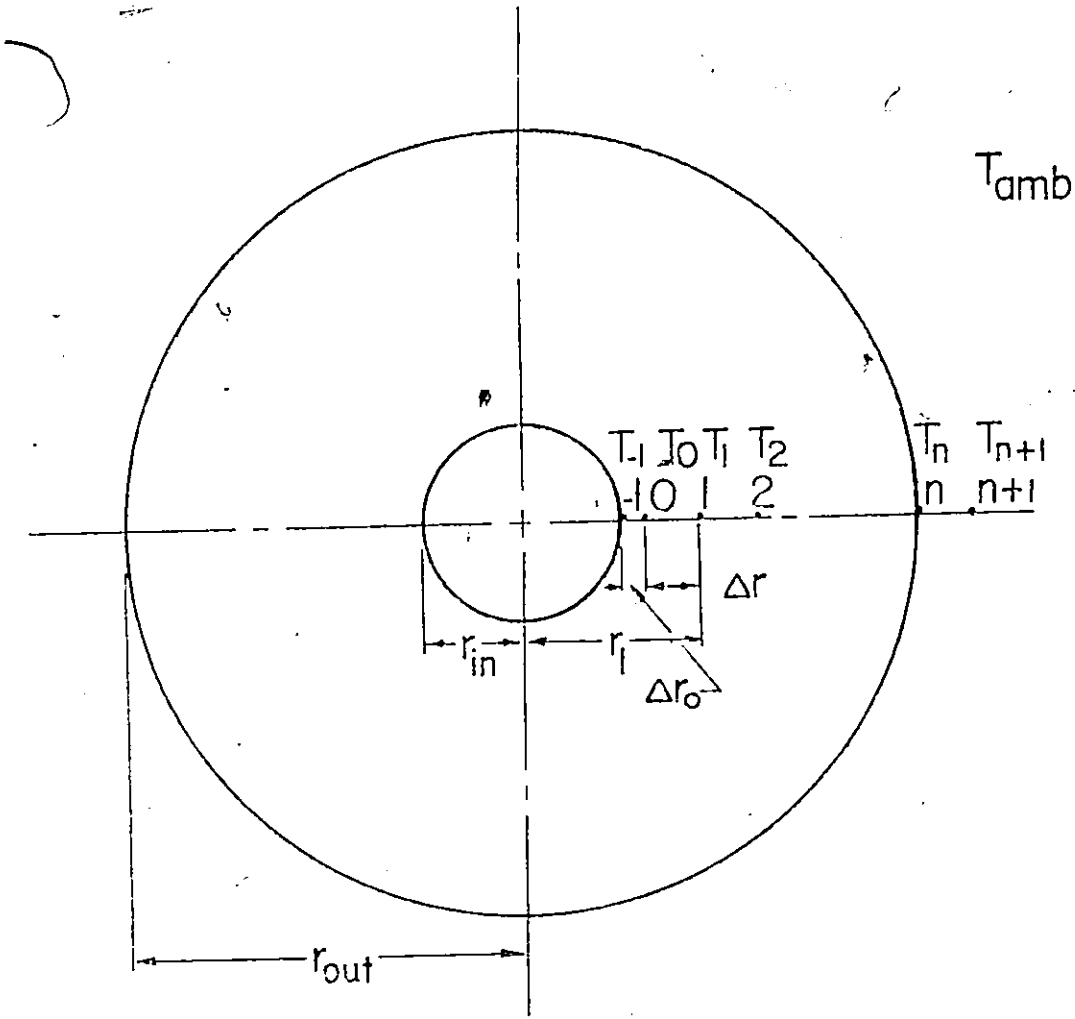

Figure 4.1 Nodal points distribution

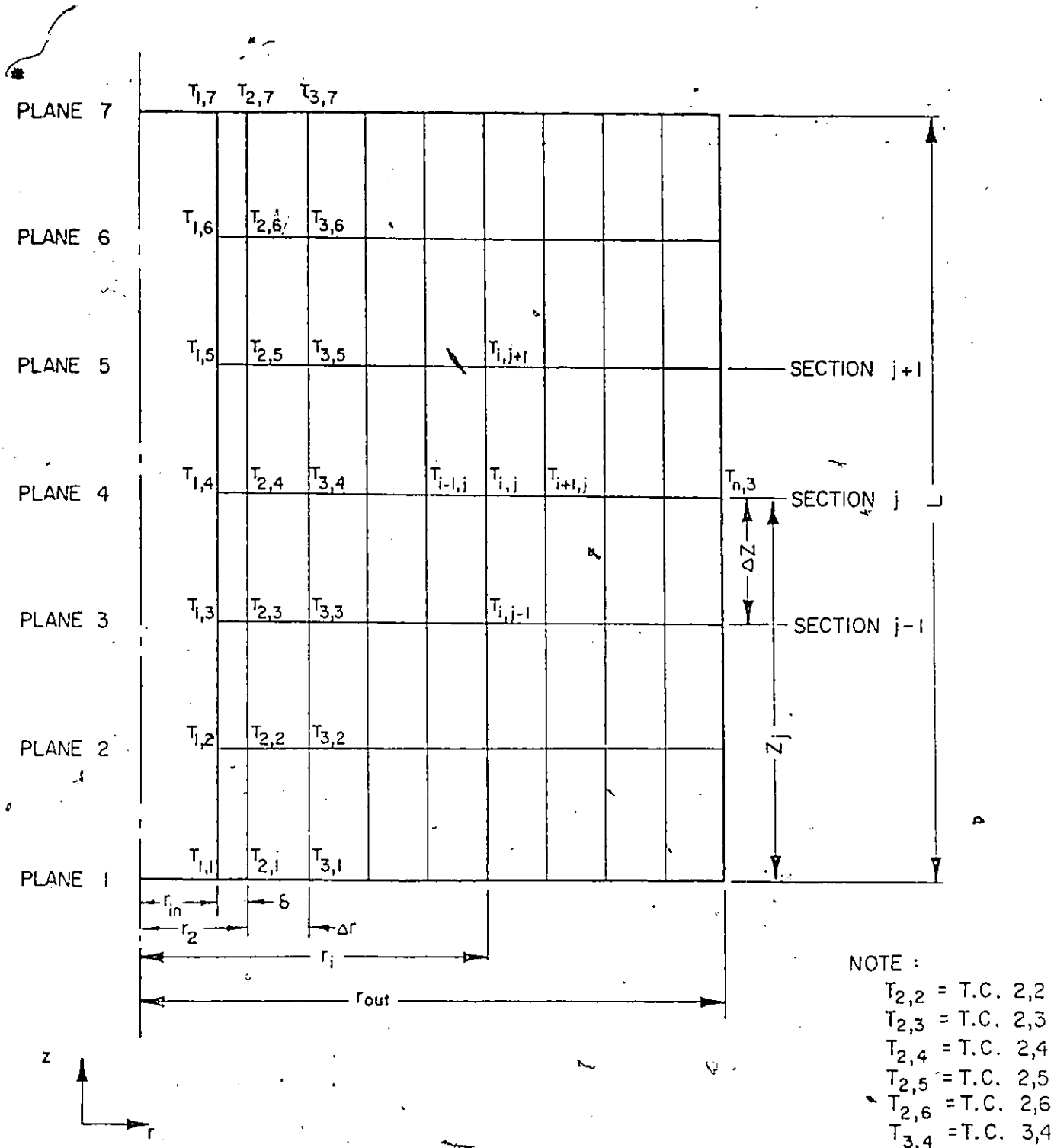

NOTE :

$T_{2,2}$ = T.C. 2,2
$T_{2,3}$ = T.C. 2,3
$T_{2,4}$ = T.C. 2,4
$T_{2,5}$ = T.C. 2,5
$T_{2,6}$ = T.C. 2,6
$T_{3,4}$ = T.C. 3,4

FIG. 4.2 NODAL NETWORK FOR TWO DIMENSIONAL MODEL IN COMPOSITE TEST SECTIONS

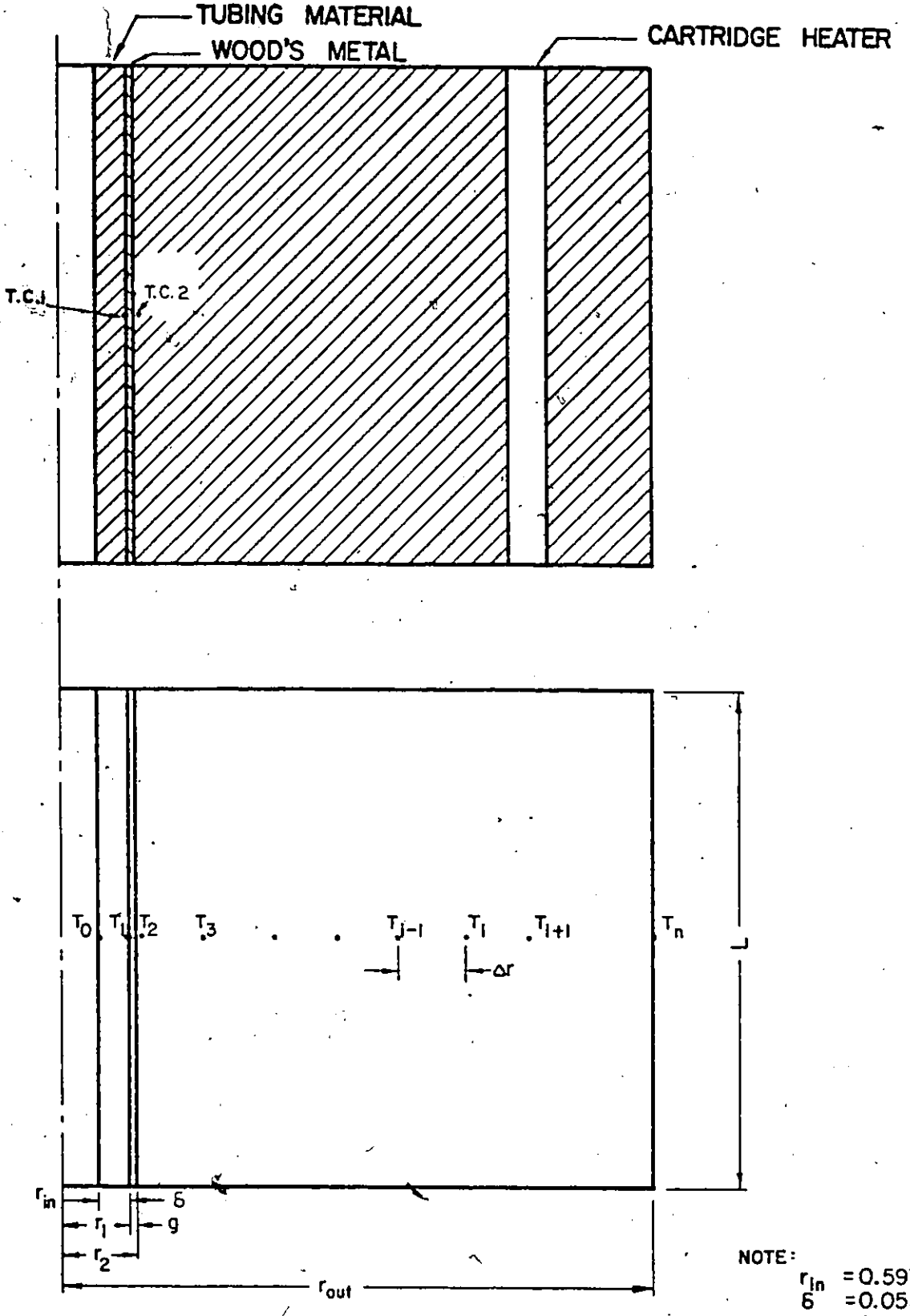

NOTE:
r_{in} = 0.597 cm
δ = 0.0559 cm
g = 0.0356 cm
r_{out} = 9.53 cm
L = 5.03 cm
T_2 = T.C. 2

FIG. 4.3 ZIRCALOY - COPPER COMPOSITE TEST SECTION & IT-S NODAL POINT DISTRIBUTION

CHAPTER 5

EXPERIMENTAL RESULTS AND DISCUSSION

5.1 Effect of Flow Conditions

5.1.1 Mass Flux

The effect of mass flux on the boiling curve was investigated within the range of 68-203 $kg.m^{-2}.s^{-1}$ for each of the test sections of Fig. 3.2. An example of the results is shown in Fig. 5.1 for the Type III test section (Inconel surface). The observed trend was identical for all other test sections: An increase in mass flux moves the boiling curve to a higher level except for the nucleate boiling regime. This is expected as both the CHF and the film boiling heat flux increase with an increase in mass flux. Since transition boiling is an intermediate heat transfer mode, the observed increase in transition boiling heat flux may be attributed to: (a) more efficient removal of bubbles because of the higher flow, (b) improved convective heat transfer during film boiling, and (c) improved wall-liquid interaction due to a higher turbulence level of the flow.

5.1.2 Inlet Subcooling

The effect of inlet subcooling was investigated in each of the test sections by varying the inlet flow subcooling from 0°C to 27°C.

Fig. 5.2 shows that for the Type III test section, the transition boiling heat flux increases with an increase in subcooling. The same trend was observed with the other test sections.

For a given inlet subcooling, the effect of local enthalpy was also observed by generating local boiling curves at different planes along the flow channel using a two-dimensional model as shown in Fig. 5.3. In general, it was found that the local boiling heat flux decreases with increased heated length and thus enthalpy.

Unlike mass flux, the inlet subcooling seems to have a significant effect on the flow stability during transition boiling. It was observed that at subcoolings greater than 27°C severe fluctuations in flow and surface temperature were accompanied by boiling noise. The flow fluctuations could be observed in a transparent flow channel installed for this purpose just upstream of the test section.

5.2 Method of Analysis

5.2.1 One-Dimensional Conduction Model (1-D Model)

Four methods of analysis were presented in Chapter 4:

a) Fourier equation method

b) Refined Fourier equation method

c) h-method

d) Two-point method

Method (a) is the least accurate method and should only be used for thin-walled test sections. Fig. 5.4 presents one of the typical results using methods (b), (c) and (d). Since method (b) assumes perfect insulation, it slightly overestimates the heat flux compared to the other two methods. Both the h-method and the two-point method yield close results except the former produces somewhat higher values in nucleat boiling and lower values in transition boiling. The h-method is recommended for 1-D analysis in transition boiling, since it is more accurate than the refined Fourier equation method, and it is simpler than the two-point method because only one data thermocouple recording is required.

5.2.2 Two-Dimensional Conduction Model (2-D Model)

Basically, the 2-D model subdivides the test section in a number of rings. It allows one to calculate heat flux from a given ring (inside the test section) by computing the rate of change in heat content of that ring, plus axial conduction from neighboring sections at the same time, t. For simplicity, the test section has been assumed to be perfectly insulated in the analysis.

A typical set of boiling curves for a mass flux of 136 $kg.m^{-2}.s^{-1}$ and an inlet subcooling of 13.9°C was constructed using the 2-D model as shown in Fig. 5.3.

A large spread in boiling curves is noticed for the 2-D results. In order to gain some insight into the cause of the spread, the test

section temperature distribution will be examined in detail. Fig. 5.5 illustrates the axial data thermocouple temperature distributions as well as the inner wall temperature distributions. The following observations can be made:

(a) At t = 100 sec, the rewet front has already gone through planes 2 and 3, while planes 4, 5 and 6 are still in the film boiling regime. A small thermocouple temperature gradient occurs between planes 5 and 6 reflecting a small amount of heat loss through the top end of the test section.

(b) Some typical temperature distributions in the transition regime which occur at t = 203 sec, are shown in the figure. At this time, the rewet front has passed through plane 4.

(c) At t = 211 sec, CHF occurs at planes 2 and 3 as evidenced by sharp temperature gradients and a large spread between the data thermocouple temperature and the corresponding inner wall temperature at each section.

(d) At t = 216 sec, CHF occurs at planes 4, 5 and 6.

(e) Some typical temperature distributions in the nucleate boiling regime which occur at t = 282 sec, are shown. From the thermocouple temperature distribution, it is clearly indicated that some axial heat loss and possibly end effects occurred at both ends of the test section.

Figs. 5.6 and 5.7 illustrate the radial temperature distributions at t = 100 sec, 211 sec and 282 sec. In general, steep temperature gradients exist near the inner wall surface (nodal point 1). At t = 100 sec and 282 sec, all five sectional radial temperature distributions are very similar except in the region close to the inner wall surface. At t = 211 sec, a large spread is observed among the five radial temperature distributions. This is because CHF occurs at planes 2 and 3 as evidenced by the existence of sharp temperature drops between nodal points 2 and 3 on both sections 2 and 3.

Examination of the boiling curves shows that the plane 6 boiling curve in the film boiling regime is always higher than the plane 5 boiling curve. This is thought to be due to neglecting axial heat losses. Also, the plane 2 boiling curve in film and transition boiling regimes, in general, is found to be noticeably higher than other boiling curves regardless of the inlet subcooling and mass flux. Ths is attributed to (a) the lower bulk fluid temperature, (b) entrance effects, and (c) neglecting axial heat losses. In the transition boiling regime, all the five boiling curves show a correct trend against the bulk fluid temperature. The radial heat loss to the surroundings should be negligibily small in comparison with a rather high level of radial conduction taking place inside the test section.

In some of the ealier tests, the Type I copper test section was equipped with thermocouples at three axial locations. Boiling curves were derived for each of the three data thermocouples using a 1-D and

2-D models[1,2]. The results showed that: (a) the mid-plane boiling curve based on either 2-D or 1-D model represents the average boiling curve for the entire test section, (b) the two mid-plane boiling curves based on 2-D and 1-D models, respectively, are approximately the same, and (c) the net effect of axial conduction on the surface heat flux at the mid-section, based on 2-D model is very small and for practical purposes can be neglected.

In the Inconel-copper composite test section, the mid-plane boiling curve of the 1-D model (taken from Fig. 5.2), is falling somewhat between the plane 3 and plane 4 boiling curves for the corresponding 2-D model (Fig. 5.3). This suggests that the zero axial conduction section has been shifted downstream from the mid-section. It also suggests that: (a) boiling curves based on a 2-D model at the mid-plane represent the average heat flux over the entire test section, and (b) boiling curves measured at the mid-plane based on a 2D model are close to those based on a 1-D model. For this reason, parametric effects on boiling curves discussed in this thesis are based on boiling curves measured at the mid-plane using a 1-D model.

5.3 Effect of Method of Operation

Measurements of boiling curves were made using two different modes of operation: the transient and the steady state mode. Fig. 5.8 shows a comparison between the transient boiling curve and the steady state data obtained for the Type I copper test section using a temperature

controller. Good agreement is observed between the steady state data and the transient boiling curve. Due to insufficient heater power in the test section, the upper portion of the steady state boiling curve could not be obtained.

Subsequent tests with a Type III test section equipped with a larger number of heaters permitted the construction of a complete steady state boiling curve as shown in Fig. 5.9. The transient boiling curve is also plotted in this figure for comparison. Again, the agreement between these two curves is reasonable with the exception of the nucleate boiling regime. The agreement of heat flux values in transition and film boiling regimes was expected, as the high thermal capacity of the test section slowed down the quenching process to make the system act in a pseudo steady state manner.

5.4 Effect of Experimental Equipment

5.4.1 General

The simplest version of test section used in these experiments is a Type I test section. The Type II test section employed a combination of two copper blocks. The Type III test section was designed to study the effect heated surface thermal properties on transition boiling, by brazing an Inconel tube into a topper block using silver solder. Because of problems in brazing a Zircaloy tube or an aluminum tube to copper a Type IV test section was designed in which Wood's metal (a

liquid metal) was used instead to provide a good thermal contact between the two materials.

Schematic drawings of these test sections were shown in Fig. 3.2. In general, boiling curves generated with these test sections are sensitive to (a) the thermal resistance between the test section and the thermocouples, (b) the exact location of the thermocouple junction, (c) the accuracy of each data thermocouple measurement, and (d) the thermal resistance between the copper block and the flow tube.

5.4.2 Effect of Upstream History

Measurements on the Type II test section (two copper blocks with the short block as an entrance heater) produced lower post-CHF heat flux values than measurements on the Type I test section (single copper block). Particularly, the heat flux with the Type II test section during the initial stage of a transient test (film boiling system) is much lower as shown in Fig. 5.10. This difference cannot be explained by the differences in local subcooling; it is thought that a more important reason is the presence of a vapour film at the entrance to the test section in the Type II test section. Here, the vapour film is established in the entrance heater and can be considerably thicker than in the Type I test section where the vapour film becomes established near the entrance of the test section. The thicker vapour film presents a greater resistance to heat transfer thus lowering the film boiling heat flux for the same equilibrium conditions compared with the Type I test section results.

5.4.3 Effect of Surface Properties of Heated Surfaces

During the course of this transition boiling study, five different heated surface materials were tested using Types I, III and IV test sections. In the Type III test section, a thin silver solder layer (0.13 mm) between the copper block and the tubing material was designed to provide a low thermal resistance path for the heat flow from the copper block. The contact resistance between the tube and the copper block is expected to have some effect on resultant boiling curves. Because of good thermal properties and wetting characteristics of the silver solder, this effect was found to be very small.

Fig. 5.11 presents the effects of k (or $\rho k c_p$) on boiling curves obtained in the Type I and Type III test sections using copper, brass and Inconel heated surfaces. In general, the values of CHF and minimum heat flux are about the same for all three heated surfaces. However, the rewetting occurs at higher wall superheat for heated surfaces having a lower k (or $\rho k c_p$). This is in agreement with experiments carried out elsewhere[3,4].

Because of problems in brazing Zircaloy and aluminum tubes to copper, a liquid metal gland (Wood's metal) was used to bring the two metals thermally into contact (Fig. 3.2, Type IV test section). In addition, copper and Inconel tubes were also used in the Type IV test section. A comparison of thermocouple signals of the Type III and IV test sections suggested a larger than expected contact resistance in the liquid metal gland, it is suspected that, due to the poor wetting

characteristics of Wood's metal, air bubbles might have remained in contact with the copper block or flow tube outside surface.

A comparison of the boiling curves obtained for the four different flow tube materials used in the Type IV test section is shown in Fig. 5.12 for standard test conditions: $G = 136\ kg.m^{-2}.s^{-1}$, $T_{sub} = 13.9°C$. The results show that the Inconel and Zircaloy heated surfaces produced an almost identical boiling curve. The copper and aluminum heated surfaces, however, produce a higher heat transfer coefficient in the film boiling region and also the transition boiling curve has a steeper negative slope for copper and aluminum as compared to Inconel and Zircaloy. The T_{CHF} and T_{min} are also smaller for copper and aluminum.

Caution should be exercised in using these results as (a) the thermal resistance of the liquid metal gland may be different for each material and may not be properly modelled, (b) the wall thickness was not kept constant (see Table 3.2), (c) axial conduction heat losses were different because of large differences in thermal conductivity (see Table 3.1), and (d) the tubes were tested as received (except for possible reduction in outside diameters) and the finish of the inside bore was not identical. However, qualitatively the results are believed to be correct as they confirm the trends observed by the Type I and III test sections (Fig. 5.11).

REFERENCES

1. S.C. Cheng, "Transition Boiling Curves Generated From Quenching Experiments Using a Two-Dimensional Model", Letters Heat Mass Transfer, Vol. 5, pp. 391-403 (1978).

2. S.C. Cheng and H. Ragheb, "Transition Boiling Data of Water on Inconel Surface Under Forced Convective Conditions", Int. J. Multiphase Flow, Vol. 5, pp. 281-291 (1979).

3. R.E. Henry, "A Correlation for the Minimum Film Boiling Temperature", AICHE Symp. Series No. 138, Vol. 70, pp. 81-90 (1974).

4. V. Magrini and E. Nannel, "On the Influence of Thickness and Thermal Properties of Heating Walls on the Heat Transfer Coefficient in Nucleate Boiling", J. Heat Transfer, Vol. 77, pp. 173-178 (1975).

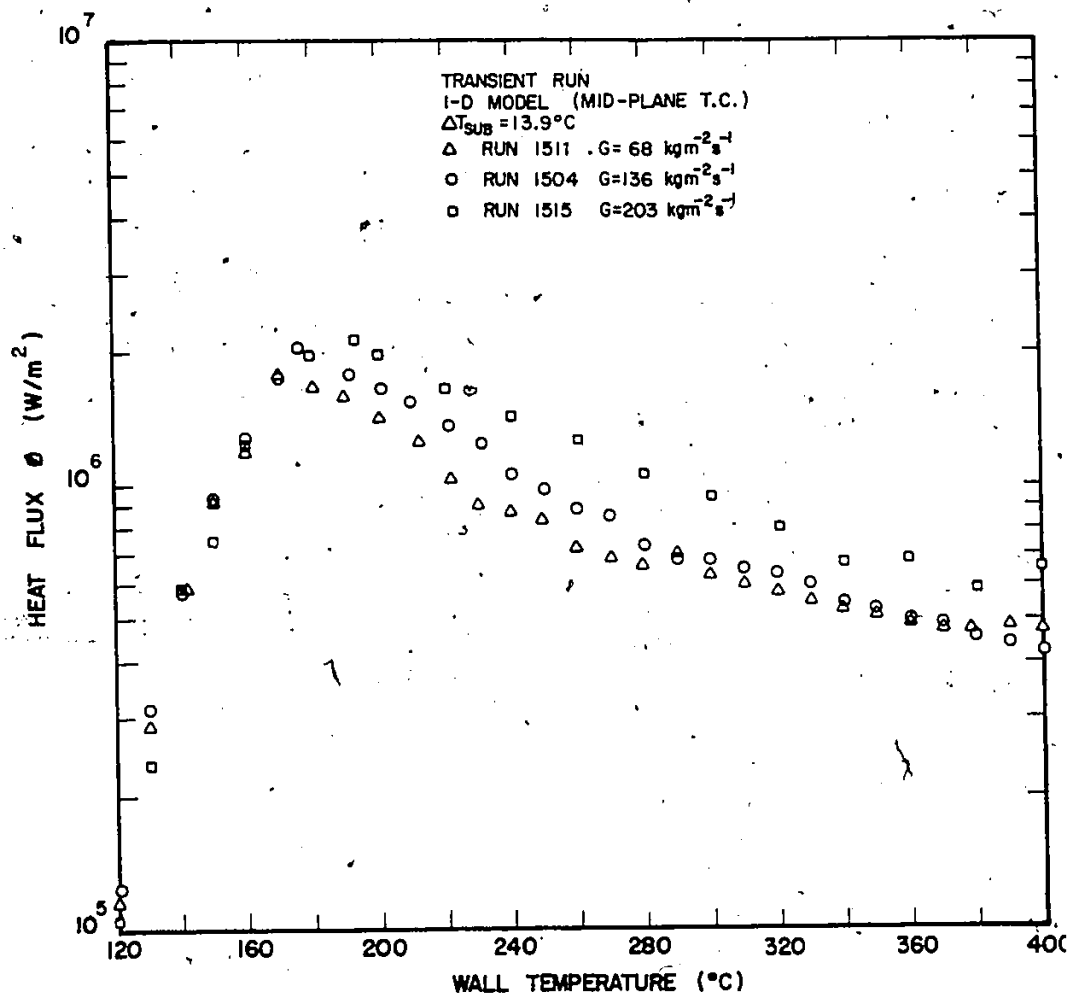

FIG.5.1 EFFECT OF MASS FLUX ON BOILING CURVE (TYPE III TEST SECTION)

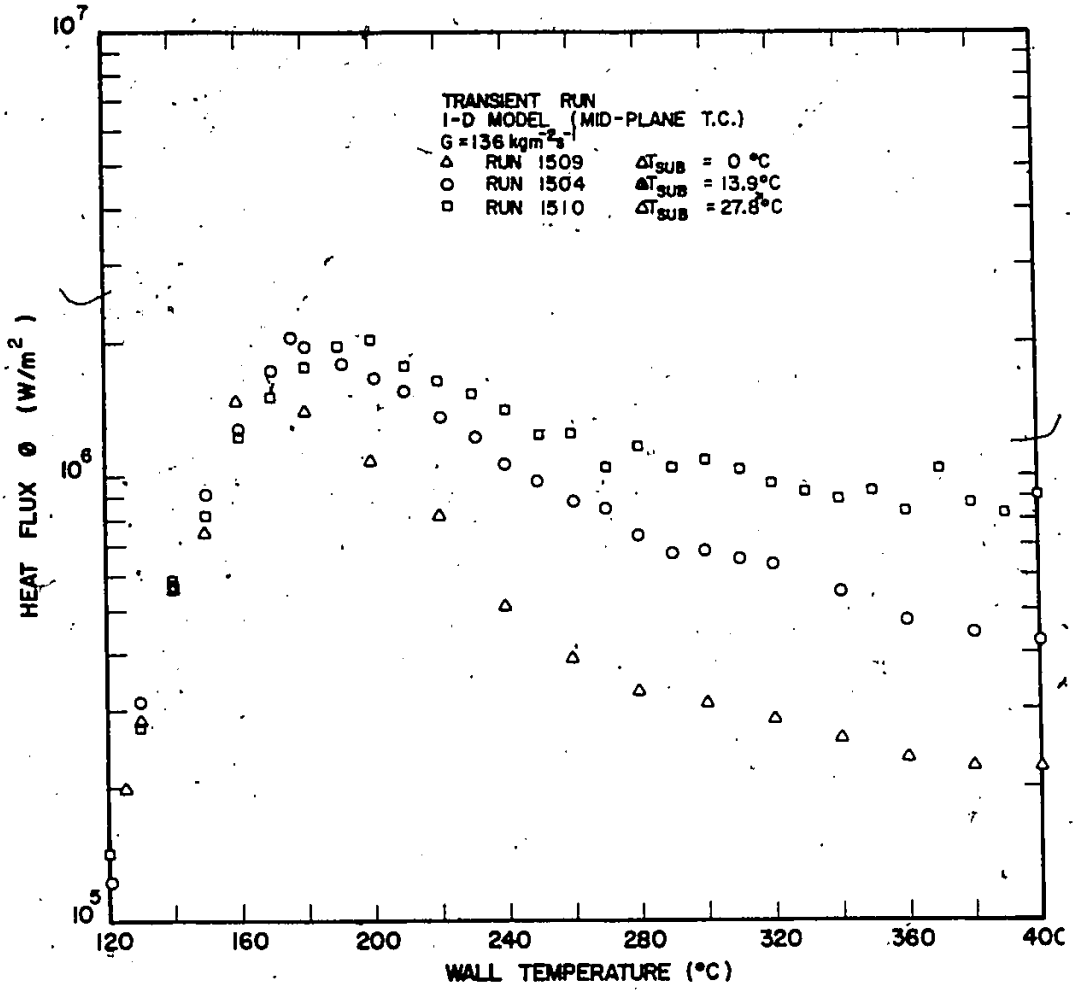

FIG.5.2 EFFECT OF INLET SUBCOOLING ON BOILING CURVE (TYPE III TEST SECTION)

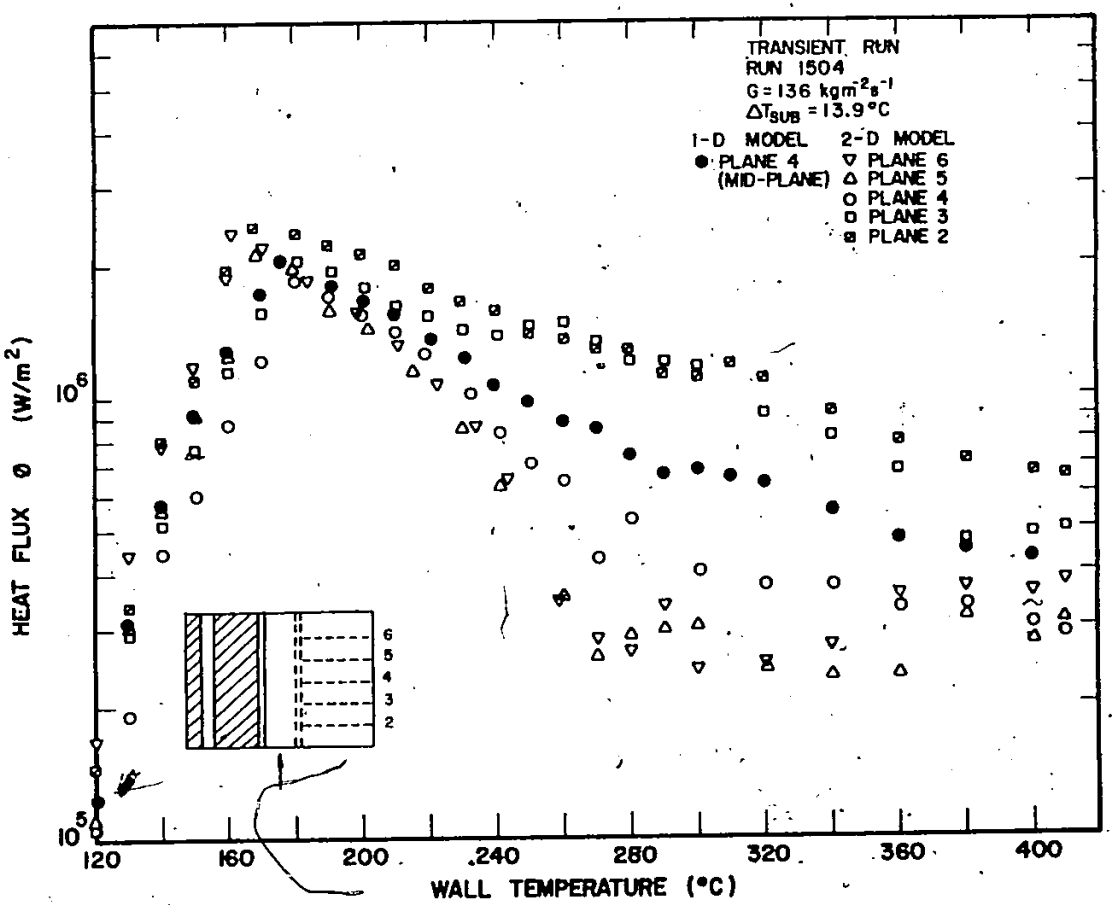

FIG. 5.3 BOILING CURVES FOR TYPE III TEST SECTION. COMPARISON OF 1-D MODEL WITH 2-D MODEL FOR FIVE THERMOCOUPLE PLANES

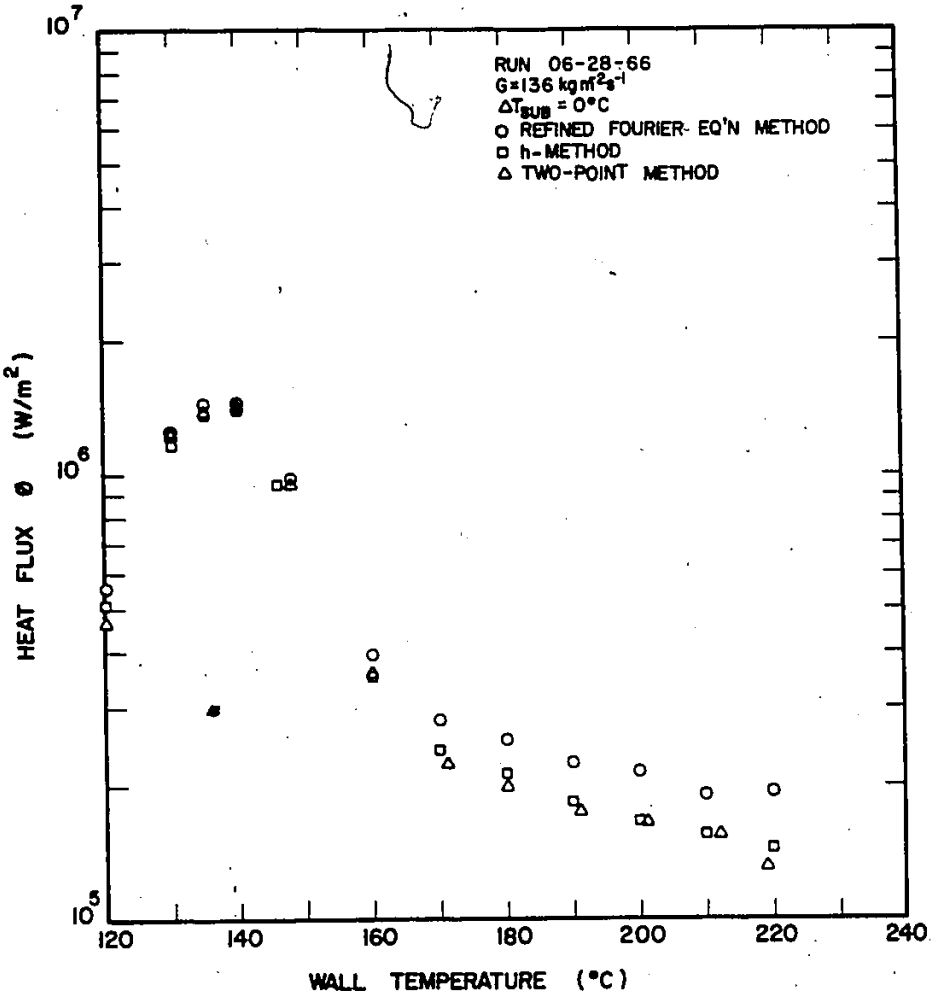

FIG. 5.4 BOILING CURVE FOR TYPE I TEST SECTION (COPPER BLOCK) USING VARIOUS ANALYTICAL METHODS (1-DIMENSIONAL CONDUCTION MODEL)

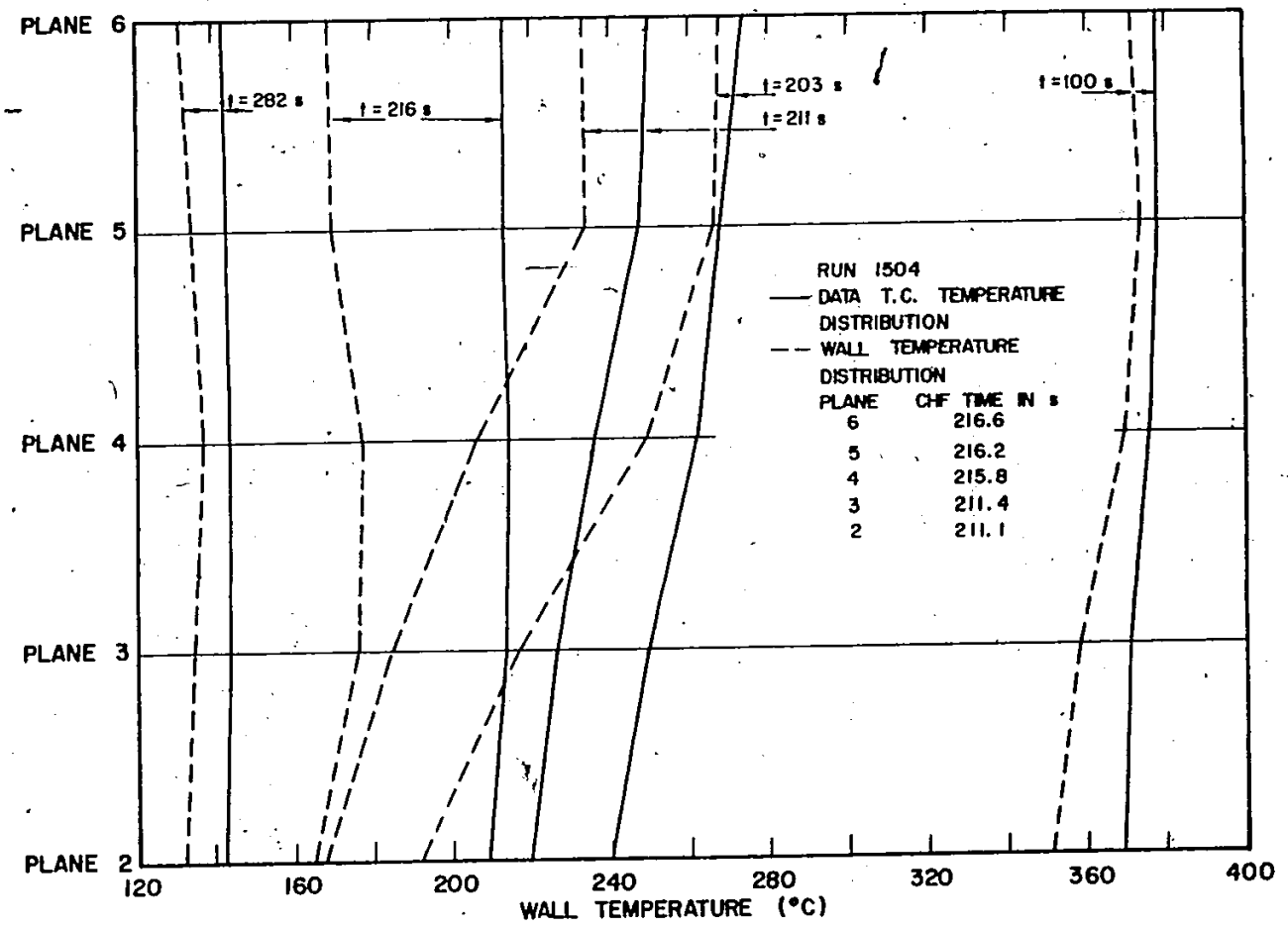

FIG. 5.5 AXIAL TEMPERATURE DISTRIBUTIONS FOR $G = 136\ kg/m^2s$ & $\Delta T_{SUB} = 13.9\ °C$, USING 2-D MODEL

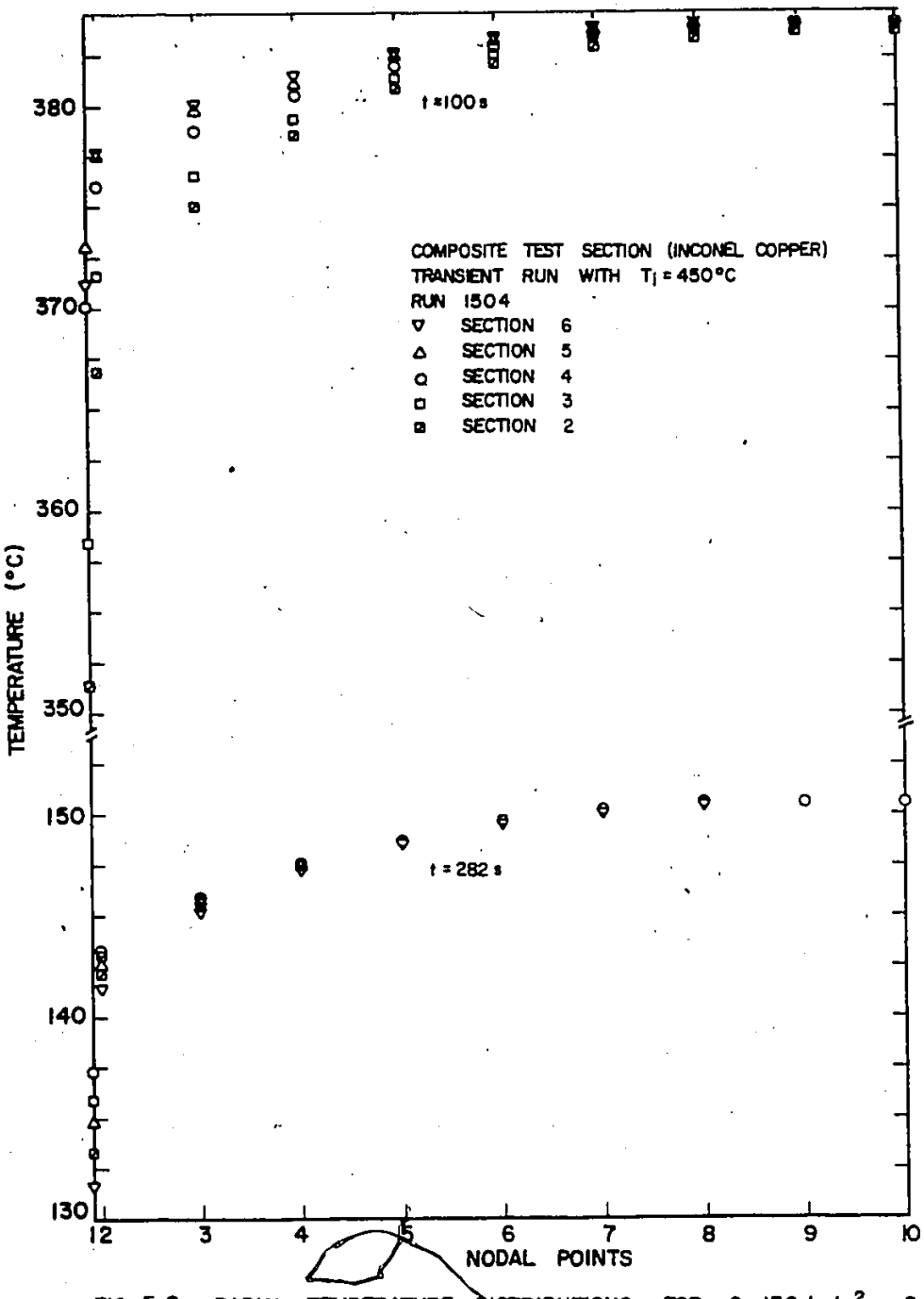

FIG. 5.6 RADIAL TEMPERATURE DISTRIBUTIONS FOR G = 136 kg/m^{2}s & ΔT_{SUB} = 13.9°C, USING 2-D MODEL (PART I)

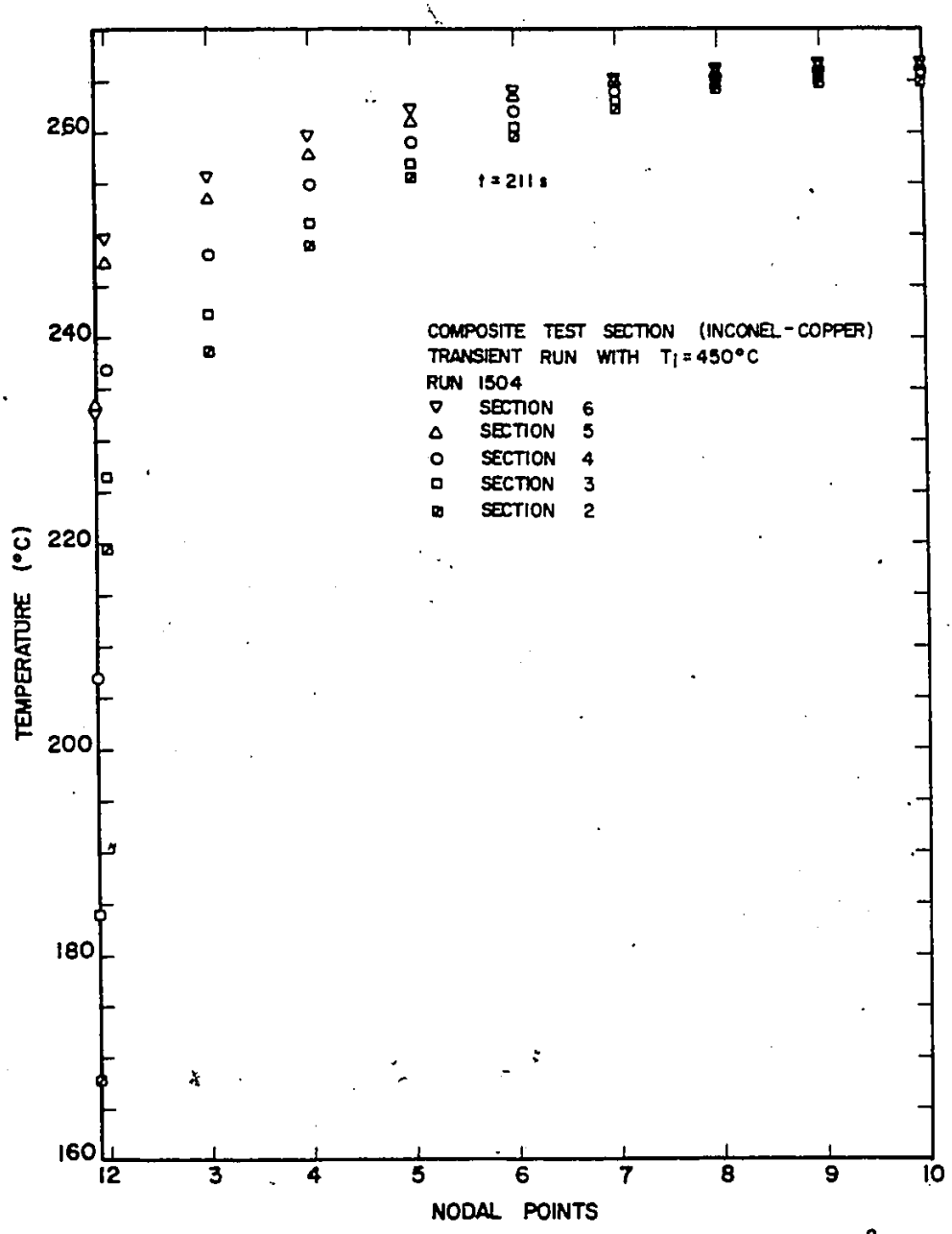

FIG. 5.7 RADIAL TEMPERATURE DISTRIBUTIONS FOR G=136 kg/m^{2}s & ΔT_{SUB} = 13.9°C, USING 2-D MODEL (PART II)

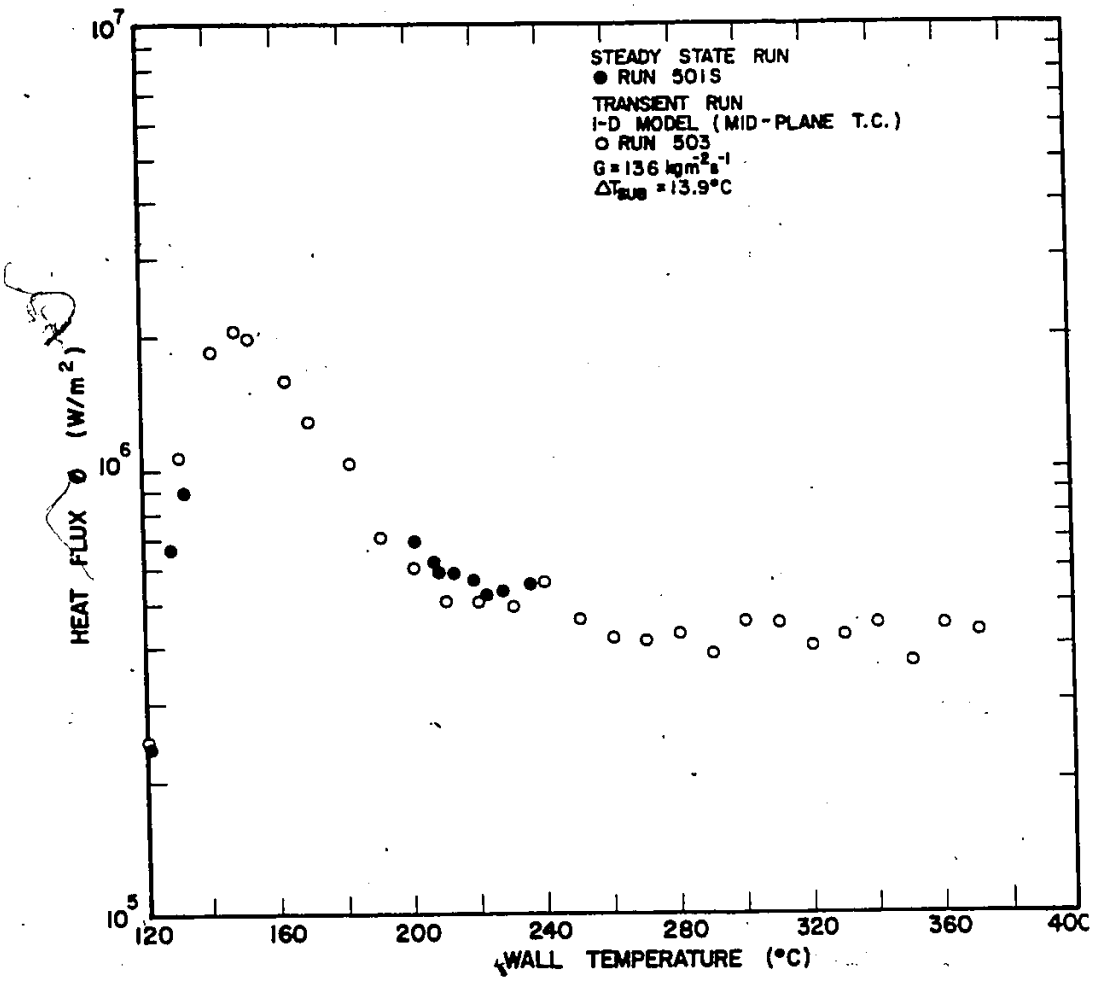

FIG. 5.8 COMPARISON OF BOILING CURVES OBTAINED FROM STEADY STATE AND TRANSIENT RUNS (TYPE I TEST SECTION, COPPER BLOCK)

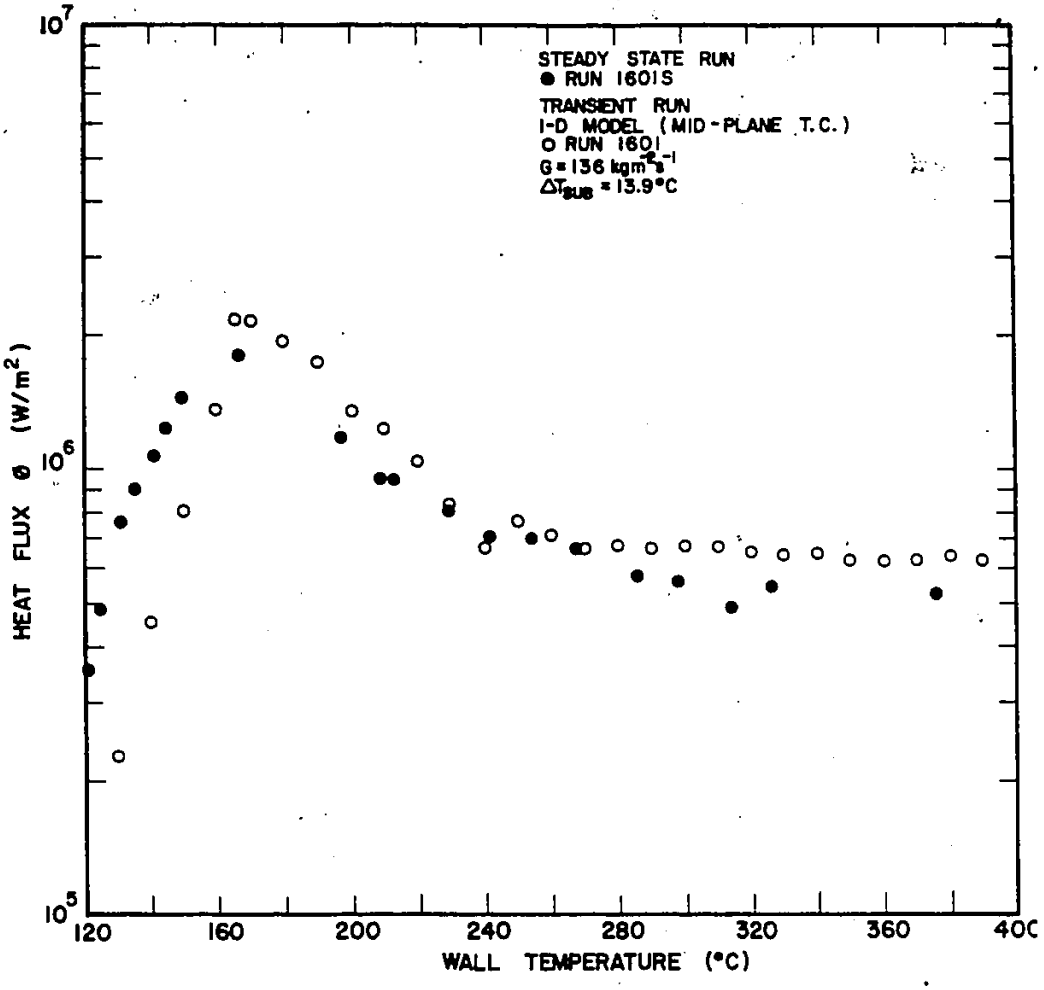

FIG.5.9 COMPARISON OF BOILING CURVES OBTAINED FROM STEADY STATE AND TRANSIENT RUNS (TYPE III TEST SECTION)

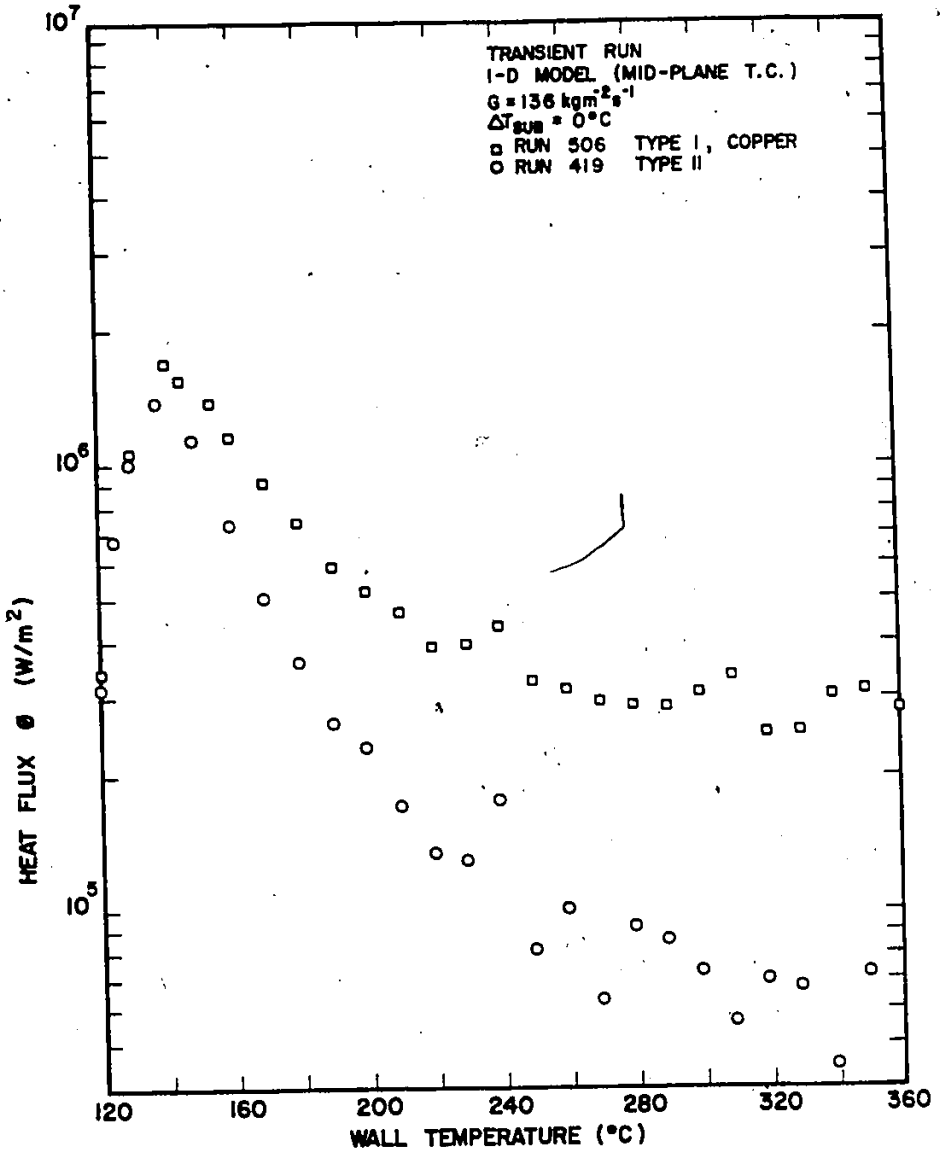

FIG. 5.10 COMPARISON OF BOILING CURVES OF TYPE I AND TYPE II TEST SECTIONS

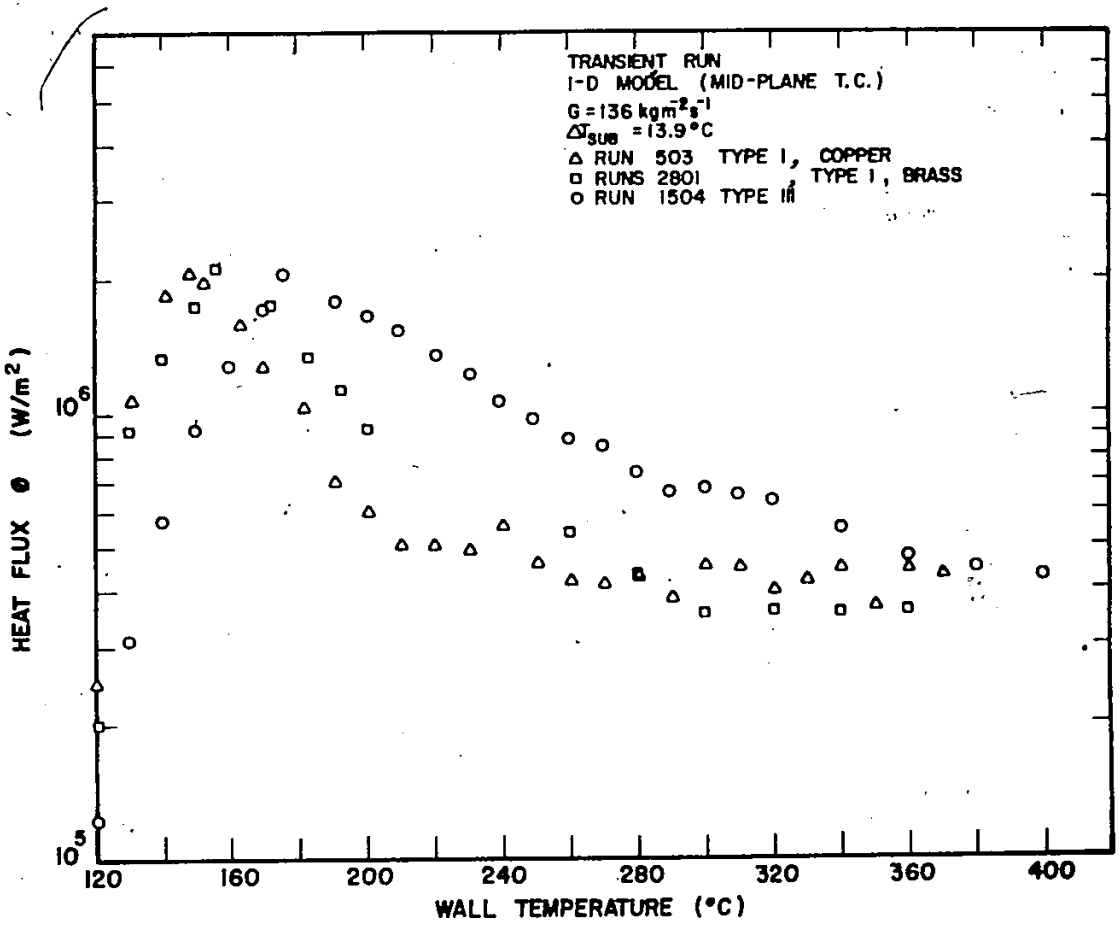

FIG. 5.11 COMPARISON OF BOILING CURVES OBTAINED FROM TYPE I AND TYPE III TEST SECTIONS: EFFECT OF HEATED SURFACE PROPERTIES

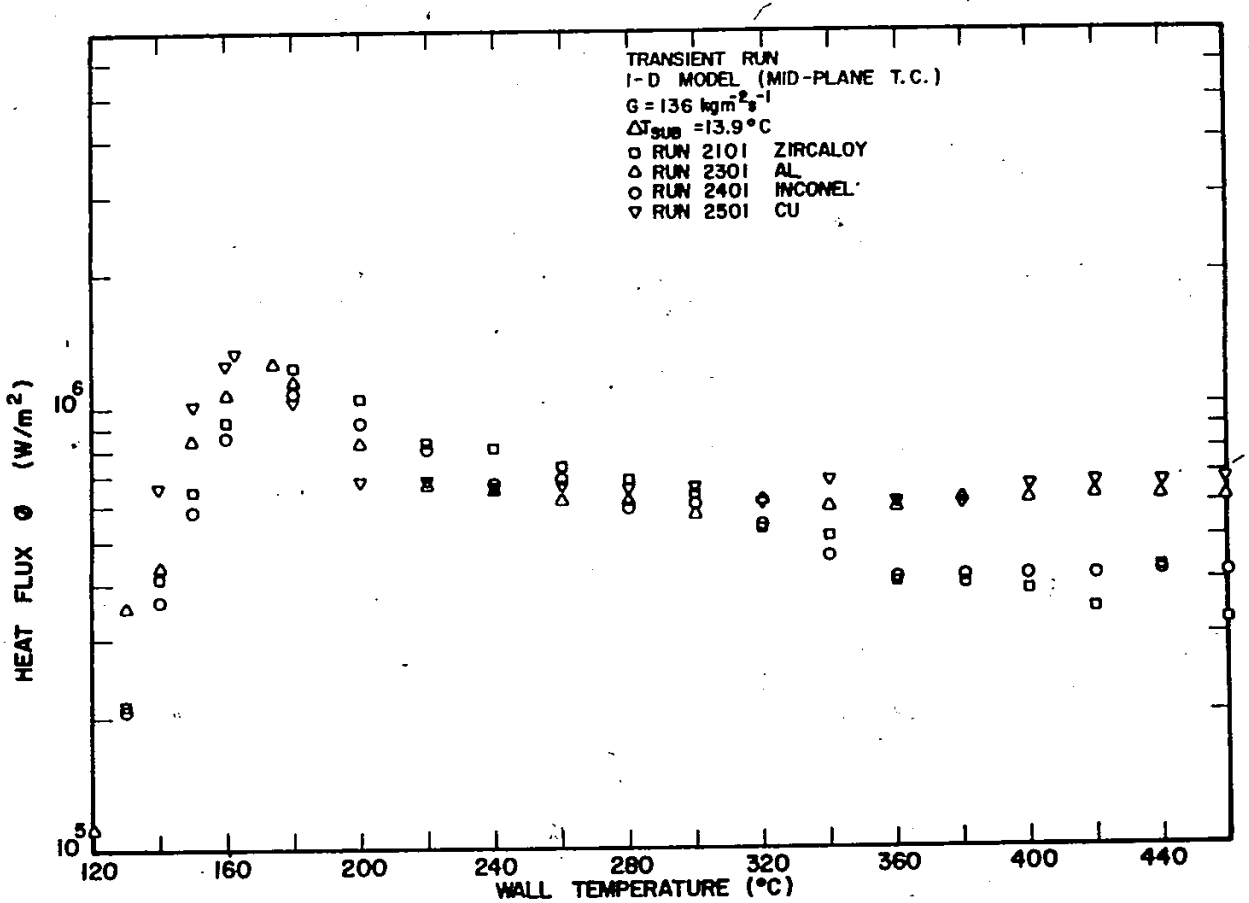

FIG. 5.12 EFFECT OF FLOW TUBE MATERIAL ON BOILING CURVE (TYPE IV TEST SECTION)

CHAPTER 6

PREDICTION OF TRANSITION BOILING HEAT TRANSFER FOR SUBCOOLED WATER AT LOW FLOW AND ATMOSPHERIC PRESSURE - A SEMI-EMPIRICAL MODEL

6.1 Introduction

This chapter presents a phenomenological model using existing correlations to predict transition boiling heat transfer for water at low flow and atmospheric pressure. The model incorporates the effects of mass flux, local enthalpy (or inlet subcooling) and thermal properties of heated surface. The proposed method establishes a general groundwork and can be easily extended after some modifications to predict transition boiling heat transfer for water as well as other fluids in the quality region at higher mass flux and higher pressure.

In developing a heat transfer correlation for the transition boiling region, several features should be sought:

(a) A correlation must have correct asymptotic trends. For example, a correlation for the transition boiling region should approach the value of film boiling heat transfer at higher wall superheats and

the critical heat flux (CHF) at lower wall superheats. Also, at a very low mass flux, the correlation should approach the value of pool boiling heat transfer.

(b) A correlation must be based on local conditions since, in many instances, the predictions deal with flow reversal situations. Under these circumstances an inlet condition is hard to define.

(c) A correlation should be based on physical understanding so that the extension to a wider range of conditions may be possible.

Although attempts have been made recently to formulate a general predictive model for the post dryout region yet better success has generally been achieved with models limited to a smaller range of conditions. Application of such models to low flow, low pressure region has become very important due to increasing studies involving heat removal from the reactor core in the absence of driving force, e.g. loss of reactor circulating pumps.

6.2 Assumptions

(a) The transition boiling mode is a combination of both unstable nucleate boiling and unstable film boiling alternately existing at any given location at the heated surface. The variation of heat

transfer rate with temperature is primarily a result of the change in the fraction of time that each boiling mode exists. This postulation is based on Berenson's description[1] which has been applied to cryogenics by Kalinin et al.[2]. The heat flux can, therefore, be expressed as

$$q_{TB} = q_{CHF}\, f + q_{FB}(1-f) \qquad (6.1)$$

where f is the fraction of surface that is wet.

(b) The fraction of wetted area f is assumed to be equal to 1 at the CHF and approaches zero at the minimum film boiling heat flux[2].

(c) The transition boiling is a violent heat transfer mode where intense mixing takes place between liquid and vapour phases. Therefore, the heat transfer coefficient is assumed to be dependent on local enthalpy and independent of heated length.

In the following section, all the terms in Eq. (6.1) will be determined for a given system pressure, flow and local enthalpy.

6.3 Formulation

6.3.1 Critical Heat Flux q_{CHF}

Basic formula. The critical heat flux is calculated based on the instability of a wave at the liquid-vapour interface using Zuber's

theory[3] of burnout. The critical heat flux for saturated pool boiling is

$$(q_{CHF})_{sat} = K\, h_{fg}\, \rho_g^{1/2} \left[\sigma g(\rho_f - \rho_g)\right]^{1/4} \quad (K = 0.12\text{-}0.15) \tag{6.2}$$

The theory provides theoretical verification of Kutateladze's equation[4], and determines the critical heat flux hydrodynamically which is independent of surface conditions. It also allows an inherent scattering of 22 percent of critical heat flux value due to the variation of K from 0.12 to 0.15.

Effect of local enthalpy. To account for the effect of subcooling ($x<0$), Kutateledze[4] proposed a semiempirical dimensionless factor that has been described by Bonilla[5], and later modified by Ivey and Morris[6].

$$(q_{CHF})_{x\leq 0} = (q_{CHF})_{sat} \left[1 + \frac{\rho_\ell}{\rho_g}^{0.75} (C_p \Delta T_{sub}/9.8\, h_{fg})\right] \tag{6.3}$$

in the above equation C_p was evaluated at

$$T' = T_{sat} - \frac{\Delta T_{sub}}{2} \tag{6.4}$$

Effect of mass flux. Based on the experimental data of Thompson and Macbeth[7] one can propose the following expression to account for the effect of mass flux

$$(q_{CHF})_{G,x\leq 0} = (q_{CHF})_{x\leq 0} \left(\frac{G}{G_{min}}\right)^{0.51} \qquad (6.5)$$

G_{min} is an arbitrary mass flux value below which the CHF approaches the pool boiling CHF.

6.3.2 Wall Temperature at CHF T_{CHF}

Bjornard and Griffith[8] suggested that T_{CHF} can be computed by Chen's correlation[9] since it is physically based and it automatically transforms into the Forester-Zuber relation for pool boiling at low flow[10]. The Chen correlation was originally derived for saturated nucleate boiling, then extended by Butterworth and Hewitt[11] to the subcooled boiling region where the F factor in Chen's correlation was set to 1 and the S factor was evaluated from the single-phase Reynolds number, GD/μ. The resulting form of correlation which is used for the present application is:

$$q_{G,x\leq 0} = F(0.023)\ \frac{k_\ell^{0.6}\, G^{0.8}\, (1-x)^{0.8}\, C_{p\ell}^{0.4}}{\mu_\ell^{0.4}\, D_e^{0.2}} (T_w - T_\ell)$$

$$+ S(0.00122)\ \frac{k_f^{0.79}\, C_{pf}^{0.45}\, \rho_f^{0.49}}{\sigma^{0.5}\, \mu_f^{0.29}\, h_{fg}^{0.24}\, \rho_g^{0.24}} (T_w - T_{sat})^{1.24} (P_w - P)^{0.75} \qquad (6.6)$$

Equating Eqs. (6.5) and (6.6), one would obtain T_w which is T_{CHF}. The solution of T_{CHF} normally requires an iterative procedure.

Effect of wall thermal properties on T_{CHF}. Magrini and Nannei[12] investigated the effect of wall thickness and thermal properties on the heat transfer of nucleate boiling. Their experiments were conducted under conditions of saturated pool boiling of water at atmospheric pressure, resulting in the following correlation

$$T_w - T_{sat} = 0.27(q)^{0.25}\left\{1 + \frac{4 \times 10^4}{\sqrt{k_w \rho_w C_{pw}}}\left[1 - e^{-4.5\times10^9 (k_w s)^3}\right]\right\}^{0.75} \quad (6.7)$$

Eq. (6.7) indicates that for a given heat flux q and wall thickness s, a heated surface with a smaller value of $k_w \rho_w C_{pw}$ will result in higher wall superheat. This confirms the present experimental data.

They found that when the wall thickness exceeds a certain value, the effect of thickness becomes negligibly small. In fact, this is the case for test sections used in the present study, thus the exponential term in Eq. (6.7) can be dropped. Furthermore, Eq. (6.7) can be rearranged to express the wall superheat of any surface material in terms of the wall superheat of copper surface under the same heat flux as

$$T_w - T_{sat} = 0.571(T_w - T_{sat})_{cu}\left(1 + \frac{4 \times 10^4}{\sqrt{k_w \rho_w C_{pw}}}\right)^{0.75} \quad (6.8)$$

where k_w, ρ_w and C_{pw} are referred to the thermal properties of any surface material. It has been found that Eq. (6.6) gives good prediction of wall superheat in nucleate boiling up to the CHF point

(when coupled with Eq. (6.5) for the copper surface. Thus for a given heat flux, the wall superheat of copper surface is obtainable from Eq. (6.6), and for the same heat flux, the wall superheat of any other surface material can be calculated via Eq. (6.8).

6.3.3 Fraction of Wetted Area f

Experimental observations[13] showed that the fraction of wetted area f during transition boiling decreases with increasing wall superheat. One can assume a possible relation between them as

$$f = a(T_w - b)^2 \tag{6.9}$$

where a and b are constants to be determined by two boundary conditions, i.e.

At $T_w = T_{CHF}$, $f = 1$;

At $T_w = T_{min}$, $f = 0$.

The expression of f then becomes

$$f = \left(\frac{T_w - T_{min}}{T_{CHF} - T_{min}}\right)^2 \tag{6.10}$$

Bjornard and Griffith[8] proposed the same expression as Eq. (6.10).

6.3.4 Minimum Stable Film Boiling Temperature T_{min}

The best available analysis that predicts the minimum surface temperature to support stable film boiling, is the model presented by Henry[14]. His correlation incorporates the effect of heated surface thermal properties of the heat transfer coefficient near the minimum film boiling point that was originally derived by Berenson[15]. Berenson's expression for the heat transfer coefficient is physically based and it combines Bromley's heat conduction model across a thin vapor film[16] with the hydrodynamic consideration of Zuber[17].

The correlation by Henry is:

$$\frac{T_{min} - (T_{min})_I}{(T_{min})_I - T_\ell} = 0.42\left[\sqrt{\frac{k_\ell \rho_\ell C_{p\ell}}{k_w \rho_w C_{pw}}}\ \frac{h_{fg}}{(\Delta T_{min})_I}\right]^{0.6} \qquad (6.11)$$

where $(T_{min})_I$ is the minimum film boiling temperature for the isothermal surface predicted by Berenson[15] and can be calculated as follows:

$$(\Delta T_{min})_I = 0.127\ \frac{\rho_g h_{fg}}{k_g}\left[\frac{g(\rho_\ell - \rho_g)}{\rho_\ell + \rho_g}\right]^{2/3}\left[\frac{\sigma}{g(\rho_\ell - \rho_g)}\right]^{1/2}\left[\frac{\mu_g}{g(\rho_\ell - \rho_g)}\right]^{1/3} \qquad (6.12)$$

6.3.5 Minimum Heat Flux q_{min}

In a series of updates to the BE (Best Estimate) Code, Hsu et al.[18] recommended Bromley's equation[16] for low void film boiling.

Bromley'sequation is based on the assumption that heat transfer through the vapor film is by molecular conduction only. Subcooled flow boiling experiments show that the film boiling heat flux can be much higher than values predicted by Bromley's equation. This could be due to the assumption that the vapor flow is laminar. It is suggested here that under flow boiling conditions, the moving liquid-vapor interface could cause the vapor flow to be turbulent. As a result, the assumption of linear temperature profile across the vapor film is not appropriate. Thus, the Bromley equation is used in the present model with a slight modification to the thermal conductivity of the vapor.

The heat transfer coefficient for film boiling given by Bromley is:

$$h_{Bromley} = 0.62 \left[\frac{k_g^3 \, g \, \rho_g (\rho_f - \rho_g) \, h_{fg}}{D \, \mu_g \, \Delta T_{sat}} \right]^{1/4} \qquad (6.13)$$

One way to account for the eddy diffusivity, is to use the simple model of Baum et al[19]. They suggested that turbulence has the effect of making heat transfer proportional to Re raised to the power of 0.8 rather than Re_0.

$$k_m = k_g \left[1 + \left(\frac{Re - Re_0}{Re_0} \right) \right]^{0.8} \qquad (6.14)$$

where Re_0 is the transition Reynolds number of 500. In the present application, a value of the vapor Reynolds number Re in the order of 10,000 was found to provide a reasonable trend in the transition boiling region when compared with experimental data.

The miminum heat flux q_{min} is then calculated by

$$q_{min} = h_{Bromley}(T_{min} - T_{sat}) \qquad (6.15)$$

This expression of q_{min} can be used to replace q_{FB} in Eq. (6.1). This is because q_{FB} in the transition boiling region is near constant for subcooled conditions and thus it can be approximated by q_{min}.[13]

6.4 Prediction

Several sets of boiling curves predicted by the present model are presented in Figs. 6.1 to 6.3 along with experimental data. Each of the boiling curves shown in these figures is constructed for a given set of parameters: mass flux, inlet subcooling and surface material. Since the model has been developed to predict heat flux as a function of local conditions, an iteration procedure was followed to calculate the local enthalpy which is in itself a function of heat flux. The iterative procedure was carried out at each point on the boiling curve and is incorporated in the computer program (Appendix III).

Figs. 6.1 to 6.3 show the effect of inlet subcooling, mass flux and heated surface material on boiling curves, respectively. In general, good agreement is observed between the predicted and experimental results in both nucleate and transition boiling regions.

In Fig. 6.3, the completed, predicted boiling curve for the copper surface is shown, this includes the film boiling region, CHF point and minimum point. Film boiling experimental data from the same surface are also added for comparison. The agreement between the predicted and experimental data in the nucleate boiling region, when Chen's correlation was used, provides more confidence in the prediction of the wall temperature at CHF. However, the present model underpredicts the film boiling data by one order of magnitude. This is not entirely unexpected. It has been shown in section 5 that film boiling is a very strong function of upstream history which itself is partially dependent on heated length. The difference in heat flux value could be as much as several orders of magnitude. In view of our very short test section, a strong entrance effect is present which tends to enhance heat transfer. No existing correlation has taken this factor into consideration.

REFERENCES

1. Berenson, P.J., "Experiments in Pool-Boiling Heat Transfer", Int. J. Heat Mass Transfer 5, 985-999, (1962).

2. Kalinin et al, "Heat Transfer in Transition Boiling of Cryogenics", Cryogenics Eng. Conf., Queen's Univ., Kingston, Ont., Canada, (1975).

3. Zuber, N., "Hydrodynamic Aspects of Boiling Heat Transfer", Ph.D. Thesis, Univ. of Calif., Los Angeles, (1959).

4. Katateladze, S.S., "A Hydrodynamic Theory of Changes in Boiling Process Under Free Convection", Izv. Akademia Nauk Otdelenie Tekh. Nauk 4, 529-536, (1951).

5. Bonilla, C.F., Nuclear Engineering, McGraw-Hill, New York, 399-431, (1957).

6. Ivey, H.J. and Morris, D.J., "On the Relevance of the Vapor-Liquid Exchange Mechanism for Subcooled Boiling Heat Transfer at High Pressure", AEEW-R137, (1962).

7. Thompson, B. and Macbeth, R.V., "Boiling Heat Transfer Burnout in Uniformly Heated Round Tubes: A Compilation of World Data with Accurate Correlations", AEEW-R356, (1964).

8. Bjornard, T.A. and Griffith, P., "PWR Blowdown Heat Transfer", Symposium on the Thermal Hydraulic Aspects of Nuclear Reactor Safety, ASME, New York, (1977).

9. Chen, J.C., "A Correlation for Boiling Heat Transfer to Saturated Fluids in Convective Flow", ASME Paper No. 63-HT-34, (1963).

10. Forster, H.K. and Zuber, N., "Dynamics of Vapor Bubbles and Boiling Heat Transfer, AEChE J. 1, 531-535, (1955).

11. Butterworth, D. and Hewitt, G.F., Two-Phase Flow and Heat Transfer, Harwell Series, Oxford University Press, 219, (1977).

12. Magrini, U. and Nannei, E., "On the Influence of Thickness and Thermal Properties of Heating Walls on the Heat Transfer Coefficients in Nucleate Pool Boiling", J. Heat Transfer 97, 173-178, (1975).

13. Ragheb, H.S. and Cheng, S.C., "Surface Wetted Area During Transition Boiling in Forced Convective Flow", J. Heat Transfer 101, 381-383 (1979).

14. Henry, R.E., "A Correlation for the Minimum Film Boiling Temperature", AIChE Symposium Series 70, 138, 81-90, (1974).

15. Berenson, P.J., "Transition Boiling Heat Transfer from a Horizontal Surface", J. Heat Transfer 83c, 351-358, (1961).

16. Bromley, L.A., "Heat Transfer in Stable Film Boiling", Chem. Eng. Prog. Symp. Ser. 46, 221-227, (1950).

17. Zuber, N., "Stability of Boiling Heat Transfer", Trans. ASME 80, 711-720, (1958).

18. Hsu, Y.Y. and Sullivan, L., "Updating of 'Best-Estimate' Heat Transfer Recommendation for Transient CHF and Post-CHF Heat Transfer Modes", CSNI Meeting on Two-Phase Flow, Los Angeles, (1981).

19. Baum, A.J., Purcupile, J.C. and Dougall, R.S., "Transition and Film Boiling Heat Transfer from Vertical Surfaces", ASME Paper No. 77-HT-82, (1977).

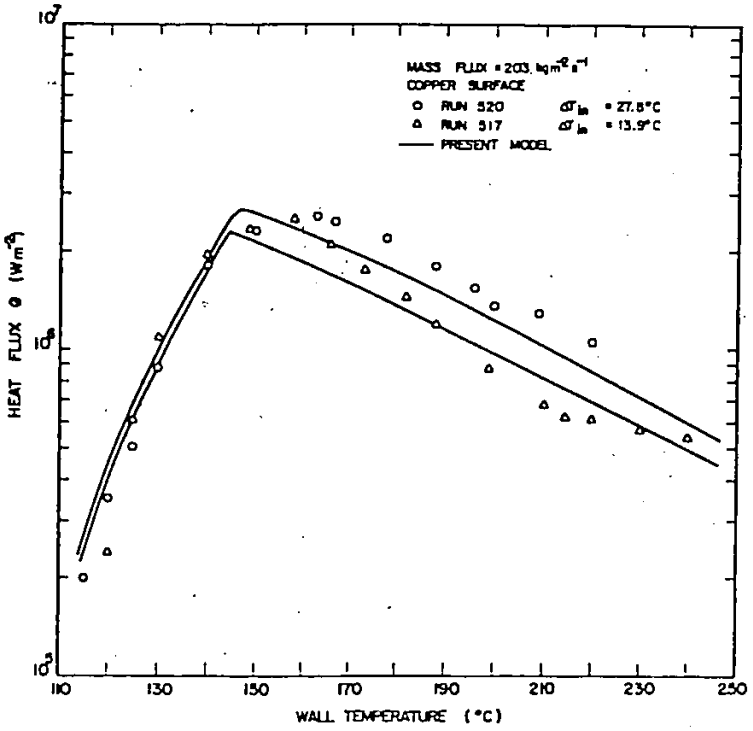

Fig. 6.1 Effect of Subcooling on Boiling Curves of Distilled Water, 500 Run Series at 203 kg/m^{2}s.

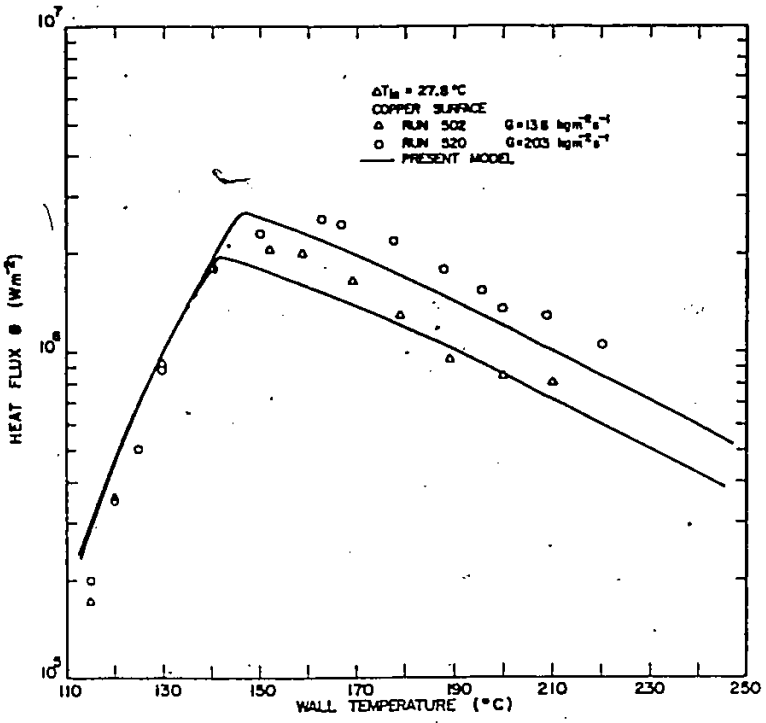

Fig 6.2 Effect of Mass Flux on Boiling Curves of Distilled Water, 500 Run Series at $\Delta T_{in} = 27.8^{o}C$.

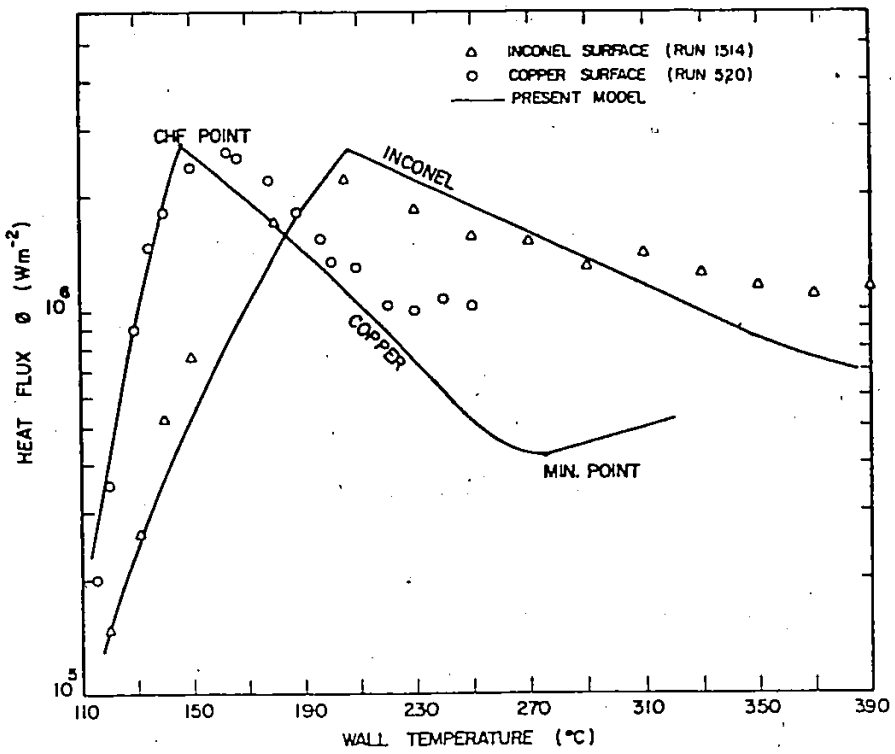

Fig 6.3 Comparison of Boiling Curves for Copper Test Section and Inconel-Copper Test Section at $G = 203\ kg/m^2s$ and $\Delta T_{in} = 27.8^{o}C$.

CHAPTER 7

PREDICTION OF TRANSITION BOILING HEAT TRANSFER FOR SUBCOOLED WATER AT LOW FLOW AND ATMOSPHERIC PRESSURE

7.1 Introduction

In this chapter, an analytical model to predict heat transfer during transition boiling is presented. The model is based on hydrodynamic considerations and is limited to the conditions of the tests, namely subcooled low flow in a vertical conduit near atmospheric pressure.

The present analysis makes use of Baum's[1] approach in analyzing the transition region in pool boiling on outside surfaces. He postulated that in inverted annular flow, the oscillations of the wavy interface are repelled from the wall by vapour being compressed as the wave approaches the wall. This mechanism is applied, in the present analysis, to subcooled flow boiling inside a vertical tube. The wave length is based on the instability of a harmonic wave travelling along a vertical liquid-vapour interface. A sketch for the flow regime analyzed is shown in Fig. 7.1.

The flowing two-phase mixture is considered as divided into an annulus vapour film and a liquid core. The mass, momentum and energy equations for the vapour annulus are solved. Heat transfer from the wall is a sum of two components; a convective component assuming laminar vapour flow adjacent to the wall and a liquid-wall conduction component assuming instantaneous contact between the oscillating wave and the wall. The effects of mass flux, wall thermal properties and degree of subcooling are also modelled. This is a unique feature of the analysis since no other analysis has reflected these effects before.

7.2 Assumptions

The following assumptions are made in order to obtain a simplified form of the momentum, continuity and energy equations:

(a) The liquid-vapour geometry is given in Fig. 7.1.

(b) Near the minimum heat flux, the wave length is unaffected by the vapour velocity and the vapour film thickness.

(c) The vapour film thickness is assumed constant in the order of 10^{-4} meter (Ref. 2).

(d) Heat is transferred through the vapour by convection. Radiation is assumed to be negligible, since the range of temperatures encountered during transition boiling in the present application is less than 600°C.

(e) Vapour flow is steady one-dimensional.

(f) Vapour generated at the liquid-vapour interface within the half wave length will eventually escape in the liquid core. This has been observed and reported earlier by this author (see section 2.2.2).

(g) The wall temperature below which the liquid-wall contact occurs is known and is set equal to the experimental T_{min} value. It can also be calculated using the proposed method by this author (see section 6.3.4).

(h) Liquid core velocity is very small compared with vapour film velocity, i.e., $V_l << V_v$.

(i) The shape of the liquid wave does not change during the contact period.

7.3 Mechanism

Referring to Fig. 7.1, the oscillations of the liquid-vapour interface do not contact the heated wall during film boiling. During their approach to the wall they are decelerated by vapour compression forces. This vapour is generated at the liquid-vapour interface due to heat transferred from the wall by convection. At the minimum film boiling point, vapour compression forces perform just enough work to bring the oscillations tangentially in contact with the wall. As the wall temperature decreases, vapour compression forces become weaker so that wave spikes will contact the wall before enough work is performed

by vapour forces to repel the wave. After the contact with the wall, vapour forces continue to perform work until the wave is repelled.

During the liquid-solid contact, heat transfer from the wall is augmented by an additional component, namely conduction between the wall and the subcooled liquid. As the wall temperature decreases the duration and extent of contact increases, thus leading to the observed trend in transition boiling where heat transfer increases with the decrease in surface temperature.

7.4 Wave Geometry

A review of the methods of application of the wave theory to the instability of liquid-vapour interface is presented in Appendix II. From the examples given in Appendix II, it seems appropriate that the postulated wavy interface in the present analysis can be treated using the Helmholtz instability, where the vertical interface stabilizes under the forces of surface tension and effects of relative velocity.

Referring to Fig. 7.2.a, Equation (II.2) can be simplified by the following assumptions which are valid for a vertical surface with forced convection:

$g = 0$ (vertical interface)

$\coth md = 1$ ($D_w = d = \infty$); the effect of vapour film thickness on the wave length is negligible[2] (7.1)

Combining Equations (7.1) and (II.2) results in the following expression for c:

$$c^2 = \frac{\sigma m}{\rho_l + \rho_v} - \frac{\rho_l \rho_v (V_v - V_l)^2}{(V_v - V_l)^2} \qquad (7.2)$$

and $$\lambda_c = 2\pi \sqrt{\frac{\sigma (\rho_l + \rho_v)}{\rho_l \rho_v (V_v - V_l)^2}} \qquad (7.3)$$

It can be seen from the above equation that for given system conditions the fluid properties (σ, ρ_l & ρ_v) are fixed. Therefore, the critical wave length is determined by the relative velocity of liquid and vapour. At atmospheric pressure: $\rho_v = 0.59$ kg/m^3 ($\rho_l >> \rho_v$) and $\sigma = 58.78 \times 10^{-3}$ $\frac{N}{m}$, thus

$$\lambda_c = \frac{0.6}{(V_v - V_l)^2} \text{ m} \qquad (7.4)$$

In this model the critical wave length λ_c is assumed in the order of 2.0 cm. Using this value in Equation (7.4) we get

$$V_v - V_l = 5.47 \text{ m/s}$$

In the present experiment $V_l = 0.2$ m/s, therefore the critical vapour velocity at the minimum film boiling point is expected to be $\simeq$5.67 m/s. This vapour velocity is to be verified by the predictions

of section 7.7. It will shown that the predicted average velocity is within 15% of the expected value.

7.5 Governing Equations

7.5.1 Momentum Equation

Momentum equation in cylindrical coordinates (r, θ, z) for the steam phase with constant ρ and μ in the z direction

$$\rho\left(\frac{\partial V_z}{\partial t} + V_r\frac{\partial V_z}{\partial r} + \frac{V_\theta}{r}\frac{\partial V_v}{\partial \theta} + V_z\frac{\partial V_z}{\partial z}\right) = \frac{-\partial p}{\partial z}$$

$$+ \mu\left(\frac{1}{r}\frac{\partial}{r}\left(r\frac{\partial V_z}{\partial r}\right) + \frac{1}{r^2}\frac{\partial^2 V_z}{\partial \theta^2} + \frac{\partial^2 V_z}{\partial z^2}\right) + \rho g_z \qquad (7.5)$$

7.5.2 Continuity Equation

$$\frac{\partial \rho}{\partial t} + \frac{1}{r}\frac{\partial}{\partial r}(\rho r v_r) + \frac{1}{r}\frac{\partial}{\partial \theta}(\rho v_\theta) + \frac{\partial}{\partial z}(\rho v_z) = 0 \qquad (7.6)$$

7.5.3 Heat Transfer

Heat transferred from the wall is a sum of two components:

1) Heat removal by instantaneous liquid-solid contact during contact periods (see Fig. 7.3.a), calculated by the model proposed by Bankoff and Mehra[3]; and

2) Heat removal by convective flow of vapour over the wall during the contact and non-contact period (see Fig. 7.3.b), calculated based on laminar flow.

Instantaneous Liquid-solid Contact Component

When the liquid of the oscillating wave at temperature T_l is brought into contact with the wall whose initial temperature is T_w, the interface immediately achieves temperature T_i which is invariant with time[4] and is given by

$$\frac{T_w - T_l}{T_i - T_l} = \sqrt{\frac{\rho_l \, C_{p_l} \, k_l}{\rho_w \, C_{p_w} k_w}} \qquad (7.7)$$

The transient conduction between the liquid and the solid is illustrated in Fig. 7.4. The predicted temperature at the interface was used by Bankoff and Mehra[3] and Henry[5] in developing their models.

The total heat transferred per contact to the liquid is determined by

$$q = 2k_l(T_i - T_l) \left(\frac{t_c}{\pi \alpha_l}\right)^{1/2} \qquad (7.8)$$

where t_c is the mean length of the contact period. Defining the thermal boundary layer thickness by

$$y = 4 \left(\frac{\alpha t_c}{\pi} \right)^{1/2} \tag{7.9}$$

Equation (7.8) can be written as:

$$q = \frac{(T_i - T_l)}{2} \frac{k_l}{\alpha_l} y \tag{7.10}$$

To account for the effect of liquid core mass flux, it is assumed here that turbulence will make the heat transfer proportional to $R_e^{0.8}$. Therefore, the normal conductivity k_l in the above equation can be modified[1] as follows:

$$k = k_l \left(1 + \frac{R - R_{eo}}{R_{eo}}\right)^{0.8} \tag{7.10.a}$$

where R_{eo} is the transition Reynolds number of 500.

The heat flux by conduction q_d is expressed as

$$q_d = q.f \tag{7.11}$$

where f is the frequency of the contacts. The heat flux is then weighted by the wetted area which is predicted from the wave position relative to the wall after contact (see section 7.7).

Heat Convection Component

Heat transferred by steam convection is based on the assumption that the flow is laminar between the wall and the liquid surface. The heat transfer coefficient is based on the Nusselt number for laminar flow between flat plates which has a value of 4.11. Referring to the geometry of a vapour flow element in Fig. 7.2.b.:

$$Nu = \frac{h\, R(1-\beta)}{k_v} = 4.11$$

The heat flux component of convection is determined by

$$q_v = 4.11\, \frac{k_v\, \Delta T}{R(1-\beta)} \left[2\, \pi\, (\beta R) \sqrt{1 + \left(\frac{d\beta}{dz}\right)^2 R^2}\; dz \right] \qquad (7.12)$$

where ΔT is the temperature difference between the wall and the liquid core.

7.6 Procedure to Formulate the Problem in Cylindrical Coordinates

1. Use Navier-Stokes equations to obtain a relationship between the pressure gradient and the velocity profile for the concentric annulus element of steam shown in Fig. 7.2.a.

2. Knowing the velocity profile, calculate the average velocity as a function of the pressure gradiant.

3. Calculate the average velocity based on the evaporation at the liquid vapour interface. The average steam velocity will be a function of wall temperature.

4. From (2) and (3) obtain an expression for the pressure in the vapour phase as a function of wall temperature and steam properties.

5. Having determined the pressure, calculate the force acting on the approaching wave and integrate it with respect to distance from the wall to obtain the energy dissipated. This energy is calculated first for a wall temperature equal to the minimum film boiling temperature which is assumed to be known.

6. Repeat steps (1) to (5) for a lower temperature. More energy will be dissipated after contact with the wall. The duration of contact will end when compression forces repell it.

7. Knowing the time and velocity of approaching wave, determine the area of contact.

8. Calculate heat transferred from the wall by convection (during non-contact and contact periods) and by conduction to liquid (during contact periods).

7.7 Solution of the Momentum and Continuity Equations

Based on assumption (f), Equation (7.5) reduces to

$$\rho_v \; V_z \frac{\partial V_z}{\partial z} = - \frac{\partial p}{\partial z} + \mu \left(\frac{1}{r} \frac{\partial}{\partial r} \left(r \frac{\partial V_z}{\partial r} \right) + \frac{\partial^2 V_z}{\partial z^2} \right) \tag{7.13}$$

Also, equation (7.6) reduces to

$$\frac{\partial V_z}{\partial z} = 0 \tag{7.14}$$

Substituting (7.14) in (7.13) gives

$$0 = - \frac{\partial p}{\partial z} + \mu \left[\frac{1}{r} \frac{\partial}{\partial r} \left(r \frac{\partial V_z}{\partial r} \right) \right] \tag{7.15}$$

Boundary Conditions

1) at $r = R$, $V_z = 0$ (no slip)

2) at $r = \beta R$, $V_z = 0$ (no slip)

(β is a function of z)

Integrating Equation (7.15) w.r.t. r

$$-\left(\frac{\partial p}{\partial z}\right)\frac{r^2}{2} + \mu\, r\, \frac{\partial V_z}{\partial r} + C_1 = 0 \qquad (7.16)$$

Integrating again,

$$-\left(\frac{\partial p}{\partial z}\right)\frac{r^2}{4} + \mu\, V_z + C_1 \ln r + C_2 = 0 \qquad (7.17)$$

Boundary condition (1) gives

$$-\left(\frac{\partial p}{\partial z}\right)\frac{R^2}{4} + C_1 \ln R + C_2 = 0 \qquad (7.18)$$

Boundary condition (2) gives

$$-\left(\frac{\partial p}{\partial z}\right)\frac{\beta^2 R^2}{4} + C_1 \ln \beta \; R + C_2 = 0 \qquad (7.19)$$

subtracting (7.18) from (7.19)

$$C_1 \ln \frac{\beta R}{R} + \frac{\partial p}{\partial z}\left(-\frac{\beta^2 R^2}{4} + \frac{R^2}{4}\right) = 0 \qquad (7.20)$$

Substituting (7.20) and (7.18) in (7.17) we get

$$-\frac{\partial p}{\partial z}\frac{r^2}{4} + \mu V_z + \frac{\partial p}{\partial z}\frac{R^2}{4} + \frac{\frac{\partial p}{\partial z}\frac{R^2}{4}(\beta^2 - 1)}{\ln \beta} \ln\left(\frac{r}{R}\right) = 0$$

or

$$V_z = \frac{1}{\mu}\frac{\partial p}{\partial z}\left[\frac{r^2}{4} - \frac{R^2}{4} - \frac{R^2}{4}\frac{(\beta^2 - 1)}{\ln \beta}\ln\left(\frac{r}{R}\right)\right]$$

$$V_z = -\frac{\partial p}{\partial z}\frac{R^2}{4\mu}\left[1 - \frac{r}{R}^2 + \frac{\beta^2 - 1}{\ln \beta}\ln\left(\frac{r}{R}\right)\right] \qquad (7.21)$$

The average vapour velocity is

$$\bar{V}_z = \frac{\int_0^{2\pi}\int_{\beta R}^{R} V_z \, r \, dr \, d\theta}{\int_0^{2\pi}\int_{\beta R}^{R} r \, dr \, d\theta} = -\left(\frac{\partial p}{\partial z}\right)\frac{R^2}{8\mu}\left(\frac{1-\beta^4}{1-\beta^2} + \frac{1-\beta^2}{\ln \beta}\right) \qquad (7.22)$$

$\bar{V}_z$ in the above equation can be determined from a heat balance at the liquid-vapour interface. The vapour flow $\Delta M°$ generated at the interface is due to the convective component q_v of equation 7.12. Therefore $\Delta M°$ can be expressed as

$$\Delta M° = \frac{q_v}{h_{fg}} \qquad (7.23)$$

The total vapour flow through the flow element is related to $\bar{V}_z$ by

$$M° + \Delta M° = \rho_v A \bar{V}_z = \rho_v \bar{V}_z \pi (1-\beta^2) R^2 \qquad (7.24)$$

where $M°$ is the vapour flow from the upstream element shown in Fig. 7.2.b.

Eliminating q_v and $\Delta M°$ from Equations (7.12), (7.23) and (7.24) and solving for $\bar{V}_z$ yields the following

$$\left[-M^{\circ}h_{fg} + \bar{V}_z\,\rho_v\pi\,(1-\beta^2)\,R^2\right]h_{fg} = \frac{k_v\,\Delta T}{R(1-\beta)}\left[2\,\pi\,(\beta R)\sqrt{1+\left(\frac{d\beta}{dz}\right)^2 R^2}\;dz\right] \quad (7.25)$$

or

$$\bar{V}_z = \frac{2\,k_v\beta\,\Delta T\,R\sqrt{1+\left(\frac{d\beta}{dz}\right)^2 R^2}\,dz + M^{\circ}\,h_{fg}\,R\,(1-\beta)}{\pi\rho_v\,h_{fg}\,R^3\,(1-\beta^2)\,(1-\beta)} \quad (7.26)$$

By substituting the above expression for $\bar{V}_z$ into equation 7.22, the pressure gradient can be determined as

$$\frac{\partial P}{\partial z} = -\frac{8\mu}{R^2\left(\frac{1-\beta 4}{1-\beta^2}+\frac{1-\beta^2}{1n\beta}\right)} \cdot \frac{2\,k_v\beta\,\Delta T\,R\sqrt{1+\left(\frac{d\beta}{dz}\right)^2 R^2}\,dz + M^{\circ}\,h_{fg}\,R\,(1-\beta)}{\pi\rho_v\,h_{fg}\,R^3\,(1-\beta^2)\,(1-\beta)} \quad (7.27)$$

Integrating to determine pressure distribution and integrating again to obtain the force acting on the liquid surface

$$F = \beta R\int_0^{2\pi}\int_0^{\lambda/2}\int_0^{z}\frac{\partial p}{\partial z}\,d_z\,d_z\,d\theta \quad (7.28)$$

The motion of the oscillation can be determined by integrating the force as a function of position normal to the wall. For each step change in wave position while approaching the wall, the work done by this force $F\,\Delta r$ is equivalent to the loss of kinetic energy of the wave mass $1/2\,m\Delta V^2$, i.e.

$$F\,\Delta r = \frac{1}{2}\,m\Delta V^2 \quad (7.29)$$

where

m = mass of wave

V = approach velocity of the wave

The total work done by vapour forces is equal to the total change in wave kinetic energy

$$\int_{r = R - d}^{r = R} F dr = \Delta KE \qquad (7.30)$$

The left hand side of the above equation is a function of the wall temperature. At the minimum temperature, the work done is just enough to decelerate the wave and make the wave velocity V = 0. It is assumed in this model that the minimum temperature is known and equal to the measured value in the experiment. Therefore, the work done by vapour compression force at the minimum temperature can be determined. This energy is referred to as E_{min} which is defined as

$$E_{min} = \int_{r = R - d}^{r = R} F dr \qquad (7.31)$$

As the wall temperature decreases, vapour compression force becomes weaker, so that at the time of contact the work done is less than E_{min}. It will take some time after the contact for the work done by compression force to reach E_{min} and to repel the wave. The contact time can, therefore, be calculated by integrating the velocity of the approaching wave with respect to the distance from the wall.

The shape of the oscillating wave approaching the wall during and before contact is shown in Fig. 7.3 a and b respectively. It is assumed that the shape of the wave does not change during contact. The wetted area can, therefore, be calculated from the relative position of the wave and the wall as shown in Fig. 7.3 a.

7.8 Results

A computer program has been constructed to perform a numerical integration of equations (7.11), (7.12) and equations (7.22) to (7.28). A listing of the computer program is given in Appendix IV. The program has a built-in water properties table and a subroutine to interpolate and extrapolate between lines.

Fig. 7.5 shows the model predictions at mass flux of 136 kg/m^2 for different degrees of subcooling on a copper surface (series 500). The agreement is good and reflects the correct observed trend, i.e.,

heat transfer decreases with the increase of surface temperature and increases with the increase of the degree of liquid subcooling.

The comparison of the predictions at different mass fluxes with the experimental measurements is shown in Fig. 7.6. The effect of mass flux in the predictions appears to agree with experimental measurements. A further verification for the model was made by comparing its predictions with the pool boiling data of Ref. 6. The comparison is shown in Fig. 7.6 and it provides also a good agreement.

The effect of wall thermal properties was predicted as shown in Fig. 7.7 in the comparison of copper and Inconel surfaces (series 500 and 1500) and provides the correct trend.

The vapour velocity at the minimum film boiling point is predicted to be in the range 4.2 to 6.4 m/s (see Appendix IV). The assumed value of 5.67 m/s lies within this range.

REFERENCES

1. Baum, A.J., Purcupile, J.C., and R.S. Dougall. "Transition and Film Boiling Heat Transfer From Vertical Surfaces, ASME paper 77-HT-82, August (1977).

2. Berenson, P.J. "Film Boiling Heat Transfer From Horizontal Surface", J. of Heat Transfer, pp. 351-358, August (1961).

3. Bankoff, S.G. and V.S. Mehra. "A Quenching Theory For Transition Boiling", I&EC Fundamentals, Vol. 1, No. 1, February (1962).

4. Carslaw, H.S. and J.G. Jaeger. "Conduction of Heat in Solids", 2nd Ed., p. 88, Oxford University Press, Oxford (1959).

5. Henry, R.E. "A correlation For the Minimum Film Boiling Temperature", AICLE Symposium Series, No. 138, Vol. 70.

6. Thibault, J. and Hoffman, T.W. "Local Boiling Heat Flux Density Around A Horizontal Cylinder Under Saturated and Subcooled Conditions", 6th International Heat Transfer Conference, Toronto, Canada, August (1978).

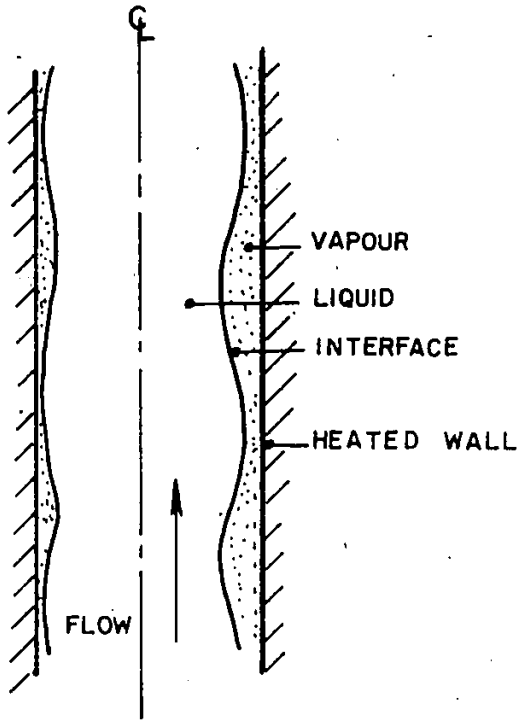

FIG. 7.1 UPWARD FLOW IN CYLINDRICAL CONDUIT

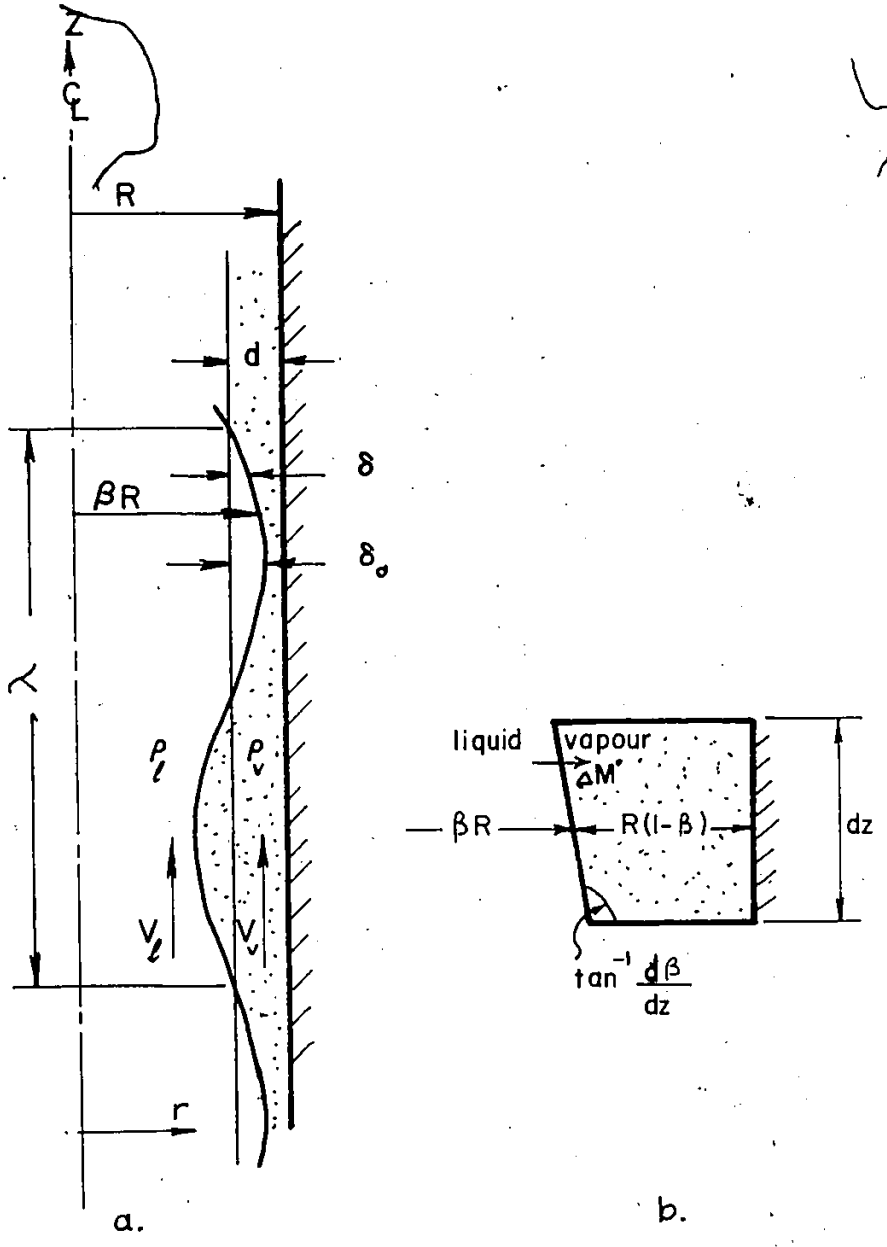

FIG. 7.2 GEOMETRY OF LIQUID-VAPOUR INTERFACE

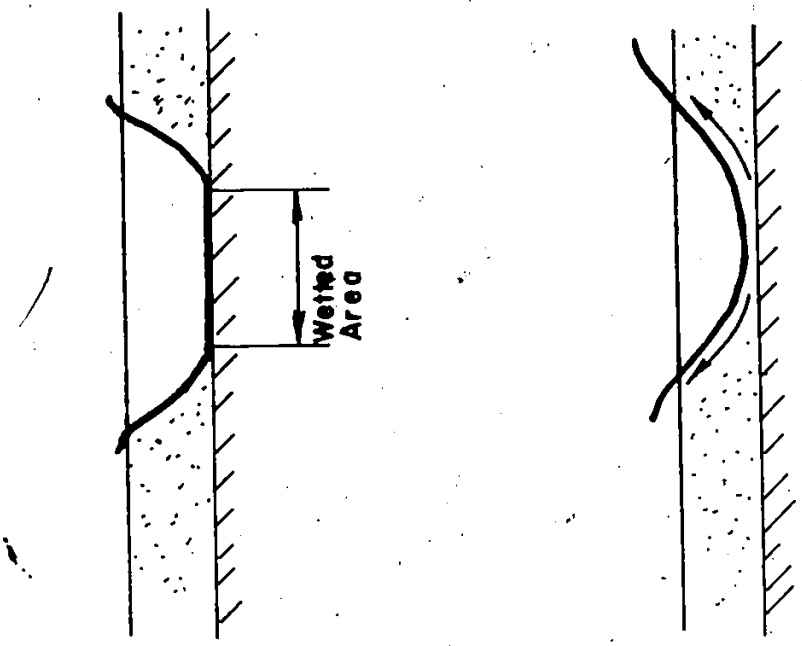

FIG. 7.3 GEOMETRY OF WAVE DURING AND BEFORE CONTACT

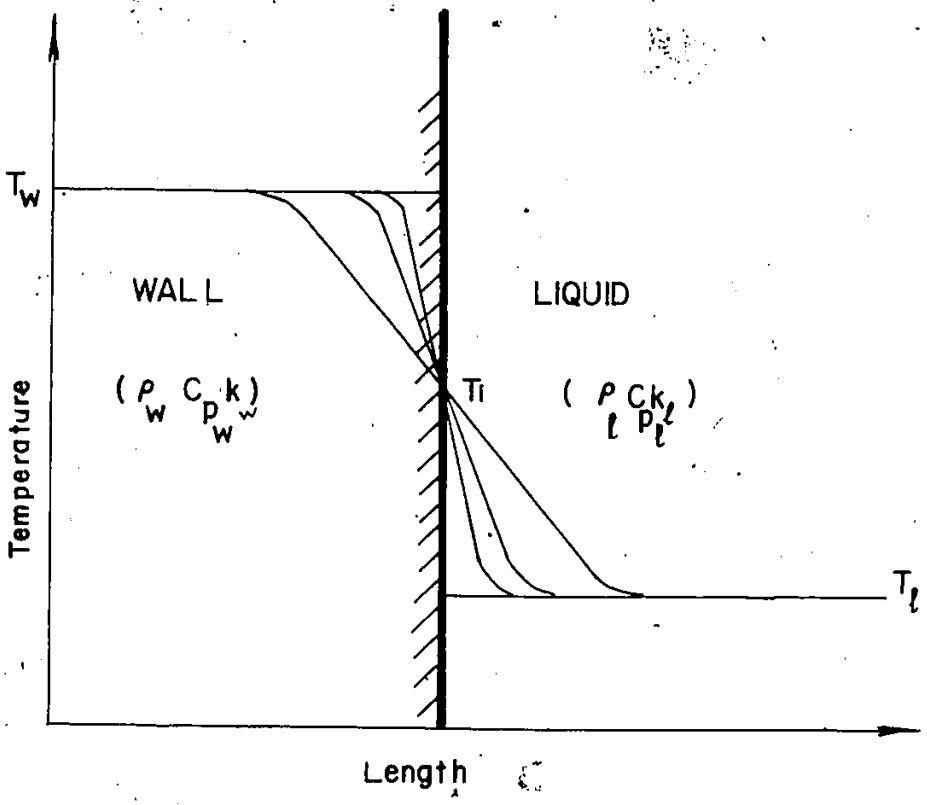

FIG. 7.4 TEMPERATURE TRANSIENTS IN SOLID AND LIQUID DUE TO INSTANTANEOUS CONTACT

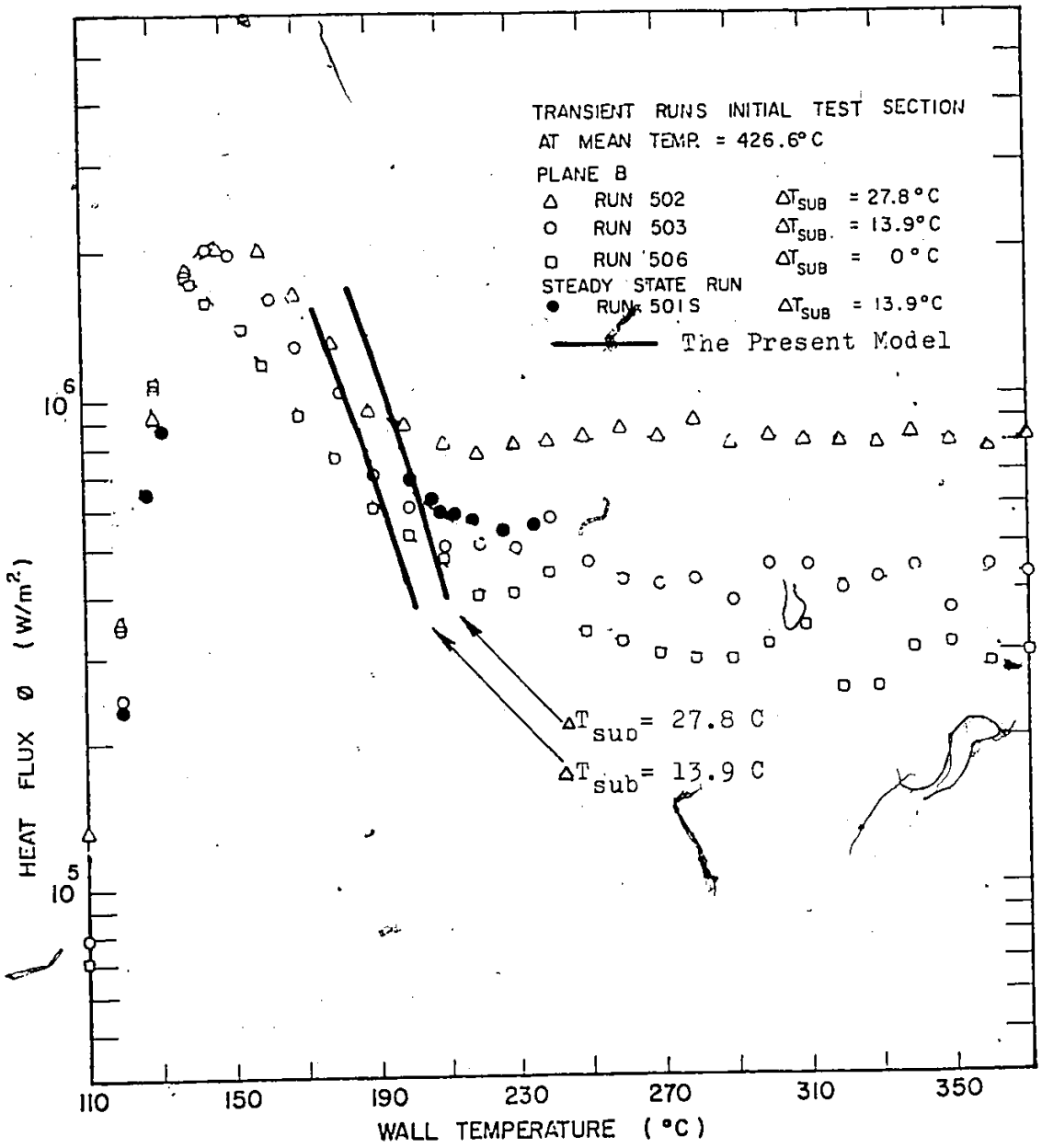

FIG. 7.5 EFFECT OF SUBCOOLING ON BOILING CURVES OF DISTILLED WATER, 500 RUN SERIES FOR G = 136 kg/m²s

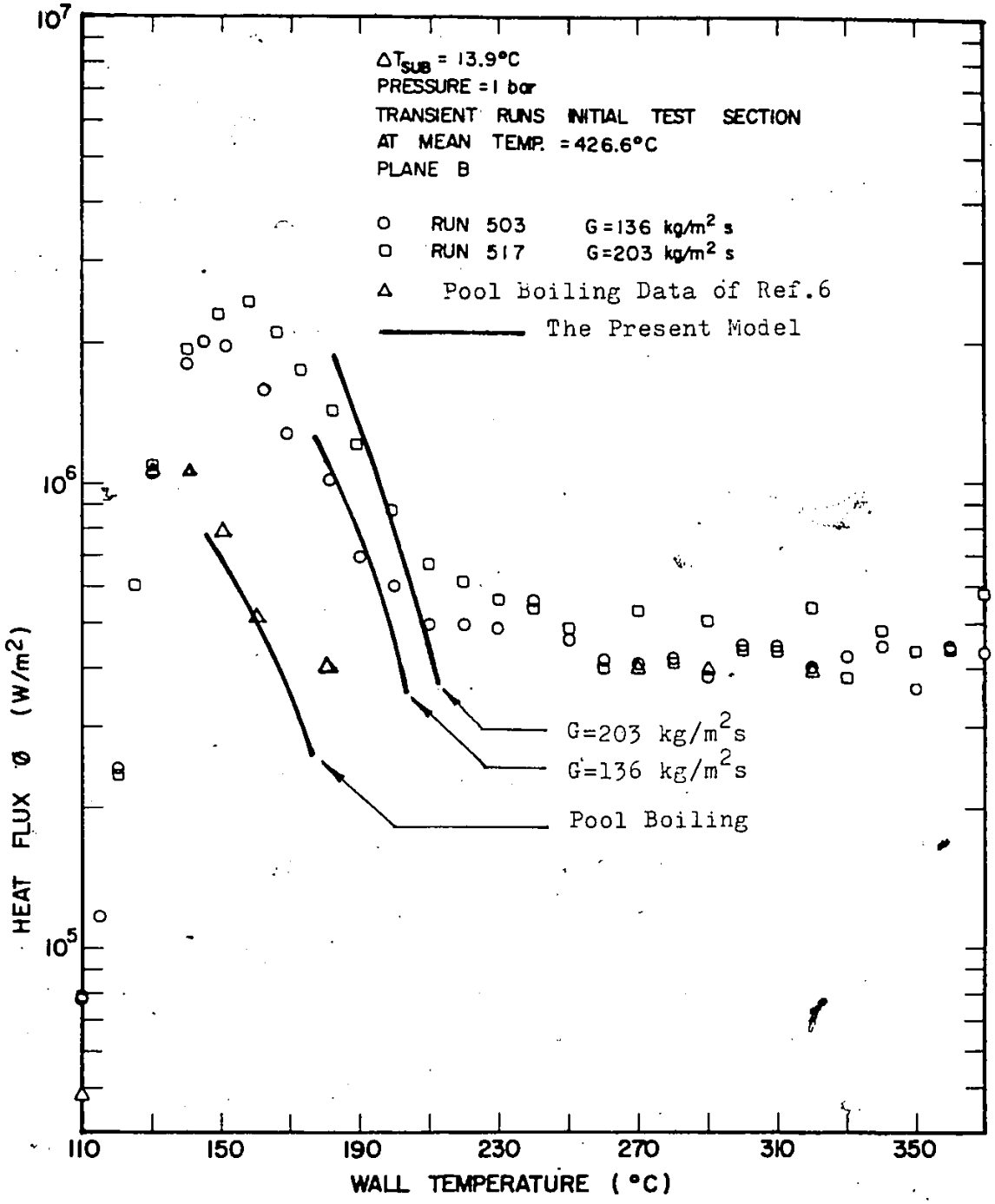

FIG. 7.6 EFFECT OF MASS FLUX ON BOILING CURVES FOR DISTILLED WATER, 500 RUN SERIES AT ΔT_{SUB} = 13.9°C

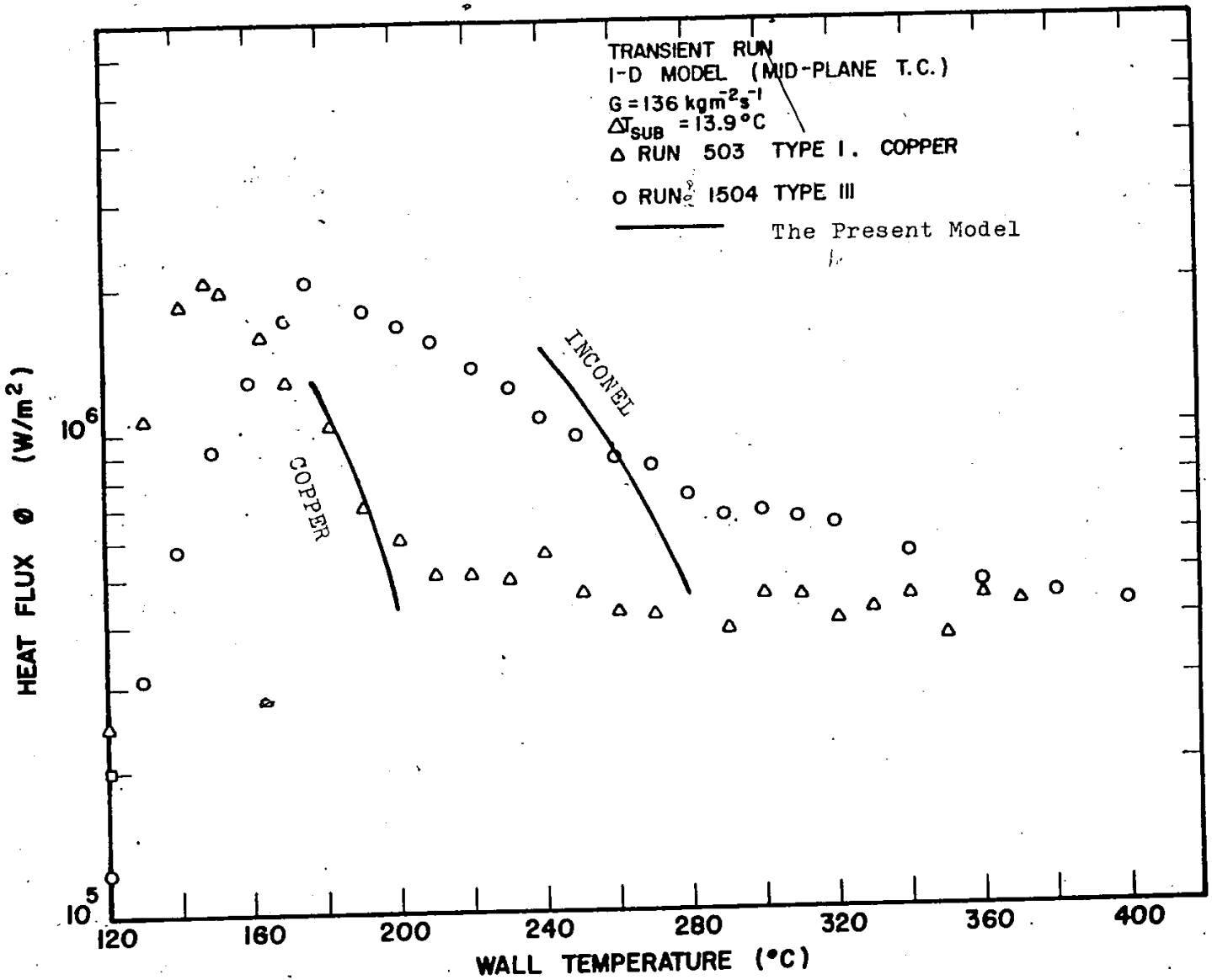

FIG. 7.7 COMPARISON OF BOILING CURVES OBTAINED FROM TYPE I AND TYPE III TEST SECTIONS: EFFECT OF HEATED SURFACE PROPERTIES

CHAPTER 8

CONCLUSIONS AND FINAL REMARKS

1. Mass flux and inlet subcooling are important parameters in transition boiling. Heat transfer increases with increasing mass flux and subcooling within the range of the flow parameters investigated; mass flux range 68 - 203 $kg.m^{-2}.s^{-1}$ and subcooling range 0 - 28°C.

2. Boiling curves generated from mid-plane thermocouples using the 1-D model represent the average heat flux for the test section and agree with the steady state data.

3. The agreement between the steady state and transient boiling curves suggests that the transient technique using a high thermal inertia test section is a simple and effective method of obtaining transition boiling data.

4. Upstream history can have a strong effect on the boiling curve. The presence of a vapour blanket just upstream of a transition boiling section tends to reduce the transition boiling heat flux considerably.

5. The heated surface properties have a strong effect on the boiling curve:
   (i) an increase in k (or $\rho k c_p$) decreases the transition boiling heat transfer coefficient.

(ii) the effect of heated surface material on CHF or the minimum heat flux is small.

(iii) an increase in k (or $\rho k c_p$) decreases the wall superheat at CHF and at rewetting (this is in agreement with the experiments carried out elsewhere).

6. A transition boiling correlation may be considered reliable if it reflects the parametric effects discussed in this study. Present transition boiling correlations do not reflect such effects.

7. An analytical model has been developed to predict transition boiling test transfer for water at low flow and atmospheric pressure. The model incorporates effects of mass flux, local enthalpy and thermal properties of heated surface. Comparison of the predicted results with experimental data show fair agreement in the transition boiling region.

APPENDIX I

Computer Program for the Two-Dimensional Conduction Model

```
                ****CONTINUOUS SYSTEM MODELING PROGRAM****

        ***PROBLEM INPUT STATEMENTS***

/       DIMENSION R(30)
 FIXED NPOINT
 FIXED IK
 FIXED IT
 PARAM CK=379.049,CSP=345.186,CRHO=4938.323
 PARAM SK=17.31,SSP=435.427,SRHO=6169.415
 INITIAL
 IK=10
 X=1.0
 Z=1.0
 CALPHA=(1.0/0.23)*2.581E-05
*
*
*
*
**
************* RUN 1502 , 300 C INIT TEMP, 25 F SUBC, 2 GMS**************
 T25=603.9
 T252=596.8
 DT5=5.0
 T24=604.3
 T242=597.2
 DT4=5.2
 T23=604.3
 T232=595.4
 DT3=4.0
 T22=604.5
 T222=590.9
 DT2=4.4
 T21=604.1
 T212=594.2
 DT1=4.0
DTDT21=(T212-T211)/DT1
 DTDT22=(T222-T221)/DT2
 DTDT23=(T232-T231)/DT3
 DTDT24=(T242-T241)/DT4
DTDT25=(T252-T251)/DT5
 RIN=(0.47/(2.0*12.0))*0.3048
 DELRO=(0.015/12.0)*0.3048
 RO=RIN+DELRO
 L=(2.0/12.0)*0.3048
 DELZ=(21.0/(64.0*12.0))*0.3048
 DELZ1=DELZ
 DELZ2=DELZ
 DELZ3=(22.0/(64.0*12.0))*0.3048
 DELZ4=DELZ3
 DZ13HF=(DELZ+DELZ3)/2.0
 DZ14HF=DZ13HF
 DZSQ=DELZ**2
 DELR=(ROUT-RIN-DELRO)/NPOINT
  DRSQ=DELR**2
 DZ12HF=(DELZ+DELZ1)/2.0
 DZ12= DZ12HF
 DZ22HF=(DELZ+DELZ2)/2.0
 DZ22= DZ22HF
 CKD =DELR*CK
 SKDRO=SK*DELRO
CRCSP=CRHO*CSP
SRCSP=SRHO*SSP
 ROUT=(3.75/(2.0*12.0))*0.3048
 NPOINT=9
 DL=(RO+DELR/2.0)**2-(RO-DELRO/2.0)**2
 KM=SK*(RO**2-(RO-DELRO/2.0)**2)/DL+X*CK*((RO+DELR/2.0)**2-RO**2)/DL
 C1=((RO**2-(RO-DELRO/2.0)**2)*SRCSP+((RO+DELR /2.0)**2-RO**2)            ...
      *CRCSP)/DL
 C2=2.0/((DELR+DELRO)*DELR)+1.0/(2.0*RO*DELR)
 D3=1.0/(2.0*RO*DELRO)-2.0/((DELR+DELRO)*DELRO)
T211=T21
T221=T22
T231=T23
T241=T24
T251=T25
 IC31=T21
IC41=T21
 IC51=T21
 IC61=T21
 IC71=T21
 IC81=T21
 IC91=T21
 ICA1=T21
 IC32=T22
 IC42=T22
 IC52=T22
 IC62=T22
 IC72=T22
 IC82=T22
 IC92=T22
 ICA2=T22
 IC33=T23
 IC43=T23
 IC53=T23
 IC63=T23
 IC73=T23
 IC83=T23
 IC93=T23
 ICA3=T23
 IC34=T24
 IC44=T24
 IC54=T24
 IC64=T24
 IC74=T24
 IC84=T24
 IC94=T24
 ICA4=T24
 IC35=T25
 IC45=T25
 IC55=T25
 IC65=T25
 IC75=T25
 IC85=T25
 IC95=T25
 ICA5=T25
 COEFFN=1.0/(2.0*3.14159*RIN)
 NOSORT
 DO 1 N=1,NPOINT
 R(N)=RO+N*DELR
 1 CONTINUE
**
*****************************************************************
****************************************************************
***************************************************************
******************************************************************
***********************************************************
********************************************************
 FUNCTION TF23=0.0,601.4,5.6,596.8,9.6,591.7,12.6,587.2,...
16.6,583.7,20.6,580.8, 23.6,577.5,27.6,574.1,31.6,570.8,35.6,569.0,...
38.6,565.3,42.6,562.4,45.6,559.5,49.6,556.5,53.6,553.9,57.6,550.8,...
60.6,540.2,73.6,539.2,88.6,529.0,103.6,518.3,118.6,507.9,...
133.6,497.1,148.6,488.9,163.6,476.3,178.6,465.8,193.6,455.1,...
```

POOR PRINT
Epreuve illisible

POOR PRINT
Epreuve illisible

```
      FUNCTION TH24=0.0,604.3,5.3,97.2,9.2,592.4,12.2,598.1,27.2,575.1,....
      FUNCTION TH23 =0.0,404.3,4.2,598.4,8.8,590.3,11.8,586.3,....
      FUNCTION TH22=0.0,604.3,5.3,97.2,9.2,592.4,12.2,598.1,27.2,575.1,....
      FUNCTION TH21=0.0,604.3,5.3,97.2,9.2,592.4,12.2,598.1,27.2,575.1,....
      DYNAMIC
      TI1 =INTGRL(IC11,DTI1)
      TI2 =INTGRL(IC12,DTI2)
      TI3 =INTGRL(IC13,DTI3)
      TI4 =INTGRL(IC14,DTI4)
      TI5 =INTGRL(IC15,DTI5)
      T11=TI1
      T12=TI2
      T13=TI3
      T14=TI4
      T15=TI5
      TA1=TA1
      TI1=INTGRL(IC31,DTI1)
      TI2=INTGRL(IC41,DTI2)
      TI3=INTGRL(IC51,DTI3)
      TI4=INTGRL(IC61,DTI4)
      TI5=INTGRL(IC71,DTI5)
      TA1=TA1
      TI2=INTGRL(IC32,DTI2)
      TI3=INTGRL(IC42,DTI3)
      TI4=INTGRL(IC52,DTI4)
      TI5=INTGRL(IC62,DTI5)
      TA2=TA2
```

```
      T33=INTGRL(IC33,DT33)
      T43=INTGRL(IC43,DT43)
      T53=INTGRL(IC53,DT53)
      T63=INTGRL(IC63,DT63)
      T73=INTGRL(IC73,DT73)
      T83=INTGRL(IC83,DT83)
      T93=INTGRL(IC93,DT93)
      TA3=T33
C*
C*
      T34=INTGRL(IC34,DT34)
      T44=INTGRL(IC44,DT44)
      T54=INTGRL(IC54,DT54)
      T64=INTGRL(IC64,DT64)
      T74=INTGRL(IC74,DT74)
      T84=INTGRL(IC84,DT84)
      T94=INTGRL(IC94,DT94)
      TA4=T94
C*
C*
      T35=INTGRL(IC35,DT35)
      T45=INTGRL(IC45,DT45)
      T55=INTGRL(IC55,DT55)
      T65=INTGRL(IC65,DT65)
      T75=INTGRL(IC75,DT75)
      T85=INTGRL(IC85,DT85)
      T95=INTGRL(IC95,DT95)
      TA5=T95
C*
C*
      T16=T13
      T26=T23
      T36=T33
      T46=T43
      T56=T53
      T66=T63
      T76=T73
      T86=T83
      T96=T93
      TA6=TA3
C*
C*
C*
C*****************************************************************
C*                                                               *
C*     FINITE DIFF. EQS. FOR PLANE  A                            *
C*                                                               *
C*****************************************************************
      DT33=CALPHA*(((T43-T33)-Z*(T33-T23))/DRSQ                  ***
           +((T43-T33)+Z*(T33-T23))/(2.0*DELR*R(1))              ***
           +((T33-T23)/DLLZ2-(T33-T34)/DELZ2)/DZ12MF)            ***
      DT43=CALPHA*(((T53-T43)*R(2)+(T43-T33)*R(1))/DRSQ          ***
           +((T43-T41)/DLLZ2-(T43-T44)/DELZ2)/DZ12MF)            ***
      DT53=CALPHA*(((T63-T53)*R(3)+(T53-T43)*R(2))/DRSQ          ***
           +((T53-T51)/DLLZ2-(T53-T54)/DELZ2)/DZ12MF)            ***
      DT63=CALPHA*(((T73-T63)*R(4)+(T63-T53)*R(3))/DRSQ          ***
           +((T63-T61)/DLLZ2-(T63-T64)/DELZ2)/DZ12MF)            ***
      DT73=CALPHA*(((T83-T73)*R(5)+(T73-T63)*R(4))/DRSQ          ***
           +((T73-T71)/DLLZ2-(T73-T74)/DELZ2)/DZ12MF)            ***
      DT83=CALPHA*(((T93-T83)*R(6)+(T83-T73)*R(5))/DRSQ          ***
           +((T83-T81)/DLLZ2-(T83-T84)/DELZ2)/DZ12MF)            ***
      DT93=CALPHA*(((TA3-T93)*R(7)+(T93-T83)*R(6))/DRSQ          ***
           +((T93-T91)/DLLZ2-(T93-T94)/DELZ2)/DZ12MF)
C*
C*    TO CALCULATE T13
C*
      HCONA=((T24-T14)/DELZ)-((T23-T34)/DELZ)/(0.5*(DELZ1+DELZ))
      DT24=DELIV(DTUT25,T25)
      T13=T23-(C1*DT24-A4-C2*CK*Z*(T34-T23))/(C2*SK)
C*
C*    TO CALCULATE HEAT FLUX AT PLANE A
C*
      HTVA=2.0*3.1415*((RIN*(T15-T14)+(-RIN*DELR*0)*(T25-T24))*0.5*SKOHO  ***
           +(0.5*(RIN+DELR*0)*(T25-T24)*R(1)*(T33-T34)*R(2)*(T43-T33)    ***
           +R(2)*(T53-T54)*R(3)*(T63-T64)*R(4)*(T73-T74)*R(5)*(T83-T84)  ***
           +R(6)*(T93-T94)*0.5*R(8)*(TA3-TA4))*CKOH)/DELZ
C*
      HCONA=2.0*3.1415*DZ12MF*((T15*(RIN+TC3*(RIN+DELRC))*DELRC*SROSP/2.0***
           +(0.5*T25*(RIN+DELR*0)+T35*R(1)+T45*R(2)+T55*R(3)+T65*R(4)    ***
           +T75*R(5)+T85*R(6)+T95*R(7)+0.5*TA5*R(8))*DELR*CRCSP)
      HTAVOD=DELIV(0.0,HCONTA)
      HTA=(-HTAS-HTVAH)*CCEFFN/DZ12MF
      ARLT=HTA  /1000.
      FT=SK*(T25-T15)/DELRC
      FLCT=HTS/100000.
C*
C*****************************************************************
C*                                                               *
C*        FINITE DIFF. EQS. FOR PLANE B                          *
C*                                                               *
C*****************************************************************
      DT34 = CALPHA*(((T44-T34)-Z*(T34-T24))/DRSQ                ***
           +((T44-T34)+Z*(T34-T24))/(2.0*DELR*R(1))              ***
           +((T35-T34)/DLLZ1 - (T24-T34)/DELZ)/DZ12MF)           ***
      DT44 = CALPHA*(((T54-2.0*T44+T34)/DRSQ + (T54-T34)/(2.0*DELR*R(2)) ***
           +((T45-T44)/DLLZ1 - (T34-T43)/DELZ)/DZ12MF)           ***
      DT54 = CALPHA*(((T64-2.0*T54+T44)/DRSQ + (T64-T44)/(2.0*DELR*R(3)) ***
           +((T55-T54)/DLLZ1 - (T44-T53)/DELZ)/DZ12MF)           ***
      DT64 = CALPHA*(((T74-2.0*T64+T54)/DRSQ + (T74-T54)/(2.0*DELR*R(4)) ***
           +((T65-T64)/DLLZ1 - (T54-T63)/DELZ)/DZ12MF)           ***
      DT74 = CALPHA*(((T84-2.0*T74+T64)/DRSQ + (T84-T64)/(2.0*DELR*R(5)) ***
           +((T75-T74)/DLLZ1 - (T64-T73)/DELZ)/DZ12MF)           ***
      DT84 = CALPHA*(((T94-2.0*T84+T74)/DRSQ + (T94-T74)/(2.0*DELR*R(6)) ***
           +((T85-T84)/DLLZ1 - (T74-T83)/DELZ)/DZ12MF)           ***
      DT94 = CALPHA*(((TA4-2.0*T94+T84)/DRSQ + (TA4-T84)/(2.0*DELR*R(7)) ***
           +((T95-T94)/DLLZ1 - (T84-T93)/DELZ)/DZ12MF)
C*
C*        TO CALCULATE T14
C*
      A4 = 0.5*((T25-T24)/DLLZ1 - (T14-T23)/DELZ)/(0.5*(DELZ1+DELZ))
      DT24=DELIV(DTUT24,T24)
      T14 = T24 - (C1*DT24-A4-C2*CK*Z*(T34-T23))/(C2*SK)
C*
C*        TO CALCULATE HEAT FLUX FOR  PLANE B
C*
      HTVB=0.5*SKOHO*(RIN*(T15-2.0*T14+T13)+(RIN+DELRC)*(T25-2.0*T24+T23))***
         + CKOH*(0.5*A4*(RIN+DELRC)*(T25-2.0*T24+T23)+R(1)*(T35-2.0*T34+T33)***
           +R(2)*(T45-2.0*T44+T43)+R(3)*(T55-2.0*T54+T53)              ***
           +R(4)*(T65-2.0*T64+T63)+R(5)*(T75-2.0*T74+T73)              ***
           +R(6)*(T85-2.0*T84+T83)+R(7)*(T95-2.0*T94+T93)              ***
           +R(8)*(TA5-2.0*TA4+TA3)*0.5)
      HTVABC=2.0*3.1415*HTVB/DELZ
      HCONT) = 2.0*3.1415*DZ12MF*((T14*(RIN+T24*(RIN+DELRC))*DELRC*SROSP/2.0***
           +(0.5*T24*(RIN+DELR*0)+T34*R(1)+T44*R(2)+T54*R(3)+T64*R(4)    ***
           +T74*R(5)+T84*R(6)+T94*R(7)+0.5*TA4*R(8))*DELR*CRCSP)
      HTP=DELIV(0.0,HCONTE)
      HTB=(-HTBS+HTVABC)*CCEFFN/DZ12MF
      FLCT=HTB  /100000.
      FT=SK*(T24-T14)/DELRC
      FLCT=HT8/100000.
```

POOR PRINT
Epreuve illisible

```
C*****************************************************************
C*                                                               *
C*      FINITE DIFF. EQNS FOR PLANE C                            *
C*                                                               *
C*****************************************************************
      DT13 = CALPHA*(((T43-T33)-Z*(T33-T23))/DRSQ                    ...
           +((T33-T32)+Z*(T33-T23))/(2.0*DELR*R(1))                  ...
           + (T32-2.0*T22+T23)/DZSQ)
      DT23 = CALPHA*(((T53-2.0*T43+T33)-Z*(T43-T23))/DRSQ +(T53-T33)/(2.0*DELR*R(2)) ...
           + (T52-2.0*T42+T43)/DZSQ)
      DT33 = CALPHA*(((T63-2.0*T53+T43)-Z*(T53-T33))/DRSQ +(T63-T43)/(2.0*DELR*R(3)) ...
           + (T62-2.0*T52+T53)/DZSQ)
      DT43 = CALPHA*(((T73-2.0*T63+T53)-Z*(T63-T43))/DRSQ +(T73-T53)/(2.0*DELR*R(4)) ...
           + (T72-2.0*T62+T63)/DZSQ)
      DT53 = CALPHA*(((T83-2.0*T73+T63)-Z*(T73-T53))/DRSQ +(T83-T63)/(2.0*DELR*R(5)) ...
           + (T82-2.0*T72+T73)/DZSQ)
      DT63 = CALPHA*(((T93-2.0*T83+T73)-Z*(T83-T63))/DRSQ +(T93-T73)/(2.0*DELR*R(6)) ...
           + (T92-2.0*T82+T83)/DZSQ)
      DT73 = CALPHA*(((T103-2.0*T93+T83)-Z*(T93-T73))/DRSQ +(T103-T83)/(2.0*DELR*R(7)) ...
           + (T102-2.0*T92+T93)/DZSQ)
C*
C*       TO CALCULATE T13
C*
      A1 = KM*((T22-2.0*T23+T24)/(DELZ**2)
      DT22=DERIV(0.0,T22,T23)
      T13 = T23 - (C1*DT23-A1-C2*CK*Z*(T33-T23))/(C3*SK)
C*
C*       TO CALCULATE HEAT FLUX -- PLANE C
C*
      HAD1= 0.5*SKOHO*PI*(R(1)*(T14-2.0*T13+T12)+(RIN+DELRC)*(T24-2.0*T23+T22))
      HAD2=CKOH*(0.5*PI*(RIN+DELRC)*(T24-2.0*T23+T22)+R(1)*(T34-2.0*T33+T32))...
           +R(2)*(T44-2.0*T43+T42)+R(3)*(T54-2.0*T53+T52)                  ...
           +R(4)*(T64-2.0*T63+T62)+R(5)*(T74-2.0*T73+T72)                  ...
           +R(6)*(T84-2.0*T83+T82)+R(7)*(T94-2.0*T93+T92)                  ...
           +R(8)*(TA4-2.0*TA3+TA2)*0.5)
      HCONTC = 2.0*3.14159*DELZ*((T13*R(1)+T23*(RIN+DELRC))*DELRC*SKOSP/2.0...
             +(0.5*T23*(RIN+DELRC)+T33*R(1)+T43*R(2)+T53*R(3)+T63*R(4)    ...
             +T73*R(5)+T83*R(6)+T93*R(7)+TA3*R(8))*0.5)*DELR*CRCSP)
      HADC=2.0*3.14159*(HAD1+HAD2)/DELZ
C*
      HTCC=DERIV(0.0,HCONTC)
      HTC=(-HTCC*HADC)*CCLFFN/DELZ
      CALLT=HTC  /100000.
      HTJ=SK*(T23-T13)/DELRC
      CLLT=HTJ/100000.
C*****************************************************************
C*                                                               *
C*      FINITE DIFF. EQS. FOR PLANE D                            *
C*                                                               *
C*****************************************************************
      DT32 = CALPHA*(((T42-T32)-Z*(T32-T22))/DRSQ                    ...
           +((T42-T32)+Z*(T32-T22))/(2.0*DELR*R(1))                  ...
           +((T31-T32)/DELZ  - (T32-T31)/DELZ2)/DZ22HF)
      DT42 = CALPHA*(((T52-2.0*T42+T32)-Z*(T42-T32))/DRSQ + (T52-T32)/(2.0*DELR*R(2)) ...
           +((T41-T42)/DELZ  - (T42-T41)/DELZ2)/DZ22HF  )
      DT52 = CALPHA*(((T62-2.0*T52+T42)-Z*(T52-T42))/DRSQ + (T62-T42)/(2.0*DELR*R(3)) ...
           +((T51-T52)/DELZ  - (T52-T51)/DELZ2)/DZ22HF)
      DT62 = CALPHA*(((T72-2.0*T62+T52)-Z*(T62-T52))/DRSQ + (T72-T52)/(2.0*DELR*R(4)) ...
           +((T61-T62)/DELZ  - (T62-T61)/DELZ2)/DZ22HF  )
      DT72 = CALPHA*(((T82-2.0*T72+T62)-Z*(T72-T62))/DRSQ + (T82-T62)/(2.0*DELR*R(5)) ...
           +((T71-T72)/DELZ  - (T72-T71)/DELZ2)/DZ22HF)
      DT82 = CALPHA*(((T92-2.0*T82+T72)-Z*(T82-T72))/DRSQ + (TA2-T82)/(2.0*DELR*R(6)) ...
           +((T91-T92)/DELZ  - (T92-T91)/DELZ2)/DZ22HF)
      DT92 = CALPHA*(((TA2-2.0*TA2+T82)-Z*(TA2-T82))/DRSQ + (TA2-T82)/(2.0*DELR*R(7)) ...
           +((TA1-TA2)/DELZ  - (TA2-TA1)/DELZ2)/DZ22HF)
C*
C*       TO CALCULATE T12
C*
      A2 = KM*((T32-T22)/DELZ-(T42-T32)/DELZ2)/(0.5*(DELZ+DELZ2))
      DT22=DERIV(0.0,T22,T23)
      T12 = T22-(C1*DT22-A2-C2*CK*Z*(T32-T22))/(C3*SK)
C*
C*       TO CALCULATE HEAT FLUX -- PLANE D --
C*
      HTVDE=0.0*3.1415*SKOHO*(RIN*(T13-2.0*T12+T11)+(RIN+DELRC)*(T23-2.0*T22+T21)) ...
           +CKOH*(0.5*PI*(RIN+DELRC)*(T23-2.0*T22+T21)                          ...
           +R(1)*(T33-2.0*T32+T31)+R(2)*(T43-2.0*T42+T41)                       ...
           +R(3)*(T53-2.0*T52+T51)+R(4)*(T63-2.0*T62+T61)                       ...
           +R(5)*(T73-2.0*T72+T71)+R(6)*(T83-2.0*T82+T81)                       ...
           +R(7)*(T93-2.0*T92+T91)+R(8)*(TA3-2.0*TA2+TA1)*0.5)
      HTVCDE=2.0*3.1415*HTVD/DELZ
C*
      HCONTD = 2.0*3.1415)*DZ22*((T12*RIN+T22*(RIN+DELRC))*DELRC*SKOSP/2.0...
             +(0.5*T22*(RIN+DELRC)+T32*R(1)+T42*R(2)+T52*R(3)+T62*R(4)    ...
             +T72*R(5)+T82*R(6)+T92*R(7)+0.5*TA2*R(8))*DELR*CRCSP)
      HTJD=DERIV(0.0,HCONTD)
      HTDE=(-HTDS*HTVCDE)*CCLFFN/DZ22HF
      CLLT=HTD  /100000.
      HTZ=SK*(T22-T12)/DELRC
      PLOT2=HTZ/100000.
C*****************************************************************
C*                                                               *
C*    FINITE DIFF. EQUATIONS FC PLANE E                          *
C*                                                               *
C*****************************************************************
      DT31= CALPHA*(((T41-T31)-Z*(T31-T21))/DRSQ                     ...
          +((T41-T31)+Z*(T31-T21))/(2.0*DELR*R(1))                   ...
          +((T32-T31)/DELZ-(T31-T30)/DELZ4)/DZ14HF)
      DT41= CALPHA* ((T51-2.0*T41+T31)/DRSQ+ (T51-T31)/(2.0*DELR*R(2))    ...
          +((T42-T41)/DELZ-(T41-T40)/DELZ4)/DZ14HF)
      DT51= CALPHA*((T61-2.0*T51+T41)/DRSQ+(T61-T41)/(2.0*DELR*R(3))      ...
          +((T52-T51)/DELZ-(T51-T50)/DELZ4)/DZ14HF)
      DT61= CALPHA*((T71-2.0*T61+T51)/DRSQ+ (T71-T51)/(2.0*DELR*R(4))     ...
          +((T62-T61)/DELZ-(T61-T60)/DELZ4)/DZ14HF)
      DT71= CALPHA* ((T81-2.0*T71+T61)/DRSQ+(T81-T61)/(2.0*DELR*R(5))     ...
          +((T72-T71)/DELZ-(T71-T70)/DELZ4)/DZ14HF)
      DT81= CALPHA*((T91-2.0*T81+T71)/DRSQ+(T91-T71)/(2.0*DELR*R(6))      ...
          +((T82-T81)/DELZ-(T81-T80)/DELZ4)/DZ14HF)
      DT91= CALPHA*((TA1-2.0*T91+T81)/DRSQ+(TA1-T81)/(2.0*DELR*R(7))      ...
          +((T92-T91)/DELZ- (T91-T90)/DELZ4)/DZ14HF)
C*
C*    TO CALCULATE T11
C*
      A1= KM*((T22-T21)/DELZ-(T21-T20)/DELZ4)/(0.5*(DELZ+DELZ4))
      DT21=DERIV(0.0,T21,T21)
      T11= T21-(C1*DT21-A1-C2*CK*Z*(T31-T21))/(C3*SK)
C*
C*    TO CALCULATE HEAT FLUX AT PLANE E
C*
      HTVDE=2.0*3.14159*((RIN*(T12-T11)+(RIN+DELRC)*(T22-T21))*0.5*SKOHO  ...
           +(0.5*K*(RIN+DELRC)*(T22-T21)+R(1)*(T32-T31)+R(2)*(T42-T41)    ...
           +R(3)*(T52-T51)+R(4)*(T62-T61)+R(5)*(T72-T71)+R(6)*(T82-T81)   ...
           +R(7)*(T92-T91)+R(8)*(TA2-TA1)*0.5)*CKOR)/DELZ
      HCONTE=2.0*3.14159*DZ14HF*((T11*RIN+T21*(RIN+DELRC))*DELRC*SKOSP/2.0...
           +(0.5*T21*(RIN+DELRC)*T21+R(1)+T41*R(2)+T51*R(3)+T61*R(4)      ...
           +T71*R(5)+T81*R(6)+T91*R(7)+0.5*TA1*R(8))*DELR*CRCSP)
      HTED=DERIV(0.0,HCONTE)
      HTE=(-HTES*HTVDE)*CCLFFN/DZ14HF
      CLLT=HTE  /100000.
      HTI=SK*(T21-T11)/DELRC
      PLOT1=HTI/100000.
      TT=TIME
      METHOD RKSEX
```

POOR PRINT
Epreuve illisible

```
      NOSORT
            IF(IT.NE.IN) GO TO 98
            WRITE(6,96) TIME
            WRITE(6,95)  T15,T25,T35,T45,T55,T65,T75,T85,T95,TA5
            WRITE(6,94)  T14,T24,T34,T44,T54,T64,T74,T84,T94,TA4
            WRITE(6,93)  T13,T23,T33,T43,T53,T63,T73,T83,T93,TA3
            WRITE(6,92)  T12,T22,T32,T42,T52,T62,T72,T82,T92,TA2
            WRITE(6,91)  T11,T21,T31,T41,T51,T61,T71,T81,T91,TA1
            WRITE(8,99)  T15 ,APLCT,T14 ,BPLCT,T13 ,CPLCT,T12 ,DPLOT,T11 ,EPLCT
            IK=IK+7
      95    FORMAT(1X,'PLANE A ',10(F 5.1,5X),/)
      94    FORMAT(1X,'PLANE B ',10(F 5.1,5X),/)
      93    FORMAT(1X,'PLANE C ',10(F 5.1,5X),/)
      92    FORMAT(1X,'PLANE D ',10(F 5.1,5X),/)
      91    FORMAT(1X,'PLANE E ',10(F 5.1,5X),/)
      96    FORMAT(30X,'TEMPERATURE DISTRIBUTION AT TIME = ',F5.1,//)
      99    FORMAT(10F5.1)
      98    CONTINUE
      SORT
      PRTPLT HTA    (T15 ,T25)
      PRTPLT HTB    (T14 ,T24)
      PRTPLT HTC    (T13 ,T23)
      PRTPLT HTD    (T12 ,T22)
      PRTPLT HTE    (T11 ,T21)
      END
      STOP
```

```
OUTPUT VARIABLE SEQUENCE
                   CALPHA DT1      T21      T211     T212     DTDT21 DT2      T22
IK       Z         DTDT22 DT3      T23      T231     T232     DTDT23 DT4      T24
T221     T222      DTDT24 DT5      T25      T251     T252     DTDT25 L        DELZ3
T241     T242      D213HF D214HF   D253     HFCINT   DELHC    FIN      RCUT     DELR
DELZ4    DELZ      D212HF D212     DELZ2    D222HF   D222     CKDR     SKDRC    X
DH50     DELZ1     KM     CRCSP    SHCSP    C1       C2       C3       IC31     IC41
HC       DL        IC71   IC81     IC91     ICA1     IC32     IC42     IC52     IC62
IC51     IC61      IC72   ICA2     IC33     IC43     IC53     IC63     IC73     IC83
IC74     IC64      IC34   IC44     IC54     IC64     IC74     IC84     IC94     ICA4
IC[illegible] IC45 IC55   IC65     IC75     IC85     IC95     ICA5     COEFFN   Z20001
IC[illegible] IC45 DT41   T31      T40      DT41     T41      T50      DT51     T51
T[illegible] T61   DT61   T70      DT71     T71      T80      DT81     T81      T90
T[illegible] DT61  T91    T22      DT32     T32      DT42     T42      DT52     T52
TA1      DT91      DT72   T72      DT82     T62      T42      DT92     T72      T23
DT[illegible] T[illegible] DT41 T43 DT33  T53      DT63     T63      DT73     T73
DT[illegible] T[illegible] TA3  DT93 T93  T24      DT34     T34      DT44     T44
DT[illegible] T[illegible] DT54 T64  DT74 T74      DT84     T84      TA4      DT94
T[illegible] T[illegible] T25   DT35 T35  T45      DT45     T45      T55      DT55
T[illegible] T[illegible] DT[illegible] T65 T76 DT75 T75  T66      DT85     T85
T[illegible] T[illegible] DT[illegible] T95 T20 A1 DT21   T11      T16      TA0
T[illegible] TA5   DT[illegible] T16 T16  TA6      A4       DT24     T14      HTVAH
T[illegible] A5    DT25   T15      HT5      PLCT5    A3       DT23     T13      HTVB
HCCNTA   HTA5      HTA    APLCT    BPLCT    HT4      PLCT4    HAB2     A2       DT22
HTV[illegible] HCCNTB HT35 HTB     HTC5     HTC      CPLCT    HT3      PLCT3    HTVD
T1[illegible] HAB1 HABC   HCCNTC   DPLCT    HT2      PLCT2    HTVDE    HCCNTE   HTES
HTVC[illegible] HCCNTD HTDS HTD    IT       Z20037   IK
HT[illegible] [illegible]PLCT HT1 PLCT1

 OUTPUTS     INPUTS      PARAMS  INTEGS + MEM BLKS  FORTRAN   DATA CDS
 2(1[illegible]) [illegible](1400)  15(400)  35+  0= 25(300)  340(600)   103

 ENDJOB
```

```
*** CSMP/360 SIMULATION DATA ***

PARAM  CK=374.0,CP=385.195,CRHO=8[illegible].323
PARAM  SK=17.31,SSP=455.427,SRHO=8169.485
FUNCTION TH1=0.0,603.4,5.6,596.3,9.6,591.9,12.6,587.3....
16.6,[illegible].7,20.6,583.9, 23.6,577.5,27.6,574.1,31.6,570.8,35.6,566.6....
[illegible].6,[illegible].4,42.6,562.4,45.6,559.5,49.6,555.5,53.6,553.9,57.6,550.8....
60.6,5[illegible].2,73.6,539.2,88.6,529.0,103.6,519.3,118.6,507.7,...
133.6,[illegible]7.1,148.6,486.4,163.6,476.3,178.6,465.4,193.6,455.1....
203.6,[illegible]7.6,213.6,440.4,223.6,432.5,233.6,423.2,243.6,417.4....
253.6,[illegible].7,263.6,401.6,273.6,393.7,283.6,385.7,293.6,377.4....
303.6,[illegible].6,313.6,359.7,322.6,350.0,333.6,339.6,138.6,334.0....
341.6,332.3,                 343.6,326.0,349.6,321.9,352.6,317.6....
356.6,313.2,360.6,308.0,362.6,304.2,367.6,299.1,371.6,294.2....
374.6,[illegible].6,378.6,293.6,382.6,279.0,385.6,272.9,389.6,266.4....
393.6,237.2,397.6,218.1,400.6,207.3,404.6,200.5,408.6,194.7....
411.6,189.4,415.6,184.4,419.6,179.8,422.6,175.5,426.6,171.7....
430.6,167.8,433.6,164.2,437.6,161.0,441.6,158.0,444.6,155.2....
448.6,152.7,452.6,150.2,456.6,148.1,459.6,146.0,463.6,144.1....
467.6,142.5,470.6,140.9,474.6,139.4,478.6,138.1,481.6,136.8....
485.6,135.6,489.6,134.6,492.6,133.5,496.6,132.6,500.6,131.6....
504.6,130.7,511.6,129.1,518.6,127.8,525.6,126.5,532.6,125.4....
542.2,123.9,572.2,120.2
FUNCTION TH24=0.0,604.3,5.2,597.2,9.2,592.4,12.2,588.1,27.2,575.1....
46.2,560.4,60.2,549.4,73.2,540.5,88.2,530.4,103.2,519.6,118.2,506.9....
133.2,496.3,148.2,487.3,162.2,477.4,178.2,466.6,193.2,455.9....
207.2,446.6,213.2,441.1,223.2,433.4,233.2,425.7,243.2,417.9....
253.2,410.2,262.2,401.9,273.2,393.8,283.2,385.5,293.2,377.2....
303.2,368.4,313.2,359.4,323.2,349.6,333.2,339.6,338.6,333.5....
341.2,329.5,345.2,325.0,349.2,320.4,352.2,316.3,356.2,311.7....
360.2,30[illegible].7,363.2,302.6,367.2,297.5,371.2,292.6,374.6,287.0....
37[illegible].2,2[illegible].1,382.2,276.[illegible],385.2,271.0,[illegible].2,264.3,393.2,2[illegible]....
397.2,223.7,400.2,210.4,404.2,203.5,408.2,197.4,411.2,191.8....
[illegible].2,177.7,430.2,169.4....
```

POOR PRINT
Epreuve illisible

POOR PRINT
Epreuve illisible

```
PRTPLT HTJ   (T12 ,T22)
PRTPLT HTE   (T11 ,T21)
END

TIMER VARIABLES
DELT  = 1.0000E-01
OUTINT= 5.7100E-05
FINTIM= 5.7100E 02
PRDEL = 7.0000E 00
OUTDEL= 5.0000E-01
```

POOR PRINT
Epreuve illisible

TEMPERATURE DISTRIBUTION AT TIME = 10.0

PLANE A	592.7	591.3	594.1	596.8	597.0	597.9	598.5	598.8	599.0	599.0
PLANE B	593.2	591.2	593.7	595.4	596.7	597.6	598.2	598.6	598.8	598.8
PLANE C	586.7	586.7	592.0	594.2	595.9	597.0	597.8	598.3	598.5	598.5
PLANE D	589.7	583.8	589.1	592.5	594.8	596.3	597.3	597.9	598.2	598.2
PLANE E	581.8	577.1	586.2	591.0	594.0	595.8	597.0	597.7	598.0	598.0

TEMPERATURE DISTRIBUTION AT TIME = 17.0

PLANE A	577.8	582.3	586.5	588.5	589.9	590.9	591.6	592.0	592.2	592.2
PLANE B	577.5	582.3	586.0	588.2	589.7	590.6	591.5	591.9	592.1	592.1
PLANE C	579.2	582.1	585.4	587.6	589.3	590.4	591.2	591.7	592.0	592.0
PLANE D	585.3	578.4	583.5	586.6	588.6	590.0	591.0	591.5	591.8	591.9
PLANE E	582.5	573.8	581.5	585.6	588.1	589.7	590.8	591.4	591.7	591.7

TEMPERATURE DISTRIBUTION AT TIME = 24.0

PLANE A	585.7	577.1	580.3	582.2	583.7	584.7	585.3	585.7	585.9	585.9
PLANE B	585.2	576.7	580.0	582.1	583.5	584.5	585.2	585.6	585.8	585.8
PLANE C	585.7	576.6	579.3	581.5	583.1	584.2	585.0	585.5	585.7	585.7
PLANE D	585.2	572.6	577.0	580.6	582.5	583.9	584.7	585.3	585.5	585.5
PLANE E	583.9	568.9	575.2	579.7	582.1	583.6	584.6	585.1	585.4	585.4

TEMPERATURE DISTRIBUTION AT TIME = 31.0

PLANE A	582.3	571.2	574.6	576.5	577.8	578.7	579.4	579.7	579.9	579.9
PLANE B	582.9	572.0	574.6	576.4	577.7	578.6	579.2	579.6	579.8	579.8
PLANE C	582.3	570.0	573.7	575.8	577.3	578.3	579.0	579.5	579.7	579.7
PLANE D	581.3	567.4	572.0	574.9	576.7	578.0	578.8	579.3	579.5	579.5
PLANE E	580.4	564.5	570.3	574.0	576.2	577.7	578.6	579.2	579.4	579.4

TEMPERATURE DISTRIBUTION AT TIME = 38.0

PLANE A	577.2	566.8	569.1	571.0	572.2	573.1	573.7	574.1	574.2	574.2
PLANE B	580.3	566.5	569.1	570.8	572.1	573.0	573.6	574.0	574.1	574.1
PLANE C	577.0	565.1	568.2	570.3	571.7	572.7	573.4	573.8	574.0	574.0
PLANE D	579.4	562.0	566.8	569.5	571.2	572.4	573.2	573.7	573.9	573.9
PLANE E	578.2	559.9	565.7	568.6	570.7	572.2	573.1	573.6	573.8	573.8

TEMPERATURE DISTRIBUTION AT TIME = 45.0

PLANE A	572.4	560.8	563.7	565.5	566.8	567.6	568.2	568.6	568.7	568.7
PLANE B	575.3	561.2	563.7	565.4	566.6	567.5	568.1	568.5	568.7	568.7
PLANE C	572.8	559.8	562.8	564.8	566.2	567.2	567.9	568.3	568.5	568.5
PLANE D	574.3	556.7	561.3	564.0	565.7	566.9	567.7	568.2	568.4	568.4
PLANE E	573.1	555.6	559.8	563.2	565.3	566.7	567.6	568.1	568.3	568.3

TEMPERATURE DISTRIBUTION AT TIME = 52.0

PLANE A	565.7	554.7	558.1	560.0	561.3	562.1	562.7	563.1	563.3	563.3
PLANE B	566.5	555.8	558.2	559.9	561.2	562.0	562.6	563.0	563.2	563.2
PLANE C	567.1	554.4	557.5	559.4	560.8	561.8	562.5	562.9	563.1	563.1
PLANE D	564.9	551.6	556.1	558.7	560.4	561.5	562.3	562.7	563.0	563.0
PLANE E	564.1	549.4	555.0	558.1	560.0	561.3	562.2	562.6	562.9	562.9

TEMPERATURE DISTRIBUTION AT TIME = 59.0

PLANE A	560.5	549.6	552.8	554.7	556.0	556.9	557.4	557.8	558.0	558.0
PLANE B	564.4	550.3	552.9	554.6	555.9	556.7	557.3	557.7	557.9	557.9
PLANE C	561.7	549.0	552.1	554.1	555.5	556.5	557.2	557.6	557.8	557.8
PLANE D	559.3	546.2	550.7	553.3	555.1	556.2	557.0	557.5	557.7	557.7
PLANE E	555.6	543.0	549.3	552.6	554.7	556.0	556.9	557.4	557.6	557.6

TEMPERATURE DISTRIBUTION AT TIME = 66.0

PLANE A	554.5	544.0	547.3	549.3	550.5	551.4	552.0	552.3	552.5	552.5
PLANE B	560.4	545.3	547.3	549.2	550.4	551.3	551.9	552.3	552.4	552.4
PLANE C	557.3	543.7	546.8	548.7	550.1	551.1	551.7	552.1	552.3	552.3
PLANE D	555.5	540.6	545.2	547.9	549.6	550.8	551.3	552.0	552.2	552.2
PLANE E	552.7	538.3	544.1	547.1	549.2	550.5	551.4	551.9	552.1	552.1

TEMPERATURE DISTRIBUTION AT TIME = 73.0

PLANE A	551.1	535.6	542.6	544.4	545.5	546.3	546.9	547.2	547.3	547.3

POOR PRINT
Epreuve illisible

PLANE C 534.8	540.0	542.4	544.1	545.2	546.1	546.7	547.0	547.2	547.2
PLANE D 526.8	537.2	541.1	543.4	544.8	545.8	546.5	546.9	547.1	547.1
PLANE E 521.2	535.0	540.1	542.8	544.3	545.7	546.4	546.8	547.0	547.0

TEMPERATURE DISTRIBUTION AT TIME = 90.0

PLANE A 526.2	534.8	537.9	539.7	540.9	541.7	542.2	542.5	542.7	542.7
PLANE B 530.7	535.9	538.2	539.7	540.8	541.6	542.1	542.5	542.6	542.6
PLANE C 530.4	535.0	537.8	539.4	540.6	541.4	542.0	542.4	542.5	542.5
PLANE D 522.4	532.6	536.5	538.8	540.2	541.2	541.9	542.2	542.4	542.4
PLANE E 516.7	530.4	535.0	537.2	539.9	541.0	541.7	542.2	542.4	542.4

TEMPERATURE DISTRIBUTION AT TIME = 87.0

PLANE A 531.4	536.0	533.2	535.0	536.2	537.0	537.5	537.8	538.0	538.0
PLANE B 529.9	531.2	533.5	535.0	536.1	536.9	537.4	537.8	537.9	537.9
PLANE C 528.8	530.8	533.1	534.7	535.9	536.7	537.3	537.7	537.8	537.8
PLANE D 517.1	527.9	531.8	534.0	535.5	536.5	537.2	537.6	537.7	537.7
PLANE E 510.3	525.4	530.6	533.5	535.2	536.2	537.1	537.5	537.7	537.7

TEMPERATURE DISTRIBUTION AT TIME = 94.0

PLANE A 516.9	525.2	528.4	530.2	531.4	532.2	532.7	533.1	533.2	533.2
PLANE B 520.4	526.3	528.6	530.2	531.3	532.1	532.7	533.0	533.2	533.2
PLANE C 520.1	526.7	528.2	529.9	531.1	531.9	532.3	532.9	533.1	533.1
PLANE D 512.3	522.8	526.3	529.2	530.7	531.7	532.4	532.8	533.0	533.0
PLANE E 505.7	520.3	525.7	528.6	530.4	531.5	532.3	532.7	532.9	532.9

TEMPERATURE DISTRIBUTION AT TIME = 101.0

PLANE A 511.3	520.2	523.4	525.2	526.4	527.2	527.8	528.1	528.3	528.3
PLANE B 515.8	521.2	523.6	525.2	526.3	527.2	527.7	528.1	528.2	528.2
PLANE C 514.6	520.1	522.9	524.8	526.1	527.0	527.6	528.0	528.2	528.2
PLANE D 506.0	517.3	521.0	524.1	525.7	526.7	527.4	527.9	528.0	528.0
PLANE E 500.3	515.1	520.5	523.5	525.3	526.5	527.3	527.8	528.0	528.0

TEMPERATURE DISTRIBUTION AT TIME = 108.0

PLANE A 506.7	515.2	518.3	520.2	521.4	522.2	522.7	523.1	523.2	523.2
PLANE B 510.4	516.1	518.5	520.1	521.3	522.1	522.7	523.0	523.2	523.2
PLANE C 509.2	514.9	517.4	519.4	521.0	521.9	522.3	522.9	523.1	523.1
PLANE D 502.1	512.1	516.4	518.9	520.6	521.6	522.1	522.6	523.0	523.0
PLANE E 495.7	510.1	515.5	518.4	520.3	521.5	522.2	522.7	522.9	522.9

TEMPERATURE DISTRIBUTION AT TIME = 115.0

PLANE A 503.1	510.3	513.4	515.2	516.3	517.2	517.7	518.0	518.2	518.2
PLANE B 506.7	511.1	513.5	515.1	516.2	517.1	517.6	518.0	518.1	518.1
PLANE C 505.1	509.9	512.8	514.6	515.9	516.9	517.5	517.9	518.0	518.0
PLANE D 498.4	507.1	511.5	513.9	515.5	516.6	517.3	517.7	517.9	517.9
PLANE E 491.3	505.3	510.5	513.4	515.3	516.4	517.2	517.7	517.9	517.9

TEMPERATURE DISTRIBUTION AT TIME = 122.0

PLANE A 497.4	506.5	509.5	511.2	511.4	512.2	512.7	513.1	513.2	513.2
PLANE B 500.7	506.2	508.5	510.1	511.3	512.1	512.7	513.0	513.2	513.2
PLANE C 499.4	505.1	507.9	509.7	511.0	511.9	512.5	512.9	513.1	513.1
PLANE D 491.1	502.3	506.0	508.0	510.0	511.7	512.4	512.8	513.0	513.0
PLANE E 485.0	500.5	505.7	508.5	510.3	511.5	512.2	512.7	512.9	512.9

TEMPERATURE DISTRIBUTION AT TIME = 129.0

PLANE A 492.1	500.4	503.5	505.2	506.5	507.3	507.8	508.1	508.3	508.3
PLANE B 495.7	501.2	503.6	505.2	506.4	507.2	507.7	508.1	508.2	508.2
PLANE C 493.9	500.3	503.0	504.8	506.1	507.0	507.6	508.0	508.1	508.1
PLANE D 486.3	497.7	501.8	504.2	505.7	506.8	507.4	507.9	508.0	508.0
PLANE E 481.6	495.8	500.8	503.7	505.4	506.6	507.3	507.8	508.0	508.0

TEMPERATURE DISTRIBUTION AT TIME = 136.0

PLANE A 488.4	495.3	498.5	500.3	501.5	502.4	502.9	503.2	503.4	503.4
PLANE B 490.5	496.2	498.7	500.3	501.5	502.3	502.8	503.2	503.3	503.3
PLANE C 489.2	495.5	498.2	500.0	501.2	502.1	502.7	503.1	503.3	503.3
PLANE D 482.0	493.0	497.0	499.3	500.9	501.9	502.6	503.0	503.2	503.2
PLANE E 476.3	490.7	495.9	498.8	500.6	501.7	502.5	502.9	503.1	503.1

TEMPERATURE DISTRIBUTION AT TIME = 143.0

PLANE A 481.2	490.3	493.5	495.4	496.6	497.4	498.0	498.3	498.5	498.5
PLANE B 485.2	491.1	493.7	495.3	496.5	497.3	497.9	498.3	498.4	498.4
PLANE C 483.8	490.3	493.1	495.0	496.3	497.2	497.8	498.2	498.3	498.3
PLANE D 477.4	488.0	492.3	494.4	495.9	496.9	497.6	498.0	498.2	498.2

POOR PRINT
Epreuve illisible

PLANE E 471.1	485.7	491.0	492.7	493.6	493.8	497.9	498.0	498.2	498.2

TEMPERATURE DISTRIBUTION AT TIME = 150.0

PLANE A 477.1	485.4	489.9	490.4	491.6	492.4	493.0	493.3	493.5	493.5
PLANE B 476.4	486.0	488.6	490.3	491.5	492.3	492.7	493.3	493.4	493.4
PLANE C 476.1	485.1	488.1	489.9	491.2	492.2	492.9	493.2	493.3	493.3
PLANE D 472.0	483.0	487.0	489.2	490.9	491.9	492.6	493.1	493.2	493.2
PLANE E 466.2	480.6	485.9	488.8	490.6	491.8	492.5	493.0	493.2	493.2

TEMPERATURE DISTRIBUTION AT TIME = 157.0

PLANE A 472.0	480.6	483.7	485.5	486.7	487.5	488.0	488.4	488.5	488.5
PLANE B 471.6	481.3	483.8	485.4	486.6	487.4	487.9	488.3	488.5	488.5
PLANE C 474.1	480.5	483.2	485.0	486.3	487.2	487.9	488.2	488.4	488.4
PLANE D 467.7	478.0	482.0	484.4	485.9	487.0	487.7	488.1	488.3	488.3
PLANE E 461.4	475.7	481.0	483.6	485.6	486.8	487.6	488.0	488.2	488.2

TEMPERATURE DISTRIBUTION AT TIME = 164.0

PLANE A 477.4	476.0	479.0	480.7	481.9	482.6	483.2	483.5	483.6	483.6
PLANE B 471.0	476.8	479.1	480.7	481.8	482.6	483.1	483.4	483.6	483.6
PLANE C 470.3	476.0	478.5	480.3	481.5	482.4	483.0	483.3	483.5	483.5
PLANE D 466.1	473.0	477.2	479.5	481.1	482.1	482.9	483.2	483.4	483.4
PLANE E 460.0	470.9	476.1	479.0	480.8	481.9	482.7	483.1	483.3	483.3

TEMPERATURE DISTRIBUTION AT TIME = 171.0

PLANE A 474.1	471.1	474.1	475.9	477.0	477.8	478.3	478.7	478.8	478.8
PLANE B 468.4	471.9	474.2	475.8	476.9	477.7	478.3	478.6	478.8	478.8
PLANE C 464.7	470.5	473.0	475.4	476.6	477.5	478.1	478.5	478.7	478.7
PLANE D 457.3	468.2	472.3	474.7	476.2	477.3	478.0	478.4	478.6	478.6
PLANE E 451.4	466.0	471.3	474.1	475.9	477.1	477.8	478.3	478.5	478.5

TEMPERATURE DISTRIBUTION AT TIME = 178.0

PLANE A 468.1	466.2	469.2	470.9	472.1	472.9	473.4	473.8	473.9	473.9
PLANE B 461.0	466.7	469.2	470.8	472.0	472.8	473.4	473.7	473.9	473.9
PLANE C 459.3	465.5	468.3	470.4	471.7	472.6	473.2	473.6	473.8	473.8
PLANE D 453.3	463.3	467.4	469.8	471.3	472.4	473.1	473.5	473.7	473.7
PLANE E 446.6	461.1	466.4	469.2	471.0	472.2	472.9	473.4	473.6	473.6

TEMPERATURE DISTRIBUTION AT TIME = 185.0

PLANE A 463.4	461.2	464.2	465.9	467.1	467.9	468.3	468.8	469.0	469.0
PLANE B 455.0	461.7	464.2	465.8	467.0	467.8	468.4	468.7	468.9	468.9
PLANE C 453.1	460.5	463.5	465.4	466.7	467.6	468.3	468.6	468.8	468.8
PLANE D 447.4	458.3	462.3	464.8	466.3	467.4	468.1	468.5	468.7	468.7
PLANE E 441.8	456.0	461.3	464.2	466.0	467.2	468.0	468.4	468.6	468.6

TEMPERATURE DISTRIBUTION AT TIME = 192.0

PLANE A 458.2	456.2	459.2	460.9	462.1	462.9	463.5	463.9	464.0	464.0
PLANE B 451.0	456.7	459.2	460.8	462.0	462.8	463.4	463.7	463.9	463.9
PLANE C 448.4	455.5	458.5	460.4	461.7	462.6	463.2	463.6	463.8	463.8
PLANE D 442.3	453.1	457.2	459.7	461.3	462.4	463.1	463.5	463.7	463.7
PLANE E 436.8	450.8	456.2	459.1	461.0	462.2	463.0	463.4	463.6	463.6

TEMPERATURE DISTRIBUTION AT TIME = 199.0

PLANE A 453.2	451.1	454.1	455.9	457.1	457.9	458.4	458.8	458.9	458.9
PLANE B 445.8	451.8	454.1	455.8	457.0	457.8	458.4	458.7	458.9	458.9
PLANE C 443.3	450.8	453.5	455.4	456.7	457.6	458.2	458.6	458.8	458.8
PLANE D 438.2	448.2	452.3	454.7	456.3	457.3	458.0	458.5	458.7	458.7
PLANE E 432.8	445.6	451.1	454.1	455.9	457.2	457.9	458.4	458.6	458.6

TEMPERATURE DISTRIBUTION AT TIME = 206.0

PLANE A 447.9	446.0	449.0	450.8	452.0	452.8	453.4	453.7	453.9	453.9
PLANE B 440.0	446.5	449.0	450.7	451.9	452.7	453.3	453.7	453.8	453.8
PLANE C 437.4	445.3	448.4	450.3	451.6	452.5	453.2	453.6	453.7	453.7
PLANE D 432.2	443.2	447.2	449.6	451.2	452.3	453.0	453.4	453.6	453.6
PLANE E 426.8	440.3	446.0	449.0	450.9	452.1	452.9	453.3	453.6	453.6

TEMPERATURE DISTRIBUTION AT TIME = 213.0

PLANE A 442.8	440.8	443.9	445.6	446.8	447.7	448.2	448.6	448.7	448.7
PLANE B 435.4	441.4	443.8	445.5	446.7	447.6	448.1	448.5	448.7	448.7
PLANE C 431.9	439.7	442.9	444.9	446.4	447.3	448.0	448.4	448.6	448.6
PLANE D 425.3	437.1	441.6	444.2	445.9	447.1	447.8	448.3	448.5	448.5
PLANE E 419.8	434.1	440.3	443.7	445.6	446.9	447.7	448.2	448.4	448.4

TEMPERATURE DISTRIBUTION AT TIME = 220.0

POOR PRINT
Epreuve illisible

PLANE A 427.2	428.4	435.1	440.2	441.5	442.4	442.7	443.3	443.4	443.4
PLANE B 426.3	435.2	435.4	440.1	441.0	442.2	442.3	443.2	443.4	443.4
PLANE C 426.3	434.3	437.6	439.6	441.0	442.0	442.7	443.1	443.2	443.3
PLANE D 420.2	431.9	436.3	439.9	440.6	441.7	442.5	442.9	443.1	443.1
PLANE E 414.1	429.5	435.2	439.3	440.3	441.5	442.4	442.8	443.1	443.1

TEMPERATURE DISTRIBUTION AT TIME = 227.0

PLANE A 421.7	429.9	433.1	434.5	436.1	437.0	437.6	437.9	438.1	438.1
PLANE B 424.5	430.3	433.0	434.6	436.0	436.9	437.5	437.9	438.0	438.0
PLANE C 421.1	429.8	432.2	434.3	435.7	436.7	437.3	437.7	437.9	437.9
PLANE D 418.1	426.5	430.9	433.5	435.2	436.4	437.1	437.6	437.8	437.8
PLANE E 408.1	424.0	429.8	432.9	434.9	436.2	437.0	437.5	437.7	437.7

TEMPERATURE DISTRIBUTION AT TIME = 234.0

PLANE A 417.4	428.0	427.9	429.6	430.8	431.7	432.2	432.6	432.7	432.7
PLANE B 418.7	425.0	427.7	429.4	430.7	431.5	432.1	432.5	432.7	432.7
PLANE C 416.3	423.7	426.9	428.9	430.3	431.3	432.0	432.4	432.6	432.6
PLANE D 408.3	420.8	425.4	428.1	429.8	431.0	431.8	432.2	432.4	432.4
PLANE E 402.0	416.2	424.2	427.5	429.5	430.8	431.6	432.1	432.3	432.3

TEMPERATURE DISTRIBUTION AT TIME = 241.0

PLANE A 411.3	419.5	422.4	424.2	425.4	426.2	426.8	427.2	427.3	427.3
PLANE B 413.3	419.6	422.3	424.0	425.2	426.1	426.7	427.1	427.3	427.3
PLANE C 411.1	419.2	421.3	423.4	424.8	425.8	426.5	426.9	427.1	427.1
PLANE D 408.3	418.6	419.0	422.5	424.3	425.5	426.3	426.8	427.0	427.0
PLANE E 396.2	412.5	418.3	421.9	423.9	425.3	426.2	426.7	426.9	426.9

TEMPERATURE DISTRIBUTION AT TIME = 248.0

PLANE A 409.2	412.9	416.0	418.7	419.9	420.7	421.3	421.6	421.8	421.8
PLANE B 409.2	414.2	416.7	418.4	419.7	420.6	421.2	421.5	421.7	421.7
PLANE C 408.3	412.7	415.3	417.8	419.3	420.3	421.0	421.4	421.6	421.6
PLANE D 398.6	409.0	414.0	416.9	418.7	419.9	420.7	421.2	421.4	421.4
PLANE E 390.3	408.8	412.9	416.2	418.4	419.7	420.6	421.1	421.3	421.3

TEMPERATURE DISTRIBUTION AT TIME = 255.0

PLANE A 401.9	408.5	411.5	413.2	414.4	415.2	415.8	416.1	416.2	416.3
PLANE B 403.1	408.7	411.3	413.0	414.2	415.1	415.7	416.1	416.2	416.2
PLANE C 399.8	407.6	410.3	412.3	413.8	414.8	415.5	415.9	416.1	416.1
PLANE D 394.3	404.3	408.7	411.5	413.3	414.5	415.2	415.7	415.9	415.9
PLANE E 388.3	401.0	407.3	410.7	412.9	414.2	415.1	415.6	415.8	415.8

TEMPERATURE DISTRIBUTION AT TIME = 262.0

PLANE A 395.3	402.9	405.3	407.0	408.3	409.0	410.2	410.6	410.7	410.7
PLANE B 396.3	402.9	405.5	407.2	408.6	409.5	410.1	410.5	410.7	410.7
PLANE C 392.2	400.9	404.4	406.6	408.1	409.2	409.9	410.3	410.5	410.5
PLANE D 385.0	397.8	402.8	405.7	407.6	408.8	409.6	410.1	410.4	410.4
PLANE E 377.2	395.0	401.4	405.0	407.2	408.6	409.5	410.0	410.3	410.3

TEMPERATURE DISTRIBUTION AT TIME = 269.0

PLANE A 390.0	397.3	400.1	401.8	403.0	403.9	404.5	404.8	405.0	405.0
PLANE B 391.1	397.1	399.8	401.5	402.8	403.7	404.3	404.7	404.9	404.9
PLANE C 388.3	395.0	398.6	400.8	402.3	403.4	404.1	404.6	404.8	404.8
PLANE D 379.1	391.9	396.9	399.8	401.7	403.0	403.9	404.4	404.6	404.6
PLANE E 373.3	388.7	395.4	399.1	401.3	402.8	403.7	404.2	404.5	404.5

TEMPERATURE DISTRIBUTION AT TIME = 276.0

PLANE A 394.4	391.7	394.4	396.1	397.3	398.1	398.7	399.1	399.2	399.2
PLANE B 391.6	391.6	394.0	395.8	397.0	397.9	398.6	399.0	399.1	399.1
PLANE C 389.8	389.3	392.8	395.0	396.5	397.6	398.3	398.8	399.0	399.0
PLANE D 373.1	386.0	391.0	394.0	395.9	397.2	398.1	398.6	398.8	398.8
PLANE E 363.0	382.4	389.4	393.1	395.4	396.9	397.9	398.4	398.7	398.7

TEMPERATURE DISTRIBUTION AT TIME = 283.0

PLANE A 379.0	386.1	388.7	390.4	391.5	392.3	392.9	393.3	393.4	393.4
PLANE B 379.3	385.6	388.2	390.0	391.2	392.1	392.8	393.1	393.3	393.3
PLANE C 375.1	383.3	386.9	389.2	390.7	391.8	392.5	392.9	393.1	393.1
PLANE D 367.3	380.0	385.1	388.1	390.0	391.3	392.2	392.7	393.0	393.0
PLANE E 356.0	376.0	383.3	387.2	389.5	391.0	392.0	392.6	392.8	392.8

TEMPERATURE DISTRIBUTION AT TIME = 290.0

PLANE A 374.0	380.4	382.9	384.5	385.7	386.5	387.0	387.4	387.6	387.6
PLANE B 373.8	379.2	382.4	384.1	385.4	386.3	386.9	387.3	387.5	387.5
PLANE C 369.0	377.8	381.0	383.2	384.8	385.9	386.6	387.1	387.3	387.3

POOR PRINT
Epreuve illisible

PLANE [illegible]	[illegible]	[illegible]	[illegible]	[illegible]	[illegible]	[illegible]	[illegible]	[illegible]	[illegible]
PLANE [illegible]	[illegible]	[illegible]	[illegible]	[illegible]	[illegible]	[illegible]	[illegible]	[illegible]	[illegible]

TEMPERATURE DISTRIBUTION AT TIME = 297.0

PLANE A	[illegible]	374.4	[illegible]	[illegible]	379.7	[illegible]	[illegible]	[illegible]	[illegible]
PLANE B	[illegible]	373.9	[illegible]	[illegible]	379.4	[illegible]	[illegible]	[illegible]	[illegible]
PLANE C	[illegible]	371.4	[illegible]	[illegible]	378.7	[illegible]	[illegible]	[illegible]	[illegible]
PLANE D	[illegible]	367.1	[illegible]	[illegible]	378.0	[illegible]	[illegible]	[illegible]	[illegible]
PLANE E	[illegible]	362.8	[illegible]	[illegible]	377.4	[illegible]	[illegible]	[illegible]	[illegible]

TEMPERATURE DISTRIBUTION AT TIME = 304.0

PLANE A	[illegible]	368.2	[illegible]	[illegible]	373.5	[illegible]	[illegible]	[illegible]	[illegible]
PLANE B	[illegible]	367.6	[illegible]	[illegible]	373.1	[illegible]	[illegible]	[illegible]	[illegible]
PLANE C	[illegible]	[illegible]	[illegible]	[illegible]	372.4	[illegible]	[illegible]	[illegible]	[illegible]
PLANE D	[illegible]	359.7	[illegible]	[illegible]	371.6	[illegible]	[illegible]	[illegible]	[illegible]
PLANE E	[illegible]	[illegible]	[illegible]	[illegible]	370.9	[illegible]	[illegible]	[illegible]	[illegible]

TEMPERATURE DISTRIBUTION AT TIME = 311.0

PLANE A	[illegible]	[illegible]	[illegible]	[illegible]	367.1	[illegible]	[illegible]	[illegible]	[illegible]
PLANE B	[illegible]	[illegible]	[illegible]	[illegible]	366.7	[illegible]	[illegible]	[illegible]	[illegible]
PLANE C	[illegible]	[illegible]	[illegible]	[illegible]	[illegible]	[illegible]	[illegible]	[illegible]	[illegible]
PLANE D	[illegible]	[illegible]	[illegible]	[illegible]	[illegible]	[illegible]	[illegible]	[illegible]	[illegible]
PLANE E	[illegible]	[illegible]	[illegible]	[illegible]	[illegible]	[illegible]	[illegible]	[illegible]	[illegible]

TEMPERATURE DISTRIBUTION AT TIME = 318.0

PLANE A	[illegible]	[illegible]	[illegible]	[illegible]	[illegible]	[illegible]	[illegible]	[illegible]	[illegible]
PLANE B	[illegible]	[illegible]	[illegible]	[illegible]	[illegible]	[illegible]	[illegible]	[illegible]	[illegible]
PLANE C	[illegible]	[illegible]	[illegible]	[illegible]	[illegible]	[illegible]	[illegible]	[illegible]	[illegible]
PLANE D	[illegible]	[illegible]	[illegible]	[illegible]	[illegible]	[illegible]	[illegible]	[illegible]	[illegible]
PLANE E	[illegible]	[illegible]	[illegible]	[illegible]	[illegible]	[illegible]	[illegible]	[illegible]	[illegible]

TEMPERATURE DISTRIBUTION AT TIME = 325.0

PLANE A	[illegible]	[illegible]	[illegible]	[illegible]	[illegible]	[illegible]	[illegible]	[illegible]	[illegible]
PLANE B	[illegible]	[illegible]	[illegible]	[illegible]	[illegible]	[illegible]	[illegible]	[illegible]	[illegible]
PLANE C	[illegible]	[illegible]	[illegible]	[illegible]	[illegible]	[illegible]	[illegible]	[illegible]	[illegible]
PLANE D	[illegible]	[illegible]	[illegible]	[illegible]	[illegible]	[illegible]	[illegible]	[illegible]	[illegible]
PLANE E	[illegible]	[illegible]	[illegible]	[illegible]	[illegible]	[illegible]	[illegible]	[illegible]	[illegible]

TEMPERATURE DISTRIBUTION AT TIME = 332.0

PLANE A	[illegible]	[illegible]	[illegible]	[illegible]	[illegible]	[illegible]	[illegible]	[illegible]	[illegible]
PLANE B	[illegible]	[illegible]	[illegible]	[illegible]	[illegible]	[illegible]	[illegible]	[illegible]	[illegible]
PLANE C	[illegible]	[illegible]	[illegible]	[illegible]	[illegible]	[illegible]	[illegible]	[illegible]	[illegible]
PLANE D	[illegible]	[illegible]	[illegible]	[illegible]	[illegible]	[illegible]	[illegible]	[illegible]	[illegible]
PLANE E	[illegible]	[illegible]	[illegible]	[illegible]	[illegible]	[illegible]	[illegible]	[illegible]	[illegible]

TEMPERATURE DISTRIBUTION AT TIME = 339.0

PLANE A	[illegible]	[illegible]	[illegible]	[illegible]	[illegible]	[illegible]	[illegible]	[illegible]	[illegible]
PLANE B	[illegible]	[illegible]	[illegible]	[illegible]	[illegible]	[illegible]	[illegible]	[illegible]	[illegible]
PLANE C	[illegible]	[illegible]	[illegible]	[illegible]	[illegible]	[illegible]	[illegible]	[illegible]	[illegible]
PLANE D	[illegible]	[illegible]	[illegible]	[illegible]	[illegible]	[illegible]	[illegible]	[illegible]	[illegible]
PLANE E	[illegible]	[illegible]	[illegible]	[illegible]	[illegible]	[illegible]	[illegible]	[illegible]	[illegible]

TEMPERATURE DISTRIBUTION AT TIME = 346.0

PLANE A	[illegible]	[illegible]	[illegible]	[illegible]	[illegible]	[illegible]	[illegible]	[illegible]	[illegible]
PLANE B	[illegible]	[illegible]	[illegible]	[illegible]	[illegible]	[illegible]	[illegible]	[illegible]	[illegible]
PLANE C	[illegible]	[illegible]	[illegible]	[illegible]	[illegible]	[illegible]	[illegible]	[illegible]	[illegible]
PLANE D	[illegible]	[illegible]	[illegible]	[illegible]	[illegible]	[illegible]	[illegible]	[illegible]	[illegible]
PLANE E	[illegible]	[illegible]	[illegible]	[illegible]	[illegible]	[illegible]	[illegible]	[illegible]	[illegible]

TEMPERATURE DISTRIBUTION AT TIME = 353.0

PLANE A	[illegible]	317.0	[illegible]	[illegible]	[illegible]	[illegible]	[illegible]	[illegible]	[illegible]
PLANE B	[illegible]	[illegible]	[illegible]	[illegible]	[illegible]	[illegible]	[illegible]	[illegible]	[illegible]
PLANE C	[illegible]	[illegible]	[illegible]	[illegible]	[illegible]	[illegible]	[illegible]	[illegible]	[illegible]
PLANE D	[illegible]	[illegible]	[illegible]	[illegible]	[illegible]	[illegible]	[illegible]	[illegible]	[illegible]
PLANE E	[illegible]	[illegible]	[illegible]	[illegible]	[illegible]	[illegible]	[illegible]	[illegible]	[illegible]

TEMPERATURE DISTRIBUTION AT TIME = 360.0

PLANE A	[illegible]	[illegible]	[illegible]	[illegible]	[illegible]	[illegible]	[illegible]	[illegible]	[illegible]
PLANE B	[illegible]	[illegible]	[illegible]	[illegible]	[illegible]	[illegible]	[illegible]	[illegible]	[illegible]
PLANE C	[illegible]	[illegible]	[illegible]	[illegible]	[illegible]	[illegible]	[illegible]	[illegible]	[illegible]
PLANE D	[illegible]	[illegible]	[illegible]	[illegible]	[illegible]	[illegible]	[illegible]	[illegible]	[illegible]
PLANE E	[illegible]	[illegible]	[illegible]	[illegible]	[illegible]	[illegible]	[illegible]	[illegible]	[illegible]

TEMPERATURE DISTRIBUTION AT TIME = 367.0

POOR PRINT
Epreuve illisible

PLANE A 294.4	299.8	302.2	304.3	305.3	306.3	307.1	307.5	307.8	307.8
PLANE B 293.4	297.5	300.6	302.8	304.5	305.6	306.7	307.2	307.3	307.5
PLANE C 282.1	292.5	297.4	300.8	302.2	304.9	306.1	306.8	307.1	307.1
PLANE D 280.3	281.5	292.4	298.1	301.7	303.9	305.4	306.3	306.7	306.7
PLANE E 247.3	278.6	290.3	296.8	300.2	303.2	305.0	305.9	306.4	306.4

TEMPERATURE DISTRIBUTION AT TIME = 374.0

PLANE A 283.7	293.1	292.7	294.6	296.0	297.0	297.8	298.3	298.5	298.5
PLANE B 291.9	288.0	291.1	293.4	295.2	296.5	297.4	298.0	298.2	298.2
PLANE C 288.9	291.7	287.2	291.1	293.7	295.5	296.7	297.4	297.8	297.8
PLANE D 285.9	270.7	282.1	288.2	292.0	294.4	296.0	296.9	297.3	297.3
PLANE E 232.1	266.6	279.5	286.6	291.0	293.8	295.5	296.6	297.0	297.0

TEMPERATURE DISTRIBUTION AT TIME = 381.0

PLANE A 275.5	290.7	283.0	284.9	286.2	287.2	288.0	288.5	288.7	288.7
PLANE B 274.4	278.1	281.3	283.6	285.4	286.7	287.6	288.2	288.5	288.5
PLANE C 269.0	272.5	277.9	281.5	284.0	285.7	286.9	287.7	288.0	288.0
PLANE D 241.2	264.4	273.4	278.8	282.4	284.7	286.2	287.1	287.5	287.5
PLANE E 219.0	259.8	269.2	276.7	281.1	284.0	285.7	286.8	287.2	287.2

TEMPERATURE DISTRIBUTION AT TIME = 388.0

PLANE A 261.4	268.7	271.7	273.8	275.4	276.7	277.6	278.2	278.4	278.4
PLANE B 257.7	266.2	269.8	272.5	274.5	276.0	277.1	277.8	278.1	278.1
PLANE C 246.7	260.0	265.9	269.9	272.8	274.9	276.3	277.1	277.5	277.5
PLANE D 223.9	239.5	260.1	266.5	270.7	273.5	275.4	276.5	277.0	277.0
PLANE E 195.1	236.3	254.3	263.6	269.1	272.6	274.7	276.0	276.6	276.6

TEMPERATURE DISTRIBUTION AT TIME = 395.0

PLANE A 226.7	246.3	259.1	258.6	261.6	263.6	265.0	265.8	266.2	266.2
PLANE B 216.5	242.3	251.5	256.9	260.5	262.9	264.4	265.4	265.8	265.8
PLANE C 201.2	239.2	247.3	254.2	258.7	261.7	263.6	264.7	265.2	265.2
PLANE D 191.2	225.8	243.2	251.6	257.0	260.5	262.7	264.0	264.7	264.7
PLANE E 171.3	221.2	239.0	249.6	255.7	259.7	262.2	263.6	264.3	264.3

TEMPERATURE DISTRIBUTION AT TIME = 402.0

PLANE A 161.0	203.3	230.1	239.8	235.9	240.2	243.0	244.7	245.5	245.5
PLANE B 155.0	205.7	221.0	230.1	236.1	240.2	243.0	244.7	245.5	245.5
PLANE C 127.0	198.4	222.5	230.7	236.4	240.4	243.1	244.7	245.5	245.5
PLANE D 170.2	206.9	242.1	230.7	236.4	240.4	243.1	244.7	245.5	245.5
PLANE E 165.3	205.9	221.2	230.3	236.2	240.3	243.0	244.7	245.5	245.5

TEMPERATURE DISTRIBUTION AT TIME = 409.0

PLANE A 180.7	194.0	206.7	214.1	219.0	222.3	224.5	225.8	226.4	226.4
PLANE B 165.7	195.9	207.0	214.5	219.2	222.4	224.5	225.8	226.4	226.4
PLANE C 174.2	196.5	208.0	215.0	219.4	222.5	224.6	225.9	226.5	226.5
PLANE D 170.3	197.4	209.2	214.9	219.4	222.5	224.6	225.9	226.5	226.5
PLANE E 166.9	194.5	207.2	214.5	219.2	222.5	224.0	225.9	226.5	226.5

TEMPERATURE DISTRIBUTION AT TIME = 416.0

PLANE A 156.2	183.3	194.4	200.6	204.7	207.4	209.2	210.3	210.9	210.9
PLANE B 161.4	185.2	195.3	201.0	204.8	207.5	209.3	210.4	210.9	210.9
PLANE C 168.1	187.9	196.1	201.4	205.0	207.6	209.3	210.4	210.9	210.9
PLANE D 164.5	186.9	195.8	201.3	205.0	207.6	209.4	210.4	210.9	210.9
PLANE E 157.4	184.6	195.0	200.9	204.9	207.6	209.3	210.4	210.9	210.9

TEMPERATURE DISTRIBUTION AT TIME = 423.0

PLANE A 151.2	175.0	184.1	189.4	192.9	195.2	196.8	197.7	198.1	198.1
PLANE B 154.8	176.3	184.7	189.7	193.0	195.3	196.8	197.7	198.1	198.1
PLANE C 161.4	176.3	185.4	190.0	193.1	195.3	196.9	197.7	198.2	198.2
PLANE D 157.3	177.2	185.1	189.8	193.1	195.3	196.8	197.7	198.2	198.2
PLANE E 151.2	175.4	184.4	189.6	193.0	195.3	196.8	197.7	198.2	198.2

TEMPERATURE DISTRIBUTION AT TIME = 430.0

PLANE A 142.9	168.3	175.8	180.1	183.0	184.9	186.2	186.9	187.3	187.3
PLANE B 152.0	169.5	176.3	180.4	183.1	184.9	186.2	186.9	187.3	187.3
PLANE C 157.9	171.3	177.0	180.6	183.2	185.0	186.2	187.0	187.3	187.3
PLANE D 154.1	170.2	176.6	180.5	183.2	185.0	186.2	187.0	187.3	187.3
PLANE E 148.7	168.5	176.0	180.3	183.1	185.0	186.2	187.0	187.3	187.3

TEMPERATURE DISTRIBUTION AT TIME = 437.0

PLANE A 144.1	161.3	167.9	171.7	174.2	175.9	177.0	177.7	178.0	178.0
PLANE B 147.6	162.6	168.4	172.0	174.3	176.0	177.1	177.7	178.1	178.1

POOR PRINT
Epreuve illisible

PLANE D 149.5	163.2	168.7	172.1	174.4	176.0	177.1	177.8	178.1	178.1
PLANE E 144.0	161.0	168.2	171.9	174.5	176.0	177.1	177.8	178.1	178.1

TEMPERATURE DISTRIBUTION AT TIME = 444.0

PLANE A 140.7	155.7	161.5	164.8	167.0	168.4	169.4	169.9	170.2	170.2
PLANE B 143.1	156.7	161.9	165.0	167.0	168.5	169.4	170.0	170.2	170.2
PLANE C 147.0	157.9	162.4	165.2	167.1	168.5	169.4	170.0	170.2	170.2
PLANE D 146.2	157.6	162.2	165.1	167.1	168.5	169.4	170.0	170.2	170.2
PLANE E 140.2	156.0	161.7	164.9	167.0	168.5	169.4	170.0	170.2	170.2

TEMPERATURE DISTRIBUTION AT TIME = 451.0

PLANE A 138.9	151.2	156.0	158.8	160.6	161.8	162.6	163.1	163.4	163.4
PLANE B 140.9	152.1	156.4	159.0	160.7	161.9	162.7	163.2	163.4	163.4
PLANE C 144.9	153.3	156.8	159.2	160.8	161.9	162.7	163.2	163.4	163.4
PLANE D 142.4	152.6	156.6	159.1	160.8	161.9	162.7	163.2	163.4	163.4
PLANE E 139.3	151.7	156.3	159.0	160.7	161.9	162.7	163.2	163.4	163.4

TEMPERATURE DISTRIBUTION AT TIME = 458.0

PLANE A 136.1	147.1	151.3	153.7	155.3	156.4	157.0	157.5	157.7	157.7
PLANE B 138.1	147.9	151.7	153.9	155.4	156.4	157.1	157.5	157.7	157.7
PLANE C 141.6	149.0	152.1	154.1	155.5	156.4	157.1	157.5	157.7	157.7
PLANE D 139.4	148.2	151.9	154.0	155.4	156.4	157.1	157.5	157.7	157.7
PLANE E 136.7	147.5	151.5	153.9	155.4	156.4	157.1	157.5	157.7	157.7

TEMPERATURE DISTRIBUTION AT TIME = 465.0

PLANE A 133.7	143.5	147.1	149.2	150.6	151.5	152.1	152.5	152.7	152.7
PLANE B 136.0	144.3	147.5	149.4	150.7	151.6	152.1	152.5	152.7	152.7
PLANE C 139.6	145.4	147.9	149.6	150.8	151.6	152.2	152.5	152.7	152.7
PLANE D 137.6	144.9	147.8	149.6	150.8	151.6	152.2	152.5	152.7	152.7
PLANE E 135.2	144.1	147.3	149.5	150.7	151.6	152.2	152.5	152.7	152.7

TEMPERATURE DISTRIBUTION AT TIME = 472.0

PLANE A 131.5	140.3	143.5	145.4	146.6	147.4	147.9	148.2	148.4	148.4
PLANE B 133.4	140.9	143.8	145.5	146.6	147.4	147.9	148.3	148.4	148.4
PLANE C 136.7	141.9	144.2	145.7	146.7	147.5	148.0	148.3	148.4	148.4
PLANE D 134.7	141.4	144.0	145.6	146.7	147.5	148.0	148.3	148.4	148.4
PLANE E 132.1	140.9	143.8	145.5	146.7	147.5	148.0	148.3	148.4	148.4

TEMPERATURE DISTRIBUTION AT TIME = 479.0

PLANE A 130.2	137.9	140.6	142.2	143.2	143.9	144.3	144.6	144.7	144.7
PLANE B 132.1	138.5	140.9	142.3	143.2	143.9	144.3	144.6	144.7	144.7
PLANE C 135.1	139.3	141.2	142.4	143.3	143.9	144.3	144.6	144.7	144.7
PLANE D 133.0	138.8	141.0	142.4	143.3	143.9	144.4	144.6	144.7	144.7
PLANE E 131.0	138.1	140.8	142.3	143.3	143.9	144.4	144.6	144.7	144.7

TEMPERATURE DISTRIBUTION AT TIME = 486.0

PLANE A 129.2	135.5	137.8	139.2	140.1	140.7	141.1	141.3	141.5	141.5
PLANE B 130.4	135.9	138.1	139.3	140.2	140.7	141.1	141.4	141.5	141.5
PLANE C 133.4	136.8	138.4	139.5	140.2	140.8	141.1	141.4	141.5	141.5
PLANE D 131.3	136.3	138.2	139.4	140.2	140.8	141.1	141.4	141.5	141.5
PLANE E 129.3	135.8	138.0	139.3	140.2	140.8	141.1	141.4	141.5	141.5

TEMPERATURE DISTRIBUTION AT TIME = 493.0

PLANE A 127.8	133.4	135.5	136.7	137.5	138.0	138.4	138.6	138.7	138.7
PLANE B 128.7	133.7	135.7	136.8	137.5	138.1	138.4	138.6	138.7	138.7
PLANE C 131.4	134.5	135.9	136.9	137.6	138.1	138.4	138.6	138.7	138.7
PLANE D 129.5	134.0	135.8	136.8	137.6	138.1	138.4	138.6	138.7	138.7
PLANE E 128.0	133.5	135.6	136.8	137.5	138.1	138.4	138.6	138.7	138.7

TEMPERATURE DISTRIBUTION AT TIME = 500.0

PLANE A 127.1	131.7	133.5	134.5	135.2	135.7	136.0	136.1	136.2	136.2
PLANE B 127.7	132.0	133.7	134.6	135.2	135.7	136.0	136.1	136.2	136.2
PLANE C 130.2	132.7	133.9	134.7	135.3	135.7	136.0	136.2	136.2	136.2
PLANE D 128.4	132.2	133.7	134.7	135.3	135.7	136.0	136.1	136.2	136.2
PLANE E 127.0	131.8	133.5	134.6	135.2	135.7	136.0	136.1	136.2	136.2

TEMPERATURE DISTRIBUTION AT TIME = 507.0

PLANE A 126.0	130.1	131.7	132.6	133.2	133.6	133.9	134.0	134.1	134.1
PLANE B 126.6	130.5	131.9	132.7	133.3	133.6	133.9	134.0	134.1	134.1
PLANE C 129.1	131.1	132.1	132.8	133.3	133.7	133.9	134.0	134.1	134.1
PLANE D 127.3	130.8	131.9	132.7	133.3	133.6	133.9	134.0	134.1	134.1
PLANE E 125.8	130.1	131.7	132.7	133.2	133.6	133.9	134.0	134.1	134.1

PLANE A 129.8	128.8	130.0	130.5	131.4	131.6	132.0	132.1	132.2	132.2
PLANE B 129.8	129.9	130.2	130.5	131.4	131.6	132.0	132.2	132.2	132.2
PLANE C 129.9	129.8	130.2	130.5	131.4	131.6	132.0	132.2	132.2	132.2
PLANE D 129.8	129.8	130.2	130.5	131.4	131.6	132.0	132.2	132.2	132.2
PLANE E 129.6	129.6	130.0	130.5	131.4	131.6	132.0	132.2	132.2	132.2

TEMPERATURE DISTRIBUTION AT TIME = 521.0

PLANE A 124.1	127.2	128.6	129.3	129.7	130.1	130.3	130.4	130.5	130.5
PLANE B 125.0	127.6	128.6	129.3	129.8	130.1	130.3	130.4	130.5	130.5
PLANE C 124.4	127.5	128.6	129.3	129.8	130.1	130.3	130.4	130.5	130.5
PLANE D 125.4	127.7	128.7	129.3	129.8	130.1	130.3	130.4	130.5	130.5
PLANE E 123.8	127.2	128.5	129.3	129.7	130.1	130.3	130.4	130.5	130.5

TEMPERATURE DISTRIBUTION AT TIME = 528.0

PLANE A 123.0	126.1	127.2	127.9	128.3	128.6	128.8	128.9	128.9	128.9
PLANE B 123.9	126.4	127.4	127.9	128.3	128.6	128.8	128.9	128.9	128.9
PLANE C 125.6	126.9	127.5	128.0	128.4	128.6	128.8	128.9	128.9	128.9
PLANE D 123.8	126.2	127.3	127.9	128.3	128.6	128.8	128.9	128.9	128.9
PLANE E 122.7	125.9	127.2	127.9	128.3	128.6	128.8	128.9	128.9	128.9

TEMPERATURE DISTRIBUTION AT TIME = 535.0

PLANE A 122.4	125.0	126.0	126.6	127.0	127.3	127.4	127.5	127.6	127.6
PLANE B 123.3	125.1	126.1	126.7	127.0	127.3	127.4	127.5	127.6	127.6
PLANE C 124.3	125.7	126.3	126.7	127.0	127.3	127.4	127.5	127.6	127.6
PLANE D 123.3	125.2	126.1	126.6	127.0	127.2	127.4	127.5	127.6	127.6
PLANE E 121.6	124.7	125.9	126.6	127.0	127.2	127.4	127.5	127.6	127.6

TEMPERATURE DISTRIBUTION AT TIME = 542.0

PLANE A 121.3	123.9	124.9	125.4	125.8	126.0	126.2	126.3	126.3	126.3
PLANE B 122.2	124.2	125.0	125.5	125.8	126.0	126.2	126.3	126.3	126.3
PLANE C 123.4	124.6	125.1	125.5	125.8	126.0	126.2	126.3	126.3	126.3
PLANE D 122.2	124.2	125.0	125.5	125.8	126.0	126.2	126.3	126.3	126.3
PLANE E 120.7	123.7	124.8	125.4	125.8	126.0	126.2	126.3	126.3	126.3

TEMPERATURE DISTRIBUTION AT TIME = 549.0

PLANE A 120.3	122.9	124.0	124.4	124.7	124.9	125.0	125.1	125.2	125.2
PLANE B 121.4	123.2	124.0	124.4	124.7	124.9	125.0	125.1	125.2	125.2
PLANE C 122.3	123.8	124.1	124.4	124.7	124.9	125.0	125.1	125.2	125.2
PLANE D 121.4	123.2	124.0	124.4	124.7	124.9	125.0	125.1	125.2	125.2
PLANE E 120.3	122.8	123.9	124.3	124.7	124.9	125.0	125.1	125.2	125.2

TEMPERATURE DISTRIBUTION AT TIME = 556.0

PLANE A 119.7	122.3	123.4	123.8	123.7	123.9	124.0	124.1	124.1	124.1
PLANE B 120.5	122.3	123.0	123.4	123.7	123.9	124.0	124.1	124.1	124.1
PLANE C 121.7	122.6	123.1	123.4	123.7	123.9	124.0	124.1	124.1	124.1
PLANE D 120.6	122.3	123.0	123.4	123.7	123.9	124.0	124.1	124.1	124.1
PLANE E 119.1	121.9	123.3	123.8	123.8	123.8	124.0	124.1	124.1	124.1

TEMPERATURE DISTRIBUTION AT TIME = 563.0

PLANE A 119.0	121.2	122.0	122.4	122.7	122.9	123.0	123.1	123.1	123.1
PLANE B 119.9	121.5	122.1	122.5	122.7	122.9	123.0	123.1	123.1	123.1
PLANE C 121.0	121.8	122.2	122.5	122.7	122.9	123.0	123.1	123.1	123.1
PLANE D 119.9	121.4	122.1	122.4	122.7	122.9	123.0	123.1	123.1	123.1
PLANE E 118.7	121.0	121.9	122.4	122.7	122.9	123.0	123.1	123.1	123.1

TEMPERATURE DISTRIBUTION AT TIME = 570.0

PLANE A 118.4	120.4	121.2	121.6	121.8	122.0	122.1	122.2	122.2	122.2
PLANE B 119.3	120.7	121.3	121.6	121.8	122.0	122.1	122.2	122.2	122.2
PLANE C 120.3	121.0	121.4	121.6	121.9	122.0	122.1	122.2	122.2	122.2
PLANE D 119.1	120.6	121.2	121.6	121.8	122.0	122.1	122.2	122.2	122.2
PLANE E 119.1	120.3	121.1	121.5	121.8	122.0	122.1	122.2	122.2	122.2

POOR PRINT
Epreuve illisible

PROBLEM DURATION 0.0 TO 3.71962 02

VARIABLE	MINIMUM	TIME	MAXIMUM	TIME
HTA	6.03406E 03	1.00000E-01	2.40009E 06	3.07700E 02
HTB	-2.32926E 04	1.00000E-01	2.04846E 06	3.00700E 02
HTC	-1.31386E 06	0.0	1.62815E 06	3.06800E 02
HTD	-2.33476E 02	0.0	1.49396E 06	3.06800E 02
HTE	6.45528E 04	1.00000E-01	2.41542E 06	3.09700E 02

POOR PRINT
Epreuve illisible

PAGE 1

MINIMUM 6.03406E 03 HTA VERSUS TIME MAXIMUM 2.40009E 06

TIME	HTA	T15	T25
0.0	3.47658E 05	6.0343E 02	6.0396E 02
1.00000E-01	1.15644E 04	5.9134E 02	6.0327E 02
1.00000E 00	1.58248E 05	5.9991E 02	6.0263E 02
2.00000E 00	1.03515E 05	5.9868E 02	6.0209E 02
3.00000E 00	1.73490E 05	5.9755E 02	6.0136E 02
4.00000E 00	1.95465E 05	5.9648E 02	6.0072E 02
5.00000E 00	2.21594E 05	5.9547E 02	6.0012E 02
6.00000E 00	2.38779E 05	5.9450E 02	5.9946E 02
7.00000E 00	2.51730E 05	5.9357E 02	5.9883E 02
8.00000E 00	2.73356E 05	5.9269E 02	5.9819E 02
9.00000E 00	2.91628E 05	5.9183E 02	5.9756E 02
1.00000E 01	3.00347E 05	5.9093E 02	5.9693E 02
1.10000E 01	3.12945E 05	5.9017E 02	5.9630E 02
1.20000E 01	3.23196E 05	5.8940E 02	5.9566E 02
1.30000E 01	3.42993E 05	5.8861E 02	5.9507E 02
1.40000E 01	3.38578E 05	5.8788E 02	5.9445E 02
1.50000E 01	3.51678E 05	5.8706E 02	5.9384E 02
1.60000E 01	3.58832E 05	5.8629E 02	5.9323E 02
1.70000E 01	3.66613E 05	5.8552E 02	5.9263E 02
1.80000E 01	3.75192E 05	5.8478E 02	5.9202E 02
1.90000E 01	3.85498E 05	5.8376E 02	5.9133E 02
2.00000E 01	4.00477E 05	5.8271E 02	5.9066E 02
2.10000E 01	4.19692E 05	5.8163E 02	5.8985E 02
2.20000E 01	4.37018E 05	5.8049E 02	5.8908E 02
2.30000E 01	4.56306E 05	5.7931E 02	5.8828C 02
2.40000E 01	4.71166E 05	5.7805E 02	5.8747E 02
2.50000E 01	4.71456E 05	5.7743E 02	5.8681E 02
2.60000E 01	4.76308E 05	5.7688C 02	5.8624E 02
2.70000E 01	4.79276E 05	5.7643E 02	5.8571E 02
2.80000E 01	4.83666E 05	5.7606E 02	5.8523E 02
2.90000E 01	4.89648E 05	5.7584E 02	5.8479E 02
3.00000E 01	4.94778E 05	5.7571E 02	5.8440E 02
3.10000E 01	4.99070E 05	5.7569E 02	5.8406E 02
3.20000E 01	4.03670E 05	5.7577E 02	5.8375E 02
3.30000E 01	4.06168E 05	5.7549E 02	5.8338E 02
3.40000E 01	4.09487E 05	5.7525E 02	5.8299E 02
3.50000E 01	4.02246E 05	5.7503E 02	5.8260C 02
3.60000E 01	4.02694E 02	5.7484E 02	5.8223E 02
3.70000E 01	3.91010E 05	5.7466E 02	5.8188E 02
3.71962E 01	3.89648E 05	5.7450E 02	5.8153E 02
3.80000E 01	3.77106E 05	5.7435E 02	5.8119E 02
3.90000E 01	3.61248E 05	5.7423E 02	5.8086E 02
4.00000E 01	3.54408E 05	5.7360E 02	5.8042E 02
4.10000E 01	3.62554E 05	5.7291E 02	5.7991E 02
4.15000E 01	3.71941E 05		

MINIMUM 6.5 AGE 03 · HTA VERSUS TIME · MAXIMUM 2.4009E 06

TIME	HTA	I	T15	T25
2.4[illegible]	3.7859E 05	---------+	5.7214E 02	5.7938E 02
2.4[illegible]	3.9154E 05	---------+	5.7130E 02	5.7882E 02
2.4[illegible]	4.0364E 05	---------+	5.7038E 02	5.7824E 02
2.4[illegible]	4.2013E 05	---------+	5.6937E 02	5.7763E 02
2.4[illegible]	4.2144E 05	---------+	5.6877E 02	5.7711E 02
2.4[illegible]	4.3124E 05	---------+	5.6817E 02	5.7663E 02
2.4[illegible]	4.3449E 05	---------+	5.6760E 02	5.7618E 02
2.4[illegible]	4.[illegible]E 05	---------+	5.6707E 02	5.7574E 02
2.4[illegible]	4.4377E 05	---------+	5.6659E 02	5.7532E 02
2.4[illegible]	4.4334E 05	---------+	5.6611E 02	5.7492E 02
2.4[illegible]	4.4158E 05	---------+	5.6568E 02	5.7454E 02
2.4[illegible]	4.4447E 05	---------+	5.6534E 02	5.7417E 02
2.4[illegible]	4.4460E 05	---------+	5.6488E 02	5.7376E 02
2.4[illegible]	4.1235E 05	---------+	5.6448E 02	5.7335E 02
2.4[illegible]	4.5071E 05	---------+	5.6408E 02	5.7293E 02
2.4[illegible]	4.4423E 05	---------+	5.6362E 02	5.7252E 02
2.4[illegible]	4.4497E 05	---------+	5.6320E 02	5.7211E 02
3.4[illegible]	4.4611E 05	---------+	5.6279E 02	5.7176E 02
3.4[illegible]	4.4216E 05	---------+	5.6233E 02	5.7129E 02
3.4[illegible]	4.4766E 05	---------+	5.6199E 02	5.7088E 02
3.4[illegible]	4.4519E 05	---------+	5.6167E 02	5.7050E 02
3.4[illegible]	4.4055E 05	---------+	5.6137E 02	5.7013E 02
3.4[illegible]	4.2953E 05	---------+	5.6109E 02	5.6976E 02
3.4[illegible]	4.3157E 05	---------+	5.6082E 02	5.6941E 02
3.4[illegible]	4.3459E 05	---------+	5.6057E 02	5.6906E 02
3.4[illegible]	4.1982E 05	---------+	5.6035E 02	5.6872E 02
3.4[illegible]	4.1459E 05	---------+	5.6014E 02	5.6839E 02
3.4[illegible]	4.0472E 05	---------+	5.5994E 02	5.6806E 02
3.4[illegible]	4.1591E 05	---------+	5.5976E 02	5.6776E 02
3.4[illegible]	4.1222E 05	---------+	5.5958E 02	5.6744E 02
3.4[illegible]	4.1936E 05	---------+	5.5942E 02	5.6716E 02
3.4[illegible]	4.4041E 05	---------+	5.5928E 02	5.6688E 02
3.4[illegible]	4.3497E 05	---------+	5.5914E 02	5.6661E 02
3.4[illegible]	4.3657E 05	---------+	5.5902E 02	5.6635E 02
3.4[illegible]	4.4069E 05	---------+	5.5891E 02	5.6610E 02
3.4[illegible]	4.4676E 05	---------+	5.5881E 02	5.6586E 02
4.4[illegible]	4.3279E 04	---------+	5.5872E 02	5.6564E 02
4.4[illegible]	4.4[illegible]E 05	---------+	5.5864E 02	5.6543E 02
4.4[illegible]	4.3514E 05	---------+	5.5857E 02	5.6523E 02
4.4[illegible]	4.2511E 05	---------+	5.5851E 02	5.6504E 02
4.4[illegible]	4.2468E 05	---------+	5.5846E 02	5.6487E 02
4.4[illegible]	4.1833E 05	---------+	5.5842E 02	5.6472E 02
4.4[illegible]	4.2450E 05	---------+	5.5839E 02	5.6459E 02
4.4[illegible]	4.1794E 05	---------+	5.5837E 02	5.6449E 02

MINIMUM 6.5 AGE 03 · HTA VERSUS TIME · MAXIMUM 2.4009E 06

TIME	HTA	I	T15	T25
4.4[illegible]	4.2233E 05	---------+	5.5308E 02	5.6138E 02
4.4[illegible]	4.1611E 05	---------+	5.5279E 02	5.6102E 02
4.4[illegible]	4.1534E 05	---------+	5.5241E 02	5.6066E 02
4.4[illegible]	4.1157E 05	---------+	5.5209E 02	5.6031E 02
4.4[illegible]	4.1337E 05	---------+	5.5174E 02	5.5997E 02
4.4[illegible]	4.0825E 05	---------+	5.5142E 02	5.5957E 02
4.4[illegible]	4.1208E 05	---------+	5.5092E 02	5.5914E 02
4.4[illegible]	4.2552E 05	---------+	5.5019E 02	5.5867E 02
4.4[illegible]	4.3803E 05	---------+	5.4951E 02	5.5819E 02
4.4[illegible]	4.4640E 05	---------+	5.4879E 02	5.5768E 02
4.4[illegible]	4.5231E 05	---------+	5.4800E 02	5.5716E 02
4.4[illegible]	4.[illegible]E 05	---------+	5.4717E 02	5.5661E 02
4.4[illegible]	4.6451E 05	---------+	5.4675E 02	5.5617E 02
4.4[illegible]	4.6601E 05	---------+	5.4641E 02	5.5577E 02
4.4[illegible]	4.6[illegible]E 05	---------+	5.4611E 02	5.5541E 02
4.4[illegible]	4.8376E 05	---------+	5.4583E 02	5.5506E 02
4.4[illegible]	4.4879E 05	---------+	5.4571E 02	5.5475E 02
4.4[illegible]	4.3805E 05	---------+	5.4561E 02	5.5446E 02
4.4[illegible]	4.2776E 05	---------+	5.4554E 02	5.5419E 02
4.4[illegible]	4.2690E 05	---------+	5.4561E 02	5.5398E 02
4.4[illegible]	4.1587E 05	---------+	5.4524E 02	5.5361E 02
4.4[illegible]	4.1750E 05	---------+	5.4489E 02	5.5322E 02
4.4[illegible]	4.1334E 05	---------+	5.4451E 02	5.5287E 02
4.4[illegible]	4.1557E 05	---------+	5.4412E 02	5.5249E 02
5.4[illegible]	4.2147E 05	---------+	5.4371E 02	5.5210E 02
5.4[illegible]	4.2124E 05	---------+	5.4327E 02	5.5170E 02
5.4[illegible]	4.2753E 05	---------+	5.4282E 02	5.5130E 02
5.4[illegible]	4.1[illegible]E 05	---------+	5.4234E 02	5.5088E 02
5.4[illegible]	4.2406E 05	---------+	5.4187E 02	5.5047E 02
5.4[illegible]	4.2954E 05	---------+	5.4138E 02	5.5004E 02
5.4[illegible]	4.3467E 05	---------+	5.4089E 02	5.4962E 02
5.4[illegible]	4.4730E 05	---------+	5.4036E 02	5.4918E 02
5.4[illegible]	4.4274E 05	---------+	5.3983E 02	5.4874E 02
6.4[illegible]	4.4634E 05	---------+	5.3927E 02	5.4829E 02
6.4[illegible]	4.5033E 05	---------+	5.3882E 02	5.4787E 02
6.4[illegible]	4.3682E 05	---------+	5.3837E 02	5.4746E 02
6.4[illegible]	4.5564E 05	---------+	5.3793E 02	5.4705E 02
6.4[illegible]	4.5540E 05	---------+	5.3751E 02	5.4665E 02
6.4[illegible]	4.5635E 05	---------+	5.3709E 02	5.4626E 02
6.4[illegible]	4.5116E 05	---------+	5.3669E 02	5.4587E 02
6.4[illegible]	4.5164E 05	---------+	5.3630E 02	5.4549E 02
6.4[illegible]	4.4940E 05	---------+	5.3592E 02	5.4511E 02
6.4[illegible]	4.4927E 05	---------+	5.3555E 02	5.4474E 02
6.4[illegible]	4.4869E 05	---------+	5.3520E 02	5.4437E 02

POOR PRINT
Epreuve illisible

HTA VERSUS TIME

MINIMUM 6.5940E 03 — MAXIMUM 2.4009E 06

TIME	HTA	T15	T25
6.6000E 01	4.5043E 05	5.3485E 02	5.4401E 02
6.6500E 01	4.4858E 05	5.3452E 02	5.4366E 02
6.7000E 01	4.5142E 05	5.3419E 02	5.4331E 02
6.7500E 01	4.4532E 05	5.3387E 02	5.4296E 02
6.8000E 01	4.4614E 05	5.3358E 02	5.4263E 02
6.8500E 01	4.4750E 05	5.3329E 02	5.4229E 02
6.9000E 01	4.4434E 05	5.3300E 02	5.4196E 02
6.9500E 01	4.3771E 05	5.3272E 02	5.4164E 02
7.0000E 01	4.3803E 05	5.3240E 02	5.4132E 02
7.0500E 01	4.4109E 05	5.3220E 02	5.4101E 02
7.1000E 01	4.2228E 05	5.3196E 02	5.4070E 02
7.1500E 01	4.2486E 06	5.3173E 02	5.4040E 02
7.2000E 01	4.2359E 05	5.3150E 02	5.4011E 02
7.2500E 01	4.2457E 05	5.3128E 02	5.3982E 02
7.3000E 01	4.2026E 05	5.3108E 02	5.3953E 02
7.3500E 01	4.1708E 05	5.3089E 02	5.3925E 02
7.4000E 01	4.1301E 05	5.3050E 02	5.3892E 02
7.4500E 01	4.1779E 05	5.3014E 02	5.3856E 02
7.5000E 01	4.1974E 05	5.2978E 02	5.3824E 02
7.5500E 01	4.1001E 05	5.2943E 02	5.3790E 02
7.6000E 01	4.1423E 05	5.2907E 02	5.3755E 02
7.6500E 01	4.1697E 05	5.2872E 02	5.3721E 02
7.7000E 01	4.1665E 05	5.2837E 02	5.3687E 02
7.7500E 01	4.2062E 05	5.2801E 02	5.3653E 02
7.8000E 01	4.2225E 05	5.2766E 02	5.3619E 02
7.8500E 01	4.1321E 05	5.2731E 02	5.3585E 02
7.9000E 01	4.1796E 05	5.2696E 02	5.3550E 02
7.9500E 01	4.1650E 05	5.2661E 02	5.3516E 02
8.0000E 01	4.2001E 05	5.2626E 02	5.3482E 02
8.0500E 01	4.1619E 05	5.2591E 02	5.3446E 02
8.1000E 01	4.1769C 05	5.2556E 02	5.3414E 02
8.1500E 01	4.1065E 05	5.2522E 02	5.3380E 02
8.2000E 01	4.2212E 05	5.2488E 02	5.3346E 02
8.2500E 01	4.2038E 05	5.2453E 02	5.3312E 02
8.3000E 01	4.2121E 05	5.2419E 02	5.3278E 02
8.3500E 01	4.2144E 05	5.2384E 02	5.3245E 02
8.4000E 01	4.1802E 05	5.2350E 02	5.3211E 02
8.4500E 01	4.1565C 05	5.2316E 02	5.3177E 02
8.5000E 01	4.2265E 05	5.2282E 02	5.3143E 02
8.5500E 01	4.2289E 05	5.2248E 02	5.3109E 02
8.6000E 01	4.1968C 05	5.2214E 02	5.3075E 02
8.6500E 01	4.2564E 05	5.2180E 02	5.3042E 02
8.7000E 01	4.1665E 05	5.2147E 02	5.3008E 02
8.7500E 01	4.2142E 05	5.2113C 02	5.2974E 02

HTA VERSUS TIME

MINIMUM 6.5940E 03 — MAXIMUM 2.4009E 06

TIME	HTA	T15	T25
8.8000E 01	4.2662E 05	5.2080E 02	5.2940E 02
8.8500E 01	4.2052E 05	5.2047E 02	5.2907E 02
8.9000E 01	4.2629E 05	5.2010E 02	5.2872E 02
8.9500E 01	4.2281E 05	5.1974E 02	5.2837E 02
9.0000E 01	4.2543E 05	5.1938E 02	5.2802E 02
9.0500E 01	4.2474E 05	5.1902E 02	5.2767E 02
9.1000E 01	4.2399E 05	5.1867E 02	5.2732E 02
9.1500E 01	4.2580E 05	5.1831E 02	5.2697E 02
9.2000E 01	4.2245E 05	5.1795E 02	5.2662E 02
9.2500E 01	4.2936E 05	5.1759E 02	5.2627E 02
9.3000E 01	4.2451E 05	5.1723E 02	5.2591E 02
9.3500E 01	4.2656E 05	5.1687E 02	5.2556E 02
9.4000E 01	4.2755E 05	5.1652E 02	5.2521E 02
9.4500E 01	4.2472E 05	5.1616E 02	5.2485E 02
9.5000E 01	4.2420E 05	5.1580E 02	5.2450E 02
9.5500E 01	4.2686E 05	5.1544E 02	5.2414E 02
9.6000E 01	4.2389E 05	5.1508E 02	5.2378E 02
9.6500E 01	4.2862E 05	5.1472E 02	5.2343E 02
9.7000E 01	4.2572E 05	5.1436E 02	5.2307E 02
9.7500E 01	4.3047E 05	5.1400E 02	5.2271E 02
9.8000E 01	4.2473E 05	5.1364E 02	5.2235E 02
9.8500E 01	4.2857E 05	5.1329E 02	5.2199E 02
9.9000E 01	4.2563E 05	5.1292E 02	5.2163E 02
9.9500E 01	4.3565E 05	5.1257E 02	5.2127E 02
1.0000E 02	4.2824E 05	5.1221E 02	5.2091E 02
1.0050E 02	4.2340E 05	5.1184E 02	5.2055E 02
1.0100E 02	4.2860E 05	5.1149E 02	5.2019E 02
1.0150E 02	4.2242E 05	5.1113E 02	5.1983E 02
1.0200E 02	4.2604E 05	5.1077E 02	5.1946E 02
1.0250E 02	4.2841E 05	5.1041E 02	5.1910E 02
1.0300E 02	4.2974E 05	5.1005E 02	5.1874E 02
1.0350E 02	4.2931E 05	5.0969E 02	5.1837E 02
1.0400E 02	4.2304E 05	5.0933E 02	5.1802E 02
1.0450E 02	4.3001E 05	5.0897E 02	5.1767E 02
1.0500E 02	4.2982E 05	5.0870E 02	5.1732E 02
1.0550E 02	4.2916E 05	5.0837E 02	5.1697E 02
1.0600E 02	4.2011E 05	5.0803E 02	5.1661E 02
1.0650E 02	4.2114E 05	5.0770E 02	5.1627E 02
1.0700E 02	4.1491E 05	5.0737E 02	5.1592E 02
1.0750E 02	4.2117E 05	5.0704E 02	5.1557E 02
1.0800E 02	4.2011E 05	5.0671E 02	5.1522E 02
1.0850E 02	4.2124E 05	5.0639E 02	5.1487E 02
1.0900E 02	4.1932E 05	5.0606E 02	5.1452E 02
1.0950E 02	4.1545E 05	5.0573E 02	5.1417E 02

POOR PRINT
Epreuve illisible

HTA VERSUS TIME

MINIMUM 6.5940E 03 — MAXIMUM 2.4009E 06

TIME	HTA	T15	T25
1.1[illegible]E 02	4.1228E 05	5.0540E 02	5.1382E 02
1.1[illegible]E 02	4.1531E 05	5.0508E 02	5.1348E 02
1.1[illegible]E 02	4.2108E 05	5.0473E 02	5.1313E 02
1.1[illegible]E 02	4.1431E 05	5.0443E 02	5.1278E 02
1.1[illegible]E 02	4.1394E 05	5.0410E 02	5.1244E 02
1.1[illegible]E 02	4.1822E 05	5.0378E 02	5.1209E 02
1.1[illegible]E 02	4.1324E 05	5.0345E 02	5.1175E 02
1.1[illegible]E 02	4.1058E 05	5.0313E 02	5.1140E 02
1.1[illegible]E 02	4.1002E 05	5.0281E 02	5.1106E 02
1.1[illegible]E 02	4.0253E 05	5.0248E 02	5.1071E 02
1.1[illegible]E 02	4.0378E 05	5.0216E 02	5.1037E 02
1.1[illegible]E 02	4.0564E 05	5.0184E 02	5.1002E 02
1.1[illegible]E 02	4.0741E 05	5.0152E 02	5.0966E 02
1.1[illegible]E 02	4.0771E 05	5.0119E 02	5.0934E 02
1.1[illegible]E 02	4.0300E 05	5.0087E 02	5.0899E 02
1.1[illegible]E 02	3.9936E 05	5.0055E 02	5.0865E 02
1.1[illegible]E 02	4.0616E 05	5.0023E 02	5.0831E 02
1.1[illegible]E 02	3.9748E 05	4.9991E 02	5.0797E 02
1.1[illegible]E 02	4.0561E 05	4.9956E 02	5.0762E 02
1.1[illegible]E 02	4.0059E 05	4.9920E 02	5.0726E 02
1.1[illegible]E 02	4.0419E 05	4.9884E 02	5.0691E 02
1.1[illegible]E 02	3.9926E 05	4.9849E 02	5.0655E 02
1.1[illegible]E 02	4.0066E 05	4.9813E 02	5.0620E 02
1.1[illegible]E 02	3.9946E 05	4.9776E 02	5.0584E 02
1.1[illegible]E 02	3.9949E 05	4.9740E 02	5.0549E 02
1.1[illegible]E 02	3.9872E 05	4.9704E 02	5.0513E 02
1.1[illegible]E 02	3.9829E 05	4.9667E 02	5.0477E 02
1.1[illegible]E 02	3.9714E 05	4.9631E 02	5.0442E 02
1.1[illegible]E 02	4.0068E 05	4.9594E 02	5.0406E 02
1.1[illegible]E 02	4.0094E 05	4.9557E 02	5.0370E 02
1.1[illegible]E 02	3.9955E 05	4.9520E 02	5.0334E 02
1.1[illegible]E 02	3.9854E 05	4.9483E 02	5.0298E 02
1.1[illegible]E 02	4.0202E 05	4.9445E 02	5.0262E 02
1.1[illegible]E 02	4.0935E 05	4.9408E 02	5.0226E 02
1.1[illegible]E 02	4.0254E 05	4.9370E 02	5.0190E 02
1.1[illegible]E 02	4.0782E 05	4.9332E 02	5.0154E 02
1.1[illegible]E 02	4.0711E 05	4.9294E 02	5.0118E 02
1.1[illegible]E 02	4.2C769E 05	4.9255E 02	5.0082E 02
1.1[illegible]E 02	4.1072E 05	4.9217E 02	5.0045E 02
1.1[illegible]E 02	4.1051E 05	4.9179E 02	5.0009E 02
1.1[illegible]E 02	4.1052E 05	4.9140E 02	4.9973E 02
1.1[illegible]E 02	4.1162E 05	4.9101E 02	4.9936E 02
1.1[illegible]E 02	4.1716E 05	4.9063E 02	4.9900E 02
1.1[illegible]E 02	4.1762E 05	4.9024E 02	4.9864E 02

HTA VERSUS TIME

MINIMUM 6.5940E 03 — MAXIMUM 2.4009E 06

TIME	HTA	T15	T25
1.[illegible]E 02	4.1812E 05	4.8984E 02	4.9827E 02
1.[illegible]E 02	4.1956E 05	4.8945E 02	4.9791E 02
1.[illegible]E 02	4.1691E 05	4.8905E 02	4.9754E 02
1.[illegible]E 02	4.1915E 05	4.8866E 02	4.9717E 02
1.[illegible]E 02	4.1720E 05	4.8830E 02	4.9681E 02
1.[illegible]E 02	4.2305E 05	4.8793E 02	4.9645E 02
1.[illegible]E 02	4.1967E 05	4.8757E 02	4.9611E 02
1.[illegible]E 02	4.2618E 05	4.8720E 02	4.9574E 02
1.[illegible]E 02	4.2145E 05	4.8684E 02	4.9538E 02
1.[illegible]E 02	4.2357E 05	4.8648E 02	4.9502E 02
1.[illegible]E 02	4.2517E 05	4.8612E 02	4.9467E 02
1.[illegible]E 02	4.2260E 05	4.8576E 02	4.9431E 02
1.[illegible]E 02	4.2213E 05	4.8543E 02	4.9395E 02
1.[illegible]E 02	4.2354E 05	4.8504E 02	4.9359E 02
1.[illegible]E 02	4.2131E 05	4.8468E 02	4.9324E 02
1.[illegible]E 02	4.2235E 05	4.8433E 02	4.9288E 02
1.[illegible]E 02	4.1981E 05	4.8397E 02	4.9252E 02
1.[illegible]E 02	4.2C30E 05	4.8362E 02	4.9216E 02
1.[illegible]E 02	4.1753E 05	4.8327E 02	4.9181E 02
1.[illegible]E 02	4.2335E 05	4.8292E 02	4.9145E 02
1.[illegible]E 02	4.1682E 05	4.8255E 02	4.9109E 02
1.[illegible]E 02	4.1615E 05	4.8222E 02	4.9074E 02
1.[illegible]E 02	4.1844E 05	4.8187E 02	4.9038E 02
1.[illegible]E 02	4.1725E 05	4.8152E 02	4.9003E 02
1.[illegible]E 02	4.2203E 05	4.8117E 02	4.8967E 02
1.[illegible]E 02	4.1737E 05	4.8083E 02	4.8931E 02
1.[illegible]E 02	4.2176E 05	4.8043E 02	4.8896E 02
1.[illegible]E 02	4.1412E 05	4.8014E 02	4.8860E 02
1.[illegible]E 02	4.1846E 05	4.7980E 02	4.8825E 02
1.[illegible]E 02	4.1962E 05	4.7946E 02	4.8789E 02
1.[illegible]E 02	4.1634E 05	4.7912E 02	4.8754E 02
1.[illegible]E 02	4.1879E 05	4.7879E 02	4.8718E 02
1.[illegible]E 02	4.0901E 05	4.7844E 02	4.8683E 02
1.[illegible]E 02	4.1452E 05	4.7803E 02	4.8647E 02
1.[illegible]E 02	4.1545E 05	4.7777E 02	4.8612E 02
1.[illegible]E 02	4.1669E 05	4.7743E 02	4.8578E 02
1.[illegible]E 02	4.1478E 05	4.7710E 02	4.8543E 02
1.[illegible]E 02	4.1333E 05	4.7678E 02	4.8509E 02
1.[illegible]E 02	4.0921E 05	4.7644E 02	4.8474E 02
1.[illegible]E 02	4.1032E 05	4.7611E 02	4.8440E 02
1.[illegible]E 02	4.1133E 05	4.7578E 02	4.8406E 02
1.[illegible]E 02	4.1057E 05	4.7545E 02	4.8372E 02
1.[illegible]E 02	4.1041E 05	4.7513E 02	4.8337E 02
1.[illegible]E 02	4.0224E 05	4.7480E 02	4.8303E 02

POOR PRINT
Epreuve illisible

HTA VERSUS TIME

MINIMUM 6.5940E 03 — MAXIMUM 2.4009E 06

TIME	HTA	T15	T25
1.6400E 02	4.0329E 05	4.7447E 02	4.8269E 02
1.6560E 02	4.0754E 05	4.7414E 02	4.8235E 02
1.6720E 02	4.0821E 05	4.7381E 02	4.8202E 02
1.6880E 02	4.0819E 05	4.7349E 02	4.8168E 02
1.7040E 02	4.0149E 05	4.7316E 02	4.8134E 02
1.7200E 02	3.9863E 05	4.7283E 02	4.8101E 02
1.7360E 02	4.0731E 05	4.7251E 02	4.8067E 02
1.7520E 02	4.0159E 05	4.7218E 02	4.8033E 02
1.7680E 02	4.0248E 05	4.7186E 02	4.8000E 02
1.7840E 02	3.9736E 05	4.7153E 02	4.7967E 02
1.8000E 02	4.0519E 05	4.7121E 02	4.7933E 02
1.8160E 02	4.0469E 05	4.7089E 02	4.7900E 02
1.8320E 02	3.9737E 05	4.7056E 02	4.7867E 02
1.8480E 02	3.9726E 05	4.7024E 02	4.7834E 02
1.8640E 02	4.0369E 05	4.6992E 02	4.7801E 02
1.8800E 02	4.0117E 05	4.6960E 02	4.7768E 02
1.8960E 02	4.0210E 05	4.6927E 02	4.7735E 02
1.9120E 02	3.9132E 05	4.6895E 02	4.7702E 02
1.9280E 02	3.9617E 05	4.6863E 02	4.7669E 02
1.9440E 02	3.9743E 05	4.6832E 02	4.7636E 02
1.9600E 02	3.9811E 05	4.6797E 02	4.7602E 02
1.9760E 02	3.9508E 05	4.6762E 02	4.7568E 02
1.9920E 02	3.9814E 05	4.6727E 02	4.7534E 02
2.0080E 02	3.9495E 05	4.6693E 02	4.7499E 02
2.0240E 02	4.0048E 05	4.6659E 02	4.7465E 02
2.0400E 02	3.9983E 05	4.6625E 02	4.7430E 02
2.0560E 02	3.9914E 05	4.6590E 02	4.7395E 02
2.0720E 02	3.9463E 05	4.6556E 02	4.7361E 02
2.0880E 02	3.9335E 05	4.6522E 02	4.7326E 02
2.1040E 02	3.9474E 05	4.6487E 02	4.7291E 02
2.1200E 02	3.9310E 05	4.6453E 02	4.7257E 02
2.1360E 02	3.9702E 05	4.6418E 02	4.7222E 02
2.1520E 02	3.9777E 05	4.6384E 02	4.7187E 02
2.1680E 02	3.9634E 05	4.6349E 02	4.7152E 02
2.1840E 02	3.9913E 05	4.6315E 02	4.7117E 02
2.2000E 02	3.9650E 05	4.6281E 02	4.7082E 02
2.2160E 02	3.9355E 05	4.6246E 02	4.7047E 02
2.2320E 02	3.9654E 05	4.6212E 02	4.7012E 02
2.2480E 02	3.9003E 05	4.6177E 02	4.6977E 02
2.2640E 02	3.9227E 05	4.6143E 02	4.6941E 02
2.2800E 02	3.9123E 05	4.6109E 02	4.6906E 02
2.2960E 02	3.9417E 05	4.6074E 02	4.6871E 02
2.3120E 02	3.9726E 05	4.6039E 02	4.6836E 02
2.3280E 02	3.9903E 05	4.6005E 02	4.6800E 02

HTA VERSUS TIME

MINIMUM 6.5940E 03 — MAXIMUM 2.4009E 06

TIME	HTA	T15	T25
1.7440E 02	3.9942E 05	4.5970E 02	4.6765E 02
1.7600E 02	3.9772E 05	4.5936E 02	4.6729E 02
1.7760E 02	3.9943E 05	4.5901E 02	4.6694E 02
1.7920E 02	3.8874E 05	4.5867E 02	4.6658E 02
1.8080E 02	3.9154E 05	4.5832E 02	4.6623E 02
1.8240E 02	3.9770E 05	4.5797E 02	4.6587E 02
1.8400E 02	3.8542E 05	4.5763E 02	4.6552E 02
1.8560E 02	3.9196E 05	4.5727E 02	4.6516E 02
1.8720E 02	3.9462E 05	4.5693E 02	4.6481E 02
1.8880E 02	3.9176E 05	4.5658E 02	4.6446E 02
1.9040E 02	3.9465E 05	4.5623E 02	4.6410E 02
1.9200E 02	3.9159E 05	4.5588E 02	4.6375E 02
1.9360E 02	3.9445E 05	4.5553E 02	4.6339E 02
1.9520E 02	3.9410E 05	4.5517E 02	4.6304E 02
1.9680E 02	3.9330E 05	4.5481E 02	4.6268E 02
1.9840E 02	3.9600E 05	4.5446E 02	4.6233E 02
2.0000E 02	3.8858E 05	4.5410E 02	4.6197E 02
2.0160E 02	3.9128E 05	4.5375E 02	4.6161E 02
2.0320E 02	3.9043E 05	4.5340E 02	4.6126E 02
2.0480E 02	3.9222E 05	4.5304E 02	4.6090E 02
2.0640E 02	3.9133E 05	4.5268E 02	4.6055E 02
2.0800E 02	3.9629E 05	4.5233E 02	4.6019E 02
2.0960E 02	3.9170E 05	4.5197E 02	4.5983E 02
2.1120E 02	3.9334E 05	4.5161E 02	4.5947E 02
2.1280E 02	3.9026E 05	4.5125E 02	4.5912E 02
2.1440E 02	3.9424E 05	4.5089E 02	4.5876E 02
2.1600E 02	3.9519E 05	4.5053E 02	4.5840E 02
2.1760E 02	3.9336E 05	4.5017E 02	4.5804E 02
2.1920E 02	3.9198E 05	4.4981E 02	4.5769E 02
2.2080E 02	3.9161E 05	4.4945E 02	4.5733E 02
2.2240E 02	3.9569E 05	4.4909E 02	4.5697E 02
2.2400E 02	3.9273E 05	4.4873E 02	4.5661E 02
2.2560E 02	3.8695E 05	4.4836E 02	4.5625E 02
2.2720E 02	3.9219E 05	4.4800E 02	4.5589E 02
2.2880E 02	3.9670E 05	4.4764E 02	4.3553E 02
2.3040E 02	3.9676E 05	4.4727E 02	4.5517E 02
2.3200E 02	3.9673E 05	4.4690E 02	4.5481E 02
2.3360E 02	3.9955E 05	4.4654E 02	4.5445E 02
2.3520E 02	3.9651E 05	4.4617E 02	4.5409E 02
2.3680E 02	3.9313E 05	4.4581E 02	4.5372E 02
2.3840E 02	3.9555E 05	4.4544E 02	4.5336E 02
2.4000E 02	3.9861E 05	4.4507E 02	4.5300E 02
2.4160E 02	3.9819E 05	4.4470E 02	4.5263E 02
2.4320E 02	3.9460E 05	4.4433E 02	4.5227E 02

POOR PRINT
Epreuve illisible

MTA VERSUS TIME

MINIMUM 6.5946E 03 — MAXIMUM 2.4009E 06

TIME	MTA	I	T1S	T2S
1.5950E 02	3.9718E 05	----------+	4.4396E 02	4.5190E 02
1.5955E 02	3.9737E 05	----------+	4.4359E 02	4.5154E 02
1.5960E 02	3.9672E 05	----------+	4.4322E 02	4.5117E 02
1.5965E 02	3.9593E 05	----------+	4.4284E 02	4.5081E 02
1.5970E 02	3.9276E 05	----------+	4.4247E 02	4.5044E 02
1.5975E 02	4.0174E 05	----------+	4.4210E 02	4.5008E 02
1.5980E 02	4.0129E 05	----------+	4.4172E 02	4.4971E 02
1.5985E 02	3.9775E 05	----------+	4.4135E 02	4.4934E 02
1.5990E 02	3.9728E 05	----------+	4.4097E 02	4.4898E 02
1.5995E 02	3.9580E 05	----------+	4.4059E 02	4.4861E 02
1.6000E 02	4.0235E 05	----------+	4.4022E 02	4.4824E 02
1.6005E 02	4.0146E 05	----------+	4.3984E 02	4.4787E 02
1.6010E 02	3.9460E 05	----------+	4.3947E 02	4.4751E 02
1.6015E 02	3.9282E 05	----------+	4.3909E 02	4.4714E 02
1.6020E 02	3.9269E 05	----------+	4.3872E 02	4.4677E 02
1.6025E 02	3.9803E 05	----------+	4.3835E 02	4.4640E 02
1.6030E 02	4.0103E 05	----------+	4.3798E 02	4.4603E 02
1.6035E 02	4.0037E 05	----------+	4.3761E 02	4.4566E 02
1.6040E 02	4.0018E 05	----------+	4.3724E 02	4.4529E 02
1.6045E 02	4.0038E 05	----------+	4.3687E 02	4.4493E 02
1.6050E 02	4.0053E 05	----------+	4.3651E 02	4.4456E 02
1.6055E 02	4.0061E 05	----------+	4.3614E 02	4.4419E 02
1.6060E 02	4.0045E 05	----------+	4.3577E 02	4.4382E 02
1.6065E 02	3.9920E 05	----------+	4.3541E 02	4.4345E 02
1.6070E 02	4.0057E 05	----------+	4.3504E 02	4.4308E 02
1.6075E 02	4.0119E 05	----------+	4.3468E 02	4.4272E 02
1.6080E 02	3.9781E 05	----------+	4.3432E 02	4.4235E 02
1.6085E 02	4.0046E 05	----------+	4.3395E 02	4.4199E 02
1.6090E 02	4.0123E 05	----------+	4.3359E 02	4.4162E 02
1.6095E 02	4.0015E 05	----------+	4.3323E 02	4.4126E 02
1.6100E 02	3.9767E 05	----------+	4.3287E 02	4.4089E 02
1.6105E 02	3.9607E 05	----------+	4.3251E 02	4.4053E 02
1.6110E 02	4.0163E 05	----------+	4.3215E 02	4.4017E 02
1.6115E 02	4.0206E 05	----------+	4.3179E 02	4.3981E 02
1.6120E 02	3.9924E 05	----------+	4.3143E 02	4.3945E 02
1.6125E 02	4.0219E 05	----------+	4.3107E 02	4.3909E 02
1.6130E 02	4.0878E 05	----------+	4.3071E 02	4.3873E 02
1.6135E 02	4.0185E 05	----------+	4.3035E 02	4.3837E 02
1.6140E 02	3.9604E 05	----------+	4.2999E 02	4.3801E 02
1.6145E 02	4.0406E 05	----------+	4.2964E 02	4.3765E 02
1.6150E 02	4.0105E 05	----------+	4.2928E 02	4.3729E 02

MTA VERSUS TIME

MINIMUM 6.5946E 03 — MAXIMUM 2.4009E 06

TIME	MTA	I	T1S	T2S
1.6155E 02	4.1242E 05	----------+	4.2721E 02	4.3640E 02
1.6160E 02	4.0760E 05	----------+	4.2678E 02	4.3604E 02
1.6165E 02	4.1217E 05	----------+	4.2635E 02	4.3568E 02
1.6170E 02	4.0784E 05	----------+	4.2591E 02	4.3532E 02
1.6175E 02	4.1230E 05	----------+	4.2548E 02	4.3496E 02
1.6180E 02	4.1344E 05	----------+	4.2504E 02	4.3459E 02
1.6185E 02	4.1779E 05	----------+	4.2459E 02	4.3423E 02
1.6190E 02	4.2183E 05	----------+	4.2415E 02	4.3387E 02
1.6195E 02	4.1633E 05	----------+	4.2380E 02	4.3350E 02
1.6200E 02	4.1756E 05	----------+	4.2344E 02	4.3314E 02
1.6205E 02	4.1750E 05	----------+	4.2308E 02	4.3278E 02
1.6210E 02	4.1662E 05	----------+	4.2274E 02	4.3242E 02
1.6215E 02	4.1664E 05	----------+	4.2239E 02	4.3205E 02
1.6220E 02	4.1643E 05	----------+	4.2205E 02	4.3169E 02
1.6225E 02	4.1413E 05	----------+	4.2172E 02	4.3133E 02
1.6230E 02	4.0559E 05	----------+	4.2139E 02	4.3096E 02
1.6235E 02	4.0315E 05	----------+	4.2106E 02	4.3060E 02
1.6240E 02	4.0650E 05	----------+	4.2074E 02	4.3024E 02
1.6245E 02	4.0712E 05	----------+	4.2042E 02	4.2988E 02
1.6250E 02	4.0126E 05	----------+	4.2011E 02	4.2952E 02
1.6255E 02	4.0434E 05	----------+	4.1981E 02	4.2917E 02
1.6260E 02	3.9960E 05	----------+	4.1951E 02	4.2881E 02
1.6265E 02	3.9440E 05	----------+	4.1921E 02	4.2846E 02
1.6270E 02	3.9725E 05	----------+	4.1891E 02	4.2810E 02
1.6275E 02	3.9126E 05	----------+	4.1863E 02	4.2775E 02
1.6280E 02	3.8810E 05	----------+	4.1834E 02	4.2739E 02
1.6285E 02	3.8493E 05	----------+	4.1807E 02	4.2704E 02
1.6290E 02	3.8168E 05	----------+	4.1779E 02	4.2668E 02
1.6295E 02	3.8427E 05	----------+	4.1751E 02	4.2633E 02
1.6300E 02	3.7787E 05	----------+	4.1724E 02	4.2597E 02
1.6305E 02	3.7593E 05	----------+	4.1696E 02	4.2562E 02
1.6310E 02	3.8163E 05	----------+	4.1668E 02	4.2526E 02
1.6315E 02	3.8628E 05	----------+	4.1641E 02	4.2491E 02
1.6320E 02	3.7770E 05	----------+	4.1613E 02	4.2455E 02
1.6325E 02	3.8777E 05	----------+	4.1586E 02	4.2420E 02
1.6330E 02	3.8197E 05	----------+	4.1558E 02	4.2384E 02
1.6335E 02	3.9403E 05	----------+	4.1532E 02	4.2349E 02
1.6340E 02	3.8703E 05	----------+	4.1505E 02	4.2313E 02
1.6345E 02	3.7991E 05	----------+	4.1478E 02	4.2278E 02
1.6350E 02	3.8447E 05	----------+	4.1452E 02	4.2242E 02
1.6355E 02	3.8540E 05	----------+	4.1425E 02	4.2207E 02
1.6360E 02	3.8719E 05	----------+	4.1398E 02	4.2171E 02
1.6365E 02	3.8662E 05	----------+	4.1372E 02	4.2136E 02
1.6370E 02	3.9962E 05	----------+	4.1345E 02	4.2100E 02
			4.1319E 02	4.2065E 02
			4.1292E 02	4.2029E 02
			4.1265E 02	4.1994E 02
			4.1239E 02	4.1958E 02
			4.1212E 02	4.1923E 02
			4.1185E 02	4.1887E 02
			4.1158E 02	4.1852E 02
			4.1132E 02	4.1816E 02
			4.1105E 02	4.1781E 02
			4.1078E 02	4.1745E 02
			4.1052E 02	4.1710E 02
			4.1025E 02	4.1674E 02
			4.0998E 02	4.1639E 02
			4.0972E 02	4.1603E 02
			4.0945E 02	4.1568E 02
			4.0918E 02	4.1532E 02
			4.0892E 02	4.1497E 02
			4.0865E 02	4.1461E 02
			4.0838E 02	4.1426E 02
			4.0812E 02	4.1390E 02
			4.0785E 02	4.1355E 02
			4.0758E 02	4.1319E 02
			4.0732E 02	4.1284E 02
			4.0705E 02	4.1248E 02
			4.0678E 02	4.1213E 02
			4.0652E 02	4.1177E 02
			4.0625E 02	4.1142E 02
			4.0598E 02	4.1106E 02
			4.0572E 02	4.1071E 02
			4.0545E 02	4.1035E 02
			4.0518E 02	4.1000E 02
			4.0492E 02	4.0964E 02
			4.0465E 02	4.0929E 02
			4.0438E 02	4.0893E 02
			4.0412E 02	4.0858E 02
			4.0385E 02	4.0822E 02
			4.0358E 02	4.0787E 02
			4.0332E 02	4.0751E 02
			4.0305E 02	4.0716E 02
			4.0278E 02	4.0680E 02
			4.0252E 02	4.0645E 02
			4.0225E 02	4.0609E 02
			4.0198E 02	4.0574E 02
			4.0172E 02	4.0538E 02
			4.0145E 02	4.0503E 02
			4.0118E 02	4.0467E 02
			4.0092E 02	4.0432E 02
			4.0065E 02	4.0396E 02
			4.0038E 02	4.0361E 02
			4.0012E 02	4.0325E 02
			3.9985E 02	4.0290E 02
			3.9958E 02	4.0254E 02
			3.9932E 02	4.0219E 02
			3.9905E 02	4.0183E 02
			3.9878E 02	4.0148E 02
			3.9852E 02	4.0112E 02
			3.9825E 02	4.0077E 02
			3.9798E 02	4.0041E 02
			3.9772E 02	4.0006E 02
			3.9745E 02	3.9970E 02
			3.9718E 02	3.9935E 02
			3.9692E 02	3.9899E 02
			3.9665E 02	3.9864E 02
			3.9638E 02	3.9828E 02
			3.9612E 02	3.9793E 02
			3.9585E 02	3.9757E 02
			3.9558E 02	3.9722E 02
			3.9532E 02	3.9686E 02
			3.9505E 02	3.9651E 02
			3.9478E 02	3.9615E 02
			3.9452E 02	3.9580E 02
			3.9425E 02	3.9544E 02
			3.9398E 02	3.9509E 02
			3.9372E 02	3.9473E 02
			3.9345E 02	3.9438E 02
			3.9318E 02	3.9402E 02
			3.9292E 02	3.9367E 02
			3.9265E 02	3.9331E 02
			3.9238E 02	3.9296E 02
			3.9212E 02	3.9260E 02
			3.9185E 02	3.9225E 02
			3.9158E 02	3.9189E 02
			3.9132E 02	3.9154E 02
			3.9105E 02	3.9118E 02
			3.9078E 02	3.9083E 02
			3.9052E 02	3.9047E 02
			3.9025E 02	3.9012E 02
			3.8998E 02	3.8976E 02
			3.8972E 02	3.8941E 02
			3.8945E 02	3.8905E 02
			3.8918E 02	3.8870E 02
			3.8892E 02	3.8834E 02
			3.8865E 02	3.8799E 02
			3.8838E 02	3.8763E 02
			3.8812E 02	3.8728E 02
			3.8785E 02	3.8692E 02
			3.8758E 02	3.8657E 02
			3.8732E 02	3.8621E 02
			3.8705E 02	3.8586E 02
			3.8678E 02	3.8550E 02
			3.8652E 02	3.8515E 02
			3.8625E 02	3.8479E 02
			3.8598E 02	3.8444E 02
			3.8572E 02	3.8408E 02
			3.8545E 02	3.8373E 02
			3.8518E 02	3.8337E 02
			3.8492E 02	3.8302E 02
			3.8465E 02	3.8266E 02
			3.8438E 02	3.8231E 02
			3.8412E 02	3.8195E 02
			3.8385E 02	3.8160E 02
			3.8358E 02	3.8124E 02
			3.8332E 02	3.8089E 02
			3.8305E 02	3.8053E 02
			3.8278E 02	3.8018E 02
			3.8252E 02	3.7982E 02
			3.8225E 02	3.7947E 02
			3.8198E 02	3.7911E 02
			3.8172E 02	3.7876E 02
			3.8145E 02	3.7840E 02
			3.8118E 02	3.7805E 02
			3.8092E 02	3.7769E 02
			3.8065E 02	3.7734E 02
			3.8038E 02	3.7698E 02
			3.8012E 02	3.7663E 02
			3.7985E 02	3.7627E 02
			3.7958E 02	3.7592E 02
			3.7932E 02	3.7556E 02
			3.7905E 02	3.7521E 02
			3.7878E 02	3.7485E 02
			3.7852E 02	3.7450E 02
			3.7825E 02	3.7414E 02
			3.7798E 02	3.7379E 02
			3.7772E 02	3.7343E 02
			3.7745E 02	3.7308E 02
			3.7718E 02	3.7272E 02
			3.7692E 02	3.7237E 02
			3.7665E 02	3.7201E 02
			3.7638E 02	3.7166E 02
			3.7612E 02	3.7130E 02
			3.7585E 02	3.7095E 02
			3.7558E 02	3.7059E 02
			3.7532E 02	3.7024E 02
			3.7505E 02	3.6988E 02
			3.7478E 02	3.6953E 02
			3.7452E 02	3.6917E 02
			3.7425E 02	3.6882E 02
			3.7398E 02	3.6846E 02
			3.7372E 02	3.6811E 02
			3.7345E 02	3.6775E 02
			3.7318E 02	3.6740E 02
			3.7292E 02	3.6704E 02
			3.7265E 02	3.6669E 02
			3.7238E 02	3.6633E 02
			3.7212E 02	3.6598E 02
			3.7185E 02	3.6562E 02
			3.7158E 02	3.6527E 02
			3.7132E 02	3.6491E 02
			3.7105E 02	3.6456E 02
			3.7078E 02	3.6420E 02
			3.7052E 02	3.6385E 02
			3.7025E 02	3.6349E 02
			3.6998E 02	3.6314E 02
			3.6972E 02	3.6278E 02
			3.6945E 02	3.6243E 02
			3.6918E 02	3.6207E 02
			3.6892E 02	3.6172E 02
			3.6865E 02	3.6136E 02
			3.6838E 02	3.6101E 02
			3.6812E 02	3.6065E 02
			3.6785E 02	3.6030E 02
			3.6758E 02	3.5994E 02
			3.6732E 02	3.5959E 02
			3.6705E 02	3.5923E 02
			3.6678E 02	3.5888E 02
			3.6652E 02	3.5852E 02
			3.6625E 02	3.5817E 02
			3.6598E 02	3.5781E 02
			3.6572E 02	3.5746E 02
			3.6545E 02	3.5710E 02
			3.6518E 02	3.5675E 02
			3.6492E 02	3.5639E 02
			3.6465E 02	3.5604E 02
			3.6438E 02	3.5568E 02
			3.6412E 02	3.5533E 02
			3.6385E 02	3.5497E 02
			3.6358E 02	3.5462E 02
			3.6332E 02	3.5426E 02
			3.6305E 02	3.5391E 02
			3.6278E 02	3.5355E 02
			3.6252E 02	3.5320E 02
			3.6225E 02	3.5284E 02
			3.6198E 02	3.5249E 02
			3.6172E 02	3.5213E 02
			3.6145E 02	3.5178E 02
			3.6118E 02	3.5142E 02
			3.6092E 02	3.5107E 02
			3.6065E 02	3.5071E 02
			3.6038E 02	3.5036E 02
			3.6012E 02	3.5000E 02
			3.5985E 02	3.4965E 02
			3.5958E 02	3.4929E 02
			3.5932E 02	3.4894E 02
			3.5905E 02	3.4858E 02
			3.5878E 02	3.4823E 02
			3.5852E 02	3.4787E 02
			3.5825E 02	3.4752E 02
			3.5798E 02	3.4716E 02
			3.5772E 02	3.4681E 02
			3.5745E 02	3.4645E 02
			3.5718E 02	3.4610E 02
			3.5692E 02	3.4574E 02
			3.5665E 02	3.4539E 02
			3.5638E 02	3.4503E 02
			3.5612E 02	3.4468E 02
			3.5585E 02	3.4432E 02
			3.5558E 02	3.4397E 02
			3.5532E 02	3.4361E 02
			3.5505E 02	3.4326E 02
			3.5478E 02	3.4290E 02
			3.5452E 02	3.4255E 02
			3.5425E 02	3.4219E 02
			3.5398E 02	3.4184E 02
			3.5372E 02	3.4148E 02
			3.5345E 02	3.4113E 02
			3.5318E 02	3.4077E 02
			3.5292E 02	3.4042E 02
			3.5265E 02	3.4006E 02
			3.5238E 02	3.3971E 02
			3.5212E 02	3.3935E 02
			3.5185E 02	3.3900E 02
			3.5158E 02	3.3864E 02
			3.5132E 02	3.3829E 02
			3.5105E 02	3.3793E 02
			3.5078E 02	3.3758E 02
			3.5052E 02	3.3722E 02
			3.5025E 02	3.3687E 02
			3.4998E 02	3.3651E 02
			3.4972E 02	3.3616E 02
			3.4945E 02	3.3580E 02
			3.4918E 02	3.3545E 02
			3.4892E 02	3.3509E 02
			3.4865E 02	3.3474E 02
			3.4838E 02	3.3438E 02
			3.4812E 02	3.3403E 02
			3.4785E 02	3.3367E 02
			3.4758E 02	3.3332E 02
			3.4732E 02	3.3296E 02
			3.4705E 02	3.3261E 02
			3.4678E 02	3.3225E 02
			3.4652E 02	3.3190E 02
			3.4625E 02	3.3154E 02
			3.4598E 02	3.3119E 02
			3.4572E 02	3.3083E 02
			3.4545E 02	3.3048E 02
			3.4518E 02	3.3012E 02
			3.4492E 02	3.2977E 02
			3.4465E 02	3.2941E 02
			3.4438E 02	3.2906E 02
			3.4412E 02	3.2870E 02
			3.4385E 02	3.2835E 02
			3.4358E 02	3.2799E 02
			3.4332E 02	3.2764E 02
			3.4305E 02	3.2728E 02
			3.4278E 02	3.2693E 02
			3.4252E 02	3.2657E 02
			3.4225E 02	3.2622E 02
			3.4198E 02	3.2586E 02
			3.4172E 02	3.2551E 02
			3.4145E 02	3.2515E 02
			3.4118E 02	3.2480E 02
			3.4092E 02	3.2444E 02
			3.4065E 02	3.2409E 02
			3.4038E 02	3.2373E 02
			3.4012E 02	3.2338E 02
			3.3985E 02	3.2302E 02
			3.3958E 02	3.2267E 02
			3.3932E 02	3.2231E 02
			3.3905E 02	3.2196E 02
			3.3878E 02	3.2160E 02
			3.3852E 02	3.2125E 02
			3.3825E 02	3.2089E 02
			3.3798E 02	3.2054E 02
			3.3772E 02	3.2018E 02
			3.3745E 02	3.1983E 02
			3.3718E 02	3.1947E 02
			3.3692E 02	3.1912E 02

POOR PRINT
Epreuve illisible

HTA VERSUS TIME

MINIMUM 6.5940E 03 — MAXIMUM 2.4009E 06

TIME	HTA	T15	T25
2.4600E 02	3.8505E 05	4.1100E 02	4.1371E 02
2.4650E 02	3.8979E 05	4.1056E 02	4.1030E 02
2.4700E 02	3.8850E 05	4.1013E 02	4.1789E 02
2.4750E 02	3.8506E 05	4.0969E 02	4.1748E 02
2.4800E 02	3.8276E 05	4.0931E 02	4.1709E 02
2.4850E 02	3.7717E 05	4.0893E 02	4.1670E 02
2.4900E 02	3.8994E 05	4.0855E 02	4.1631E 02
2.4950E 02	3.9326E 05	4.0817E 02	4.1592E 02
2.5000E 02	3.9135E 05	4.0779E 02	4.1553E 02
2.5050E 02	3.8987E 05	4.0741E 02	4.1515E 02
2.5100E 02	3.9148E 05	4.0703E 02	4.1476E 02
2.5150E 02	3.9001E 05	4.0666E 02	4.1437E 02
2.5200E 02	3.8638E 05	4.0628E 02	4.1399E 02
2.5250E 02	3.8884E 05	4.0590E 02	4.1360E 02
2.5300E 02	3.8756E 05	4.0553E 02	4.1322E 02
2.5350E 02	3.8431E 05	4.0516E 02	4.1283E 02
2.5400E 02	3.8120E 05	4.0477E 02	4.1245E 02
2.5450E 02	3.8435E 05	4.0441E 02	4.1207E 02
2.5500E 02	3.8780E 05	4.0404E 02	4.1168E 02
2.5550E 02	3.8567E 05	4.0367E 02	4.1130E 02
2.5600E 02	3.8673E 05	4.0330E 02	4.1092E 02
2.5650E 02	3.8183E 05	4.0293E 02	4.1054E 02
2.5700E 02	3.8049E 05	4.0255E 02	4.1016E 02
2.5750E 02	3.8135E 05	4.0220E 02	4.0978E 02
2.5800E 02	3.8552E 05	4.0180E 02	4.0938E 02
2.5850E 02	3.7946E 05	4.0143E 02	4.0899E 02
2.5900E 02	3.8204E 05	4.0100E 02	4.0859E 02
2.5950E 02	3.8423E 05	4.0060E 02	4.0819E 02
2.6000E 02	3.8622E 05	4.0020E 02	4.0779E 02
2.6050E 02	3.8077E 05	3.9980E 02	4.0739E 02
2.6100E 02	3.8206E 05	3.9940E 02	4.0699E 02
2.6150E 02	3.8104E 05	3.9900E 02	4.0659E 02
2.6200E 02	3.8331E 05	3.9860E 02	4.0618E 02
2.6250E 02	3.7985E 05	3.9820E 02	4.0578E 02
2.6300E 02	3.8190E 05	3.9779E 02	4.0538E 02
2.6350E 02	3.8516E 05	3.9739E 02	4.0497E 02
2.6400E 02	3.8671E 05	3.9699E 02	4.0456E 02
2.6450E 02	3.8038E 05	3.9658E 02	4.0415E 02
2.6500E 02	3.8247E 05	3.9617E 02	4.0374E 02
2.6550E 02	3.8090E 05	3.9577E 02	4.0333E 02
2.6600E 02	3.8167E 05	3.9537E 02	4.0292E 02
2.6650E 02	3.8418E 05	3.9496E 02	4.0251E 02
2.6700E 02	3.8032E 05	3.9455E 02	4.0210E 02
2.6750E 02	3.8529E 05	3.9414E 02	4.0168E 02

HTA VERSUS TIME

MINIMUM 6.5940E 03 — MAXIMUM 2.4009E 06

TIME	HTA	T15	T25
2.6800E 02	3.8439E 05	3.9377E 02	4.0128E 02
2.6850E 02	3.8003E 05	3.9339E 02	4.0088E 02
2.6900E 02	3.8073E 05	3.9301E 02	4.0048E 02
2.6950E 02	3.8201E 05	3.9264E 02	4.0008E 02
2.7000E 02	3.8028E 05	3.9226E 02	3.9969E 02
2.7050E 02	3.7141E 05	3.9189E 02	3.9929E 02
2.7100E 02	3.7962E 05	3.9151E 02	3.9889E 02
2.7150E 02	3.7722E 05	3.9114E 02	3.9849E 02
2.7200E 02	3.7560E 05	3.9077E 02	3.9810E 02
2.7250E 02	3.7696E 05	3.9043E 02	3.9770E 02
2.7300E 02	3.6962E 05	3.9003E 02	3.9731E 02
2.7350E 02	3.7024E 05	3.8966E 02	3.9691E 02
2.7400E 02	3.7451E 05	3.8929E 02	3.9652E 02
2.7450E 02	3.7286E 05	3.8893E 02	3.9613E 02
2.7500E 02	3.6772E 05	3.8856E 02	3.9573E 02
2.7550E 02	3.6927E 05	3.8820E 02	3.9534E 02
2.7600E 02	3.6429E 05	3.8784E 02	3.9495E 02
2.7650E 02	3.6278E 05	3.8747E 02	3.9456E 02
2.7700E 02	3.6102E 05	3.8711E 02	3.9417E 02
2.7750E 02	3.6065E 05	3.8676E 02	3.9378E 02
2.7800E 02	3.5844E 05	3.8639E 02	3.9338E 02
2.7850E 02	3.5677E 05	3.8601E 02	3.9299E 02
2.7900E 02	3.5020E 05	3.8563E 02	3.9259E 02
2.7950E 02	3.5681E 05	3.8525E 02	3.9219E 02
2.8000E 02	3.5643E 05	3.8488E 02	3.9179E 02
2.8050E 02	3.5942E 05	3.8451E 02	3.9139E 02
2.8100E 02	3.5002E 05	3.8413E 02	3.9099E 02
2.8150E 02	3.4922E 05	3.8376E 02	3.9059E 02
2.8200E 02	3.5174E 05	3.8339E 02	3.9019E 02
2.8250E 02	3.4450E 05	3.8301E 02	3.8979E 02
2.8300E 02	3.4679E 05	3.8264E 02	3.8939E 02
2.8350E 02	3.4562E 05	3.8227E 02	3.8899E 02
2.8400E 02	3.4455E 05	3.8189E 02	3.8859E 02
2.8450E 02	3.4304E 05	3.8152E 02	3.8819E 02
2.8500E 02	3.3845E 05	3.8114E 02	3.8779E 02
2.8550E 02	3.3993E 05	3.8077E 02	3.8739E 02
2.8600E 02	3.4077E 05	3.8039E 02	3.8699E 02
2.8650E 02	3.3865E 05	3.8002E 02	3.8659E 02
2.8700E 02	3.4270E 05	3.7964E 02	3.8618E 02
2.8750E 02	3.3673E 05	3.7926E 02	3.8578E 02
2.8800E 02	3.3743E 05	3.7887E 02	3.8537E 02
2.8850E 02	3.3159E 05	3.7848E 02	3.8496E 02
2.8900E 02	3.2876E 05	3.7808E 02	3.8456E 02
2.8950E 02	3.3493E 05	3.7768E 02	3.8415E 02

POOR PRINT
Epreuve illisible

HTA VERSUS TIME

MINIMUM 6.5940E 03 I

MAXIMUM 2.4009E 06 I

TIME	HTA		T15	T25
[illegible]	3.2940E 03	-------+	3.7728E 02	3.8374E 02
[illegible]	3.3717E 05	-------+	3.7688E 02	3.8332E 02
[illegible]	3.3332E 05	-------+	3.7649E 02	3.8291E 02
[illegible]	3.3222E 05	-------+	3.7608E 02	3.8250E 02
[illegible]	3.3710E 05	-------+	3.7567E 02	3.8208E 02
[illegible]	3.2897E 05	-------+	3.7527E 02	3.8167E 02
[illegible]	3.3335E 05	-------+	3.7485E 02	3.8125E 02
[illegible]	3.3431E 05	-------+	3.7445E 02	3.8084E 02
[illegible]	3.3135E 05	-------+	3.7404E 02	3.8042E 02
[illegible]	3.3229E 05	-------+	3.7362E 02	3.8000E 02
[illegible]	3.3159E 05	-------+	3.7321E 02	3.7959E 02
[illegible]	3.3194E 05	-------+	3.7279E 02	3.7917E 02
[illegible]	3.3140E 05	-------+	3.7237E 02	3.7875E 02
[illegible]	3.2993E 05	-------+	3.7196E 02	3.7833E 02
[illegible]	3.2966E 05	-------+	3.7153E 02	3.7791E 02
[illegible]	3.3370E 05	-------+	3.7111E 02	3.7748E 02
[illegible]	3.3442E 05	-------+	3.7069E 02	3.7706E 02
[illegible]	3.3119E 05	-------+	3.7026E 02	3.7663E 02
[illegible]	3.3004E 05	-------+	3.6982E 02	3.7620E 02
[illegible]	3.1147E 05	-------+	3.6939E 02	3.7577E 02
[illegible]	3.4211E 05	-------+	3.6895E 02	3.7533E 02
[illegible]	3.2230E 05	-------+	3.6852E 02	3.7490E 02
[illegible]	3.3147E 05	-------+	3.6804E 02	3.7446E 02
[illegible]	3.2291E 05	-------+	3.6764E 02	3.7403E 02
[illegible]	3.3062E 05	-------+	3.6721E 02	3.7359E 02
[illegible]	3.3076E 05	-------+	3.6677E 02	3.7315E 02
[illegible]	3.4273E 05	-------+	3.6632E 02	3.7271E 02
[illegible]	3.3419E 05	-------+	3.6588E 02	3.7227E 02
[illegible]	3.2854E 05	-------+	3.6544E 02	3.7183E 02
[illegible]	3.3456E 05	-------+	3.6499E 02	3.7138E 02
[illegible]	3.3311E 05	-------+	3.6454E 02	3.7094E 02
[illegible]	3.3412E 05	-------+	3.6409E 02	3.7049E 02
[illegible]	3.3119E 05	-------+	3.6365E 02	3.7004E 02
[illegible]	3.3660E 05	-------+	3.6320E 02	3.6959E 02
[illegible]	3.3203E 05	-------+	3.6274E 02	3.6914E 02
[illegible]	3.3581E 05	-------+	3.6227E 02	3.6869E 02
[illegible]	3.3165E 05	-------+	3.6186E 02	3.6825E 02
[illegible]	3.2629E 05	-------+	3.6144E 02	3.6780E 02
[illegible]	3.3134E 05	-------+	3.6101E 02	3.6736E 02
[illegible]	3.2617E 05	-------+	3.6058E 02	3.6692E 02
[illegible]	3.3283E 05	-------+	3.6016E 02	3.6647E 02
[illegible]	3.2935E 05	-------+	3.5973E 02	3.6603E 02
[illegible]	3.4345E 05	-------+	3.5931E 02	3.6558E 02
[illegible]	3.3000E 05	-------+	3.5888E 02	3.6514E 02

HTA VERSUS TIME

MINIMUM 6.5940E 03 I

MAXIMUM 2.4009E 06 I

TIME	HTA		T15	T25
[illegible]	3.2784E 05	-------+	3.5846E 02	3.6470E 02
[illegible]	3.2790E 05	-------+	3.5804E 02	3.6425E 02
[illegible]	3.2747E 05	-------+	3.5761E 02	3.6381E 02
[illegible]	3.2943E 05	-------+	3.5720E 02	3.6336E 02
[illegible]	3.2759E 05	-------+	3.5678E 02	3.6292E 02
[illegible]	3.2592E 05	-------+	3.5636E 02	3.6247E 02
[illegible]	3.2903E 05	-------+	3.5593E 02	3.6202E 02
[illegible]	3.1834E 05	-------+	3.5552E 02	3.6158E 02
[illegible]	3.1422E 05	-------+	3.5510E 02	3.6113E 02
[illegible]	3.1534E 05	-------+	3.5468E 02	3.6068E 02
[illegible]	3.1249E 05	-------+	3.5427E 02	3.6024E 02
[illegible]	3.1927E 05	-------+	3.5386E 02	3.5979E 02
[illegible]	3.1439E 05	-------+	3.5337E 02	3.5933E 02
[illegible]	3.1501E 05	-------+	3.5293E 02	3.5888E 02
[illegible]	3.1703E 05	-------+	3.5247E 02	3.5839E 02
[illegible]	3.1734E 05	-------+	3.5201E 02	3.5792E 02
[illegible]	3.1065E 05	-------+	3.5154E 02	3.5744E 02
[illegible]	3.0961E 05	-------+	3.5107E 02	3.5697E 02
[illegible]	3.1151E 05	-------+	3.5059E 02	3.5649E 02
[illegible]	3.0945E 05	-------+	3.5011E 02	3.5601E 02
[illegible]	3.0981E 05	-------+	3.4963E 02	3.5553E 02
[illegible]	3.1240E 05	-------+	3.4913E 02	3.5505E 02
[illegible]	3.1775E 05	-------+	3.4866E 02	3.5456E 02
[illegible]	3.1664E 05	-------+	3.4817E 02	3.5407E 02
[illegible]	3.1403E 05	-------+	3.4768E 02	3.5358E 02
[illegible]	3.1866E 05	-------+	3.4718E 02	3.5309E 02
[illegible]	3.1502E 05	-------+	3.4668E 02	3.5260E 02
[illegible]	3.1861E 05	-------+	3.4617E 02	3.5210E 02
[illegible]	3.1764E 05	-------+	3.4567E 02	3.5161E 02
[illegible]	3.1632E 05	-------+	3.4515E 02	3.5111E 02
[illegible]	3.2035E 05	-------+	3.4464E 02	3.5060E 02
[illegible]	3.1737E 05	-------+	3.4413E 02	3.5010E 02
[illegible]	3.2194E 05	-------+	3.4362E 02	3.4960E 02
[illegible]	3.1585E 05	-------+	3.4312E 02	3.4909E 02
[illegible]	3.2068E 05	-------+	3.4262E 02	3.4859E 02
[illegible]	3.2122E 05	-------+	3.4212E 02	3.4808E 02
[illegible]	3.2049E 05	-------+	3.4161E 02	3.4757E 02
[illegible]	3.1841E 05	-------+	3.4111E 02	3.4706E 02
[illegible]	3.1775E 05	-------+	3.4060E 02	3.4654E 02
[illegible]	3.1900E 05	-------+	3.4010E 02	3.4603E 02
[illegible]	3.2163E 05	-------+	3.3960E 02	3.4553E 02
[illegible]	3.1697E 05	-------+	3.3909E 02	3.4495E 02
[illegible]	3.1785E 05	-------+	3.3859E 02	3.4447E 02
[illegible]	3.1784E 05	-------+	3.3808E 02	3.4395E 02

POOR PRINT
Epreuve illisible

MINIMUM 6.5940E 03 HTA VERSUS TIME MAXIMUM 2.4009E 06

TIME	HTA	I	T15	T25
3.3[illegible] 02	3.2062E 05	------+	3.3758E 02	3.4342E 02
3.3[illegible] 02	3.1899E 05	------+	3.3707E 02	3.4290E 02
3.3[illegible] 02	3.1873E 05	------+	3.3656E 02	3.4237E 02
3.3[illegible] 02	3.1720E 05	------+	3.3606E 02	3.4184E 02
3.3[illegible] 02	3.1655E 05	------+	3.3555E 02	3.4131E 02
3.3[illegible] 02	3.1475E 05	------+	3.3505E 02	3.4078E 02
3.3[illegible] 02	3.1124E 05	------+	3.3454E 02	3.4024E 02
3.3[illegible] 02	3.1072E 05	------+	3.3401E 02	3.3971E 02
3.3[illegible] 02	3.1014E 05	------+	3.3342E 02	3.3916E 02
3.3[illegible] 02	3.1933E 05	------+	3.3282E 02	3.3861E 02
3.3[illegible] 02	3.2002E 05	------+	3.3221E 02	3.3806E 02
3.3[illegible] 02	3.2633E 05	------+	3.3158E 02	3.3750E 02
3.3[illegible] 02	3.2284E 05	------+	3.3095E 02	3.3695E 02
3.3[illegible] 02	3.2806E 05	------+	3.3031E 02	3.3638E 02
3.3[illegible] 02	3.3593E 05	------+	3.2965E 02	3.3582E 02
3.3[illegible] 02	3.4009E 05	------+	3.2899E 02	3.3525E 02
3.3[illegible] 02	3.4120E 05	------+	3.2832E 02	3.3469E 02
3.3[illegible] 02	3.4659E 05	------+	3.2764E 02	3.3411E 02
3.3[illegible] 02	3.4987E 05	------+	3.2696E 02	3.3352E 02
3.3[illegible] 02	3.5257E 05	------+	3.2625E 02	3.3292E 02
3.3[illegible] 02	3.4973E 05	------+	3.2575E 02	3.3230E 02
3.3[illegible] 02	3.5154E 05	------+	3.2517E 02	3.3169E 02
3.3[illegible] 02	3.5083E 05	------+	3.2461E 02	3.3106E 02
3.3[illegible] 02	3.4654E 05	------+	3.2403E 02	3.3043E 02
3.3[illegible] 02	3.4639E 05	------+	3.2351E 02	3.2984E 02
3.3[illegible] 02	3.4792E 05	------+	3.2303E 02	3.2927E 02
3.3[illegible] 02	3.3913E 05	------+	3.2255E 02	3.2871E 02
3.3[illegible] 02	3.3484E 05	------+	3.2209E 02	3.2817E 02
3.3[illegible] 02	3.3567E 05	------+	3.2162E 02	3.2763E 02
3.3[illegible] 02	3.2642E 05	------+	3.2113E 02	3.2711E 02
3.3[illegible] 02	3.2550E 05	------+	3.2074E 02	3.2660E 02
3.3[illegible] 02	3.2242E 05	------+	3.2035E 02	3.2611E 02
3.3[illegible] 02	3.1671E 05	------+	3.1991E 02	3.2558E 02
3.3[illegible] 02	3.1301E 05	------+	3.1948E 02	3.2506E 02
3.3[illegible] 02	3.1658E 05	------+	3.1907E 02	3.2454E 02
3.3[illegible] 02	3.0410E 05	------+	3.1867E 02	3.2403E 02
3.3[illegible] 02	3.0551E 05	------+	3.1827E 02	3.2352E 02
3.3[illegible] 02	2.9179E 05	-----+	3.1789E 02	3.2301E 02
3.3[illegible] 02	2.8718E 05	-----+	3.1751E 02	3.2250E 02
3.3[illegible] 02	2.7872E 05	-----+	3.1716E 02	3.2200E 02
3.3[illegible] 02	2.9077E 05	-----+	3.1633E 02	3.2136E 02
3.3[illegible] 02	2.9256E 05	-----+	3.1553E 02	3.2072E 02
3.3[illegible] 02	3.0229E 05	------+	3.1474E 02	3.2002E 02
3.3[illegible] 02	3.1204E 05	------+	3.1382E 02	3.1930E 02

MINIMUM 6.5940E 03 HTA VERSUS TIME MAXIMUM 2.4009E 06

TIME	HTA	I	T15	T25
3.[illegible] 02	3.1751E 05	------+	3.1285E 02	3.1954E 02
3.[illegible] 02	3.1764E 05	------+	3.1178E 02	3.1776E 02
3.[illegible] 02	3.1733E 05	------+	3.1114E 02	3.1708E 02
3.[illegible] 02	3.1566E 05	------+	3.1052E 02	3.1645E 02
3.[illegible] 02	3.1004E 05	------+	3.0993E 02	3.1584E 02
3.[illegible] 02	3.2783E 05	------+	3.0939E 02	3.1525E 02
3.[illegible] 02	3.2778E 05	------+	3.0888E 02	3.1468E 02
3.[illegible] 02	3.2715E 05	------+	3.0841E 02	3.1414E 02
3.[illegible] 02	3.1645E 05	------+	3.0798E 02	3.1361E 02
3.[illegible] 02	3.1499E 05	------+	3.0762E 02	3.1310E 02
3.[illegible] 02	3.1156E 05	------+	3.0697E 02	3.1252E 02
3.[illegible] 02	3.1492E 05	------+	3.0633E 02	3.1191E 02
3.[illegible] 02	3.1920E 05	------+	3.0568E 02	3.1130E 02
3.[illegible] 02	3.1672E 05	------+	3.0502E 02	3.1067E 02
3.[illegible] 02	3.2324E 05	------+	3.0435E 02	3.1005E 02
3.[illegible] 02	3.2664E 05	------+	3.0366E 02	3.0941E 02
3.[illegible] 02	3.2533E 05	------+	3.0295E 02	3.0878E 02
3.[illegible] 02	3.2765E 05	------+	3.0225E 02	3.0813E 02
3.[illegible] 02	3.3328E 05	------+	3.0160E 02	3.0756E 02
3.[illegible] 02	3.2921E 05	------+	3.0096E 02	3.0686E 02
3.[illegible] 02	3.3097E 05	------+	3.0034E 02	3.0623E 02
3.[illegible] 02	3.3055E 05	------+	2.9973E 02	3.0556E 02
3.[illegible] 02	3.3247E 05	------+	2.9912E 02	3.0496E 02
3.[illegible] 02	3.2945E 05	------+	2.9852E 02	3.0433E 02
3.[illegible] 02	3.2710E 05	------+	2.9793E 02	3.0369E 02
3.[illegible] 02	3.2722E 05	------+	2.9734E 02	3.0306E 02
3.[illegible] 02	3.2668E 05	------+	2.9675E 02	3.0242E 02
3.[illegible] 02	3.2630E 05	------+	2.9617E 02	3.0178E 02
3.[illegible] 02	3.2037E 05	------+	2.9558E 02	3.0114E 02
3.[illegible] 02	3.1879E 05	------+	2.9500E 02	3.0051E 02
3.[illegible] 02	3.1833E 05	------+	2.9442E 02	2.9987E 02
3.[illegible] 02	3.2030E 05	------+	2.9382E 02	2.9923E 02
3.[illegible] 02	3.1552C 05	------+	2.9324E 02	2.9860E 02
3.[illegible] 02	3.1397E 05	------+	2.9267E 02	2.9798E 02
3.[illegible] 02	3.1015E 05	------+	2.9209E 02	2.9736E 02
3.[illegible] 02	3.0610E 05	------+	2.9151E 02	2.9674E 02
3.[illegible] 02	3.0673E 05	------+	2.9093E 02	2.9614E 02
3.[illegible] 02	3.0411E 05	------+	2.9035E 02	2.9553E 02
3.[illegible] 02	3.0560E 05	------+	2.8977E 02	2.9492E 02
3.[illegible] 02	3.0053E 05	------+	2.8924E 02	2.9432E 02
3.[illegible] 02	3.1127E 05	------+	2.8868E 02	2.9358E 02
3.[illegible] 02	3.2271E 05	------+	2.8723E 02	2.9278E 02
3.[illegible] 02	3.4307E 05	------+	2.8615E 02	2.9194E 02
3.[illegible] 02	3.4042E 05	------+	2.8501E 02	2.9106E 02

POOR PRINT
Epreuve illisible

MINIMUM 6.5940E 03 — MTA VERSUS TIME — MAXIMUM 2.4009E 06

TIME	MTA	T1S	T2S
3.7460E 02	1.5896E 05	2.8381E 02	2.9014E 02
3.7450E 02	1.7294E 05	2.8252E 02	2.8916E 02
3.7500E 02	1.7044E 05	2.8179E 02	2.8838E 02
3.7550E 02	1.7383E 05	2.8165E 02	2.8763E 02
3.7600E 02	1.7219E 05	2.8039E 02	2.8691E 02
3.7650E 02	1.6669E 05	2.7971E 02	2.8622E 02
3.7700E 02	1.6956E 05	2.7913E 02	2.8555E 02
3.7750E 02	1.6631E 05	2.7859E 02	2.8491E 02
3.7800E 02	1.5714E 05	2.7811E 02	2.8430E 02
3.7850E 02	1.4291E 05	2.7771E 02	2.8371E 02
3.7900E 02	1.4033E 05	2.7720E 02	2.8310E 02
3.7950E 02	1.3883E 05	2.7673E 02	2.8250E 02
3.8000E 02	1.2988E 05	2.7630E 02	2.8190E 02
3.8050E 02	1.2382E 05	2.7591E 02	2.8132E 02
3.8100E 02	1.1270E 05	2.7555E 02	2.8074E 02
3.8150E 02	1.0119E 05	2.7522E 02	2.8019E 02
3.8200E 02	2.9138E 05	2.7494E 02	2.7964E 02
3.8250E 02	2.7414E 05	2.7473E 02	2.7916E 02
3.8300E 02	2.4990E 05	2.7457E 02	2.7872E 02
3.8350E 02	3.0795E 05	2.7234E 02	2.7741E 02
3.8400E 02	3.2283E 05	2.7104E 02	2.7644E 02
3.8450E 02	3.4165E 05	2.6954E 02	2.7540E 02
3.8500E 02	3.6984E 05	2.6796E 02	2.7430E 02
3.8550E 02	3.9324E 05	2.6621E 02	2.7314E 02
3.8600E 02	3.9294E 05	2.6525E 02	2.7217E 02
3.8650E 02	3.8708E 05	2.6431E 02	2.7127E 02
3.8700E 02	3.9560E 05	2.6344E 02	2.7041E 02
3.8750E 02	3.9475E 05	2.6263E 02	2.6958E 02
4.0000E 02	4.0002E 05	2.6189E 02	2.6878E 02
3.8850E 02	3.5149E 05	2.6122E 02	2.6800E 02
3.8900E 02	3.8852E 05	2.6061E 02	2.6726E 02
3.8950E 02	3.7514E 05	2.6017E 02	2.6654E 02
3.9000E 02	3.9195E 05	2.5896E 02	2.6586E 02
3.9050E 02	3.6796E 05	2.5776E 02	2.6457E 02
3.9100E 02	4.0351E 05	2.5652E 02	2.6349E 02
4.1250E 02	4.1473E 05	2.5524E 02	2.6237E 02
3.9200E 02	4.2367E 05	2.5392E 02	2.6120E 02
3.9250E 02	4.3001E 05	2.5255E 02	2.6000E 02
3.9300E 02	4.4544E 05	2.5113E 02	2.5875E 02
3.9350E 02	4.4985E 05	2.4995E 02	2.5746E 02
4.0750E 02	9.2515E 05	2.4322E 02	2.5464E 02
4.1000E 02	7.6435E 05	2.3582E 02	2.5101E 02
4.1500E 02	9.0662E 05	2.2754E 02	2.4692E 02
3.9500E 02	1.2017E 06	2.1829E 02	2.4236E 02

MINIMUM 6.5940E 03 — MTA VERSUS TIME — MAXIMUM 2.4009E 06

TIME	MTA	T1S	T2S
4.1750E 02	1.4463E 06	2.0404E 02	2.3733E 02
4.2000E 02	1.7015E 06	1.9689E 02	2.3145E 02
4.2250E 02	1.9871E 06	1.8873E 02	2.2537E 02
4.2500E 02	2.3235E 06	1.7695E 02	2.1944E 02
4.2750E 02	2.3304E 06	1.6795E 02	2.1574E 02
4.3000E 02	2.3187E 06	1.6529E 02	2.1316E 02
4.3250E 02	2.3154E 06	1.6345E 02	2.1108E 02
4.3500E 02	2.2814E 06	1.6258E 02	2.0942E 02
4.3750E 02	2.2302E 06	1.6271E 02	2.0919E 02
4.4000E 02	2.1440E 06	1.6384E 02	2.0746E 02
4.4250E 02	2.1414E 06	1.6281E 02	2.0623E 02
4.4500E 02	2.1170E 06	1.6208E 02	2.0501E 02
4.4750E 02	2.0901E 06	1.6161E 02	2.0393E 02
4.5000E 02	2.0556E 06	1.6136E 02	2.0299E 02
4.5250E 02	2.0240E 06	1.6131E 02	2.0218E 02
4.5500E 02	1.9744E 06	1.6147E 02	2.0156E 02
4.5750E 02	1.9377E 06	1.6183E 02	2.0097E 02
4.6000E 02	1.8734E 06	1.6261E 02	2.0056E 02
4.6250E 02	1.8577E 06	1.6223E 02	1.9988E 02
4.6500E 02	1.8236E 06	1.6199E 02	1.9911E 02
4.6750E 02	1.8030E 06	1.6181E 02	1.9836E 02
4.7000E 02	1.7724E 06	1.6165E 02	1.9762E 02
4.7250E 02	1.7443E 06	1.6151E 02	1.9690E 02
4.7500E 02	1.7149E 06	1.6139E 02	1.9626E 02
4.7750E 02	1.6858E 06	1.6129E 02	1.9551E 02
4.8000E 02	1.6659E 06	1.6124E 02	1.9483E 02
4.8250E 02	1.6416E 06	1.6074E 02	1.9404E 02
4.8500E 02	1.6233E 06	1.6022E 02	1.9320E 02
4.8750E 02	1.6070E 06	1.5966E 02	1.9233E 02
4.9000E 02	1.5946E 06	1.5905E 02	1.9144E 02
4.9250E 02	1.5813E 06	1.5838E 02	1.9053E 02
4.9500E 02	1.5740E 06	1.5760E 02	1.8959E 02
4.9750E 02	1.5536E 06	1.5731E 02	1.8879E 02
5.0000E 02	1.5295E 06	1.5704E 02	1.8807E 02
5.0250E 02	1.5072E 06	1.5680E 02	1.8738E 02
5.0500E 02	1.4854E 06	1.5662E 02	1.8673E 02
5.0750E 02	1.4601E 06	1.5648E 02	1.8612E 02
5.1000E 02	1.4354E 06	1.5639E 02	1.8554E 02
5.1250E 02	1.4114E 06	1.5635E 02	1.8500E 02
5.1500E 02	1.3814E 06	1.5642E 02	1.8450E 02
5.1750E 02	1.3678E 06	1.5619E 02	1.8392E 02
5.2000E 02	1.3474E 06	1.5597E 02	1.8333E 02
5.2250E 02	1.3273E 06	1.5577E 02	1.8274E 02
5.2500E 02	1.3094E 06	1.5558E 02	1.8217E 02

POOR PRINT .
Epreuve illisible

MINIMUM 6.5940E 03 HTA VERSUS TIME MAXIMUM 2.4009E 06

TIME	HTA	T1S	T2S
4.1600E 02	1.2884E 06	1.5539E 02	1.8156E 02
4.1650E 02	1.2812E 06	1.5521E 02	1.8103E 02
4.1700E 02	1.2751E 06	1.5502E 02	1.8046E 02
4.1750E 02	1.2312E 06	1.5487E 02	1.7991E 02
4.2000E 02	1.2234E 06	1.5440E 02	1.7927E 02
4.2050E 02	1.2140E 06	1.5390E 02	1.7855E 02
4.2100E 02	1.2059E 06	1.5336E 02	1.7788E 02
4.2150E 02	1.1994E 06	1.5278E 02	1.7716E 02
4.2200E 02	1.1920E 06	1.5216E 02	1.7642E 02
4.2250E 02	1.1901E 06	1.5144E 02	1.7566E 02
4.2300E 02	1.1714E 06	1.5118E 02	1.7502E 02
4.2350E 02	1.1574E 06	1.5096E 02	1.7445E 02
4.2400E 02	1.1380E 06	1.5078E 02	1.7392E 02
4.2450E 02	1.1227E 06	1.5066E 02	1.7342E 02
4.2500E 02	1.1107E 06	1.5059E 02	1.7295E 02
4.2550E 02	1.0924E 06	1.5058E 02	1.7252E 02
4.2600E 02	1.0660E 06	1.5062E 02	1.7213E 02
4.2650E 02	1.0373E 06	1.5076E 02	1.7177E 02
4.2700E 02	1.0274E 06	1.5059E 02	1.7131E 02
4.2750E 02	1.0143E 06	1.5026E 02	1.7083E 02
4.2800E 02	1.0024E 06	1.5001E 02	1.7035E 02
4.2850E 02	9.8963E 05	1.4973E 02	1.6986E 02
4.2900E 02	9.7915E 05	1.4943E 02	1.6937E 02
4.2950E 02	9.6866E 05	1.4919E 02	1.6886E 02
4.3000E 02	9.6004E 05	1.4883E 02	1.6839E 02
4.3050E 02	9.5014E 05	1.4859E 02	1.6790E 02
4.3100E 02	9.4503E 05	1.4810E 02	1.6735E 02
4.3150E 02	9.4143E 05	1.4760E 02	1.6678E 02
4.3200E 02	9.3729E 05	1.4706E 02	1.6619E 02
4.3250E 02	9.3143E 05	1.4649E 02	1.6559E 02
4.3300E 02	9.2570E 05	1.4589E 02	1.6497E 02
4.3350E 02	9.2703E 05	1.4521E 02	1.6433E 02
4.3400E 02	9.2440E 05	1.4492E 02	1.6386E 02
4.3450E 02	9.1614E 05	1.4467E 02	1.6332E 02
4.3500E 02	9.0259E 05	1.4446E 02	1.6287E 02
4.3550E 02	8.9021E 05	1.4433E 02	1.6245E 02
4.3600E 02	8.7823E 05	1.4417E 02	1.6206E 02
4.3650E 02	8.6261E 05	1.4413E 02	1.6176E 02
4.3700E 02	8.4665E 05	1.4412E 02	1.6136E 02
4.3750E 02	8.2894E 05	1.4419E 02	1.6106E 02
4.3800E 02	8.2194E 05	1.4398E 02	1.6069E 02
4.3850E 02	8.1197E 05	1.4379E 02	1.6031E 02
4.3900E 02	8.0114E 05	1.4360E 02	1.5993E 02
4.3950E 02	7.9239E 05	1.4342E 02	1.5955E 02

MINIMUM 6.5940E 03 HTA VERSUS TIME MAXIMUM 2.4009E 06

TIME	HTA	T1S	T2S
4.4000E 02	7.8079E 05	1.4322E 02	1.5918E 02
4.4050E 02	7.7394E 05	1.4303E 02	1.5881E 02
4.4100E 02	7.6858E 05	1.4283E 02	1.5844E 02
4.4150E 02	7.6540E 05	1.4266E 02	1.5807E 02
4.4200E 02	7.5330E 05	1.4231E 02	1.5765E 02
4.4250E 02	7.4665E 05	1.4194E 02	1.5721E 02
4.4300E 02	7.4348E 05	1.4156E 02	1.5675E 02
4.4350E 02	7.4179E 05	1.4115E 02	1.5628E 02
4.4400E 02	7.3768E 05	1.4072E 02	1.5580E 02
4.4450E 02	7.3606E 05	1.4022E 02	1.5530E 02
4.4500E 02	7.2975E 05	1.4002E 02	1.5489E 02
4.4550E 02	7.1962E 05	1.3984E 02	1.5451E 02
4.4600E 02	7.1019E 05	1.3969E 02	1.5416E 02
4.4650E 02	7.0032E 05	1.3957E 02	1.5384E 02
4.4700E 02	6.9304E 05	1.3947E 02	1.5353E 02
4.4750E 02	6.7899E 05	1.3944E 02	1.5325E 02
4.4800E 02	6.6577E 05	1.3943E 02	1.5299E 02
4.4850E 02	6.5201E 05	1.3948E 02	1.5275E 02
4.4900E 02	6.4764E 05	1.3929E 02	1.5245E 02
4.4950E 02	6.4065E 05	1.3911E 02	1.5214E 02
4.5000E 02	6.3325E 05	1.3893E 02	1.5183E 02
4.5050E 02	6.2702E 05	1.3874E 02	1.5151E 02
4.5100E 02	6.2117E 05	1.3854E 02	1.5120E 02
4.5150E 02	6.1484E 05	1.3833E 02	1.5089E 02
4.5200E 02	6.1022E 05	1.3812E 02	1.5058E 02
4.5250E 02	6.0568E 05	1.3790E 02	1.5026E 02
4.5300E 02	5.9980E 05	1.3776E 02	1.4997E 02
4.5350E 02	5.9580E 05	1.3764E 02	1.4969E 02
4.5400E 02	5.8241E 05	1.3752E 02	1.4942E 02
4.5450E 02	5.7567E 05	1.3741E 02	1.4915E 02
4.5500E 02	5.6847E 05	1.3731E 02	1.4889E 02
4.5550E 02	5.5969E 05	1.3722E 02	1.4864E 02
4.5600E 02	5.5152E 05	1.3714E 02	1.4839E 02
4.5650E 02	5.4315E 05	1.3708E 02	1.4815E 02
4.5700E 02	5.4229E 05	1.3679E 02	1.4785E 02
4.5750E 02	5.3863E 05	1.3649E 02	1.4752E 02
4.5800E 02	5.3884E 05	1.3616E 02	1.4718E 02
4.5850E 02	5.3929E 05	1.3579E 02	1.4682E 02
4.5900E 02	5.4040E 05	1.3540E 02	1.4646E 02
4.5950E 02	5.4340E 05	1.3496E 02	1.4608E 02
4.6000E 02	5.3654E 05	1.3478E 02	1.4576E 02
4.6050E 02	5.3218E 05	1.3460E 02	1.4548E 02
4.6100E 02	5.2587E 05	1.3446E 02	1.4522E 02
4.6150E 02	5.2006E 05	1.3434E 02	1.4497E 02

POOR PRINT
Epreuve illisible

MINIMUM 6.5940E 03 — HTA VERSUS TIME — MAXIMUM 2.4009E 06

TIME	HTA	I	T1S	T2S
4.6200E 02	5.1147E 05	----------+	1.3425E 02	1.4474E 02
4.6350E 02	5.0436E 05	----------+	1.3420E 02	1.4452E 02
4.6500E 02	4.9674E 05	----------+	1.3417E 02	1.4432E 02
4.6650E 02	4.8813E 05	----------+	1.3418E 02	1.4413E 02
4.6800E 02	4.8117E 05	----------+	1.3407E 02	1.4393E 02
4.6950E 02	4.7564E 05	----------+	1.3398E 02	1.4371E 02
4.7100E 02	4.6926E 05	----------+	1.3390E 02	1.4351E 02
4.7250E 02	4.6364E 05	----------+	1.3383E 02	1.4330E 02
4.7400E 02	4.5525E 05	----------+	1.3376E 02	1.4310E 02
4.7550E 02	4.5014E 05	----------+	1.3369E 02	1.4291E 02
4.7700E 02	4.4471E 05	----------+	1.3363E 02	1.4272E 02
4.7850E 02	4.3802E 05	---------+	1.3360E 02	1.4254E 02
4.8000E 02	4.3583L 05	---------+	1.3340E 02	1.4231E 02
4.8150E 02	4.3160E 05	---------+	1.3319E 02	1.4206E 02
4.8300E 02	4.2944E 05	---------+	1.3297E 02	1.4180E 02
4.8450E 02	4.2990E 05	---------+	1.3273E 02	1.4153E 02
4.8600E 02	4.2996E 05	---------+	1.3247E 02	1.4125E 02
4.8750E 02	4.2867E 05	---------+	1.3217E 02	1.4096E 02
4.8900E 02	4.2318E 05	---------+	1.3204E 02	1.4072E 02
4.9050E 02	4.2062E 05	---------+	1.3192E 02	1.4050E 02
4.9200E 02	4.1561E 05	---------+	1.3181E 02	1.4029E 02
4.9350E 02	4.1012E 05	---------+	1.3171E 02	1.4010E 02
4.9500E 02	4.0384E 05	---------+	1.3164E 02	1.3991E 02
4.9650E 02	3.9774E 05	---------+	1.3157E 02	1.3974E 02
4.9800E 02	3.9240E 05	---------+	1.3153E 02	1.3958E 02
4.9950E 02	3.8740E 05	--------+	1.3151E 02	1.3943E 02
5.0100E 02	3.8331E 05	--------+	1.3142E 02	1.3926E 02
5.0250E 02	3.7814E 05	--------+	1.3134E 02	1.3909E 02
5.0400E 02	3.7425E 05	--------+	1.3127E 02	1.3892E 02
5.0550E 02	3.6830E 05	--------+	1.3120E 02	1.3876E 02
5.0700E 02	3.6264E 05	--------+	1.3114E 02	1.3860E 02
5.0850E 02	3.5956E 05	--------+	1.3108E 02	1.3844E 02
5.1000E 02	3.5437E 05	--------+	1.3103E 02	1.3828E 02
5.1150E 02	3.4741E 05	--------+	1.3099E 02	1.3813E 02
5.1300E 02	3.4670E 05	--------+	1.3082E 02	1.3794E 02
5.1450E 02	3.4762E 05	--------+	1.3064E 02	1.3774E 02
5.1600E 02	3.4432E 05	--------+	1.3045E 02	1.3753E 02
5.1750E 02	3.4489E 05	--------+	1.3024E 02	1.3731E 02
5.1900E 02	3.4298E 05	--------+	1.3002E 02	1.3708E 02
5.2050E 02	3.4538E 05	--------+	1.2977E 02	1.3685E 02
5.2200E 02	3.4174E 05	-------+	1.2966E 02	1.3665E 02
5.2350E 02	3.3864E 05	-------+	1.2956E 02	1.3648E 02
5.2500E 02	3.3373E 05	-------+	1.2943E 02	1.3631E 02
5.2650E 02	3.2870E 05	-------+	1.2941E 02	1.3615E 02

MINIMUM 6.5940E 03 — HTA VERSUS TIME — MAXIMUM 2.4009E 06

TIME	HTA	I	T1S	T2S
5.2800E 02	3.2515E 05	-------+	1.2930E 02	1.3601E 02
5.2950E 02	3.1742E 05	-------+	1.2932E 02	1.3587E 02
5.3100E 02	3.1459E 05	-------+	1.2931E 02	1.3574E 02
5.3250E 02	3.0648E 05	-------+	1.2931E 02	1.3562E 02
5.3400E 02	3.0577E 05	-------+	1.2925E 02	1.3549E 02
5.3550E 02	3.0153E 05	-------+	1.2920E 02	1.3536E 02
5.3700E 02	2.9649E 05	-------+	1.2916E 02	1.3523E 02
5.3850E 02	2.9120E 05	------+	1.2912E 02	1.3510E 02
5.4000E 02	2.8855E 05	------+	1.2909E 02	1.3498E 02
5.4150E 02	2.8486E 05	------+	1.2905E 02	1.3486E 02
5.4300E 02	2.7926E 05	------+	1.2902E 02	1.3474E 02
5.4450E 02	2.7403E 05	------+	1.2901E 02	1.3462E 02
5.4600E 02	2.7454E 05	------+	1.2886E 02	1.3447E 02
5.4750E 02	2.7320E 05	------+	1.2871E 02	1.3430E 02
5.4900E 02	2.7190E 05	------+	1.2853E 02	1.3412E 02
5.5050E 02	2.7254E 05	------+	1.2834E 02	1.3394E 02
5.5200E 02	2.7496E 05	------+	1.2813E 02	1.3374E 02
5.5350E 02	2.7260E 05	------+	1.2789E 02	1.3354E 02
5.5500E 02	2.7200E 05	------+	1.2781E 02	1.3338E 02
5.5650E 02	2.6945E 05	------+	1.2774E 02	1.3324E 02
5.5800E 02	2.6503E 05	------+	1.2768E 02	1.3311E 02
5.5950E 02	2.6316E 05	------+	1.2765E 02	1.3299E 02
5.6100E 02	2.5743E 05	------+	1.2763E 02	1.3288E 02
5.6250E 02	2.5248E 05	------+	1.2763E 02	1.3278E 02
5.6400E 02	2.4810E 05	------+	1.2765E 02	1.3269E 02
5.6550E 02	2.4135E 05	-----+	1.2770E 02	1.3261E 02
5.6700E 02	2.4024E 05	-----+	1.2762E 02	1.3250E 02
5.6850E 02	2.3730E 05	-----+	1.2755E 02	1.3238E 02
5.7000E 02	2.3462E 05	-----+	1.2747E 02	1.3226E 02
5.7150E 02	2.3315E 05	-----+	1.2738E 02	1.3214E 02
5.7300E 02	2.3105E 05	-----+	1.2729E 02	1.3201E 02
5.7450E 02	2.2932E 05	-----+	1.2720E 02	1.3188E 02
5.7600E 02	2.2678E 05	-----+	1.2709E 02	1.3176E 02
5.7750E 02	2.2706E 05	-----+	1.2698E 02	1.3163E 02
5.7900E 02	2.2994E 05	-----+	1.2691E 02	1.3151E 02
5.8050E 02	2.2321E 05	-----+	1.2683E 02	1.3139E 02
5.8200E 02	2.2125E 05	-----+	1.2676E 02	1.3127E 02
5.8350E 02	2.1829E 05	-----+	1.2669E 02	1.3116E 02
5.8500E 02	2.1554E 05	-----+	1.2661E 02	1.3105E 02
5.8650E 02	2.1513E 05	-----+	1.2654E 02	1.3094E 02
5.8800E 02	2.1269E 05	-----+	1.2647E 02	1.3083E 02
5.8950E 02	2.1029E 05	-----+	1.2641E 02	1.3072E 02
5.9100E 02	2.0791E 05	-----+	1.2632E 02	1.3061E 02
5.9250E 02	2.0640E 05	-----+	1.2624E 02	1.3050E 02

POOR PRINT
Epreuve illisible

HTA VERSUS TIME

MINIMUM 6.59406E 03 — MAXIMUM 2.40096E 06

TIME	HTA	I	T1S	T2S
0.0	2.0527E 05	----+	1.2615E 02	1.3338E 02
0.0	2.0534E 05	----+	1.2607E 02	1.3027E 02
0.0	2.0309E 05	----+	1.2599E 02	1.3016E 02
0.0	2.0263E 05	----+	1.2589E 02	1.3004E 02
0.0	2.0027E 05	----+	1.2580E 02	1.2993E 02
0.0	2.0022E 05	----+	1.2571E 02	1.2981E 02
0.0	1.9860E 05	----+	1.2562E 02	1.2970E 02
0.0	1.9795E 05	----+	1.2552E 02	1.2958E 02
0.0	1.9672E 05	----+	1.2543E 02	1.2947E 02
0.0	1.9563E 05	----+	1.2533E 02	1.2935E 02
0.0	1.9532E 05	----+	1.2524E 02	1.2924E 02
0.0	1.9517E 05	----+	1.2514E 02	1.2912E 02
0.0	1.9147E 05	----+	1.2508E 02	1.2902E 02
0.0	1.9116E 05	----+	1.2502E 02	1.2892E 02
0.0	1.8866E 05	----+	1.2496E 02	1.2882E 02
0.0	1.8532E 05	----+	1.2490E 02	1.2872E 02
0.0	1.8499E 05	----+	1.2485E 02	1.2862E 02
0.0	1.8234E 05	----+	1.2480E 02	1.2852E 02
0.0	1.8043E 05	----+	1.2476E 02	1.2843E 02
0.0	1.7666E 05	----+	1.2472E 02	1.2834E 02
0.0	1.7464E 05	----+	1.2467E 02	1.2825E 02
0.0	1.7432E 05	----+	1.2463E 02	1.2816E 02
0.0	1.6963E 05	----+	1.2460E 02	1.2807E 02
0.0	1.6930E 05	----+	1.2456E 02	1.2798E 02
0.0	1.6650E 05	----+	1.2452E 02	1.2790E 02
0.0	1.6483E 05	----+	1.2449E 02	1.2782E 02
0.0	1.6134E 05	----+	1.2442E 02	1.2773E 02
0.0	1.6006E 05	----+	1.2435E 02	1.2763E 02
0.0	1.5946E 05	----+	1.2428E 02	1.2754E 02
0.0	1.5921E 05	----+	1.2421E 02	1.2745E 02
0.0	1.5859E 05	----+	1.2414E 02	1.2735E 02
0.0	1.5727E 05	----+	1.2406E 02	1.2726E 02
0.0	1.5634E 05	----+	1.2399E 02	1.2717E 02
0.0	1.5613E 05	----+	1.2390E 02	1.2708E 02
0.0	1.5527E 05	----+	1.2381E 02	1.2698E 02
0.0	1.5436E 05	----+	1.2372E 02	1.2689E 02
0.0	1.5417E 05	----+	1.2363E 02	1.2680E 02
0.0	1.5157E 05	----+	1.2354E 02	1.2670E 02
0.0	1.5100E 05	----+	1.2344E 02	1.2661E 02
0.0	1.5050E 05	----+	1.2335E 02	1.2652E 02
0.0	1.5025E 05	----+	1.2325E 02	1.2643E 02
0.0	1.4986E 05	----+	1.2322E 02	1.2635E 02
0.0	1.4962E 05	----+	1.2316E 02	1.2626E 02
0.0	1.4858E 05	----+	1.2311E 02	1.2618E 02

HTA VERSUS TIME

MINIMUM 6.59406E 03 — MAXIMUM 2.40096E 06

TIME	HTA	I	T1S	T2S
0.0	1.4866E 05	----+	1.2305E 02	1.2610E 02
0.0	1.4852E 05	----+	1.2300E 02	1.2602E 02
0.0	1.4749E 05	----+	1.2295E 02	1.2594E 02
0.0	1.4710E 05	----+	1.2291E 02	1.2586E 02
0.0	1.4695E 05	----+	1.2286E 02	1.2579E 02
0.0	1.4690E 05	----+	1.2282E 02	1.2571E 02
0.0	1.4627E 05	----+	1.2279E 02	1.2563E 02
0.0	1.4592E 05	----+	1.2275E 02	1.2556E 02
0.0	1.4515E 05	----+	1.2272E 02	1.2549E 02
0.0	1.4376E 05	----+	1.2266E 02	1.2541E 02
0.0	1.4192E 05	----+	1.2263E 02	1.2534E 02
0.0	1.4262E 05	----+	1.2257E 02	1.2526E 02
0.0	1.4107E 05	----+	1.2251E 02	1.2518E 02
0.0	1.4085E 05	----+	1.2244E 02	1.2510E 02
0.0	1.4029E 05	----+	1.2238E 02	1.2502E 02
0.0	1.3987E 05	----+	1.2231E 02	1.2495E 02
0.0	1.3846E 05	----+	1.2223E 02	1.2487E 02
0.0	1.3747E 05	----+	1.2218E 02	1.2479E 02
0.0	1.3734E 05	----+	1.2211E 02	1.2471E 02
0.0	1.3659E 05	----+	1.2204E 02	1.2463E 02
0.0	1.3634E 05	----+	1.2197E 02	1.2456E 02
0.0	1.3634E 05	----+	1.2189E 02	1.2448E 02
0.0	1.3744E 05	----+	1.2182E 02	1.2440E 02
0.0	1.3549E 05	----+	1.2174E 02	1.2432E 02
0.0	1.3412E 05	----+	1.2166E 02	1.2424E 02
0.0	1.3434E 05	----+	1.2158E 02	1.2416E 02
0.0	1.3427E 05	----+	1.2150E 02	1.2409E 02
0.0	1.3492E 05	----+	1.2142E 02	1.2401E 02
0.0	1.3434E 05	----+	1.2133E 02	1.2393E 02
0.0	1.3413E 05	----+	1.2126E 02	1.2386E 02
0.0	1.3373E 05	----+	1.2120E 02	1.2378E 02
0.0	1.3340E 05	----+	1.2113E 02	1.2371E 02
0.0	1.3341E 05	----+	1.2107E 02	1.2364E 02
0.0	1.3396E 05	----+	1.2100E 02	1.2356E 02
0.0	1.3230E 05	----+	1.2094E 02	1.2349E 02
0.0	1.3257E 05	----+	1.2088E 02	1.2342E 02
0.0	1.3245E 05	----+	1.2081E 02	1.2335E 02
0.0	1.3133E 05	----+	1.2075E 02	1.2328E 02
0.0	1.3056E 03	----+	1.2069E 02	1.2321E 02
0.0	1.2117E 05	----+	1.2063E 02	1.2314E 02
0.0	1.2059E 05	----+	1.2057E 02	1.2307E 02
0.0	1.2017E 05	----+	1.2051E 02	1.2300E 02
0.0	1.1933E 05	----+	1.2046E 02	1.2293E 02
0.0	1.1794E 05	----+	1.2040E 02	1.2286E 02

POOR PRINT
Epreuve illisible

MTA VERSUS TIME

MINIMUM 6.5940E 03 — MAXIMUM 2.4009E 06

TIME	MTA	T15	T25
5.6600E 02	1.1769E 05	1.2034E 02	1.2279E 02
5.6700E 02	1.1799E 05	1.2029E 02	1.2273E 02
5.6800E 02	1.1671E 05	1.2023E 02	1.2266E 02
5.6900E 02	1.1620E 05	1.2019E 02	1.2259E 02
5.7000E 02	1.1598E 05	1.2013E 02	1.2253E 02
5.7100E 02	1.1365E 05	1.2007E 02	1.2246E 02
5.7200E 02	1.1344E 05	1.2002E 02	1.2240E 02
5.7300E 02	1.1326E 05	1.1996E 02	1.2233E 02
5.7400E 02	1.1307E 05	1.1991E 02	1.2227E 02
5.7500E 02	1.1150E 05	1.1986E 02	1.2220E 02
5.7600E 02	1.1209E 05	1.1980E 02	1.2214E 02
5.7700E 02	1.1188E 05	1.1975E 02	1.2208E 02
5.7800E 02	1.1031E 05	1.1970E 02	1.2201E 02
5.7900E 02	1.1200E 05	1.1965E 02	1.2195E 02
5.8000E 02	1.0982E 05	1.1960E 02	1.2189E 02
5.8100E 02	1.0831E 05	1.1954E 02	1.2183E 02
5.8200E 02	1.0966E 05	1.1949E 02	1.2176E 02
5.8300E 02	1.0769E 05	1.1944E 02	1.2170E 02
5.8400E 02	1.0780E 05	1.1939E 02	1.2164E 02
5.8500E 02	1.0725E 05	1.1935E 02	1.2159E 02
5.8600E 02	1.0736E 05	1.1930E 02	1.2152E 02
5.8700E 02	1.0794E 05	1.1925E 02	1.2147E 02
5.8800E 02	1.0522E 05	1.1920E 02	1.2141E 02
5.8900E 02	1.0675E 05	1.1915E 02	1.2135E 02
5.9000E 02	1.0413E 05	1.1911E 02	1.2129E 02
5.9100E 02	1.0375E 05	1.1906E 02	1.2123E 02
5.9200E 02	1.0372E 05	1.1901E 02	1.2118E 02
5.9300E 02	1.0407E 05	1.1897E 02	1.2112E 02
5.9400E 02	1.0329E 05	1.1892E 02	1.2106E 02
5.9500E 02	1.0145E 05	1.1888E 02	1.2101E 02
5.9600E 02	1.0223E 05	1.1883E 02	1.2094E 02
5.9700E 02	1.0089E 05	1.1879E 02	1.2090E 02
5.9800E 02	1.0053E 05	1.1875E 02	1.2084E 02
5.9900E 02	1.0069E 05	1.1870E 02	1.2079E 02
6.0000E 02	9.8688E 04	1.1866E 02	1.2073E 02
6.0100E 02	9.9417E 04	1.1862E 02	1.2068E 02
6.0200E 02	9.7947E 04	1.1858E 02	1.2063E 02
6.0300E 02	9.7169E 04	1.1854E 02	1.2058E 02
6.0400E 02	9.7118E 04	1.1850E 02	1.2052E 02
6.0500E 02	9.5459E 04	1.1846E 02	1.2047E 02
6.0600E 02	9.3670E 04	1.1842E 02	1.2042E 02
6.0700E 02	9.5721E 04	1.1838E 02	1.2037E 02
		1.1834E 02	1.2032E 02

POOR PRINT
Epreuve illisible

APPENDIX II

Application of the Wave Theory to Boiling Heat Transfer

II.1 General

To analyze the wavy liquid-vapour interface, it is postulated that harmonic waves travel along the interface separating the two media (liquid and vapour) which flow concurrently and parallel to the interface as illustrated in Fig. II.1.

The harmonic wave at the interface can be defined as:

$$\delta = \delta_o \, e^{-int} \cos mz$$

$$\delta = \delta_o \, e^{bt} \cos mz \qquad \text{(II.1)}$$

where

δ = distance perpendicular to liquid-vapour interface

n = wave frequency

$b = -in$ = growth coefficient

m = wave number $= \frac{2\pi}{\lambda}$

where λ is the wave length

The definitions of all terms used in this appendix are given in the nomenclature. It is seen, in the above equation, that if n is real, the surface disturbance is periodic in time and, therefore, stable. If n is imaginary, the disturbance grows exponentially with time.

Expressions for n as a function of fluid properties, gravity, surface tension, fluid velocity parallel to the interface, fluid depth

and wave speed $c(c^2 = n^2/m^2)$ have been derived and reported in (1, 2 & 3). Van Stralen[4] derived a general expression for the velocity of harmonic waves from (1, 2 & 3) which is written as

$$-b^2 = m^2c^2 = n^2 = \frac{\sigma m^3}{\rho_l + \rho_v \coth md} - \frac{g(\rho_l - \rho_v)\, m}{\rho_l + \rho_v \coth md}$$

$$- \frac{\rho_l \rho_v (\coth md)(V_v - V_l)^2 m^2}{(\rho_l + \rho_v \coth md)^2} - \frac{2\sigma m}{D_w^2 (\rho_l + \rho_v \coth md)} \qquad \text{(II.2)}$$

Before applying the above formula to our case, we shall briefly review the special cases reported in the literature where Equation (II:2) was applied.

II.2 Application of the Wave Theory at the Minimum Heat Flux Point

Zuber[5] used a simplified version of Equation (II.2) to predict the minimum heat flux on a flat horizontal surface. His model is shown in Fig. II.2. For $V_v = 0$ and $D_w = d \to \infty$ (both media are infinitely extended), Equation (II.2) reduced to

$$-\frac{b^2}{m^2} = c^2 = \frac{\sigma m}{\rho_v + \rho_l} - \frac{g}{m}\frac{\rho_l - \rho_v}{\rho_l + \rho_v} \qquad \text{(II.3)}$$

From Equation (II.1), it is seen that if n is real, the disturbance is periodic in time and, therefore, stable. Consequently, instability occurs when c^2 (in Equation (II.3)) becomes negative, and

the critical value for the wave length can be found by setting c^2 to zero:

$$m_c = \sqrt{\frac{g\,(\rho_1 - \rho_v)}{\sigma}} \qquad \text{(II.4)}$$

The critical wave length becomes

$$\lambda_c = \frac{2\pi}{m_c} = 2\pi\sqrt{\frac{\sigma}{g\,(\rho_1 - \rho_v)}} \qquad \text{(II.5)}$$

The physical meaning of λ_c can be explained by rewriting Equation (II.5) as

$$\frac{1}{2}\, g\,(\rho_1 - \rho_v)\,\delta_o^2 = \frac{2\pi}{\lambda_c}\,\frac{\pi\sigma}{\lambda_c}\,\delta_o^2 \qquad \text{(II.6)}$$

which means that, at the critical wave length, the surface tension energy equals the total mechanical energy. This type of instability occurs in the absence of relative velocity $(V_v - V_l)$, and is

referred to as Taylor's instability. All perturbations with wave length longer than the critical one λ_c are unstable.

As a consequence of Taylor's instability, Zuber[5] expected a definite geometrical configuration which is shown in Fig. II.2.e. The liquid-vapour interface consists of spikes of liquids and rounded vapour regions similar to cylindrical bubbles which rise into the liquid. When these spikes fall downward and contact the hot surface, rapid evaporation occurs and vapour flows in the region between two spikes. This region resembles rising bubbles, and after a row of bubbles is released an unstable interface is formed again and the process continues.

To quantify the heat flux, Zuber made a simplifying assumption by approximating the vapour slugs by spheres of radius = $\lambda/4$. He also used the experimental results of Lewis[6] to predict the frequency of bubble release. Knowing the frequency of bubble release and the energy needed to generate an amount of vapour equivalent to one vapour slug, he arrived at an expression for the heat transfer rate at the minimum heat flux point.

II.3 Application of the Wave Theory at the Critical Heat Flux Point

Zuber[5] and Zuber and Tribus[7], used a simplified version of Equation (II.2) to derive an expression for the critical heat flux where

the relative velocity of rising columns of vapour and falling liquid is important. Their model is shown in Fig. II.3 where the liquid vertical interface is vertical. They assumed g = 0 (vertical interface) and $D_w = d = \infty$; Equation (II.2) reduced to

$$c^2 = \frac{\sigma m}{\rho_l + \rho_v} - \frac{\rho_l \rho_v}{(\rho_l + \rho_v)^2} (V_v - V_l)^2 \qquad (II.6)$$

This type of instability is referred to as Helmholtz instability. The condition for stability is that c must be real. The velocity in the liquid phase is obtained from the continuity equation:

$$\rho_v V_v = \rho_l V_l \qquad (II.7)$$

Substituting V_l from Equation (II.7) into Equation (II.6) the critical vapour velocity can be obtained as

$$V_v = \left(\frac{\sigma m}{\rho_v}\right)^{1/2} \left(\frac{\rho_l}{\rho_l + \rho_v}\right)^{1/2} \qquad (II.8)$$

The wave number was calculated from Rayleigh's analysis[8] who examined the stability of a circular gas jet in a liquid and found that the instability occurs only for disturbances whose wave length is longer than the circumference of the jet. Therefore, the wave length is given by

$$\lambda = 2 \pi R \qquad (II.9)$$

where R is the radius of the jet. The wave length λ is related to wave number by the following relationship:

$$m = \frac{2\pi}{\lambda} \tag{II.10}$$

Substituting (II.9) and (II.10) in (II.8) the critical vapour velocity then becomes.

$$V_v = \left(\frac{\sigma}{\rho_v R}\right)^{1/2} \left(\frac{\rho_l}{\rho_l+\rho_v}\right)^{1/2} \tag{II.11}$$

Having determined the critical vapour velocity, the vapour mass flow rate can be calculated. Thus, the energy needed to generate the vapour flow leads to an expression for the critical heat flux.

II.4 Application of the Wave Theory to Determine the Minimum Film Boiling Temperature

Berenson[9] started with Equation (II.2) to derive an expression for the heat transfer coefficient at the minimum film boiling temperature. His model is shown in Fig. II.4. By setting the liquid velocity $V_l = 0$ (stagnant pool over a horizontal flat surface), Equation (II.2) becomes

$$-\frac{b^2}{m} = c^2 = \frac{\sigma m}{\rho_l+\rho_v/md} - \frac{g(\rho_l-\rho_v)}{m(\rho_l+\rho_v/md)} - \frac{\rho_l\rho_v V_v^2}{(\rho_l+\rho_v/md)md} \qquad \text{(II.12)}$$

Since both gravity and velocity terms appeared in Equation (II.12), it has become conventional to refer to Equation (II.12) as the combined Taylor-Helmholtz instability.

The parameter of interest in predicting the growth of the two-phase boundary is the coefficient b defined in Equation (II.1). Berenson introduced different simplying assumptions and studied their effect on the value of c and therefore the growth coefficient b:

1) Assume the effect of vapour velocity and depth are negligible, i.e., $V_v = 0$ and coth md = 1

2) Assume the effect of vapour velocity is negligible and that the vapour thickness is very small, i.e., $V_v = 0$ and coth $md = \frac{1}{md}$

3) Assume the effect of vapour thickness is negligible, i.e., coth md = 1.

4) Assume that the vapour film is very thin, i.e., coth $md = \frac{1}{md}$

The results of introducing the above assumptions to Equation (II.2) indicated that in the neighbourhood of the minimum film boiling temperature, the effect of vapour velocity and film thickness on the growth rate of the wave is negligible.

The vapour velocity was estimated from an analysis of the physical model shown in Fig. II.5 Assuming that the heat transfer is by conduction and that the vapour flows radially into the bubble, Berenson obtained an expression for the vapour velocity as a function of the temperature difference $(T_w - T_l)$ and the wave length. Applying the momentum equation he arrived at an expression for the vapour film thickness d. The heat transfer coefficient at the minimum film boiling point was then defined by

$$h = \frac{k_v}{d} \qquad \text{(II.13)}$$

This result combined with the minimum heat flux predicted by Zuber[9] (see section II.2), made it possible to predict the temperature difference at the minimum film boiling point, ΔT_{min}.

REFERENCES

1. Jordan, D.P. "Film and Transition Boiling", "Advances in Heat Transfer", Vol. 5, pp. 55-128, Academic, New York (1968).

2. Lamb, H. "Hydrodynamics" 6th Ed., University Press, Cambridge (1957).

3. Milne-Thompson, L.M. "Theoretical Hydrodynamics", 3rd Ed., Macmillan, New York (1955).

4. Stralen, S. "Boiling Phenomena", Vol. 2, Hemisphere Publishing Corporation (1979).

5. Zuber, N. "Hydrodynamic Aspects of Boiling Heat Transfer", AECU-4439, June (1959).

6. Lewis, D.J. "The instability of liquid surfaces when accelerated in a direction prependicular to their Planes II", Proc. Roy, Soc. London, A-2-2, 1950, Rept. LA-1600 (1954).

7. Zuber, N. and M. Tribus. "Further Remarks on the Stability of Boiling Heat Transfer", Report AECU-3631, January (1958).

8. Lord Rayleigh, Theory of Sound, Dover Publishers, New York (1945).

9. Berenson, P.J. "Film Boiling Heat Transfer From a Horizontal Surface", J. of Heat Transfer, pp. 351-358, August 1961.

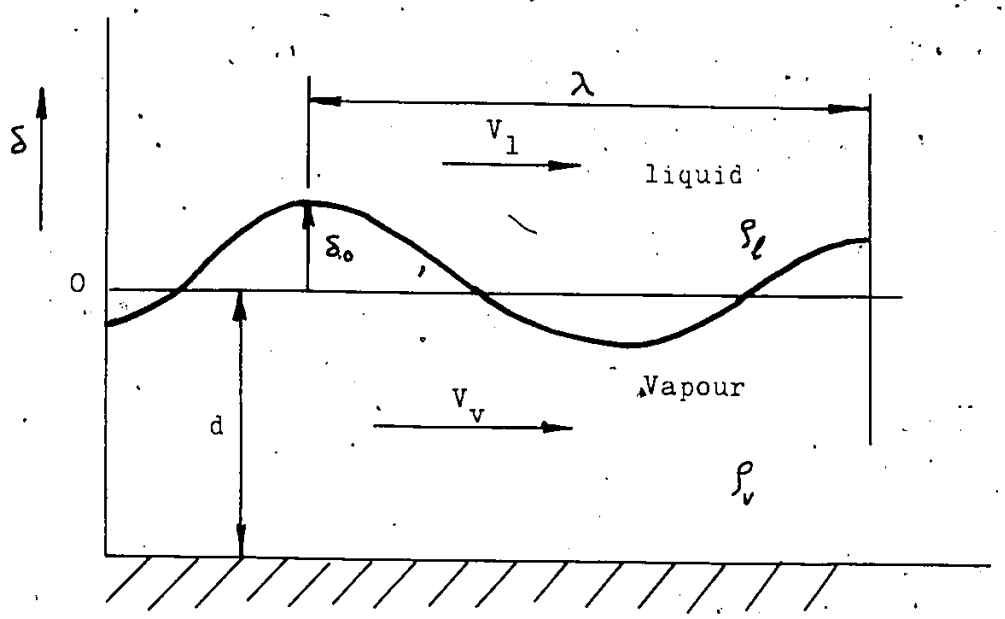

Fig. II.1 Surface Tension Waves at Liquid-Vapour Interface

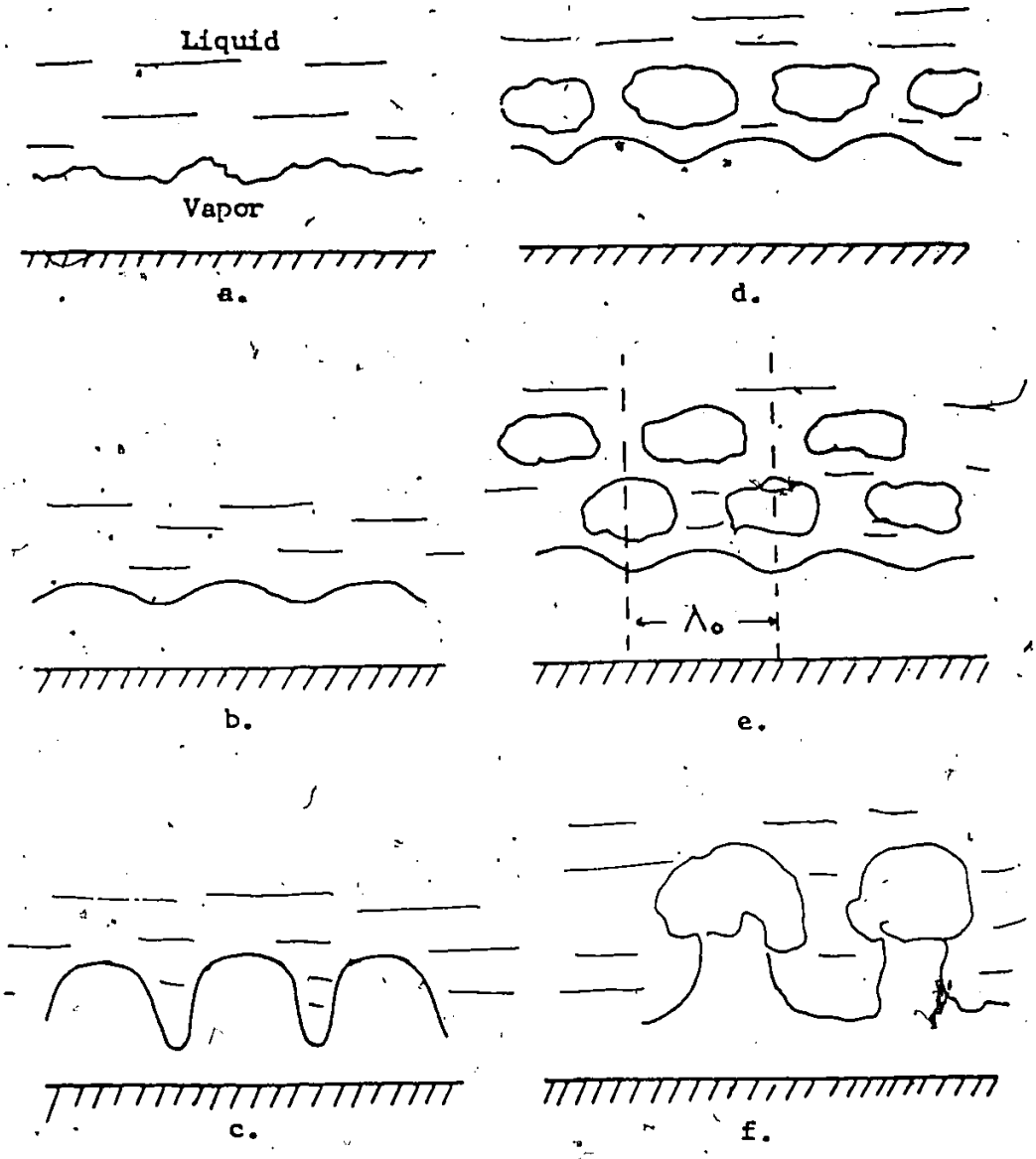

Fig. II.2 Schematic Representation of the Process of Transitional Boiling (Zuber 1958)

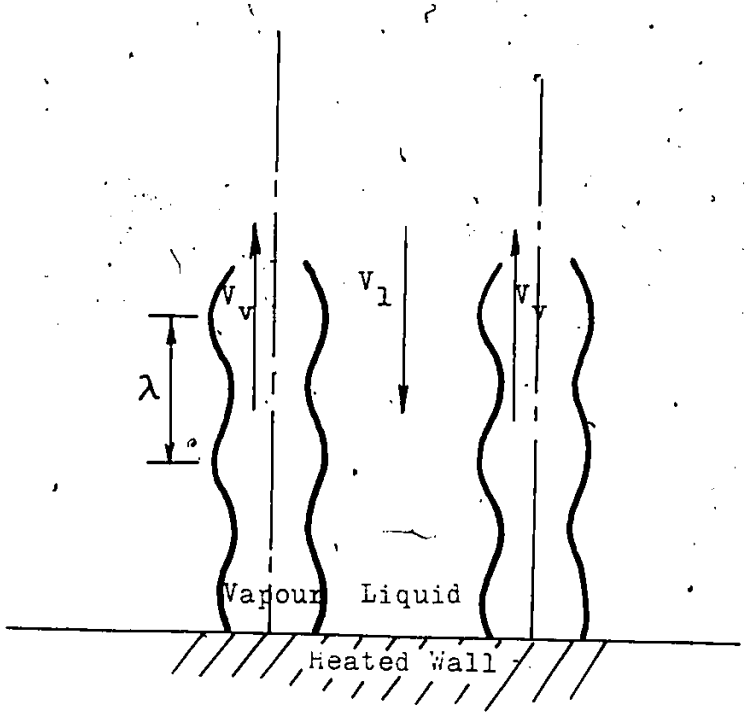

Fig. II.3 Instability Model of Zuber and Tribus at the Critical Heat Flux.

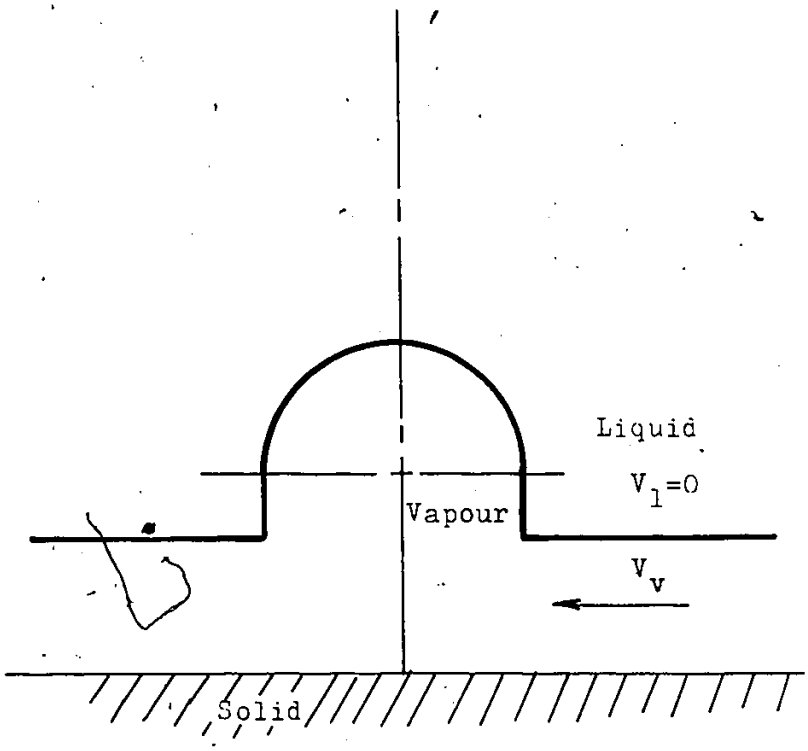

Fig. II.4 Berenson's Model of Film Boiling From a Horizontal Surface

APPENDIX III

Computer Program for the Semi-Empirical Model

```
FTN4X,Q
      PROGRAM BOIL
      REAL TT(35),TP(35),TVG(35),THF(35),THG(35),TCPF(35),TSIGMA(35)
      REAL TMUF(35),TKF(35),TMUG(35),TKG(35),TVF(35),TCPG(35)
      REAL  FITB(40),T(50),TEMP(100),HFLUX(100),TEMPI(30),HFLUXI(30)
      COMMON/AREA6/TT,TP,TVG,THF,THG,TCPF,TSIGMA,TMUF,TKF,TMUG
     1,TKG,TVF,TCPG
      COMMON/AREA1/D,X,P,G,DTSAT,TSAT,VISCG,VISCF,CPF,CONDF,VG,VF,HG,
     *SIGMA,PWALL,HC,HNCB,HCHEN,FICHEN,HF,FINCB,FIC,EL,F,CPG,Z,HFI,IFIC
      COMMON/AREA2/DTSUB,CHFPOL,ES,ALPHA,AK1,AK2,AK3,CHF
      COMMON/AREA3/TWALL,DTMINI,DTMINI,HMIN,TMINI,RATIO,TLOCAL,EM
     1,TMIN,CONDM,ROHM,CPM,FIMIN,FITRY,CONDAV,VISCAV,VGAV,TAV,IAV
      COMMON/AREA4/K,FITB,T,TTB,CHFTOT,TCHF
      COMMON/AREA5/ANU,FIKAL,EBROM,HFILM
      COMMON/AREA7/IGESS
      COMMON/AREA9/TEMP,HFLUX,IJ,TMAX
C
C
C     READ PROPERTY TABLES OF WATER
C     -----------------------------
C
      READ(51,1) TT
      READ(51,2)TP
      READ(51,3)TVF
      READ(51,2)TVG
      READ(51,4) THF,THG,TCPF,TSIGMA
      READ(51,1)TMUF
      READ(51,4)TKF,TCPG,TMUG,TKG
C
      DO 8 I=1,35
      THF(I)=THF(I)*1000.0
      TKG(I)=TKG(I)*0.001
      TMUG(I)=TMUG(I)*0.000001
      TCPF(I)=TCPF(I)*1000.0
      TCPG(I)=TCPG(I)*1000.0
      THG(I)=THG(I)*1000.0
    8 TSIGMA(I)=TSIGMA(I)*0.001
C
C
C     READ GEOMETRY AND INLET/LOCAL CONDITIONS
C     ----------------------------------------
C
      READ(51,5) D,Z,EL
   10 READ(51,5)G,TIN,P,ROHM,CPM,CONDM
      IF(G.EQ.999.0)STOP
      IAV=0
      IFIC=0
      CALL PRPRT
      CALL PCAL(TIN,TT,THF,HFI)
C
C
C     CALCULATE LOCAL CONDITIONS IF INLET CONDITIONS ARE GIVEN
C     --------------------------------------------------------
C
C
```

```
C
C              OBTAIN A GUESS VALUE FOR HEAT FLUX FROM ZUBER'S POOL BOILING
C              AND DTSAT OF THOM'S CORRELATION
C              ------------------------------------------------------------
C
      IGESS=1
      CALL ZUBER
      IGESS=0
      FITRY=CHFPOL
      DTSAT=0.0225*FITRY**0.5*EXP(-P/87.0)
C
      ETRF=0.0
   15 CALL LOCON
C
C
C     CALCULATE CHF AND CRITICAL TEMPERATURE USING MODIFIED ZUBER
C     CORRELATION AND CHEN'S CORRELATION. ITERATE TO MATCH LOCAL
C     CONDITIONS.
C     ------------------------------------------------------------
C
      GMIN=68.0
   30 CALL ZUBER
      ETR=0.0
   35 TWALL=TSAT+DTSAT
      CALL CHEN
      CHFTOT=CHF*(G/GMIN)**0.51
      VAR=FICHEN-CHFTOT
      IF(ABS(VAR).LE.100000.)GO TO 40
      DTSAT=DTSAT-0.50*(ABS(VAR)/VAR)
      ETR=ETR+1.0
      IF(ETR.EQ.80.0)GO TO 40
      GO TO 35
   40 VARP=FITRY-CHFTOT
      IF(ABS(VARP).LE.100000.) GO TO 49
      FITRY=FITRY-0.05 *  (ABS(VARP)/VARP)*ABS(VARP)
      ETRF=ETRF+1.0
      IF(ETRF.EQ.120.0) GO TO 49
      GO TO 15
   49 TCHF=TWALL
   50 CONTINUE
C
C
C     CALCULATE THE NUCLEATE BOILING HEAT FLUX USING CHEN'S
C     CORRELATION. START WITH CHF AND ITERATE TO MATCH LOCAL
C     CONDITIONS
C     ------------------------------------------------------
C
      IJ=1
      TWALL=TCHF-5.0
      FITRY=CHFTOT
   53 DTSAT=TWALL-TSAT
      IF(DTSAT.LE.5.0)GO TO 59
      ETRN=0.0
   55 CALL LOCON
      CALL CHEN
      ETRN=ETRN+1.0
```

```
      IF(ETRM.GE.40) GO TO 58
      VAR=FITRY-FICHEN
      VARP=VAR/EICHEN
      IF(ABS(VARP).LE.0.05) GO TO 58
      FITRY=FITRY-0.5*(ABS(VAR)/VAR)*ABS(VAR)
      GO TO 55
   58 CONTINUE
      TEMP1(IJ)=(TWALL-TSAT)*(1.0+40000./SQRT(CONDM*ROHM*C PM))**0.75/
     11.75+TSAT
      HFLUX1(IJ)=FICHEN
      IJ=IJ+1
      TWALL=TWALL-5.0
      GO TO 53
   59 CONTINUE
C
C---c-CHANGE ORDER OF PLOT ARRAYS-------
C
      IL=IJ-1
      DO 57 IK=1,IL
      TEMP(IK)=TEMP1(IJ-IK)
      HFLUX(IK)=HFLUX1(IJ-IK)
   57 CONTINUE
C
C
C     CALCULATE MINIMUM FILM BOILING TEMP AND HEAT HFLUX
C     ITERATE TO MATCH  LOCAL CONDITIONS
C     ----------------------------------------
C
C
      TWALL=TCHF
      ETRM=0.0
   61 IAV=1
      CALL PRPRT
      IAV=0
      CALL LOCON
      CALL HENRY
      FITRY=FIMIN
      VAR=FITRY-FIMIN
      VARP=VAR/EIMIN
      IF(ABS(VARP).LE.0.05)GO TO 69
      FITRY=FITRY-0.5*(ABS(VAR)/VAR)*ABS(VAR)
      ETRM=ETRM+1.0
      IF(ETRM.GE.40.0) GO TO 69
      GO TO 61
C
C
   69 CONTINUE
      DTSAT=TMIN-TSAT
      CALL HENRY
      HFILM=FBROM
      CALL HELMY
   71 CALL HENRY
      TWALL=DTSAT+TSAT
      FFILM=FBROM
      TEMP(IJ)=TWALL
```

```
      HFLUX(IJ)=EEILM
      DTSAT=DTSAT+20.0
      IF(DTSAT.GE.400.0) GO TO 80
      IJ=IJ+1
      GO TO 71
   80 CONTINUE
      WRITE(6,6)G,TIN,P,ROHM,CPM,CONDM,CHFTOT,TMAX,HEILM,TMIN
      DO 81 I=1,IJ
   81 WRITE(6,777)TEMP(I),HFLUX(I)
      GO TO 10
    1 FORMAT(7E10.2)
  111 FORMAT(7(1X,E10.2))
    2 FORMAT(7F10.6)
    3 FORMAT(7E10.4)
    4 FORMAT(7F10.3)
    5 FORMAT(8E10.3)
  555 FORMAT(8(1X,E10.3))
    6 FORMAT(1H1,30X," HEAT TRANSFER PREDICTIONS FOR:  ",//,30X,
     *"MASS FLUX=",F7.2," KG/M2/S",5X,"INLET TEMP=",F5.2," C",
     *5X,"PRESSRE=",E10.2," BAR",//,30X,"WALL DENSITY=",F10.3,
     *" KG/M3",5X,"WALL CP",F10.3," J/KG C",5X,"WALL COND=",E10.3
     *,"W/M",//,30X,"CHF=",E10.3,"W/M2",5X,"TMAX=",F7.2," C",5X,"HMIN=",
     *E10.3," W/M2",5X,"MIN TEMP=",F7.2,"C",//
     *,30X,"SURFACE TEMPERATURE",5X,"HEAT FLUX",/)
  777 FORMAT(30X,F10.1,15X,E10.4)
  999 FORMAT(10(2X,E10.3))
      END
      SUBROUTINE CHEN
      REAL TT(35),TP(35),TVG(35),THF(35),THG(35),TCPF(35),TSIGMA(35)
      REAL TMUF(35),TKF(35),TMUG(35),TKG(35),TVF(35),TCPG(35)
      REAL    FITB(40),T(50)
      COMMON/AREA6/TT,TP,TVG,THF,THG,TCPF,TSIGMA,TMUF,TKF,TMUG
     1,TKG,TVF,TCPG
      COMMON/AREA1/D,X,P,G,DTSAT,TSAT,VISCG,VISCF,CPF,CONDF,VG,VF,HG,
     *SIGMA,PWALL,HC,HNCB,HCHEN,FICHEN,HF,FINCB,FIC,EL,F,CPG,Z,HFI,IFIC
      COMMON/AREA2/DTSUB,CHFPOL,ES,ALPHA,AK1,AK2,AK3,CHF
      COMMON/AREA3/TWALL,DTMIN1,DTMIN1,HMIN,TMINI,RATIO,FLOCAL,EM
     1,TMIN,CONDM,ROHM,CPM,FIMIN,FITRY,CONDAV,VISCAV,VGAV,TAV,IAV
      COMMON/AREA4/K,FITB,T,TTB,CHFTOT,TCHF
      COMMON/AREA5/ANU,FIKAL,FBROM,HFIEM
      CALL PCAL(TWALL,TT,TP,PWALL)
      HFG=HG-HF
      ROHG=1/VG
      ROHF=1/VF
      REF=D*G*(1-X)/VISCF
      IF(X.LE.0.0)REF=D*G /VISCF
    8 FORMAT(8(E10.3,2X))
      F=1.0
      IF(X.LE.0.01)GO TO 1
      XTTINV=((X/(1-X))**0.9)*((ROHF/ROHG)**0.5)*
     1((VISCG/VISCF)**0.1)
      F=((XTTINV+0.213)**0.736)*2.35
      IF(XTTINV.LE.0.1)F=1.0
    1 PRF=CPF*VISCF/CONDF
```

```
      HC=0.023*(REF**0.8)*(PRF**0.4)*(CONDF/D)*E*(1.0+(D/EL)**0.7)
      FIC=HC*DTSAT
      IF(IFIC.EQ.1) RETURN
      RETP=REF*(F**1.25)*0.0001
      S=1/(1+0.42*RETP**0.78)
      IF(RETP.LT.32.5)S=1/(1+0.12*RETP**1.14)
      IF(RETP.GE.70.0)S=0.1
      DPSAT=(PWALL-P)*100000.0
      HNCB1=0.00122*((CONDF**0.79)*(CPF**0.45)*(ROHF**0.49))/((SIGMA**0.
     *5)*(VISCF**0.29)*(HFG**0.24)*(ROHG**0.24))
      HNCB2=S*(DTSAT**0.24)*(DPSAT**0.75)
      HNCB=HNCB2*HNCB1
      FINCB=HNCB*DTSAT
      IF(X.LE.0.0)FIC=HC*(DTSAT+DTSUB)
      HCHEN=HC+HNCB
      FICHEN=FINCB+FIC
      RETURN
      END
      SUBROUTINE PCAL(VARI,TBI,TBD,VARD)
C
C
C     THIS SUBROUTINE INTERPOLATES OR EXTRAPOLATES IN TABLES TO
C     OBTAIN THE CORRESPONDING VALUE OF AN INDEPENDANT VARIABLE:
C
C     VARI= INDEPENDANT VARIABLE
C     TBI =    "   "      TABLE
C     TBD = DEPENDENT   TABLE
C     VARD=    "   "      VARIABLE
C
      REAL TBI(35),TBD(35)
      DO 20 I=1,40
      DIF=TBI(I)-VARI
      IF(DIF)20,30,30
   20 CONTINUE
   30 VARD=TBD(I-1)+(VARI-TBI(I-1))*(TBD(I)-TBD(I-1))/(TBI(I)-TBI(I-1))
      RETURN
      END
      SUBROUTINE ZUBER
      REAL TT(35),TP(35),TVG(35),THF(35),THG(35),TCPF(35),TSIGMA(35)
      REAL TMUF(35),TKF(35),TMUG(35),TKG(35),TVF(35),TCPG(35)
      REAL FITB(40),T(50)
      COMMON/AREA6/TT,TP,TVG,THF,THG,TCPF,TSIGMA,TMUF,TKF,TMUG
     1,TKG,TVF,TCPG
      COMMON/AREA1/D,X,P,G,DTSAT,TSAT,VISCG,VISCF,CPF,CONDF,VG,VF,HG,
     *SIGMA,PWALL,HC,HNCB,HCHEN,FICHEN,HF,FINCB,FIC,EL,F,CPG,Z,HFI,IFIC
      COMMON/AREA2/DTSUB,CHFPOL,ES,ALPHA,AK1,AK2,AK3,CHF
      COMMON/AREA3/TWALL,DTMIN1,DTMIN1,HMIN,TMINI,RATIO,TLOCAL,EM
     1,TMIN,CONDM,ROHM,CPM,FIMIN,FITRY,CONDAV,VISCAV,VGAV,TAV,IAV
      COMMON/AREA4/K,FITB,I,TTB,CHFTOT,TCHF
      COMMON/AREA5/ANU,FIKAL,FB,ROM,HFGM
      COMMON/AREA7/IGESS
      HFG=HG-HF
      ROHF=1.0/VF
      ROHG=1.0/VG
      CHFPOL=0.16*HFG*(ROHG**0.5)*((9.8*SIGMA*(ROHF-ROHG))**0.25)
```

```
      IF(IGESS.EQ.1)RETURN
      VAR=-0.016
      ES=((ROHF/ROHG)**0.205)*((G*D /VISCF)**VAR)
      ALPHA=X/(X+ROHG*ES*(1.0-X)/ROHF)
      IF(X.LT.0.01.AND.X.GT.0.0)DTSUB=0.0
      AK1=1.0+0.1*((ROHF/ROHG)**0.75)*CPF*DTSUB/HFG
      IF(X.GE.0.01)AK1=(1.0-ALPHA)**1.0
      AK2=1.0
      AK3=1.0
      CHF=CHFPOL*AK1*AK2*AK3
      RETURN
      END
      SUBROUTINE HENRY
      REAL TT(35),TP(35),TVG(35),THF(35),THG(35),TCPF(35),TSIGMA(35)
      REAL TMUF(35),TKF(35),TMUG(35),TKG(35),TVF(35),TCPG(35)
      REAL     FITB(40),T(50)
      COMMON/AREA6/TT,TP,TVG,THF,THG,TCPF,TSIGMA,TMUF,TKF,TMUG
     1,TKG,TVF,TCPG
      COMMON/AREA1/D,X,P,G,DTSAT,TSAT,VISCG,VISCF,CPF,CONDF,VG,VF,HG,
     *SIGMA,PWALL,HC,HNCB,HCHEN,FICHEN,HF,FINCB,FIC,EL,F,CPG,Z,HFI,IFIC
      COMMON/AREA2/DTSUB,CHFPOL,ES,ALPHA,AK1,AK2,AK3,CHF
      COMMON/AREA3/TWALL,DTMINI,DTMINI,HMIN,TMINI,RATIO,TLOCAL,EM
     1,TMIN,CONDM,ROHM,CPM,FIMIN,FITRY,CONDAV,VISCAV,VGAV,TAV,IAV
      COMMON/AREA4/K,FITB,T,TTB,CHFTOT,TCHF
      COMMON/AREA5/ANU,FIKAL,FBROM,HFILM
      ROHG=1.0/VG
      ROHF=1.0/VF
      HFG=HG-HF
      ROHGAV=1.0/VGAV
      DTMINI=0.127*(ROHGAV*HFG/CONDAV)*((9.8*(ROHF-ROHGAV)/
     1(ROHF+ROHGAV))**0.67)*((SIGMA/9.8/(ROHF-ROHGAV))**0.5)*
     2((VISCAV/9.8/(ROHF-ROHGAV))**0.333)
      HMIN=0.425*((CONDAV**3.0)*9.8*ROHGAV*(HG-HF)*(ROHF-ROHGAV)/
     1VISCAV/((SIGMA/9.8/(ROHF-ROHGAV))**0.5))**0.25
      REO=500.0
      REN=35000.0
      CONDI=CONDAV*(1.+((REN-REO)/REO)**0.8)
      HBROM=0.62*((COND1**3)*9.8*ROHGAV*(HG-HF)*(ROHF-ROHGAV)/
     1VISCAV/DTSAT)**  .25
      FBROM=HBROM*DTSAT
      FIMIN=0.09*ROHGAV*(HG-HF)*(9.8*SIGMA*(ROHF-ROHGAV)/((ROHF
     1+ROHGAV)**2.0))**0.25
      DTMINI=(FIMIN/HMIN)**1.333
      TMINI=DTMINI+TSAT
      RATIO=0.42*(((CONDF*ROHF*CPF)/(CONDM*ROHM*CPM))
     1**0.5*(HG-HF)/DTMINI/CPM)**0.6
      TMIN=TMINI+RATIO*(TMINI-TLOCAL)
      RETURN
      END
      SUBROUTINE KALIN
      REAL TT(35),TP(35),TVG(35),THF(35),THG(35),TCPF(35),TSIGMA(35)
      REAL TMUF(35),TKF(35),TMUG(35),TKG(35),TVF(35),TCPG(35)
      REAL     FITB(40),T(50)
      COMMON/AREA6/TT,TP,TVG,THF,THG,TCPF,TSIGMA,TMUF,TKF,TMUG
     1,TKG,TVF,TCPG
```

```
      COMMON/AREA1/D,X,P,G,DTSAT,TSAT,VISCG,VISCF,CPF,CONDF,VG,VF,HG,
     *SIGMA,PWALL,HC,HNCB,HCHEN,FICHEN,HF,FINCB,FIC,EL,F,CPG,Z,HFI,IFIC
      COMMON/AREA2/DTSUB,CHFPOL,ES,ALPHA,AK1,AK2,AK3,CHF
      COMMON/AREA3/TWALL,DTMIN1,DTMINI,HMIN,TMINI,RATIO,TLOCAL,EM
     1,TMIN,CONDM,ROHM,CPM,FIMIN,FITRY,CONDAV,VISCAV,VGAV,TAV,IAV
      COMMON/AREA4/K,FITB,T,ITB,CHFTOT,TCHF
      COMMON/AREA5/ANU,FIKAL,FBROM,HFILM
      CALL PRPRF
      ANU=0.0012*(G*D/VISCF)**((CPF*VISCF/CONDF)**0.4)*(1.0+22*EXP(
     1-0.038*EL/D))
      FIKAL=(ANU*CONDF/D)*(TSAT-TLOCAL)
      RETURN
      END
      SUBROUTINE HELMY
      REAL TT(35),TP(35),TVG(35),THF(35),THG(35),TCPF(35),TSIGMA(35)
      REAL TMUF(35),TKF(35),TMUG(35),TKG(35),TVF(35),TCPG(35)
      REAL     FITB(40),T(50) ,TEMP(100),HFLUX(100)
      COMMON/AREA6/TT,TP,TVG,THF,THG,TCPF,TSIGMA,TMUF,TKF,TMUG
     1,TKG,TVF,TCPG
      COMMON/AREA1/D,X,P,G,DTSAT,TSAT,VISCG,VISCF,CPF,CONDF,VG,VF,HG,
     *SIGMA,PWALL,HC,HNCB,HCHEN,FICHEN,HF,FINCB,FIC,EL,F,CPG,Z,HFI,IFIC
      COMMON/AREA2/DTSUB,CHFPOL,ES,ALPHA,AK1,AK2,AK3,CHF
      COMMON/AREA3/TWALL,DTMIN1,DTMINI,HMIN,TMINI,RATIO,TLOCAL,EM
     1,TMIN,CONDM,ROHM,CPM,FIMIN,FITRY,CONDAV,VISCAV,VGAV,TAV,IAV
      COMMON/AREA4/K,FITB,T,ITB,CHFTOT,TCHF
      COMMON/AREA5/ANU,FIKAL,FBROM,HFILM
      COMMON/AREA9/TEMP,HFLUX,IJ,TMAX
C-------- EFFECT OF WALL PROPERTIES ON TCHF ----------------
C
C
      TMAX=(TCHF-TSAT)*(1.0+40000./SQRT((CONDM*ROHM*CPM)**0.75/1.75+
     1TSAT
      MAXT=TMAX
      MINT=TMIN
      K=1
      IJ=IJ-1
      DO 9 IT=MAXT,MINT,5
      T(K)=FLOAT(IT)
      DELTA=(T(K)-TMIN)**2/(TMAX-TMIN)**2
      IF(DELTA.LT.0)DELTA=0
      IF(DELTA.GT.1.0)DELTA=1.0
      FI=DELTA*CHFTOT+(1.0-DELTA)*HFILM
      TEMP(IJ)=T(K)
      HFLUX(IJ)=FI
      IJ=IJ+1
  111 FORMAT(2X,F10.4,2X,F12.4,5(2X,F10.4))
      K=K+1
    9 CONTINUE
      IJ=IJ-1
      RETURN
      END
      SUBROUTINE LOCON
C
C
C       THIS SUBROUTINE CALCULATES LOCAL CONDITIONS IF INLET
```

```
C       CONDITIONS ARE KNOWN
C       ---------------------------------------------------
C
      REAL TT(35),TP(35),TVG(35),THF(35),THG(35),TCPF(35),TSIGMA(35)
      REAL TMUF(35),TKF(35),TMUG(35),TKG(35),TVF(35),TCPG(35)
      COMMON/AREA6/TT,TP,TVG,THF,THG,TCPF,TSIGMA,TMUF,TKF,TMUG
     1,TKG,TVF,TCPG
      COMMON/AREA1/D,X,P,G,DTSAT,TSAT,VISCG,VISCF,CPF,CONDF,VG,VF,HG,
     *SIGMA,PWALL,HC,HNCB,HCHEN,FICHEN,HF,FINCB,FIC,EL,F,CPG,Z,HFI,IFIC
      COMMON/AREA2/DTSUB,CHFPOL,ES,ALPHA,AK1,AK2,AK3,CHF
      COMMON/AREA3/TWALL,DTMIN1,DTMIN1,HMIN,TMINI,RATIO,TLOCAL,EM
     1,TMIN,CONDM,ROHM,CPM,FIMIN,FITRY,CONDAV,VISCAV,VGAV,TAV,IAV
      DELH=Z*4.0*FITRY/G/D
      HLOCAL=HFI+DELH
      X=(HLOCAL-HF)/(HG-HF)
      CALL PCAL(HLOCAL,THF,TT,TLOCAL)
      IF(TLOCAL.GE.TSAT)TLOCAL=TSAT
      DTSUB=TSAT-TLOCAL
      RETURN
      END
      SUBROUTINE PRPRT
      REAL TT(35),TP(35),TVG(35),THF(35),THG(35),TCPF(35),TSIGMA(35)
      REAL TMUF(35),TKF(35),TMUG(35),TKG(35),TVF(35),TCPG(35)
      REAL     FITB(40),T(50)
      COMMON/AREA6/TT,TP,TVG,THF,THG,TCPF,TSIGMA,TMUF,TKF,TMUG
     1,TKG,TVF,TCPG
      COMMON/AREA1/D,X,P,G,DTSAT,TSAT,VISCG,VISCF,CPF,CONDF,VG,VF,HG,
     *SIGMA,PWALL,HC,HNCB,HCHEN,FICHEN,HF,FINCB,FIC,EL,F,CPG,Z,HFI,IFIC
      COMMON/AREA2/DTSUB,CHFPOL,ES,ALPHA,AK1,AK2,AK3,CHF
      COMMON/AREA3/TWALL,DTMIN1,DTMIN1,HMIN,TMINI,RATIO,TLOCAL,EM
     1,TMIN,CONDM,ROHM,CPM,FIMIN,FITRY,CONDAV,VISCAV,VGAV,TAV,IAV
      COMMON/AREA4/K,FITB,T,TTB,CHFTOT,TCHF
      COMMON/AREA5/ANU,FIKAL,EBROM,HFILM
      IF(IAV.EQ.1) GO TO 1
      CALL PCAL(P,TP,TT,TSAT)
      CALL PCAL(P,TP,TMUG,VISCG)
      CALL PCAL(P,TP,TMUF,VISCF)
      CALL PCAL(P,TP,TCPF,CPF)
      CALL PCAL(P,TP,TCPG,CPG)
      CALL PCAL(P,TP,TKF,CONDF)
      CALL PCAL(P,TP,TVG,VG)
      CALL PCAL(P,TP,TVF,VF)
      CALL PCAL(P,TP,THG,HG)
      CALL PCAL(P,TP,THF,HF)
      CALL PCAL(P,TP,TSIGMA,SIGMA)
      GO TO 2
1     TAV=TSAT
      CALL PCAL(TAV,TT,TKG,CONDAV)
      CALL PCAL(TAV,TT,TMUG,VISCAV)
      CALL PCAL(TAV,TT,TVG,VGAV)
2     RETURN
      END
      BLOCK DATA AREAS,ANYTHING
      REAL TT(35),TP(35),TVG(35),THF(35),THG(35),TCPF(35),TSIGMA(35)
      REAL TMUF(35),TKF(35),TMUG(35),TKG(35),TVF(35),TCPG(35)
```

```
      REAL FITB(40),T(50),TEMP(100),HFLUX(100),TEMP1(30),HFLUX1(30)
      COMMON/AREA6/TT,TP,TVG,THF,THG,TCPF,TSIGMA,TMUF,TKF,TMUG
     1,TKG,TVF,TCPG
      COMMON/AREA1/D,X,P,G,DTSAT,TSAT,VISCG,VISCF,CPF,CONDF,VG,VF,HG,
     *SIGMA,PWALL,HC,HNCB,HCHEN,FICHEN,HF,FINCB,FIC,EL,F,CPG,Z,HFI,IFIC
      COMMON/AREA2/DTSUB,CHFPOL,ES,ALPHA,AK1,AK2,AK3,CHF
      COMMON/AREA3/TWALL,DTMIN1,DTMIN1,HMIN,TMIN1,RATIO,TLOCAL,EM
     1,TMIN,CONDM,ROHM,CPM,FIMIN,FITRY,CONDAV,VISCAV,VGAV,TAV,IAV
      COMMON/AREA4/K,FITB,T,TTB,CHFTOT,TCHF
      COMMON/AREA5/ANU,FIKAL,FBROM,HFILM
      COMMON/AREA7/IGESS
      COMMON/AREA9/TEMP,HFLUX,IJ,TMAX
      END
      ENDS
```

0.01	+00 10.0	+00 20.0	+00 30.0	+00 40.0	+00 50.0	+00 60.0	+00
70.0	+00 80.0	+00 90.0	+00 100.0	+00 110.0	+00 120.0	+00 130.0	+00
140.0	+00 150.0	+00 160.0	+00 170.0	+00 180.0	+00 190.0	+00 200.0	+00
210.0	+00 220.0	+00 230.0	+00 240.0	+00 250.0	+00 260.0	+00 270.0	+00
280.0	+00 290.0	+00 300.0	+00 310.0	+00 320.0	+00 330.0	+00 340.0	+00
0.006112	0.012271	0.023368	0.042418	0.073750	0.12335	0.19919	
0.31161	0.47358	0.70109	1.01325	1.4327	1.9854	2.7011	
3.6136	4.7597	6.1804	7.9202	10.027	12.553	15.550	
19.080	23.202	27.979	33.480	39.776	46.941	55.052	
64.191	74.449	85.917	98.694	112.89	128.64	146.08	
1.0002	-031.0004	-031.0018	-031.0044	-031.0079	-031.0121	-031.0171	-03
1.0228	-031.0290	-031.0359	-031.0435	-031.0515	-031.0603	-031.0697	-03
1.0798	-031.0906	-031.1021	-031.1144	-031.1275	-031.1415	-031.1565	-03
1.1726	-031.1900	-031.2087	-031.2291	-031.2512	-031.2755	-031.3023	-03
1.3321	-031.3655	-031.4036	-031.4475	-031.4992	-031.5620	-031.6390	-03
206.146	106.422	57.836	32.929	19.546	12.045	7.6776	
5.0453	3.4083	2.3609	1.6730	1.2101	0.89171	0.66832	
0.50866	0.39257	0.30685	0.24262	0.19385	0.15635	0.12719	
0.104265	0.086062	0.071472	0.059674	0.050056	0.042149	0.035599	
0.030133	0.025537	0.021643	0.018316	0.015451	0.012967	0.010779	
0.000061	41.99	83.86	125.66	167.47	209.3	251.1	
293.0	334.9	376.9	419.1	461.3	503.7	546.3	
589.1	632.2	675.5	719.1	763.1	807.5	852.4	
897.7	943.7	990.3	1037.6	1085.8	1135.0	1185.2	
1236.8	1290.0	1345.0	1402.0	1462.0	1526.0	1596.0	
2501.0	2519.0	2538.0	2556.0	2574.0	2592.0	2609.0	
2626.0	2643.0	2660.0	2676.0	2691.0	2706.0	2720.0	
2734.0	2747.0	2758.0	2769.0	2778.0	2786.0	2793.0	
2798.0	2802.0	2803.0	2803.0	2801.0	2796.0	2790.0	
2780.0	2766.0	2749.0	2727.0	2700.0	2666.0	2623.0	
4.218	4.194	4.182	4.179	4.179	4.181	4.185	
4.191	4.198	4.207	4.218	4.230	4.244	4.262	
4.282	4.306	4.334	4.366	4.403	4.446	4.494	
4.550	4.613	4.685	4.769	4.866	4.985	5.134	
5.307	5.520	5.794	6.143	6.604	7.241	8.225	
75.60	74.24	72.78	71.23	69.61	67.93	66.19	
64.40	62.57	60.69	58.78	56.83	54.85	52.83	
50.79	48.70	46.59	44.44	42.26	40.05	37.81	
35.53	33.23	30.90	28.56	26.19	23.82	21.44	
19.07	16.71	14.39	12.11	9.89	7.75	5.71	
1786.0	-061304.0	-061002.0	-06798.3	-06653.9	-06547.8	-06467.3	-06
404.8	-06355.4	-06315.6	-06283.1	-06254.8	-06231.0	-06210.9	-06
194.1	-06179.8	-06167.7	-06157.4	-06148.5	-06140.7	-06133.9	-06
127.9	-06122.4	-06117.5	-06112.9	-06108.7	-06104.8	-06101.1	-06
097.5	-06094.1	-06090.7	-06087.2	-06083.5	-06079.5	-06075.4	-06
0.569	0.587	0.603	0.618	0.631	0.643	0.653	
0.662	0.670	0.676	0.681	0.684	0.687	0.688	
0.668	0.687	0.684	0.681	0.677	0.671	0.664	
0.657	0.648	0.639	0.628	0.616	0.603	0.589	
0.574	0.558	0.541	0.523	0.503	0.482	0.460	
1.863	1.870	1.880	1.890	1.900	1.912	1.924	
1.946	1.970	1.999	2.034	2.076	2.125	2.180	
2.245	2.320	2.406	2.504	2.615	2.741	2.883	
3.043	3.223	3.426	3.656	3.918	4.221	4.575	
4.996	5.509	6.148	6.968	8.060	9.580	11.87	

08.105	08.504	08.903	09.305	09.701	10.10	10.50
10.89	11.29	11.67	12.06	12.45	12.83	13.20
13.57	13.94	14.30	14.66	15.02	15.37	15.72
16.07	16.42	16.78	17.14	17.51	17.90	18.31
18.74	19.21	19.73	20.30	20.95	21.70	22.70
17.6	18.2	18.8	19.5	20.2	20.9	21.6
22.4	23.2	24.0	24.9	25.8	26.7	27.8
28.9	30.0	31.3	32.6	34.1	35.7	37.4
39.4	41.5	43.9	46.5	49.5	52.8	56.6
60.9	66.0	71.9	79.1	87.7	99.0	114.0

12.7 −03 0.254−01 50.800+00

20.3	+01	00.72	+02	1.0	+00	8.938	+03	3.85	+02	3.79	+02	1.00	+00	
13.6	+01	00.72	+02	1.0	+00	8.938	+03	3.85	+02	3.79	+02	1.00	+00	
13.6	+01	00.86	+02	1.0	+00	8.938	+03	3.85	+02	3.79	+02	1.00	+00	
20.3	+01	00.72	+02	1.0	+00	8.169	+03	4.35	+02	0.17	+02	1.00	+00	
99.9	+01	00.72	+02	1.0	+00	8.169	+03	4.35	+02	0.17	+02	1.00	+00	

HEAT TRANSFER PREDICTIONS FOR:

ASS FLUX= 203.00 KG/M2/S INLET TEMP=72.00 C PRESSRE= .10E+01 BAR

ALL DENSITY= 8938.000 KG/M3 WALL CP 385.000 J/KG C WALL COND= .379E+03W/

HF= .270E+07W/M2 TMAX= 147.83 C HMIN= .414E+06 W/M2 MIN TEMP= 276.49C

URRACE TEMPERATURE	HEAT FLUX
107.8	.1305E+06
112.8	.2281E+06
117.8	.3741E+06
122.8	.5790E+06
127.8	.8467E+06
132.8	.1191E+07
137.8	.1616E+07
147.0	.2699E+07
152.0	.2553E+07
157.0	.2385E+07
162.0	.2223E+07
167.0	.2069E+07
172.0	.1921E+07
177.0	.1780E+07
182.0	.1646E+07
187.0	.1519E+07
192.0	.1399E+07
197.0	.1286E+07
202.0	.1180E+07
207.0	.1080E+07
212.0	.9878E+06
217.0	.9023E+06
222.0	.8236E+06
227.0	.7518E+06
232.0	.6870E+06
237.0	.6290E+06
242.0	.5779E+06
247.0	.5338E+06
252.0	.4965E+06
257.0	.4662E+06
262.0	.4427E+06
267.0	.4261E+06
276.5	.4137E+06
296.5	.4483E+06
316.5	.4820E+06
336.5	.5150E+06
356.5	.5473E+06
376.5	.5789E+06
396.5	.6100E+06
416.5	.6406E+06
436.5	.6707E+06
7456.5	.7003E+06
476.5	.7295E+06
496.5	.7584E+06

HEAT TRANSFER PREDICTIONS FOR:

ASS FLUX= 136.00 KG/M2/S INLET TEMP= 72.00 C PRESSRE= .10E+01 BAR

ALL DENSITY= 8938.000 KG/M3 WALL CP 385.000 J/KG C WALL COND= .379E+03W/

HF= .200E+07W/M2 TMAX= 411.83 C HMIN= .414E+06 W/M2 MIN TEMP= 276.40C

URFACE TEMPERATURE	HEAT FLUX
106.8	.9677E+05
111.8	.1839E+06
116.8	.3223E+06
121.8	.5162E+06
126.8	.7785E+06
131.8	.1112E+07
141.0	.1999E+07
146.0	.1902E+07
151.0	.1790E+07
156.0	.1683E+07
161.0	.1579E+07
166.0	.1480E+07
171.0	.1386E+07
176.0	.1296E+07
181.0	.1210E+07
186.0	.1129E+07
191.0	.1052E+07
196.0	.9794E+06
201.0	.9112E+06
206.0	.8474E+06
211.0	.7879E+06
216.0	.7329E+06
221.0	.6822E+06
226.0	.6359E+06
231.0	.5940E+06
236.0	.5564E+06
241.0	.5232E+06
246.0	.4944E+06
251.0	.4700E+06
256.0	.4500E+06
261.0	.4343E+06
266.0	.4230E+06
271.0	.4161E+06
276.4	.4135E+06
296.4	.4482E+06
316.4	.4819E+06
336.4	.5149E+06
356.4	.5471E+06
376.4	.5788E+06
396.4	.6099E+06
416.4	.6404E+06
436.4	.6705E+06
456.4	.7002E+06
476.4	.7294E+06
496.4	.7583E+06

HEAT TRANSFER PREDICTIONS FOR:

ASS FLUX= 136.00 KG/M2/S INLET TEMP=86.00 C PRESSRE= .10E+01 BAR

ALL DENSITY= 8938.000 KG/M3 WALL CP 385.000 J/KG C WALL COND= .379E+03W/

HF= .368E+06W/M2 TMAX= 121.34 C HMIN= .393E+05 W/M2 MIN TEMP= 264.89C

URFACE TEMPERATURE	HEAT FLUX
106.3	.6800E+05
111.3	.1502E+06
121.0	.3677E+06
126.0	.3693E+06
131.0	.3710E+06
136.0	.3726E+06
141.0	.3742E+06
146.0	.3757E+06
151.0	.3771E+06
156.0	.3785E+06
161.0	.3798E+06
166.0	.3811E+06
171.0	.3823E+06
176.0	.3834E+06
181.0	.3845E+06
186.0	.3855E+06
191.0	.3864E+06
196.0	.3873E+06
201.0	.3881E+06
206.0	.3889E+06
211.0	.3896E+06
216.0	.3902E+06
221.0	.3908E+06
226.0	.3913E+06
231.0	.3918E+06
236.0	.3922E+06
241.0	.3925E+06
246.0	.3928E+06
251.0	.3930E+06
256.0	.3931E+06
264.9	.3932E+06
284.9	.4284E+06
304.9	.4626E+06
324.9	.4960E+06
344.9	.5286E+06
364.9	.5606E+06
384.9	.5921E+06
404.9	.6229E+06
424.9	.6533E+06
444.9	.6832E+06
464.9	.7126E+06
484.9	.7417E+06

HEAT TRANSFER PREDICTIONS FOR:

ASS FLUX= 203.00 KG/M2/S INLET TEMP=72.00 C PRESSRE= .10E+01 BAR

ALL DENSITY= 8169.000 KG/M3 WALL CP 435.000 J/KG C WALL COND= .170E+02W/

HF= .270E+07W/M2 TMAX= 207.26 C HMIN= .617E+06 W/M2 MIN TEMP= 400.90C

URFACE TEMPERATURE	HEAT FLUX
118.0	.1305E+06
129.2	.2281E+06
140.3	.3741E+06
151.5	.5790E+06
162.6	.8467E+06
173.8	.1191E+07
184.9	.1616E+07
207.0	.2699E+07
212.0	.2598E+07
217.0	.2495E+07
222.0	.2394E+07
227.0	.2296E+07
232.0	.2201E+07
237.0	.2309E+07
242.0	.2019E+07
247.0	.1932E+07
252.0	.1848E+07
257.0	.1767E+07
262.0	.1688E+07
267.0	.1613E+07
272.0	.1540E+07
277.0	.1469E+07
282.0	.1402E+07
287.0	.1337E+07
292.0	.1276E+07
297.0	.1217E+07
302.0	.1160E+07
307.0	.1107E+07
312.0	.1056E+07
317.0	.1008E+07
322.0	.9628E+06
327.0	.9204E+06
332.0	.8807E+06
337.0	.8439E+06
342.0	.8098E+06
347.0	.7784E+06
352.0	.7499E+06
357.0	.7241E+06
362.0	.7011E+06
367.0	.6809E+06
372.0	.6634E+06
377.0	.6487E+06
382.0	.6368E+06
387.0	.6277E+06
392.0	.6213E+06
401.0	.6169E+06
421.0	.6473E+06
441.0	.6773E+06
461.0	.7069E+06
481.0	.7360E+06

APPENDIX IV

Computer Program for the Transition Boiling Model

```
FTN4X
      PROGRAM WAVE(4,99),TB
      REAL TT(35),TP(35),TVG(35),THF(35),THG(35),TCPF(35),TSIGMA(35)
      REAL TMUF(35),TKF(35),TMUG(35),TKG(35),TVF(35),TCPG(35)
      COMMON/AREA6/TT,TP,TVG,THF,THG,TCPF,TSIGMA,TMUF,TKF,TMUG
     1,TKG,TVF,TCPG
      COMMON/AREA1/D,P,G,TSAT,VISCG,VISCF,CPF,CONDF,VG,VF,HG,CPG,
     *SIGMA,CONDG,ALFAF,TAV
C
C
C     READ PROPERTY TABLES OF WATER
C     -----------------------------
C
      READ(51,1) TT
      READ(51,2)TP
      READ(51,3)TVF
      READ(51,2)TVG
      READ(51,4) THF,THG,TCPF,TSIGMA
      READ(51,1)TMUF
      READ(51,4)TKF,TCPG,TMUG,TKG
C
      DO 8 I=1,35
      THF(I)=THF(I)*1000.0
      TKG(I)=TKG(I)*0.001
      TMUG(I)=TMUG(I)*0.000001
      TCPF(I)=TCPF(I)*1000.0
      TCPG(I)=TCPG(I)*1000.0
      THG(I)=THG(I)*1000.0
    8 TSIGMA(I)=TSIGMA(I)*0.001
C
C
C     READ GEOMETRY, INLET CONDITIONS AND BOUNDARY COND.
C     --------------------------------------------------
C
      READ(51,5) D,Z,EL
      READ(51,5)G1,G2,REQ,AK,ALMDA,BETAO
      READ(51,5) TIN1,TIN2,TIN3,TIN4
      READ(51,5) TMIN1,TMIN2,TMIN3,TMIN4,TMIN5
      READ(51,5) STEPW,STEPL,STEPD
      READ(51,5) TFIN1,TFIN2,TFIN3
   41  READ(51,5)G,TIN,P,ROHM,CPM,CONDM,SURF
      ALFAM=CONDM/ROHM/CPM
      IF(G.EQ.999.0)STOP
      IF(SURF.EQ.1.0.AND.G.EQ.G1 )TMIN=TMIN1
      IF(SURF.EQ.1.0.AND.TIN.EQ.TIN2)TMIN=TMIN3
      IF(G.EQ.G2.AND.TIN.EQ.TIN3 )TMIN=TMIN2
      IF(G.EQ.G1.AND.TIN.EQ.TIN2 )TMIN=TMIN2
      IF(SURF.EQ.1.0.AND.TIN.EQ.TIN1)TMIN=TMIN4
      IF(SURF.EQ.2.0)TMIN=TMIN5
      TWALL=TMIN
      TAV=(TWALL+TIN )/2.0
      CALL PRPRT
      CONDG1=4.1*CONDG
      QQ2=0.0
```

```
      QQ=0.0

      ENMIN=0.0
      ICONT=0
      ROG=1.0/VG
      U=G*VF
      REF=D*U/VF/VISCF
      CONRF=CONDF*(1.0+((REF-REO)/REO)**0.8)
      ALFAF=CONRF*VF/CPF
      AR=D/2.0
      DEE=AR*BETAO
      IF(SURF.EQ.2.0) GO TO 16
      WRITE(1,558)TIN,G,P
      GO TO 13
 16   WRITE(1,557) TIN,G,P
 13   CONTINUE
  6   ZFIN=ALMDA/4.
      DZED=ALMDA/STEPL
      DD=DEE/STEPD
      DDO=DD*0.10
      DELTA=DD
      TYM=0.0
      Q2=0.0
      T1=0.0
      ENERG=0.
      SVEL=0.
      CALL PCAL(TIN,TT,THF,HLOCA)
      DELH=4.0*Z*QQ*AK/G/D
      HLOC =HLOCA+DELH
      CALL PCAL(HLOC,THF,TT,TLIQ)
      IF(TLIQ.GE.TSAT)TLIQ=TSAT
      IF(AK.EQ.0.0)TLIQ=TIN
   7  ZED=0.
  17  HEIT=DELTA*COS(2.0*3.14*ZED/ALMDA)
      IF(HEIT.LT.DEE) GO TO 18
      ZED=ZED+DZED
      Z1=ZED
      GO TO 17
  18  CONTINUE
      SUMQ2=0.0
      SUMF=0.
      SUMV=0.0
      FLM=0.0
      S1=0.
      P1=0.
      DTEM=TWALL-TLIQ
C
C
C---  CALCULATE MASS AND FORCE ON WAVE SURFACE FOR A GIVEN POSITION
    9 BETA=(AR-DEE+DELTA*COS(2.0*3.14*ZED/ALMDA))/AR
      IF(BETA.GE.0.995)BETA=0.995
      DBDZ=-2.0*3.14*DELTA*SIN(2.0*3.14*ZED/ALMDA)/AR/ALMDA
      IF(DBDZ.GT.0.)DBDZ=0.
      QELM=CONDG1*DTEM*2.0*3.14*BETA*AR*SQRT(1.0+AR**2*DBDZ**2)
     ,*DZED/(AR*(1.0-BETA))
```

```
      DMDOT=QELM/(HG-HF)
      FLM=FLM+DMDOT
      VZAV=(2.0*CONDG1*DTEM*BETA*AR*3.14*SQRT(1.+AR**2*DBDZ**2)*DZED
     ,+FLM*(HG-HF)*AR*(1.0-BETA))/
     ,(3.14*ROG*(HG-HF)*(1.-BETA)*(1.-BETA**2)*AR**3)
      REN=VZAV*DEE/VG/VISCG
      BTERM=BETA*SQRT(1.+AR**2*DBDZ**2)/(1.-BETA)/(1.-BETA**4+
     ,(1.-BETA**2)**2/ALOG(BETA))
C
      DNOM=(1.0-BETA**4)/(1.0-BETA**2)+(1.0-BETA**2)/ALOG(BETA)
      DPDZ=(-1.0)*8.0*VZAV*VISCG/DNOM/(AR**2)
      DP=DPDZ*DZED
      S2=COS(2.0*3.14*ZED/ALMDA)
      VOLE=DELTA*DZED*(S2+S1)*(AR-DEE)*3.14
      SUMQ2=SUMQ2+QELM
      SUMV=SUMV+VOLE
      P2=P1+DP
      PAV=(P1+P2)/2.0
      EF=2.0*3.14*BETA*PAV*DZED*SQRT(1.0+(AR*DBDZ)**2)*AR
      SUMF=SUMF+EF
      ZED=ZED+DZED
      P1=P2
      S1=S2
      IF(ZED.GE.ZFIN )GO TO 10
      GO TO 9
   10 CONTINUE
      ZFIN=ZED
      WMAS=SUMV/VF
      DIST=DD*COS(2.0*3.14*ZED/ALMDA)/2.0
      DWORK=(-1.)*SUMF*DIST
      ENERG=ENERG+DWORK
      DVEL=SQRT(2.0*DWORK/WMAS)
      DTYM=DD/DVEL
      IF(ICONT.EQ.1)DTYM=DD/(VMIN-DVEL)
      DQ2=SUMQ2*DTYM
      Q2=Q2+DQ2
      TYM=TYM+DTYM
      SVEL=SVEL+DVEL
      VAR=DELTA/DEE
      IF(VAR.GT.0.85)DD=DDO
      DELTA=DELTA+DD
      IF(ICONT.EQ.1)GO TO 12
      IF(DELTA.GE.DEE) GO TO 20
      GO TO 7
C---  CONTINUE INTEGRATION OF ENERGY AFTER CONTACT-------
   12 CONTINUE
      IF(ENERG.GE.ENMIN) GO TO 30
      IF(DELTA.LE.DEE)T1=TYM
      GO TO 7
   20 CONTINUE
C
C------ ENERGY AT THE MINIMUM HEAT FLUX POINT ------------
C
C
C
```

```
      QMIN=Q2/TYM/(3.14*D*ALMDA/4.0)
      VMIN=SVEL
      ENMIN=ENERG
      VZAV1=VZAV
      TYMIN=TYM
      OTYM=4.0*TYM
      FRMIN=1.0/OTYM
   28 CONTINUE
      TWALL=TWALL-STEPW
      TAV=(TWALL+TLIQ)/2.0
      CALL RRPRT
      IF(TWALL.LE.TFIN1.AND.SURF.EQ.2.)GO TO 40
      IF(TWALL.LE.TFIN2.AND.TIN.LT.TIN4) GO TO 40
      IF(TWALL.LE.TFIN3) GO TO 40
      ICONT=1
      GO TO 6
   30 CONTINUE
C
C
      T2=TYM
      TCONA=(T2+T1)*0.5
      OTYM=4.0*T2
      FREQ=1./OTYM
C
      RATIO=1.0+4.0*(ZFIN-Z1)/ALMDA
C
C---- HEAT TRANSFER DURING LIQUID CONTACT----------
C
      TE=(TWALL-TLIQ)/(1.+CONRF*SQRT(ALFAM/ALFAF)/CONDM)
      Q=2.0*CONRF*TE*RATIO*SQRT(TCONA/3.14/ALFAF)
      QQN=Q*FREQ
C
C
C----------HEAT TRANSFER BEFORE CONTACT------------
      QQ2=Q2/TYM/(3.14*D*ALMDA/4.0)
      QQ=QQ1+QQ2
      WRITE(1,559)TWALL,QQ
      GO TO 28
   40 CONTINUE
      WRITE(1,596)VZAV1
      GO TO 41
    1 FORMAT(7E10.2)
    2 FORMAT(7F10.6)
    3 FORMAT(7E10.4)
    4 FORMAT(7F10.3)
    5 FORMAT(8E10.3)
  558 FORMAT(1H1,///,20X,"TRNSITION BOILING HEAT TRANSFER FOR COPPER
     *SURFACE",//,20X,"LIQUID TEMPERATURE (C) = ",F8.2," MASS FLUX(KG/
     * M**2/ S)=",E10.3," PRESSURE (BAR)= ",E10.3,
     *      ///,20X,"WALL TEMPERATURE(C)",10X,"HEAT FLUX(W/M**2)"
     *,//)
  557 FORMAT(1H1,//,20X," TRANSITION BOILING HEAT TRANSFER FOR INCONEL
     *SURFACE",//,20X,"LIQUID TEMPERATURE (C) = ",E10.3,"MASS FLUX(KG/
     * M**2/ S)=",E10.3," PRESSURE (BAR)= ",E10.3,
     *      ///,20X,"WALL TEMPERATURE(C)",10X,"HEAT FLUX(W/M**2)"
```

```
     *,//)
 556   FORMAT(//,20X,"AVERAGE VAPOUR VELOCITY = ",F5.1," M/SEC")
 559 FORMAT(25X,F6.2,20X,E8.3,2X,3F6.1)
     END
     SUBROUTINE PCAL(VARI,TBI,TBD,VARD)
C
C
C      THIS SUBROUTINE INTERPOLATES OR EXTRAPOLATES IN TABLES TO
C      OBTAIN THE CORRESPONDING VALUE OF AN INDEPENDANT VARIABLE:
C
C      VARI= INDEPENDANT VARIABLE
C      TBI =    ,,,,,,    TABLE
C      TBD = DEPENDENT    TABLE
C      VARD=    ,,,,,,    VARIABLE
C
      REAL TBI(35),TBD(35)
      DO 20 I=1,40
      DIF=TBI(I)-VARI
      IF(DIF)20,30,30
   20 CONTINUE
   30 VARD=TBD(I-1)+(VARI-TBI(I-1))*(TBD(I)-TBD(I-1))/(TBI(I)-TBI(I-1))
      RETURN
      END
      SUBROUTINE PRPRT
      REAL TT(35),TP(35),TVG(35),THF(35),THG(35),TCPF(35),TSIGMA(35)
      REAL TMUF(35),TKF(35),TMUG(35),TKG(35),TVF(35),TCPG(35)
      COMMON/AREA6/TT,TP,TVG,THF,THG,TCPF,TSIGMA,TMUF,TKF,TMUG
     1,TKG,TVF,TCPG
      COMMON/AREA1/D,P,G,TSAT,VISCG,VISCF,CPF,CONDF,VG,VF,HG,CPG,
     *SIGMA,CONDG,ALFAF,TAV
      CALL PCAL(P,TP,TT,TSAT)
      CALL PCAL(P,TP,TMUG,VISCG)
      CALL PCAL(P,TP,TMUF,VISCF)
      CALL PCAL(P,TP,TCPF,CPF)
      CALL PCAL(P,TP,TCPG,CPG)
      CALL PCAL(P,TP,TKF,CONDF)
      CALL PCAL(P,TP,TKG,CONDG)
      CALL PCAL(P,TP,TVG,VG)
      CALL PCAL(P,TP,TVF,VF)
      CALL PCAL(P,TP,THG,HG)
      CALL PCAL(P,TP,THF,HF)
      CALL PCAL(P,TP,TSIGMA,SIGMA)
      TAV=TSAT
      CALL PCAL(TAV,TT,TKG,CONDG)
      CALL PCAL(TAV,TT,TMUG,VISCG)
      CALL PCAL(TAV,TT,TVG,VG)
    2 RETURN
      END
      BLOCK DATA AREAS,COMMON
      REAL TT(35),TP(35),TVG(35),THF(35),THG(35),TCPF(35),TSIGMA(35)
      REAL TMUF(35),TKF(35),TMUG(35),TKG(35),TVF(35),TCPG(35)
      COMMON/AREA6/TT,TP,TVG,THF,THG,TCPF,TSIGMA,TMUF,TKF,TMUG
     1,TKG,TVF,TCPG
      COMMON/AREA1/D,P,G,TSAT,VISCG,VISCF,CPF,CONDF,VG,VF,HG,CPG,
     *SIGMA,CONDG,ALFAF,TAV
```

END
ENDS

0.01 +00	10.0 +00	20.0 +00	30.0 +00	40.0 +00	50.0 +00	60.0 +00	
70.0 +00	80.0 +00	90.0 +00	100.0 +00	110.0 +00	120.0 +00	130.0 +00	
140.0 +00	150.0 +00	160.0 +00	170.0 +00	180.0 +00	190.0 +00	200.0 +00	
210.0 +00	220.0 +00	230.0 +00	240.0 +00	250.0 +00	260.0 +00	270.0 +00	
280.0 +00	290.0 +00	300.0 +00	310.0 +00	320.0 +00	330.0 +00	340.0 +00	
0.006112	0.012271	0.023368	0.042418	0.073750	0.12335	0.19919	
0.31161	0.47358	0.70109	1.01325	1.4327	1.9854	2.7011	
3.6136	4.7597	6.1804	7.9202	10.027	12.553	15.550	
19.080	23.202	27.979	33.480	39.776	46.941	55.052	
64.191	74.449	85.917	98.694	112.89	128.64	146.08	
1.0002 -031	1.0004 -031	1.0018 -031	1.0044 -031	1.0079 -031	1.0121 -031	1.0171 -03	
1.0228 -031	.0290 -031	.0359 -031	.0435 -031	.0515 -031	.0603 -031	.0697 -03	
1.0798 -031	.0906 -031	.1021 -031	.1144 -031	.1275 -031	.1415 -031	.1565 -03	
1.1726 -031	.1900 -031	.2087 -031	.2291 -031	.2512 -031	.2755 -031	.3023 -03	
1.3321 -031	.3655 -031	.4036 -031	.4475 -031	.4992 -031	.5620 -031	.6390 -03	
206.146	106.422	57.836	32.929	19.546	12.045	7.6776	
5.0453	3.4083	2.3609	1.6730	1.2101	0.89171	0.66832	
0.50866	0.39257	0.30685	0.24262	0.19385	0.15635	0.12719	
0.104265	0.086062	0.071472	0.059674	0.050056	0.042149	0.035599	
0.030133	0.025537	0.021643	0.018316	0.015451	0.012967	0.010779	
0.00061	41.99	83.86	125.66	167.47	209.3	251.1	
293.0	334.9	376.9	419.1	461.3	503.7	546.3	
589.1	632.2	675.5	719.1	763.1	807.5	852.4	
897.7	943.7	990.3	1037.6	1085.8	1135.0	1185.2	
1236.8	1290.0	1345.0	1402.0	1462.0	1526.0	1596.0	
2501.0	2519.0	2538.0	2556.0	2574.0	2592.0	2609.0	
2626.0	2643.0	2660.0	2676.0	2691.0	2706.0	2720.0	
2734.0	2747.0	2758.0	2769.0	2778.0	2786.0	2793.0	
2798.0	2802.0	2803.0	2803.0	2801.0	2796.0	2790.0	
2780.0	2766.0	2749.0	2727.0	2700.0	2666.0	2623.0	
4.218	4.194	4.182	4.179	4.179	4.181	4.185	
4.191	4.198	4.207	4.218	4.230	4.244	4.262	
4.282	4.306	4.334	4.366	4.403	4.446	4.494	
4.550	4.613	4.685	4.769	4.866	4.985	5.134	
5.307	5.520	5.794	6.143	6.604	7.241	8.225	
75.60	74.24	72.78	71.23	69.61	67.93	66.19	
64.40	62.57	60.69	58.78	56.83	54.85	52.83	
50.79	48.70	46.59	44.44	42.26	40.05	37.81	
35.53	33.23	30.90	28.56	26.19	23.82	21.44	
19.07	16.71	14.39	12.11	9.89	7.75	5.71	
1786.0 -061	304.0 -061	002.0 -06	798.3 -06	653.9 -06	547.8 -06	467.3 -06	
404.8 -063	55.4 -063	15.6 -062	83.1 -062	54.8 -062	31.0 -062	10.9 -06	
194.1 -061	79.8 -061	67.7 -061	57.4 -061	48.5 -061	40.7 -061	33.9 -06	
127.9 -061	22.4 -061	17.5 -061	12.9 -061	08.7 -061	04.8 -061	01.1 -06	
097.5 -060	94.1 -060	90.7 -060	87.2 -060	83.5 -060	79.5 -060	75.4 -06	
0.569	0.587	0.603	0.618	0.631	0.643	0.653	
0.662	0.670	0.676	0.681	0.684	0.687	0.688	
0.668	0.687	0.684	0.681	0.677	0.671	0.564	
0.657	0.648	0.639	0.628	0.616	0.603	0.589	
0.574	0.558	0.541	0.523	0.503	0.482	0.460	
1.863	1.870	1.880	1.890	1.900	1.912	1.924	
1.946	1.970	1.999	2.034	2.076	2.125	2.180	
2.245	2.320	2.406	2.504	2.615	2.741	2.883	
3.043	3.223	3.426	3.656	3.918	4.221	4.575	
4.996	5.509	6.148	6.968	8.060	9.580	11.87	

08.105	08.504	08.903	09.305	09.701	10.10	10.50
10.89	11.29	11.67	12.06	12.45	12.83	13.20
13.57	13.94	14.30	14.66	15.02	15.37	15.72
16.07	16.42	16.78	17.14	17.51	17.90	18.31
18.74	19.21	19.73	20.30	20.95	21.70	22.70
17.6	18.2	18.8	19.5	20.2	20.9	21.6
22.4	23.2	24.0	24.9	25.8	26.7	27.8
28.9	30.0	31.3	32.6	34.1	35.7	37.4
39.4	41.5	43.9	46.5	49.5	52.8	56.6
60.9	66.0	71.9	79.1	87.7	99.0	114.0
12.7	-03	0.254-01	50.800+00			
20.3	+01	13.6 +01	50.0 +01	0.3 +00	0.02 +00	0.33 -01
9.7	+01	8.6 +01	7.2 +01	9.6 +01		
23.0	+01	22.0 +01	21.0 +01	1.9 +02	2.9 +02	
2.0	+00	10.0 +01	2.0 +01			
2.4	+02	1.8 +02	1.52 +02			
20.3	+01	00.72 +02	1.0 +00	8.938 +03	3.85 +02	3.79 +02 1.00 +00
20.3	+01	00.86 +02	1.0 +00	8.938 +03	3.85 +02	3.79 +02 1.00 +00
13.6	+01	00.72 +02	1.0 +00	8.938 +03	3.85 +02	3.79 +02 1.00 +00
0.1	+01	00.97 +02	1.0 +00	8.938 +03	3.85 +02	3.79 +02 1.00 +00
13.6	+01	00.86 +02	1.0 +00	8.938 +03	3.85 +02	3.79 +02 1.00 +00
13.6	+01	00.86 +02	1.0 +00	8.169 +03	4.35 +02	0.17 +02 2.00 +00
99.9	+01	00.86 +02	1.0 +00	8.169 +03	74.35 +02	0.17 +02 1.00 +00

TRNSITION BOILING HEAT TRANSFER FOR COPPER SURFACE

LIQUID TEMPERATURE (C) = 72.00 MASS FLUX(KG/ M**2/ S) = .203E+03 PRESSURE (BAR) = .100E+01

WALL TEMPERATURE(C)	HEAT FLUX(W/M**2)
228.00	.252E+06
226.00	.336E+06
224.00	.360E+06
222.00	.460E+06
220.00	.507E+06
218.00	.620E+06
216.00	.637E+06
214.00	.675E+06
212.00	.822E+06
210.00	.851E+06
208.00	.100E+07
206.00	.104E+07
204.00	.122E+07
202.00	.126E+07
200.00	.143E+07
198.00	.148E+07
196.00	.167E+07
194.00	.171E+07
192.00	.191E+07
190.00	.213E+07
188.00	.212E+07
186.00	.233E+07
184.00	.253E+07
182.00	.271E+07

AVERAGE VAPOUR VELOCITY = 4.9 M/SEC

TRNSITION BOILING HEAT TRANSFER FOR COPPER SURFACE

LIQUID TEMPERATURE (C) = 86.00 MASS FLUX(KG/ M**2/ S) = .203E+03 PRESSURE (BAR) = .100E+01

WALL TEMPERATURE(C)	HEAT FLUX(W/M**2)
218.00	.210E+06
216.00	.301E+06
214.00	.381E+06
212.00	.398E+06
210.00	.412E+06
208.00	.524E+06
206.00	.552E+06
204.00	.669E+06
202.00	.708E+06
200.00	.844E+06
198.00	.871E+06
196.00	.102E+07
194.00	.118E+07
192.00	.122E+07
190.00	.139E+07
188.00	.156E+07
186.00	.173E+07
184.00	.173E+07
182.00	.190E+07

AVERAGE VAPOUR VELOCITY = 4.2 M/SEC

TRNSITION BOILING HEAT TRANSFER FOR COPPER SURFACE

LIQUID TEMPERATURE (C) = 72.00 MASS FLUX(KG/ M**2/ S)= .136E+03 PRESSURE (BAR)= .100E+01

WALL TEMPERATURE(C)	HEAT FLUX(W/M**2)
218.00	.222E+06
216.00	.288E+06
214.00	.392E+06
212.00	.408E+06
210.00	.423E+06
208.00	.535E+06
206.00	.563E+06
204.00	.661E+06
202.00	.703E+06
200.00	.823E+06
198.00	.855E+06
196.00	.101E+07
194.00	.104E+07
192.00	.119E+07
190.00	.135E+07
188.00	.139E+07
186.00	.155E+07
184.00	.173E+07
182.00	.173E+07

AVERAGE VAPOUR VELOCITY = 4.6 M/SEC

TRNSITION BOILING HEAT TRANSFER FOR COPPER SURFACE

LIQUID TEMPERATURE (C) = 86.00 MASS FLUX(KG/ M**2/ S)= .136E+03 PRESSURE (BAR)= .100E+01

WALL TEMPERATURE(C)	HEAT FLUX(W/M**2)
208.00	.182E+06
206.00	.253E+06
204.00	.316E+06
202.00	.345E+06
200.00	.433E+06
198.00	.455E+06
196.00	.547E+06
194.00	.576E+06
192.00	.683E+06
190.00	.802E+06
188.00	.836E+06
186.00	.960E+06
184.00	.110E+07
182.00	.124E+07

AVERAGE VAPOUR VELOCITY = 3.9 M/SEC

TRNSITION BOI LING HEAT TRANSFER FOR COPPER SURFACE

LIQUID TEMPERATURE (C) = 97.00 MASS FLUX(KG/ M**2/ S)= .100E+01 PRESSURE (BAR)= .100E+01

WALL TEMPERATURE(C)	HEAT FLUX(W/M**2)
188.00	.118E+06
186.00	.145E+06
184.00	.168E+06
182.00	.172E+06
180.00	.199E+06
178.00	.230E+06
176.00	.237E+06
174.00	.269E+06
172.00	.303E+06
170.00	.339E+06
168.00	.374E+06
166.00	.413E+06
164.00	.413E+06
162.00	.477E+06
160.00	.508E+06
158.00	.558E+06
156.00	.583E+06
154.00	.549E+06

AVERAGE VAPOUR VELOCITY = 2.9 M/SEC

TRANSITION BOILING HEAT TRANSFER FOR INCONEL SURFACE

LIQUID TEMPERATURE (C) = .860E+02MASS FLUX(KG/ M**2/ S)= .136E+03 PRESSURE (BAR)= .100E+01

WALL TEMPERATURE(C)	HEAT FLUX(W/M**2)
288.00	.279E+06
286.00	.350E+06
284.00	.371E+06
282.00	.367E+06
280.00	.452E+06
278.00	.471E+06
276.00	.488E+06
274.00	.585E+06
272.00	.600E+06
270.00	.634E+06
268.00	.740E+06
266.00	.769E+06
264.00	.778E+06
262.00	.909E+06
260.00	.930E+06
258.00	.951E+06
256.00	.108E+07
254.00	.113E+07
252.00	.114E+07
250.00	.128E+07
248.00	.132E+07
246.00	.148E+07
244.00	.151E+07
242.00	.167E+07

AVERAGE VAPOUR VELOCITY = 6.4 M/SEC